TOWARDS A NEW TENSEGRITY SYSTEM

D. NGO

DELFT, 07/2017

TOWARDS A NEW TENSEGRITY SYSTEM
FOR LARGE-SPAN STRUCTURES

Date	07/2017
Name	Duc Ngo
Student number	4504526
Address	------
Postal code	------
Telephone number	------
E-mail address	ducngo123@gmail.com
University	Delft University of Technology
Faculty	Architecture and Built Environment
Department	Architectural Engineering and Technology
Graduation Track	Building Technology
Main mentor	Assistant Professor ir. A. Borgart
	Chair of Structural Mechanics
Second mentor	Assistant Professor dr. ir. P. Nourian
	Chair of Design Informatics
External Examiner	Assistant Professor dr. T.E. Jylhä
	Chair of Real Estate Management

Abstract

Throughout the long history of
architecture, the effect of gravity
is always present in any structures.
Surprisingly in tensegrity composition,
this primary law of nature seems to be
absent. This is because the discontinuous
set of struts in the continuous network
of proportionally thin cables makes the
structures look like floating in the
air. However, there has not been much
application of tensegrity principle in
the construction field due to the lack
of design methods and its complexity. By
developing a large-span structure using
tensegrity systems, a design method and
an analysis technique are introduced
along to define double-surface tensegrity
systems. The design approach explores an
innovative way to determine the structural
topology and geometry of such the systems.
The form-finding process and structural
analysis are conducted to discover an
appropriate way of analyzing tensegrity
and ensuring that the systems are stable.

*Keyword: tensegrity, double-surface
tensegrity, form-finding, complex geometry,
large-span structure, structural topology*

Preface

Towards A Tensegrity System is the graduation thesis for the Master of Science Architecture, Urbanism and Building Sciences by Duc Ngo as the final project at the Faculty of Architecture and Built Environment at Delft University of Technology, the Netherlands. This work is produced in Building Technology Graduation Studio.

I am thankful for the brilliant guidance by a group of inspiring and talented people.

First of all, I received a great help with a thorough knowledge on structural complexity from my first mentor, Andrew Borgart from the Chair of Structural Mechanics. Secondly, there is a significant support on computational design and methodology from my second mentor, Pirouz Nourian from the Chair of Design Informatics. In addition, I am grateful for the technical supports of Jon Mirtschin, Arend van Waard, and Thomas Li.

Duc Ngo, Delft, May 2017

Table of contents

Chapter 1. Introduction

The Introduction is dedicated to the research framework which is the starting point of this graduation thesis towards a new tensegrity system.

1.1. Background

For more than 50 years, tensegrity is considered an innovative structural concept and it has the potentials to become a super-efficient structural system. In this system, the coupling between forces and forms is very tight, and this relation is made visible by structural components themselves. Everyone is fascinated by seeing the very particular type of structural composition in which struts seem to float in the air. This character is also the key point since people, engineers and architects more than the others, are surprised by this new kind of flow of forces. They are used to gravity effect, and in this case, gravity seems to be absent.
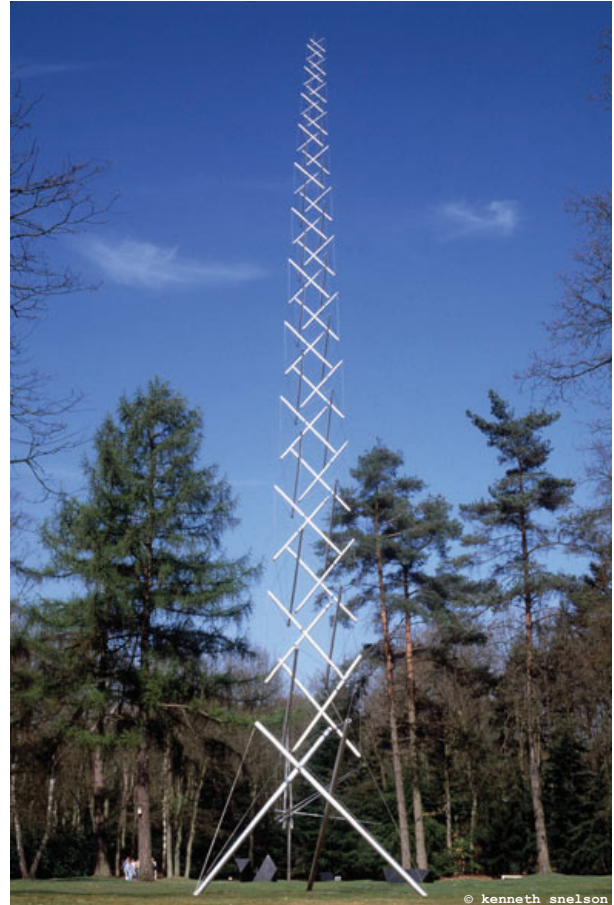
Regardless its potentials, there has not been much application of tensegrity principle in the construction field. Examples have remained at the prototype state for lack of adequate technological design studies. By studying the complexity of tensegrity and applying it to a football stadium, this thesis focuses on exploring a design method which could help to realize this structural composition in architectural practice.

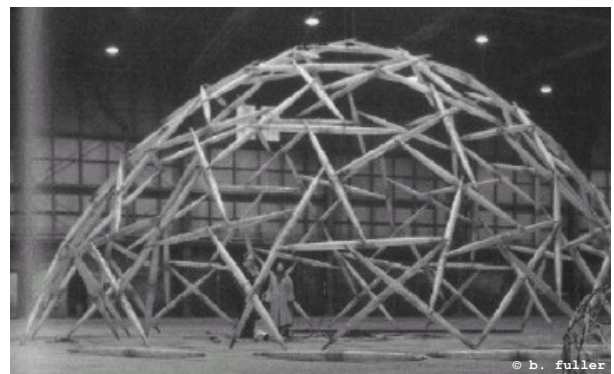1.1. Tensegrity needle tower, Kenneth Snelson

1.2. Problem Statement

The issue of form-finding is central in the study of tensegrity system due to the lack of design and analysis techniques, especially when the system is complex with a large number of struts and cables. The composition of struts in a network of cables could not be manually handled anymore. On the other hand, spherical and domical structures of tensegrity are enormously sophisticated which can lead to difficulties in fabrication and assembling. When the structure spans a long distance, it is almost impossible to predict the structural behavior to ensure whether or not they are stable in reality.

Hypotheses

By designing a large-span structure using

1.2. Tensegrity dome, Buckminster Fuller

tensegrity systems, a design method and an analysis technique will be developed along to define the structural composition of struts and cables, visualize structural performance, and ensure the stability of such a complex system.

1.3. Research Question

Main question:
How to design a stable tensegrity system for a large span structure to cover a stadium?

Sub-questions:
How can a software work-flow help in designing tensegrity structure?
What is the tessellation of tensegrity that should be investigated?
What is the structural morphology of tensegrity systems?
What is the topology of tensegrity systems?
How to apply structural principles to analyze tensegrity systems?
How to translate mathematical principles of tensegrity to digital tools?
How to study tensegrity structures using physical models?
How to visualize mechanic behaviors of tensegrity systems?
How can designers optimize the geometric form, the material efficiency, and the cross section of structural components in tensegrity systems?

1.4. Design Assignment

Design a new roof for Feyenoord stadium using tensegrity structure.

In the 1930s, Leen van Zandviet, Feyenoord's president came up with the idea of building an entirely new stadium, unlike any other on the continent, with two free hanging tiers, and no obstacles blocking the view. This design was an incredibly innovative use of technology for structure in architecture, which inspires several great stadiums around Europe, Camp Nou is a famous example. After almost 80 years in service, De Kuip needs to have a new roof structure which could continue its innovative tradition.

Tensegrity structure could write the next chapter of the story. By using this type of structure, the efficiency of the structure would be maximized, the slenderness of structural members would be pushed to the edges. As a result, the pressure on the existing system can be decreased, and the transparency can be achieved. Eventually, an extraordinary space inside the stadium would be absolutely an ideal present for football lovers.

1.5. Method Description

The research is started with literature studies related to tensegrity systems, rigidity theory, and large-span structures. Studies in areas of form-finding, pattern, tessellation, morphology, and topology of the structure systems would be further investigated. Along with literature review, modeling techniques will be conducted manually and computationally to acquire more understanding about computational design as well as the structural composition of tensegrity systems.

After that, a generic design method will be introduced to construct a large-span dome (240x200x45m) with a huge central opening. The technique would be transformed into the design of a new tensegrity roof for Feyenoord stadium in Rotterdam, the Netherlands. Based on this particular case, there would be practical inputs and requirements for the performance of the structural model and optimization regarding cross-sectional properties, material efficiency, geometrical rigidity, stability, and constructibility.

Finally, a fabrication method and technique will be produced according to the structural model in a way that it would help the model to perform better structurally. For the constructibility, important details would be developed to help the construction process of the tensegrity structure in large scales.

1.6. Relevance

On the scientific aspect, this thesis would contribute to constructing to the library of tensegrity structures with a design method for application in large-scale construction. It helps to resolve the obstacles posed by the complexity of such the systems by the innovative use of computational tools. Besides, a way of improving the rigidity and usability of tensegrity in mega-structure is explored, which paves a way to realize the construction and fabrication of the buildings using this structural system.

The collaboration between the architect and the engineer would be developed along with the process of this graduation project. The work-flow proposed by this

thesis could lead to better communication between different disciplines working on a common parametric platform.

On the social aspect, a new way of tensegrity application can reflect the technological innovation of our time in a complex type of building covering a vast open space, a stadium. A stadium is a major component in social interaction in the culture around the world. It is currently the place where people can come together to celebrate sport, enjoy a concert, or congregate for self-expression, or some other similar social events. Society will obviously benefit from the impact of using tensegrity systems for the redevelopment of a current urban context.
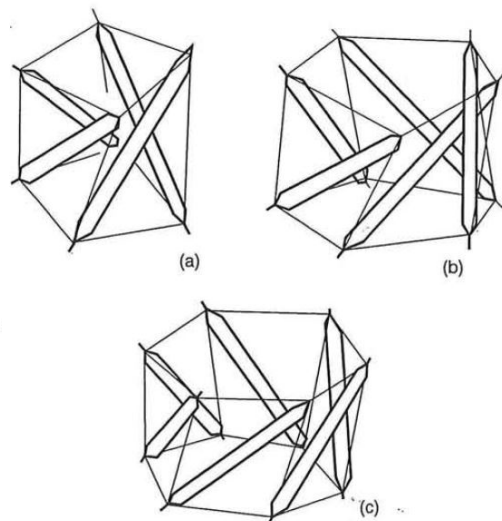
1.3. Tesegrity structures based on twisted prisms. a - 4 struts, b - 5 struts, c - 6 struts

Chapter 2. Tensegrity Structures

2.1. Introduction to Tensegrity Structures

The term 'tensegrity' was invented from the words 'tensile' and 'integrity' by Fuller (1962). In his patent, tensegrity was described as 'Islands of compression inside an ocean of tension'. Fourteen years later, Pugh (1976) introduced a comprehensive definition: 'A tensegrity system is established when a set of discontinuous compression components interacts with a set of continuous tensile elements to define a stable volume in space'. In practice, tensegrity structures are usually modeled as a set of weightless discontinuous struts and continuous cables connected by frictionless ball joints. The struts bear compression, while the cables carry tensile forces. Both struts and cables are pre-stressed and subjected to an axial load. Over the last few decades, tensegrity structures have attracted considerable attention from many fields, such as architecture, mathematics, material sciences, and biology.

2.1. Buckminster Fuller with his tensegrity sphere.

2.2. Rigidity Theory

To be able to understand structural principles of tensegrity structures, one needs to understand the essential knowledge about rigidity.
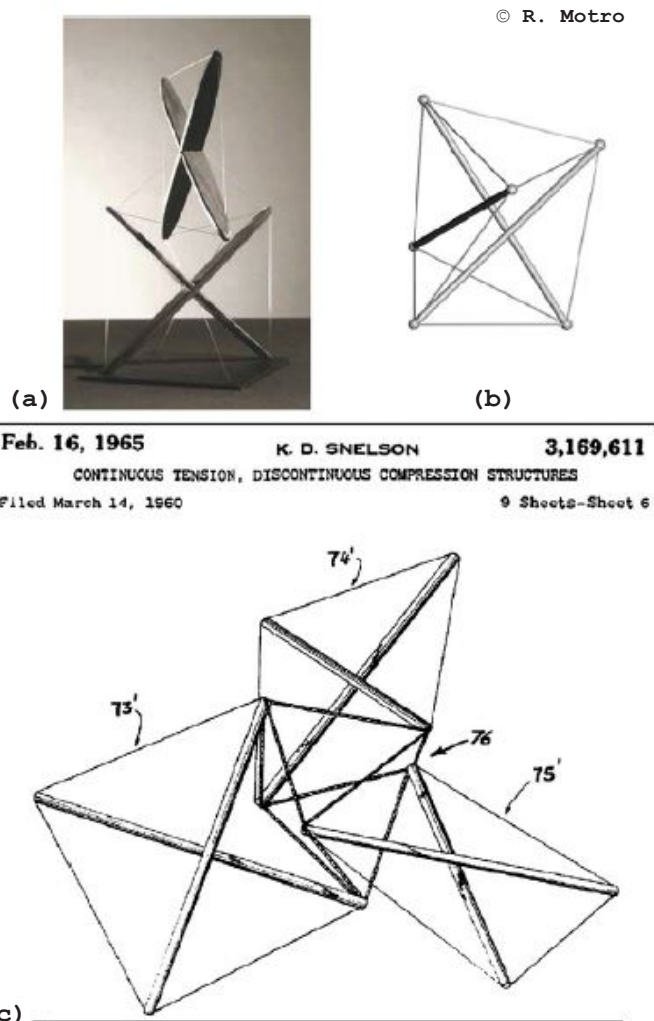
There are several compositions of tensegrity systems which need to prove that whether or not a given tensegrity structure is rigid. This question is obviously difficult to answer. Most of the cases, tensegrity structures were tested with a physical model, and there are a few the systems that were conducted using computational tools.

In two dimensions, the easiest way of constructing a rigid truss is by arranging the bars to form a sequence of triangles. A triangle consisting of pin-jointed bars is the simplest two-dimensional rigid structure, and two triangles with a side in common also form a rigid structure in two dimensions (but not in three dimensions, as one of the triangles can move out of plane by rotating about the common side).

To extend this approach to three dimensions, i.e. to construct in a three-dimensional (Euclidean) space, one can use the simplest three-dimensional structure that is rigid, i.e. the tetrahedron;

(a)   **(b)**

Feb. 16, 1965   K. D. SNELSON   3,169,611
CONTINUOUS TENSION, DISCONTINUOUS COMPRESSION STRUCTURES
Filed March 14, 1960   9 Sheets-Sheet 6

(c)

2.2. Double-X(a), simplex(b), triple-X(c)

or alternatively one can form a closed
surface that is completely triangulated.
These approaches are often followed in
the design of practical structures, but
there are also many rigid structures that
are not triangulated. Therefore, it is
important to have a general way of proving
whether or not a given three-dimensional
structure is rigid.

According to Miura and Pellegrino, in two
dimensions, each joint has two degrees of
freedom, i.e. two independent translation
components, and hence for a structure with
j joints the total number of degrees of
freedom is 2j. Denoting by k the total
number of kinematic constraints, where
– for example – connecting a joint to
a foundation counts as two because it
suppresses both translation components,
and by b the total number of pin-jointed
bars – each bar counts one as it imposes a
single 'distance' constraint between the
joints it connects – we require that

$$2j - k - b \leq 0 \quad (1.1)$$

This is known as Maxwell's equation
(Maxwell, 1964). Consider, for example,
the structure shown in figure 2.3(a). It
consists of four triangles, the first
of which is connected to a foundation,
and therefore, it is obviously a rigid
structure. Substituting j = 6, k = 4, b =
8 (obviously, there is no need for a bar
between the two foundation joints) into
Eq. 1.1. this is obtained:

$$2 \times 6 - 4 - 8 = 0$$

Therefore, it could be concluded that this
structure has sufficient amount of bars to
be rigid.

It is crucial to realize that a structure
that has enough bars to be rigid may not,
in fact, be rigid, as its bars maybe
'incorrectly' placed. For example, if in
figure 2.3(a) we relocate the bar bracing
the left-hand square, so that the right-
hand square is now doubly braced, as shown
in figure 2.3(b), we obtain a structure
that still satisfies Eq. 1.1. and yet is
clearly not rigid. In this case, we have a
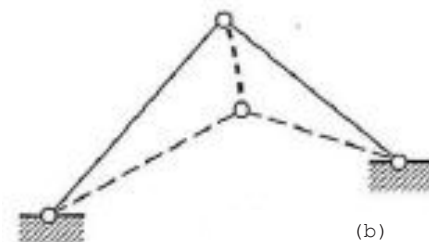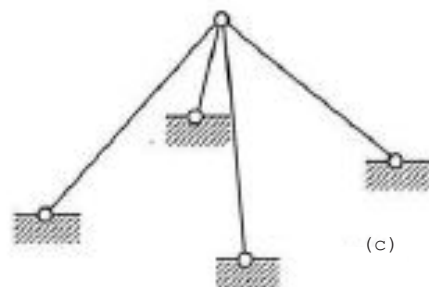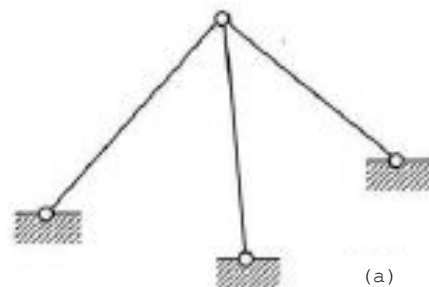single-degree-of-freedom mechanism, figure
2.3.c).

A structure that admits no mechanisms is
called kinematically determinate.

Note that the doubly-braced square on
the right-hand side of the structure in
figure 2.3(b) declares a state of self-
stressed, there is a set of non-zero bar
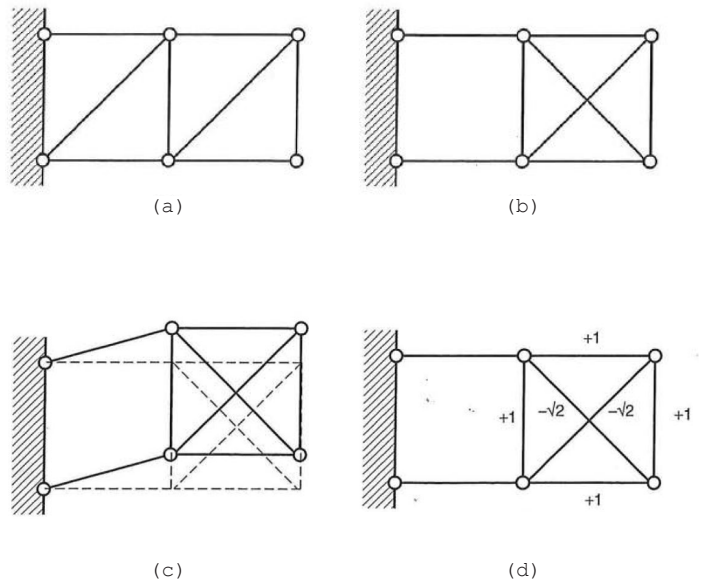
2.3. 2-d trusses.   © Miura + Pellegrino

2.4. Examples of simple three-dimensional trusses.

8

forces that are in equilibrium with zero external forces, as shown in figure 2.3(d). A structure that admits no states of self-stressed is called statically determinate.

Denoting by m the number of independent mechanisms of a structure, and by s the number of states of independent states of self-stress, for the structure of figure we have s = 0 and m = 0 (statically and kinematically determinate), whereas for the structure of figure 2.3(b) we have s = 1 and m = 1 (statically and kinematically indeterminate). Here, by independent we mean that if any mechanism is represented by a vector, whose components correspond to the tangent motions of the joint, and any state of self-stress by a vector whose components correspond to the bar forces, it is not possible to obtain one of the vectors as a linear combination of the others.

Therefore, Maxwell's equation in the form of equation 1.1. is the only necessary condition for the kinematic determinacy of pin-jointed structures, but not a sufficient condition. It will be shown in the general, most useful way, of writing Maxwell's equation is

$$dj - b - k = m - s \quad (1.2)$$

where d = 2, or 3 depending on the dimensions of the (Euclidean) space in which the structure is considered.

Considering the three-dimensional structures, d = 3, shown in figure 2.4 The tripod structure in fig 2.4(a) has a single free joint plus three fully constrained joints; so j = 4 and k = 9. The unconstrained joint is connected by three non-coplanar bars, b = 3, to the foundation joints. It has no states of self-stress, s = 0, as the condition for the joint to be equilibrium in three directions without external forces requires that the bar forces be zero. Substituting into Eq. 1.2 gives

$$3 \times 4 - 3 - 9 = 0 = m - 0 \quad (1.3)$$

Having established that s = 0 for the structure of fig 2.4(a), obviously, s will remain unchanged if a bar is removed, figure 2.4(b). Hence, for this structure j = 3, k = 6, and b = 2. Substituting into Maxwell's equation

$$3 \times 3 - 2 - 6 = m - 0 \quad (1.4)$$

This gives m = 1. The mechanism involves a rotation of the two bars about an axis

passing through the two foundation joints, as shown in figure 2.4(b).
By an analogous argument, the structure of figure 2.4(a), has m = 0, from Maxwell's equation, s = 1.

The existence of structures with infinitesimal mechanisms was first discovered by J. Clerk Maxwell (1864), but it was only more recently that it was realized that they could be given a first-order (geometric) stiffness through a state of pre-stress (Calladine, 1986). This property has been successfully exploited in the design of pre-stressed cable nets and tensegrity structures.

Cubic Truss

The next example provided by Pellegrino is the cubic truss in figure 2.5(a), with members of length a lying on the edges of a cube plus four diagonal bracing members on the side faces, of length a√2. The four joints at the bottom are fully constrained. This truss has j = 8, b = 12, and k = 12; substituting these values into Maxwell's equation

$$3 \times 8 - 12 - 12 = 0 = m - s \quad (1.10)$$

Giving m - s = 0. It can be shown by the matrix method that this truss is both statically and kinematically determinate (m = s = 0).

Now, consider varying the shape of this truss by rotating the upper square in an anti-clockwise sense, without translating. Obviously, the lengths of both the diagonal members and of the members that were originally vertical, e.g. AF and AE respectively, vary during this process.

According to Tarnai, the coefficient matrix of the system of equilibrium equationshas full rank, equal to 12, normally. However, the matrix becomes rank deficient, with rank of 11, in four special configurations. Of these, the configurations that are of greatest practical interest are those that are obtained for a rotation of the upper square though 45, figure 2.5(b), and 135, figure 2.5(c).

In each of these configurations the static and kinematic properties of the structure change from m = s = 0 to m = s = 1. The states of self-stress and mechanisms for these configurations are shown in figures 2.6 and 2.7. In figure 2.3 note that the bar forces in the top square are alternatively positive and negative as one goes round the square, whereas in

fig. 2.7 the bar forces in the top square
are all of the same sign. There is an
important difference between these two
special configurations: in the first one,
the mechanism allows a finite amplitude
distortion of the structure, whereas the
mechanism of the second configuration
allows only an infinitesimal motion.

In practice, imposing a state of pre-
stress on the first structure, e.g. by
varying the length of one of its members
with a turnbuckle, is impossible, as the
structure will change shape instead of
becoming self-stressed. On the other hand,
the structure of figure 2.5(c) has the same
type of behavior of the structure in figure
2.6(b). It is an example of a tensegrity
structure.

According to Tarnai, the existence of
special configurations that are both
statically and kinematically indeterminate
is a general feature of trusses based
on two interconnected regular polygons
with n-sides (in figure 2.5 n = 4) and,
in particular, configurations that admit
finite amplitude inextensional mechanisms
exist for all trusses with n even and ≥
4. However, for n odd, there are no such
special configurations.

Truss structures with a layout similar to
figure 2.5(b) have been used for several
applications, often in preference to the
layout in figure 2.5(a), because their
higher degree of symmetry leads to the
expectation of a 'more uniform' stiffness
distribution.

2.3. Topology

The tensegrity pattern can be interpreted
mathematically and structurally through a
connectivity topology of the tessellation.
In such the system, the relationships
between vertices, edges, and faces are
informed. A topology does not provide
information about the distance, magnitude
or geometry of structural members in
Euclidian space. Therefore a multitude of
different physical representations of one
topology can be identified. However, the
same joints are always connected via the
similar bars.

A connectivity topology consists of data
about the unique identifiers of joints and
bars, and the start and end nodes of every
bar. This information describes a singular
way of connection the bars via nodes. As
identifiers, the joints and bars often get
a numeric label, to distinguish between
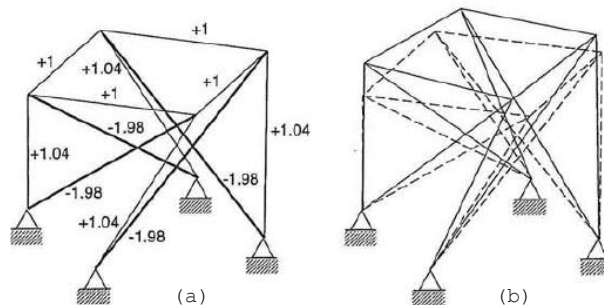joints and bars the latter can be written
between square brackets.
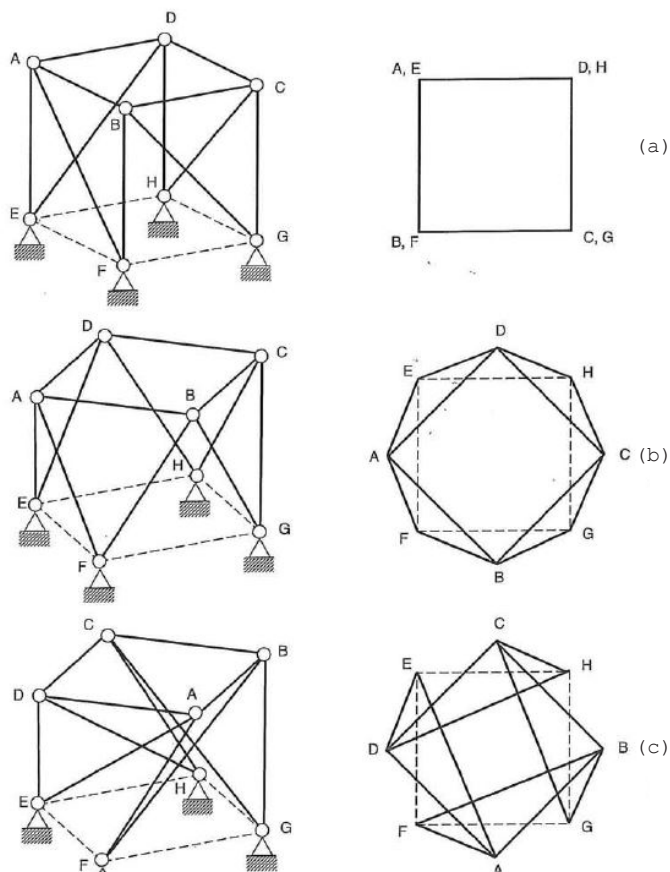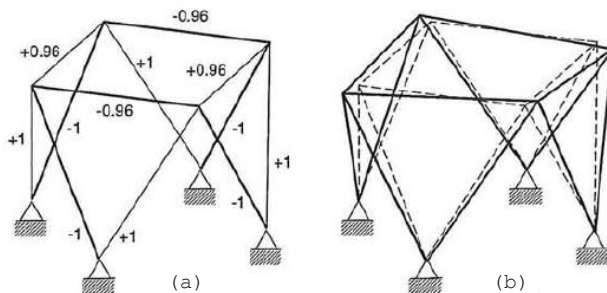
2.5. Cubic truss

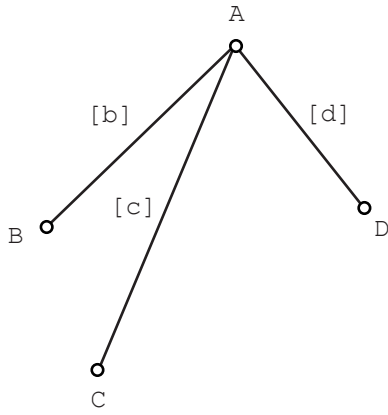2.6. (a) state of self-stress and (b) inextensional
mechanism of first special configuration of cubic
truss.

2.7. (a) state of self-stress and (b) inextensional
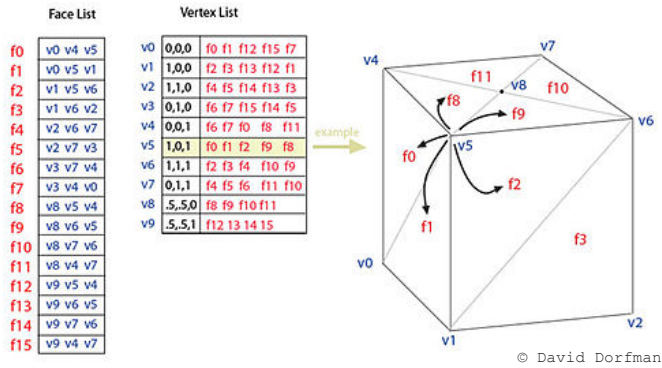mechanism of second special configuration of cubic
truss.

A

[b]   [d]

[c]

B   D

C

2.8. Topology of a frame

edge	start vertex	end vertex
[b]	A	B
[c]	A	C
[d]	A	D

2.9. Face-vertex topology of a cube

2.10. Vertex-vertex topology of a cube

Consider the example in figure 2.8 consisting of three bars and four joints. In one matrix or with two named arrays we can describe the connectivity of this simple framework.

There are also other possibilities of connectivity matrices for the same configuration. This depends on the chosen numbering and which is considered as start joint for a bar and which is considered as end joint. In graph theory, this can be considered a simple directed graph. In combination with joint coordinates, this approach is useful for creating the equilibrium matrix of a framework. The directedness of the graph is not strictly necessary to describe frameworks since the topology does not change by reverting bars. So mathematically a connection topology can be written as the ordered pair: G = (V, E), where V is the set of vertices or nodes (joints), and E is the set of edges.

Looking at figures 2.9 and 2.10, there is an introduction of using a combination of a face-vertex graph in combination with the vertex-vertex graph for the description of a topology of a given geometry. For the equilibrium matrix setup, a network graph will be used with its directional ordered pair written in form D = (V, A), where the order of every 2-element in A determines the start and end joint of a bar.

Cubic Graph

In the mathematical field of graph theory, a cubic graph is a graph in which all vertices have degree three. In other words, a cubic graph is a 3-regular graph. Cubic graphs are also called trivalent graphs.

Cubic graphs arise naturally in topology in several ways. For example, if one considers a graph to be 1-dimensional CW complex, cubic graphs are generic in that most 1-cell attaching maps are disjoint from the 0-skeleton of the graph. Cubic graphs are also formed such as the graphs of simple polydedra in three dimensions, polyhedra such as the regular dodecahedron with the property that three faces meet at every vertex.
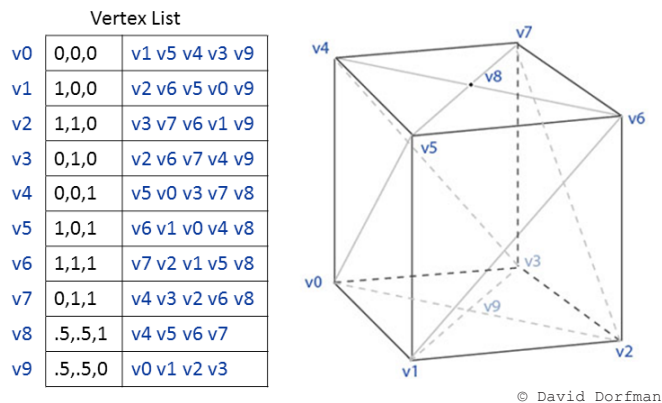
An arbitrary graph embedding on a two-dimensional surface may be represented as a cubic graph structure known as a graph-encoded map. In this structure, each vertex of a cubic graph represents a

flag of the embedding, a mutually incident triple of a vertex, edge, and face of the surface. The three neighbors of each flag are the three flags that may be obtained from it by changing one of the members of this mutually incident triple and leaving the order members unchanged.

2.4. Single-surface Tensegrity Structures

As discussed previously, there exist a number of methods to assemble tensegrity structures based on elementary cells. For example, the triplex and quadruplex tensegrity prisms have often been selected as the elementary cells. A triplex tensegrity prism has three struts and nine cables, and a quadruplex tensegrity prism contains four struts and 12 cables. It is a more flexible method to assemble tensegrity structures based on much simpler elementary cells containing only one strut. In contrast to the existing methods, the elementary cells adopted here are not complete tensegrity structures by themselves, but they can be used to construct almost all types of tensegrity structures. The provement and examples in this section are rooted from the work of Y. Li et al. in *'Constructing tensegrity structures from one-strut elementary cells'*.

The definition of the elementary cells will follow Pugh's definition of tensegrity in that no connection is allowed between two struts. Only those tensegrity structures in which each node has one and only one strut is considered. The elementary cell adopted will consist of one strut and a few cables. In such a design approach, the number of elementary cells, c, will always be equal to the total number of struts, b, in a structure. As each strut has two nodes, the total number of nodes, n is then twice c, i.e.

$$n = 2b = 2c \quad (2.1)$$

Assuming each node in the structure is shared by two elementary cells, we have

$$n = \tfrac{1}{2}.(n_c)c \quad (2.2)$$

where n_c denotes the number of nodes in each cell and $\langle n_c \rangle$ is the expectation of n_c. It follows from equations (2.1) and (2.2) that $\langle n_c \rangle = 4$. If a tensegrity structure is assembled from elementary cells with the same topology, then there should be four nodes in each cell, i.e. $\langle n_c \rangle = 4$.

Figure 2.11 lists all of the ten possible topology graphs of elementary cells containing one strut and four nodes. They are classified into four groups according to the number of cables. The type-0 cell has five cables, and it can be considered as the basis for other cells. By removing one, two, or three cables from the type-0 cell, we obtain elementary cells of the other nine types.

The elementary cells can be used to assemble almost all types of tensegrity structures. For example, the expandable octahedral, cylindrical and truncated regular tetrahedral tensegrity structures can be assembled from type-1, type-4, and type-3, respectively, while planar tensegrity structures can be constructed from the type-7 cell.

In the sequel, the type-3 will be selected, referred as 'Z-shaped cell' for its shape, as the main elementary cell to construct tensegrity structures. The reason for this selection is as follow. Firstly, if a node in a tensegrity structure has only two cables and one strut connected, force balance would require that they must lie in the same plane and the corresponding structure will be planar. Therefore, in a three-dimensional tensegrity structure, there should be at least three cables connected to a node, i.e.

$$s_n \geq 3 \quad (2.3)$$

Where s_n denotes the number of cables connected to each node. As each cable in the constructed structure has two nodes, it follows from equations (2.1) and (2.3) that the total number of cables must satisfy

$$s = \tfrac{1}{2}.ns_n \geq \tfrac{1}{2}.3n = 3c \quad (2.4)$$

If no cable is shared by two cells, the number of cables, sc, in each cell of a spatial tensegrity structure should satisfy

$$s_c = s/c \geq 3 \quad (2.5)$$

The cells of type 7-9 contains only two cables each and cannot be used to construct three-dimensional tensegrity structure. Secondly, adding cables to a stable tensegrity structure will not make it unstable, while removing cables is likely to lead to instability. Therefore, it is focused on tensegrity structures in which the ratio between the numbers of cables and struts is as small as possible. Therefore, the cells of types

© Li et al
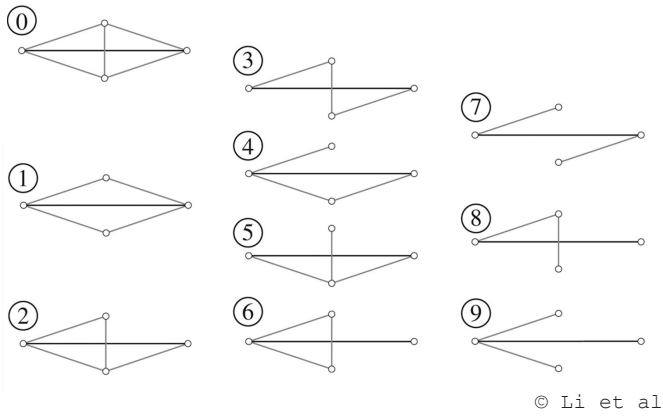
2.11. The topology graph of all elementary tensegrity cells containing one strut and 4 nodes.

© Li et al

2.12. Typical tensegrity structures assembled from elementary cells
(a) octahedral tensegrity from type-1 cells
(b) cylindrical tensegrity from type-4 cells
(c) truncated tetrahedral from type-3 cells
(d) planar tensegrity from type-7 cells

0-2, which contain four or five cables, will not be considered further in this section. Thirdly, among the cells of type 3-6 each of which contains three cables, the type-3 or Z-shaped cell can be made a pre-stressed and self-equilibrated one-dimensional structure, while the other three types cannot. This means that it should be easier to design a structure under pre-stress stability based on the Z-shaped cell than on the other three types. Therefore, the tensegrity structures assembled from the Z-shaped cell will be focused to develop further. The obtained assemblies will be referred to as the Z-based tensegrity.

Topology of Z-based Tensegrity

Topology determination is the first and an important step to designing tensegrity structures. In this study, the topology of a Z-based tensegrity will be determined in two steps. The first step is to specify the topology of cables, and the second is to add struts into the cable network. Provided that the process of adding struts is achievable for the specified topology of cables, one can readily obtain the topology of a Z-based tensegrity. From equation (2.4) and (2.5), it is known that each note in a Z-based tensegrity must be connected by three cables, i.e. $s_n = 3$. In the terminology of the graph theory, the topology of the cables is said to be a cubic graph, also called a 3-regular graph.

It should be noted that there are a large number of cubic graphs. The following questions then arise: can all the cubic graphs be used to construct Z-based tensegrity; and if not, what are the conditions for a cubic graph to be selected?

As the three cables in a Z-shaped cell are linked end to end, their topology constitutes a path including three edges according to the graph theory. The two end vertices of the cable path also correspond to the two nodes of the strut in the same cell. Therefore, once a 3-path decomposition of the cubic graph is admitted, one can easily add the struts into the topology. Here a pertinent theorem proved by Heinrich et al. (1999) is quoted.

Theorem

Let G be a simple connected 3m-regular graph, which, when m is odd, has no cut edge. Then G admits a balanced 3-path
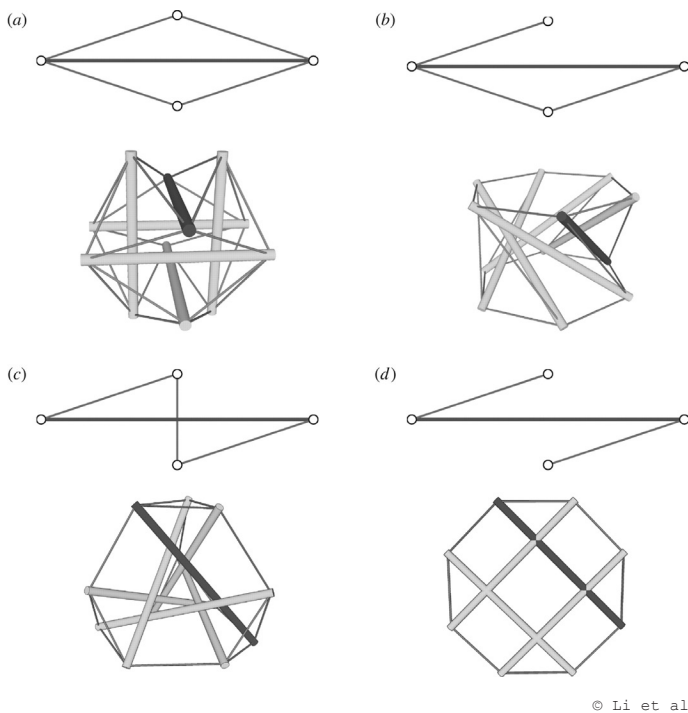
decomposition.

In the case of m = 1, this theorem is reduced to following proposition: 'Every simple bridgeless cubic graph G admits a balanced 3-path decomposition'.

Here, balanced path decomposition means that 'each vertex of G is an end of s paths of the decomposition for some fixed s' (Heinrich et al. 1999). It is evidence that s can only be equal to 1 for the 3-path decomposition of a cubic graph. From the viewpoint of a tensegrity structure, this ensures that there is no connection between struts. The balanced decomposition also excludes the situation where the two end vertices of a path coincide. This means that the two nodes of an added strut must be different or, in other words, no strut of zero length can exist in a tensegrity structure. Such a structure perfectly matches the tensegrity definition. Therefore, the above proposition provides a sufficient condition for those cubic graphs, which can be used as the cable topology of a Z-based tensegrity. Furthermore, we can prove that the restrictions of the cubic graphs in the proposition are also necessary for designing a practical tensegrity structure. Firstly, the topology of cables in the tensegrity structures of interest must also be bridgeless. In the graph theory, a bridge is defined as an edge (or a cable in the tensegrity structure under study) whose removal will disconnect the graph into two separate parts. Thus, a structure with a 'bridge' is unstable and impractical.
From the above proposition and discussions, the following corollary for Z-based tensegrity structures is achieved.

Corollary

A Z-based tensegrity structure can be constructed by adding to a cable net if and only if the topology of cables is a simple and bridgeless cubic graph. Based on this corollary, one can construct the topology of the structure from a cubic graph. Once the topology is determined, the next step is to set proper original lengths and stiffness of the struts and cables before using a form-finding procedure. As the two parameters are not independent for the form-finding of a tensegrity, for the sake of simplicity, we set the stiffness of all elements as unity. Generally, to keep a tensegrity structure in a state of pre-stress stability, its cables are all in tension and struts in compression. An obvious way to achieve such a pre-stressed state is to set the strut length in each cell to be longer than the total length of its three cables.

Example

To illustrate some applications of the proposed topology design method, a number of simple examples will be given in the following. It can be shown that all polyhedra with three edges connected at each node satisfy the topology requirements in the corollary. This has inspired us to construct Z-based tensegrity structures following the topology of a polyhedron.

For cable nets with a regular cubic graph topology, struts can be manually added for tensegrity. For instance, take the pentagonal prism as the topology of a cable net, as shown in figure 2.13.(a). The topology after adding struts is shown in figure 2.13.(b), and the final form-finding result of the tensegrity is shown in figure 2.13(c). The obtained structure is named as $D^{1,2}_5$ prismatic tensegrity, which is also special case of tradition cylindrical tensegrity consisting of five struts. As all the prisms are cubic graphs, many other cylindrical tensegrity structures can be constructed in a similar way.

Next, there is a more interesting example, in which the topology of cable is a sphericon-like polyhedron assembled from two half-prisms, as shown in figure 2.14(a). The corresponding typology after adding struts and form-finding are given in figure 2.14(b,c), respectively. This structure resembles a configuration of two half-cylindrical Tensegrities fused together.

Another cubic graph family is the hexagonal mesh shown in figure 2.15(a). For the hexagonal topology, there are two different modes of adding struts, as colored by cyan and magenta in figure 5a, respectively. Such hexagonal configuration has been used by Motro (2006) to classify and define the geodesic 'Z' tensegrity system, which always has a spherical shape. Here, nanostructures such as Bucky balls (figure 2.15(b)) and capped carbon nanotubes (figure 2.16(a)) are taken as inspirations. After adding struts and form-finding, it is possible to construct not only spherical structures resembling a Bucky ball but also tubular structures like a carbon nanotube, as shown in figure 2.15(c) and 2.16(b), respectively.
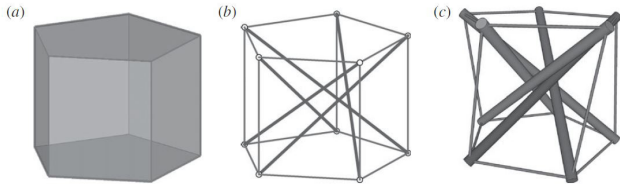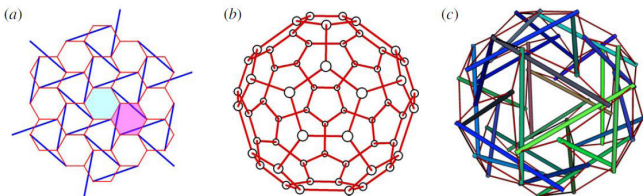
2.13. Construction of Z-based tensegrity based on a pentagonal prism. (a) The topology of a pentagonal prism (b) The topology of the pentaplex tensegrity prism (c) The form-finding result of the pentaplex tensegrity prism
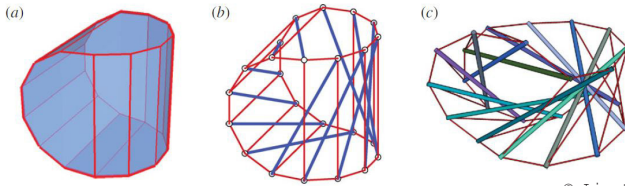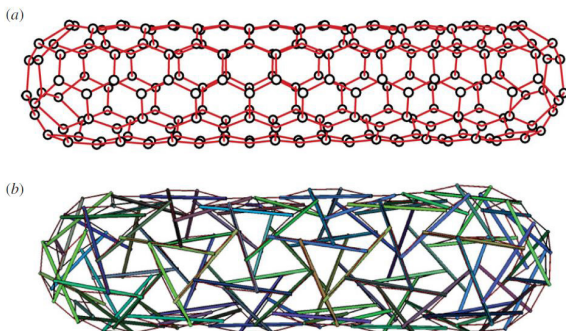

2.14. Construction of Z-based tensegrity based on a sphericon-like polyhedron. (a) The topology of a sphericon-like polyhedron assembled by two perpendicular half-prisms (b) The topology of struts (c) The form-finding result

2.15. Construction of Z-based Bucky ball tensegrity. (a) A hexagonal mesh. There are two different modes of adding struts, which are colored by cyan and magenta, respectively (b) The topology of C_{60} Bucky ball (c) The form-finding result

2.16. Construction of Z-based tensegrity resembling a capped carbon nanotube. (a) The topology of a capped (5,5) carbon nanotube (b) The form-finding result

2.5. Further Developments

By now it may be apparent that there are more Tensegrity systems than could be described in this research. This part describes various methods by which further systems can be evolved, and gives brief descriptions of a few families of figures which have not been mentioned previously.

Four Methods of Evolving New Tensegrity Systems

One way of evolving new figures is to define a new concept of Tensegrity or to modify an existing idea. For example, it might be possible to find a different interpretation of the soap bubble analogy.

A second method is to discover a new relationship between struts and cables. There are several ways of doing it, as will be suggested later.

A third method, will be discussed in detail later on, is to discover or develop new polyhedral figures which can be used as bases for Tensegrity systems using an already established relationship between struts and cables.

A fourth method is to extend an existing idea or figure.

New Relationship between Struts and Cables

According to Pugh, there are several ways of discovering new relationships between struts and cables, the first being to interpret the relationship between the struts and cables of an existing figure in a different way. For example, the expanded octahedron could be regarded as a figure composed of six struts, each of which is surrounded by a diamond arrangement of cables. Alternatively, the same system could be regarded as a figure composed of six struts which are contained by eight triangles of cables. Though this new description of the relationship does not produce further figures, in this case, it does illustrate the general idea.

Another method of evolving a new relationship between struts and cables is to manipulate the struts and cables of an existing figure until a new pattern is produced. A good example of this method appears in the truncated tetrahedron, with its zigzag arrangement of struts and cables, is evolved from the expanded octahedron, with its diamond patterns of struts and cables.

A final approach is to consider the various ways in which struts and cables can be related to each other. For example, most of the systems described have had a strut on the other side of each strut. In the diamond-pattern systems, they were directly opposite one another, and in zigzag-pattern systems they were staggered. Since there must be a strut end on the other side of each strut, so that its cables can be fixed to something, then the only other possibility would appear to be to have more than one strut on one or both sides.

All the relationships shown so far have had single struts suspended in space or joined end-to-end in circuits. Other relationships could be established by joining more than two strut ends together and then creating stable configurations by adding components.

Basing Tensegrity Systems on Other Polyhedra

Perhaps the easiest way of evolving further Tensegrity systems is to find additional polyhedra which can be used as bases for such figures. Further polyhedra often are found in various publications or evolved from one's own studies. In the latter case, a background knowledge of polyhedra is invaluable. In this case, a polyhedron is used to determine the approximate configuration of the tensegrity structure in design and obtain the topology of cables by its vertex truncation. The polyhedron is truncated by cutting all its original vertical and creating a new polygonal facet around each vertex. No matter how many edges are connected at a vertex in the original polyhedron, the truncation will make each new vertex having just three edges connected. That is, the new polyhedron is guaranteed to be an appropriate cubic graph for the design of Z-based tensegrity structures. For instance, figure 2.17(a) shows a pyramid, which is originally not a cubic graph because the vertex G has four edges. However, the polyhedron, after truncation, has evidently become a cubic graph with three edges at each vertex.

The truncation method is not convenient in constructing cubic graphs to be used as the topology of cables but also in the addition of struts. We still take the pyramid in figure 2.17(a) as an example. The red lines denote the new edges generated owing to the truncation, named the 'truncating-edge cables', and the magenta lines denote the remaining segment of the edges in the original pyramid,

© Li et al
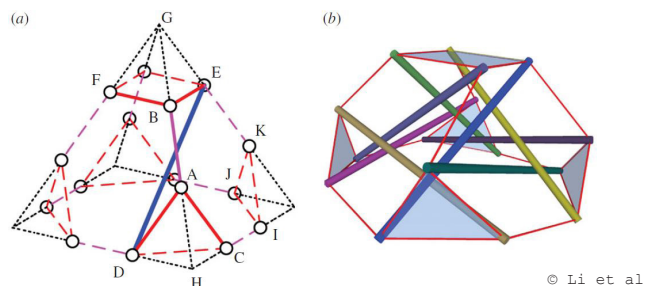
2.17. Construction of Z-based tensegrity from a truncated pyramid. (a) A truncated pyramid. The red lines stand for new edges produced by truncation, the megenta lines stand for the remaining edges of the original pyramid and the blue line stands for the added strut (b) The form-finding result

© Li et al
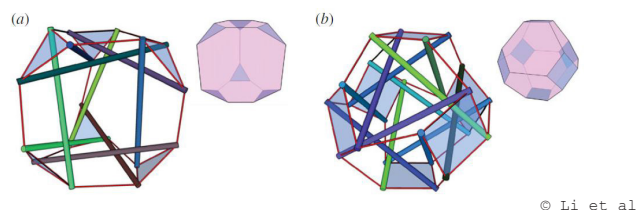
2.18. Construction of Z-based tensegrity from (a) A truncated triplex prism and (b) regular truncated octahedral

© Li et al
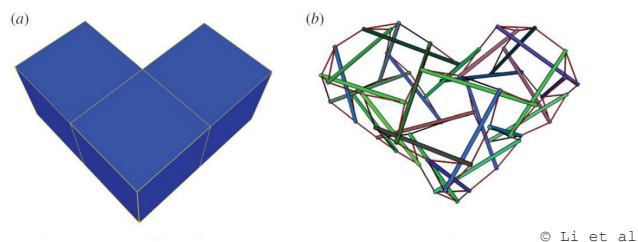
2.19. Construction of Z-based tensegrity from a concave polyhedron (a) A concave shaped polyhedron (b) The form-finding result

called the 'remaining-edge cables'. Once the topology of cables has been obtained, we can add the struts in a truncated polyhedron according to the following two rules:

(i)   Each cell contains only one remaining-edge cable, and this cable must be in the middle of two others;
(ii)   The two nodes of each strut must be on two different polygon faces.

If one adds a strut between D and E as the blue line in figure 2.17(a), the cell containing the next remaining-edge cable CI will be uniquely determined by repeating the same procedure. The final form-finding result of the truncated pyramid tensegrity structure is shown in figure 2.17(b).

Examples

Comparing figure 2.17(a,b), it is seen that the equilibrium configuration of the obtained tensegrity is similar to the shape of a truncated pyramid. Therefore, this method makes it convenient to design tensegrity structures from specific polyhedra. To construct a tensegrity structure with a required configuration, one just needs to choose a polyhedron with a similar shape and to perform the above described manipulation in a canonical manner.

Using the polyhedral truncation scheme, for instance, we have constructed tensegrity structures having the approximate shapes of a truncated triangular prism and a truncated regular octahedron from the corresponding polyhedra. The form-finding results are shown in figure 2.18(a,b), respectively. Similarly, the structure in figure 5c can also be achieved easily by this truncation scheme from an icosahedron.

It is worth pointing out that the truncation method is applicable not only for polyhedra, but one can also use this scheme to design tensegrity structures of many other different shapes, e.g. concave polyhedron shapes. As an example, figure 11a shows a concave polyhedron, which then leads to a heart-shaped tensegrity, as shown in figure 2.19(b).

2.6. Constructing Physical Models of based on the Outputs of Digital Models

A proper understanding of Tensegrity can only be gained by building and studying models of the figures. Depending on the type of tensegrity models, the different methods are applied, there is no method especially in favor. However, with large and complex model of tensegrity structures, it is recommended that one should build the model bottom-up, and one by one at a time, in the end the finished model will be achieved and minor adjustments can be added. The physical model techniques presented in this thesis represents the combination of cutting-edge technology and the craftsmanship of low-tech construction.

Nowadays tensegrity structures are still designed in a way that purely based on physical models or mathematical complexity. From the beginning of the design process, designers would use all struts with the same length and approximate the length of rubber bands based on the elastic performance of these bands. This way limited the development of tensegrity structures enormously because the figure achieved in the end may be a different version of what the designer expected. The other way is that designers would use complex mathematical equations and computations to solve the geometrical complexity of tensegrity to figure the exact lengths of structural elements in such the system. This way demands very high background knowledge of mathematics which is normally not applicable for most of designers who think visually.

The method I propose is that by studying some principles of the topology of tensegrity structures, the relationships between struts and cables, one could make easily the 3d model in a computer program, Rhinoceros for example, and export all the information, lengths of structural elements, structural topology and geometry, from this digital model to build the physical ones. There is always a need to check between the computational result and physical model because having a tensegrity on the screen does not mean that it can stand stably in reality. This seems similar to the way of checking back and forth between hand calculation and computational results because it is very easy to come up with a mistake in the computer or the process simulated in the software does not match with what happens in reality.

In reality, one needs to pay attention that the length of the cable will be slightly shorter than the length in the digital model to provide pre-stress forces to the cables. One could make the fastening system for every single cable

and adjust after finishing the construction of the whole model. But this way is very time-consuming and not very practical for such a small scale model of tensegrity. Also without pre-stress from the beginning, a tensegrity structure cannot achieve its equilibrium state. So I would suggest that making a 3D digital model is a necessary condition, and building a physical one is a sufficient condition to have a successful tensegrity design.

It is best to creat a model in two stages. In the first stage a set of rough 'working' struts and cables is assembled, to form a crude model of the figure. In the second stage, the struts and cables of that model are replaced, one at a time, by better component, to complete the model. Though this may appear time-consuming, it is actually quicker and results in much more accurate models than if the final version were built straight away.

Most of the simple tensegrity figures described in this thesis are based on polyhedra or prism, and it is useful to be able to refer to a model of the appropriate polyhedron when constructing a model. Larger and more complex models are the combination or multiple of one or several types of simple tensegrity figures.

Struts

One of the best materials for struts is dowel – long, circular wooden rods which can be bought at many hardware stores, hobby shops, and stationary shops.
Dowel 3-5mm in diameter is suitable for most models. Because dowel is a natural material, so its properties are not guaranteed. In additional, one should select lengths which are as straight as possible, as bent dowel often has a grain which is not straight and so many splits when being loaded. Also if they are not straight, bending moment will be created within the system, which will cause the impurity of the system.
Dowel usually comes in 1m lengths, so each length can be cut with a knife to provide several struts following the length given by the digital models. At two ends of one strut, there is 5mm extra in length as the space for fitting the cables. The ones, which are shorter or longer than this range, are difficult to handle by human hands.

Fitting Cables

As mentioned above, while cutting the struts, one should pay attention to cut
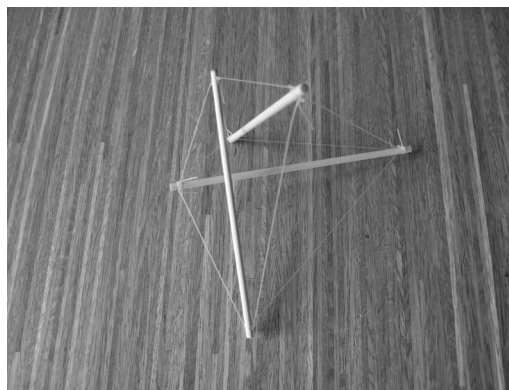
2.20. The simplex
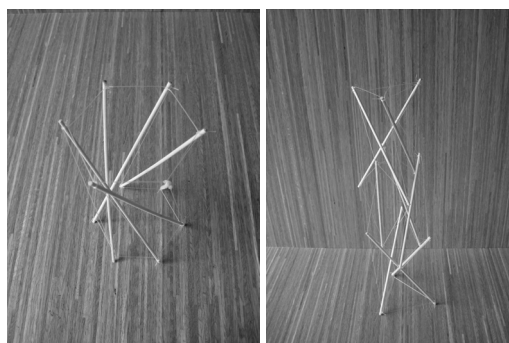
2.21. A hexagonal cylindrical tensegrity and A tensegrity column
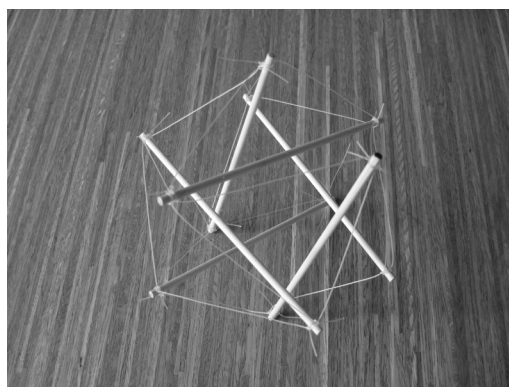
2.22. Icosahedral tensegrity
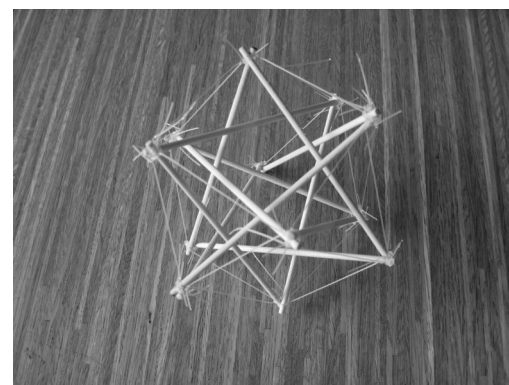
2.23. Dodecagonal tensegrity

extra 5mm at each end of the stick to leave space to fit cables. The other side of a knife is used to make a convex ring at two ends to keep the cable knots in places that it will not slip along the strut. By doing this, it helps to prevent of splitting if one driving a nail into a strut.

Also, all joints in a tensegrity system are pin-jointed nodes. By using a knotting technique, it makes the joints becoming very flexible and can be well-considered pin-jointed connections.

Cables

The best cable material I have found is braided nylon fishing line can be easily found in every fishing shop in town. A line with a breaking strength of 10 kg is stiff enough for most models. They are slender, transparent and very lightweight.
One of the main advantages of a nylon line is that it is slightly elastic, but not over-elastic, so it can be tied very tightly to produce high tensioned models. The slight elasticity helps take up the inevitable inaccuracies; if the cables are inelastic and one cable slightly too long, the figure would be slack and look very untidy. The fishing line can return to its original length after it has been loaded as well. In fact, I always make the cables shorter than the lengths from digital models to give it slightly more pre-stress, so in the end, the figure will be better self-equilibrium.

Tying the Cables

When one started tying the cables, one should cut the fishing lines as few times as possible. This way will save time, as each time the line is cut, its ends must be tied securely to prevent their coming undone. A lot of time can be also saved if the cables are tied with simple loops formed by thumb knots and half hitches. Though fancier knots can be used, they take longer to tie and are no more efficient.

Once the line has been fastened to the strut, a cable can be measured and tied to the next strut. Rather than measure each length with a ruler, it is quicker to cut a measuring stick of an appropriate length from a waste piece of dowel and measure each cable against it. This saves all the time involved in trying to read the calibrations on a ruler.

There are several points concerning the length of the cables. The first is that it is important to measure all the cables when they are pulled tight and to measure every length at about that same tension. The second point is that as one builds, allowances must be made for the elasticity of cables; otherwise, a very floppy model will result. Often, especially with a large figure, it may appear that the cables are much too short and that the saucer-shaped figure being produced cannot possibly become spherical. However, it is important not to try to compensate by tying the rest of the cables slightly longer. The rest of the cables should be tied the same length. When the figure is complete, they will all stretch equally to produce a spherical model.

Since so many hinges on the degree of model-making accuracy and on the stretching quality of fishing line, one of the best ways of finding out how long to tie the cables is by the experience of building models. The lessons gained from one model can be used on the other, related models, even if they are not exactly similar.

The only way to know the lengths of struts and cables is using computational modeling and extract the lengths of these elements from the digital model. For strut cutting, the distance between two convex rings is the same with the lengths from the digital model. The distance from the convex ring to the end is 5 mm. For cable tying, the distances between two knots are always (5 mm) shorter than the lengths of the element from a digital model.

2.7. Geiger's Dome

A number of long span 'Tensegrity' dome type structures have been realized in the previous decade following the inventions of R. Buckminster Fuller (Fuller) and David H. Geiger (Geiger). These structures have demonstrated structural efficiency in many long-span roof applications. While these domes can be covered with a variety of roof systems, all the tensegrity domes built to date have been clad with tensioned membranes. As a consequence of the sparseness of the Cable-dome network, these structures are less than determinate in classical linear terms and have a number of independent mechanisms or inextensional modes of deformation (Pellegrino). In these modes, a load is primarily resisted by changes in the geometry of the tensile network. The relative flexibility of these structures to asymmetric loading has made the use of

tensile membranes for the roof a logical choice.

In 1984 David Geiger developed the idea of the "Cable-dome" and realized for the Sun Coast Dome in St Peterburg, Florida (diameter 210 m). Figure 2.24 shows the dome during construction. This is a lightweight membrane roof supported by a pre-stressed cable-and-strut structure that was invented by David Geiger (Geiger, Stefaniuk, and Chen 1986). Geiger's structure was a successful, practical realization of an earlier tensegrity dome concept invented by Buckminster Fuller (1964).

The cable-and-strut structure consists of 24 radial cable-and-strut trusses, which are pre-stressed by four cable hoops, two inner tension rings, and a perimeter compression ring. Each of the radial trusses, see figure 2.25 for nomenclature details, consists of a ridge cable that connects the top tension ring to the perimeter, of 5 vertical struts and five diagonal cables, which join the ridge hoops, also the top tension ring to the bottom one. Note that the cable hoops are connected only to the bottom ends of the struts.

The concept of the supporting structure for this dome is best explained with reference to the smaller version shown in figure 2.25 following Pellegrino's explaination. This dome consists of only twenty-four cable segments and eight struts.

Structural Behavior

In figure 2.26, it will now be shown that s = 1 for this structure. A radical, taken in isolation from the rest of the dome, is in equilibrium if two forces of magnitude √2 are applied at joints 1 and 5, and a force of magnitude 2√2 is applied at joint 13, all forces act radically inwards, as shown in figure 2.26. This loading induces tensile forces of magnitude √3 in the ridge element 1-9 and the diagonal element 5-9, and of magnitude 2√3 in 9-17 and 13-17. It also induces compressive forces in the vertical elements 1-5 and 9-13, respectively of magnitude 1 and 2. A similar set of three radical forces can be applied to the other three beams in the dome. Now, turning to the two tension rings and the hoop, we note that they are in equilibrium if radical forces of equal magnitude are applied at each corner: outward forces of magnitude √2 would induce tensile forces of magnitude 1

© Geiger Engineers

2.24. Sun Coast dome during construction

© Miura + Pellegrino

2.25. Small-scale version of structure of Sun Coast dome
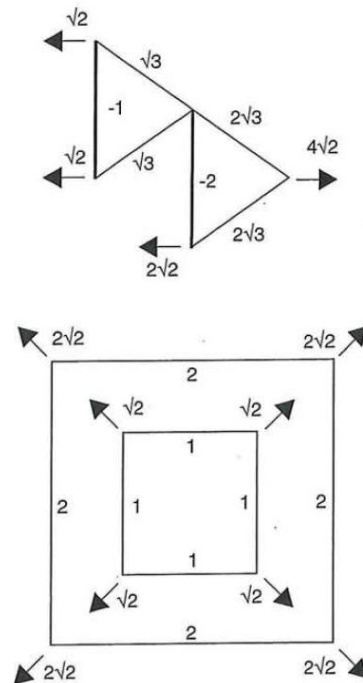
© Miura + Pellegrino

2.26. State of self-stress

20
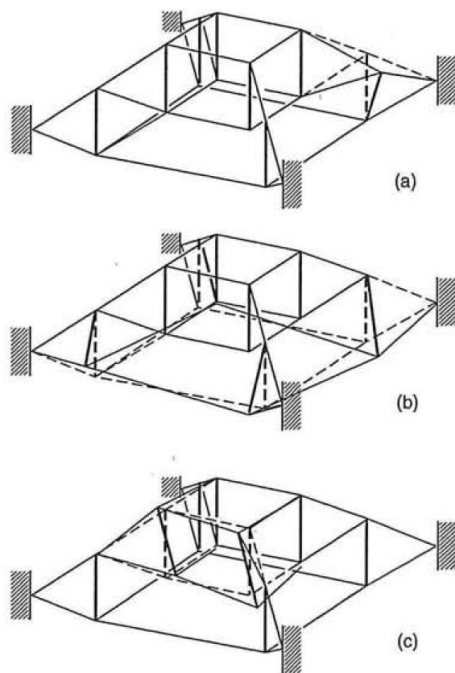
2.27. Mechanisms of the simple dome

2.28. Physical model of the simple dome

in the hoops, etc., figure 2.26. However, these external forces can be transmitted by the joints between the beams, the rings and the hoop, and therefore the set of axial forces obtained above is in equilibrium without any external loads. Having found one state of self-stress for the structure, it is natural to ask whether any more independent states of self-stress can be generated by a similar process. For equilibrium of the rings and the hoop, all states of self-stress must be 4-fold rotationally symmetric. In addition, the forces applied to each radical truss can only be radical and in the ration 1:1:2, or in-plane equilibrium would be violated. With these constraints, there is only one independent solution, for zero external forces.

For $s = 1$, $m = 13$, Pellegrino classified these mechanisms into following four groups:

- Out-of-plane displacement of the mid-ridge joints. There are four independent mechanisms of this type, which involve displacements of joints 9, 10, 11, 12. For instance, in one of these four mechanisms:
- joint 9 moves by equal amounts in the direction x and −y.
- Rotation of the two tensions and the hoop about the z-axis, see figure 2.27. These three mechanisms are independent.
- In-plane distortion of the square 'four-strut' links formed by two corresponding elements of the top and bottom inner rings, and the two struts which connect them. The four joints at the corner of the square move in a diagonal direction, alternatively in and out as shown in figure 2.27.

Although the dome contains four different square 'four-strut' links, only (any) three mechanisms of this type are independent. The fourth mechanism can be obtained as a linear combination of the other three mechanisms in this set, and of the two ring rotations in the previous set.

- Global mechanism, such as a rigid-body rotation of the prism formed by the inner rings and the four struts joining them, about any horizontal axis through the centre of the prism.

2.8. La Plata Stadium

La Plata, in Buenos Aires, Argentina, is a 53,000-seat capacity stadium originally opened in 2003, is formed from the intersection of two 85 m circles, with 48 m between their two centers. Designed
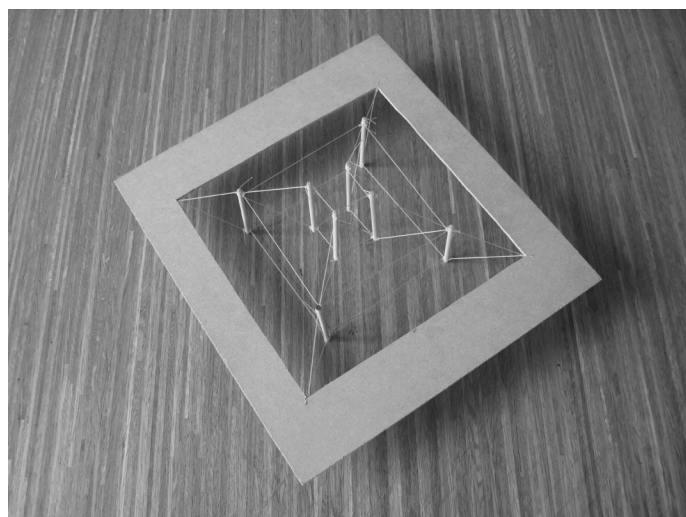
by architect Roberto Ferreira, the stadium is receiving a 29,036 m^2 tensile roof featuring Birdair's steel cable systems and PTFE, a Teflon®-coated woven fiberglass membrane. Around the perimeter is the octet steel tube compression ring consisting of 45 octahedron/tetrahedron modules, forming a load bearing ring that will support the roof. The top chords of this ring are the starting line for a dome formed by a triangulated cable network. The system features tensioned steel cable hoops at three different levels, together with vertical columns, diagonal cables, and ridge cables, thus deploying a tensegrity design. True to its tensegrity deployment, PTFE panels will be added as cladding, and will not play a supporting function; they will float in the tensegrity structure, pulled stiff in the same way that a drum head is tautened.

© estadiolp.gba.gov.ar

2.29. The tensegrity roof of La Plata stadium

Chapter 3. Computational Design of Tensegrity Systems for Large-span Structures

This chapter is a collective of several discoveries done using computational tools, specifically: Rhino+Grasshopper, two associative parametric 3D modeling programs, and Oasys GSA, a structural finite elements analysis (FEA) software. Several experiments on structural design are conducted to develop the idea on how to use computational structural design at the beginning of the design process.

The purpose is to investigate the use of computational structural tools for designers. During the process of investigation a variety methods, the way in which a designer interacts with the model were explored. This is only the modest part of the wide range of possibilities that can be done.

Combining computational design and structural design brings several advantages. It is a reduction of the workload when analyzing multiple and complex models. While traditionally one would have to export the geometry of the structure to FEM software and then add structural properties to the geometrical model; this step has become obsolete: the structural data (beams, nodes, loads, constraints) have become part of the computational model.

The combination of structural design and computational tools also allows for direct feedback on the model in the very early stage of design to show whether or not the proposed design alternative is feasible. This supports a concept that it is possible to obtain more information about the structural performance in early stages of the design when all design goals are still vague. Exploring this possibility can give the power to a designer to be aware of the possibilities and impossibilities of the design and to make informed decisions on choosing design directions. In a way, the method helps to bring back the position of a master-builder in the computational era of 21st century.

Computational Modeling

+GEOMETRYGYM

Form-finding and Structural Analysis

3.1. Programs in use

```
STRUCTURAL TOPOLOGY + GEOMETRY
          TESSELLATION
                              (0)


    GEOMETRIC COMPUTATIONAL MODEL
                              (1)


   PHYSICAL MODEL        STRUCTURAL MODEL
            (2.1)                   (2.2)


        COMPARING STRUCTURAL
             BEHAVIORS
                              (3)


              SIMILAR
             STRUCTURAL          NO
             BEHAVIORS


                 YES


         COMPUTATIONAL
        FORM-FINDING METHOD
                              (4)

   NO

             EXPECTED FORM


                 YES


         STRUCTURAL ANALYSIS
                              (5)


          ANALYSIS RESULTS
                              (6)
```

———— manual

———— digital

3.2. Design method

24
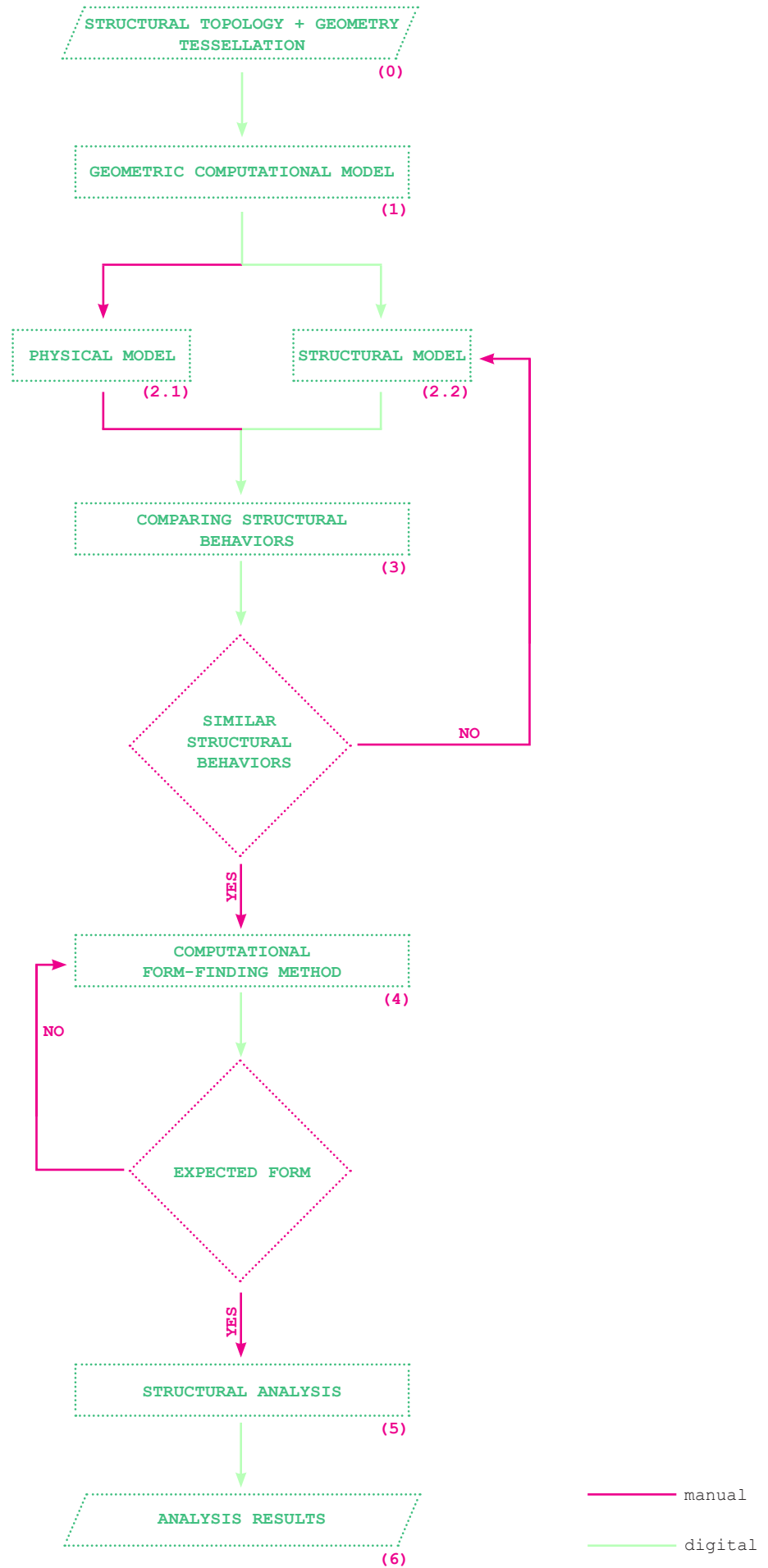
3.1. A Design Method

This section is a summary of the design method for a computational and structural model of complex tensegrity structures using Rhinoceros, Grasshopper and Oasys GSA in combination. The implementation of the workflow is shown by these steps in diagram 3.2 which identifies several stages in the construction of a computational structural model. Sometimes, it costs a enormous amount of time to go back and forth within options before figuring out the appropriate way to go.

(1) Geometric Computational Model

Acquiring topological and geometrical knowledge about tensegrity structures (0), one can start design some simple alternatives with a smooth surface as the starting point. This simple surface can always be simplified to a rectangular shape with u, v divisions which can be built on a quadrangular grid of vertices. One needs to transform this surface into a tessellation of singe-surface tensegrity and then double-surface tensegrity systems having networks of struts and cables spatially articulated (will be explained in detail later on). A new computational method of constructing double-surface tensegrity systems will be extensively discussed in this chapter.

(2.1) Building Physical Model

By taking information of element dimensions from a geometric computational model (1), one can build a physical model to see if the designed tensegrity works in reality with the real influence of gravity. Understanding behaviors of tensegrity structures through the real models remains the best way to study such a complex structural system.

(2.2) Build Structural Model

Using GeometryGym - a plugin of Grasshopper, all structural elements (nodes, beams, supports, sectional properties, materials) are defined beforehand in Grasshopper as a parametric model. Then this model is exported to Oasys GSA which is only considered a calculation platform in this case. There is a possibility to even conduct the calculation in Grasshopper, but since structural performances of tensegrity systems are complex, it is better to do it in Oasys GSA.

(3) Comparing structural behavior

One can try to apply some similar load cases (Gravity, Node loading) to both the physical model and structural model to see whether they perform similarly. If the performances are similar (the way they deform), the right form-finding method is achieved. Otherwise, one needs to go back to the structural model and try other form-finding options.

(4) Form-finding

The appropriate form-finding method found in (3) with the option 'ignore form-finding properties' in Oasys GSA together with the right way of applying pre-stress forces to the systems. One can continue to find the expected form which has some similarities with the designed structure in (2).

(5) Structural Analysis

When the expected form is achieved, some more load cases are applied to the model to check its structural performances and stability.

(6) Analysis Results

After all the experimentations, some conclusions on the way of doing will be provided as well as some recommendations for further studies and developments.

3.2. Bucky's Dome with a Central Opening

Bucky's dome and Geiger's dome were investigated previously, and these designs were realized in large-scale projects such as stadium or concert hall. But they are all fully closed domes, without any openings. To achieve a good design for an open-air stadium, it should have a large opening in the center as a typical typology; otherwise, they will become a place for indoor sports which is a different type.

Digital Model

For studying this type of topology, Bucky's design of the dome was taken, and a big opening was added in the center of the dome. This combination forms a new concept of tensegrity for large-span projects. The dome has a span of 80 meters in diameter, and the diameter of the central opening is 40 meters without any interrupting structural elements in the opening. From outside in, there is a large compression ring providing 12 pinned supports for the entire dome. These supports are connected to 12 struts in the next circle with 48 cables. The tops of these struts are connected to 12 struts in the next round with again 48 cables. The logic is continued to the third ring with other 12 struts, and the final ring will be formed by 12 struts connected, one by one. This inner ring is in tension, which means it only needs to be made from cables to bear the forces. But cables are very flexible, and there are a lot of displacements so that the inner ring is made by bar elements to from a stiff circle.

Regarding structural principles of behaviors, the dome performed similarly to Bucky's dome. This can be explained by the similarity of structural composition or structural topology of cables and struts. To simplify, it can also be explained in the way of K. Miura and S. Pellegrino in 'Structural Concepts' for categorizing its state of self-stress and mechanisms.

The dome could be considered constructed from a simple cell which is the combination of one strut, five cables, and four nodes. In total, the system contains 24 struts of 10 meters, 12 struts of 11 meters, 216 cables Ø10 with three different lengths.

Physical Model

The physical model was built pretty much
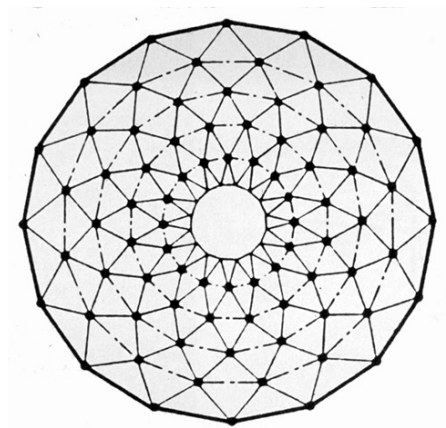
3.3. Bucky's dome, B. Fuller, 1964
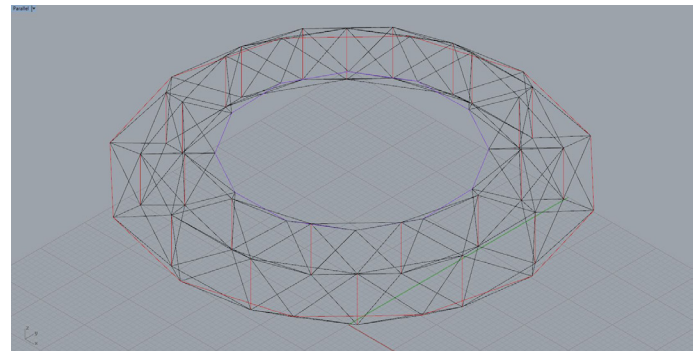
3.4. Digital model of Bucky's dome with a central opening in Rhinoceros
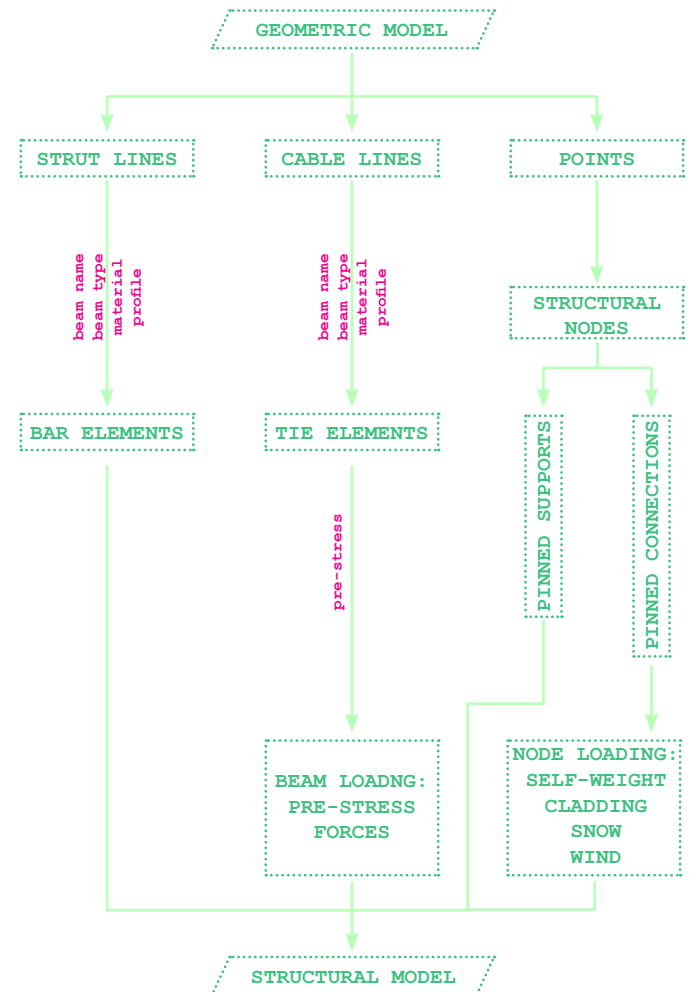
3.5. Generating structural model

(a) Plan of Bucky's dome

Analysing this simple system helps to understand and to figure out the right form-finding method for more complex systems afterward.

After conducting form-finding with option 'ignore form-finding properties' in Oasys GSA, the tops of struts slightly deformed inwards, which is similar to the physical model. So this form-finding technique is the right choice for more complex ones.

Diameter: 80m
opening diameter: 40m
cantilever: 20m
Strut length: 10M
Cable: Ø10MM
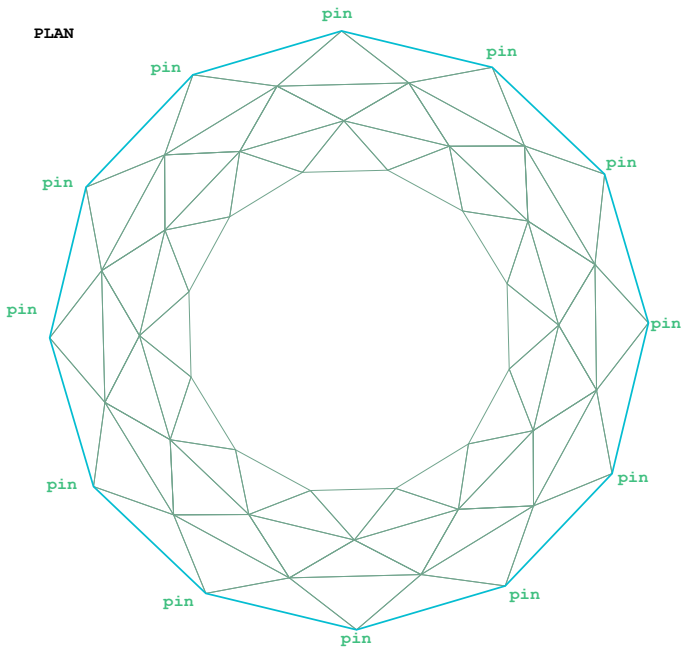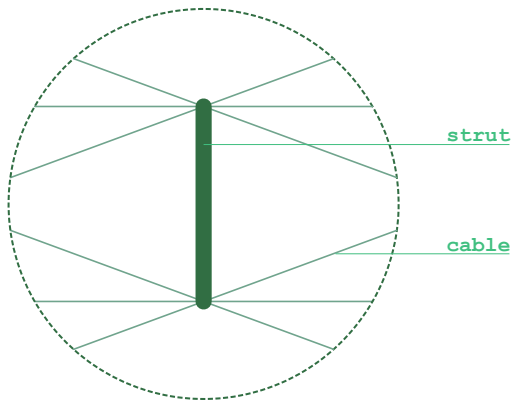
(c) Cell topology
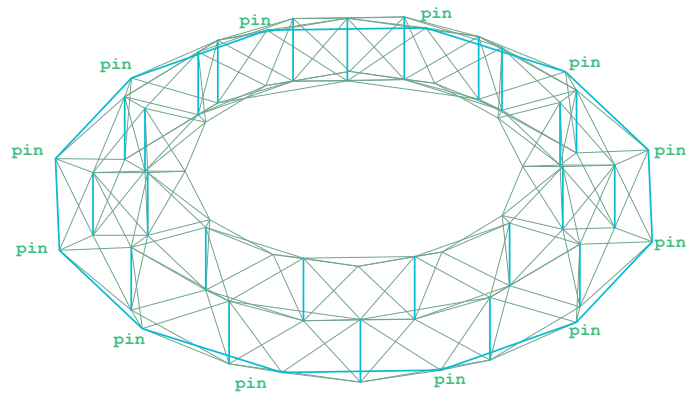
(b) Bucky's dome with a central opening

3.6. Bucky's dome with a central opening
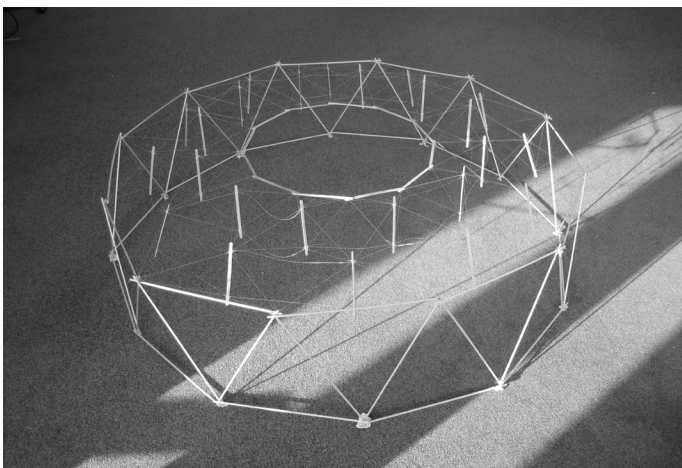
3.7. Physical model
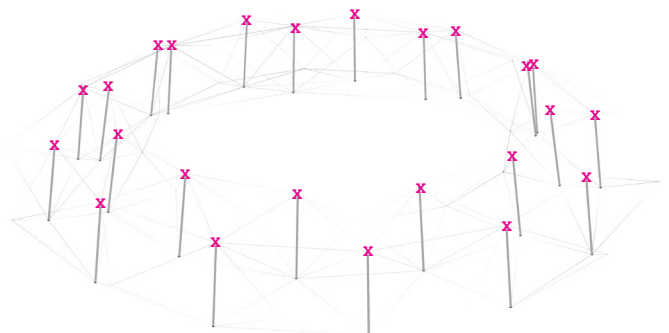
3.8. Form-finding result
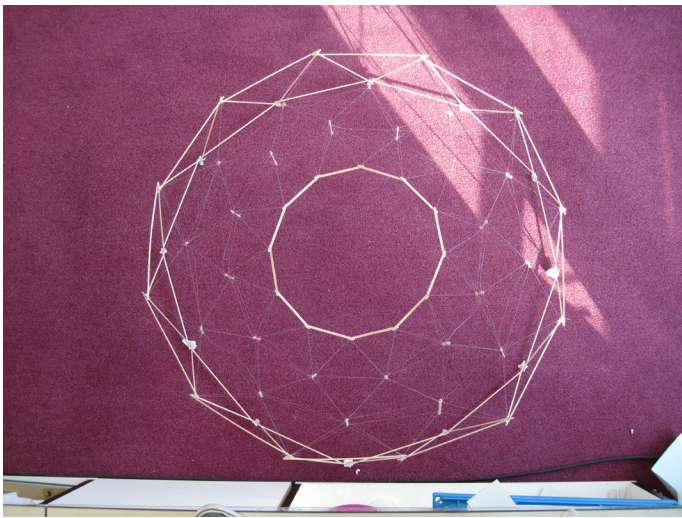
(a)
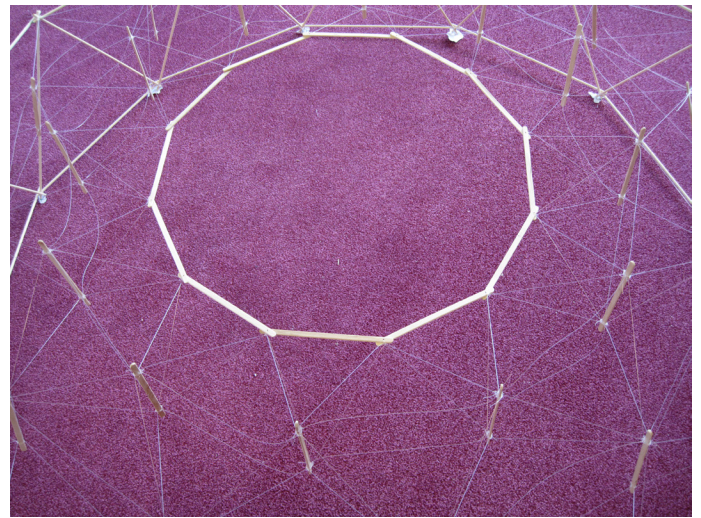
(b)
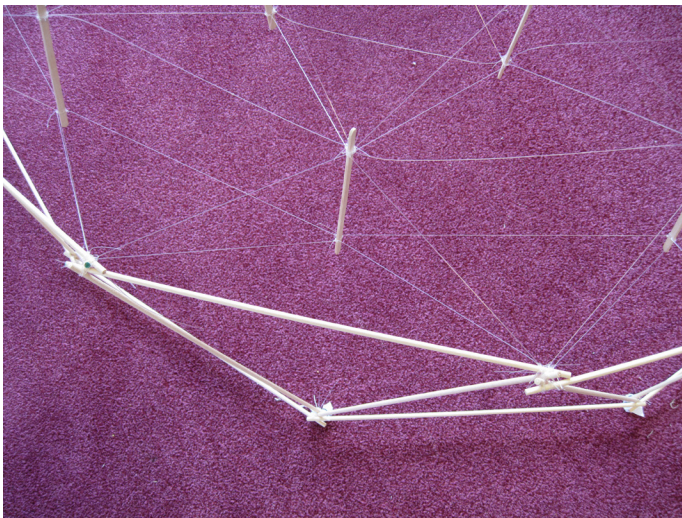
(c)

(d)
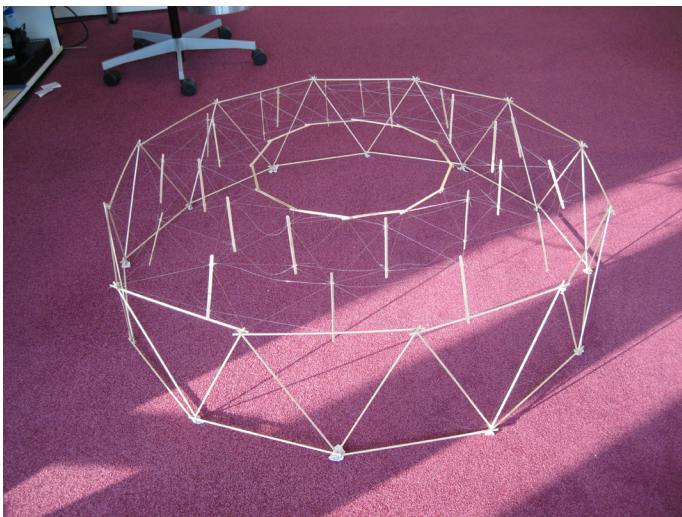
(e)

(f)

3.9. Physical model of Bucky's dome with a central opening
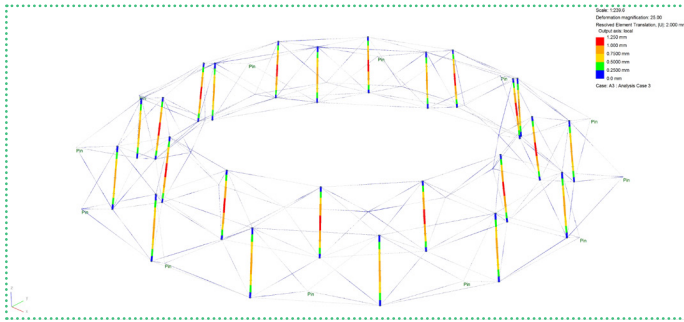
(a) Beam displacements | Max: 1.25mm
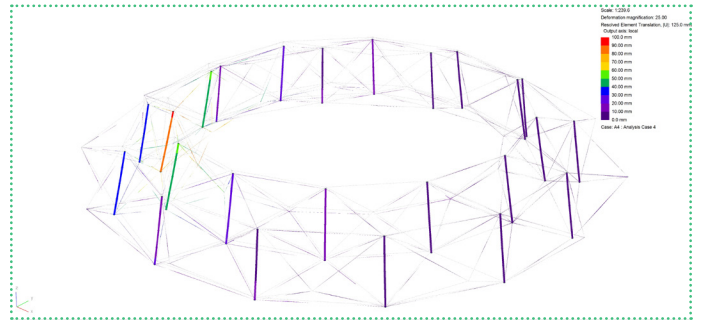
(a) Beam displacements | Max: 100 mm
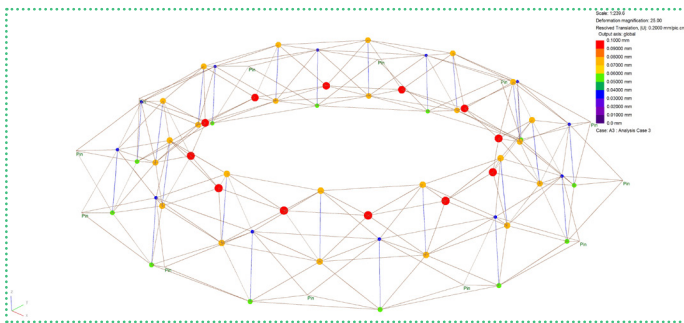
(b) Node displacements | Max: 0.1mm
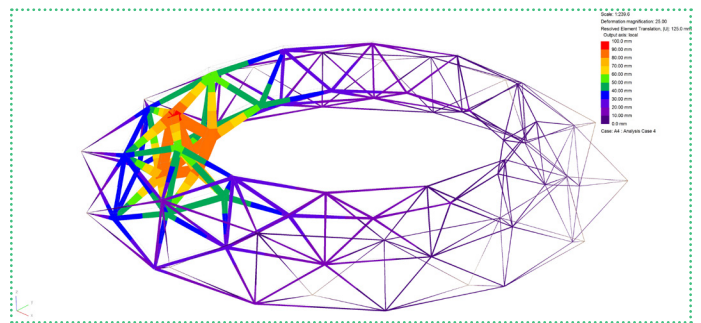
(b) Beam displacements | Max: 100 mm
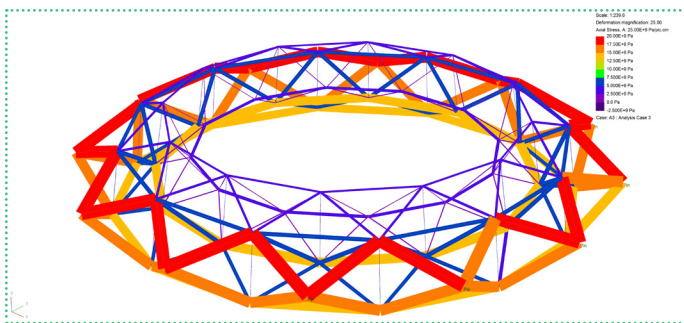
(c) Axial stresses | Max: 20e9 Pa
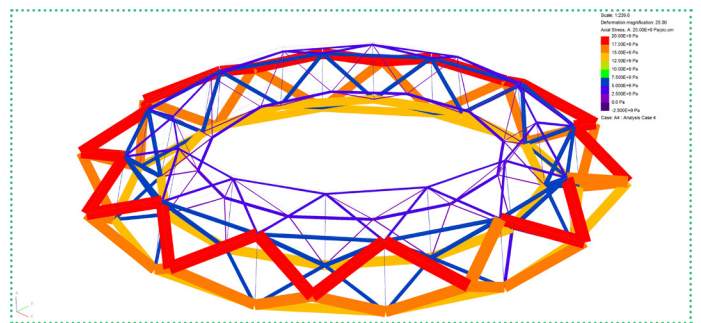
(c) Axial stresses | Max: 20e9 Pa

3.10. Structural performance under Pre-stress forces and Gravity

3.11. Structural performance under Pre-stress forces, Gravity and Node loading
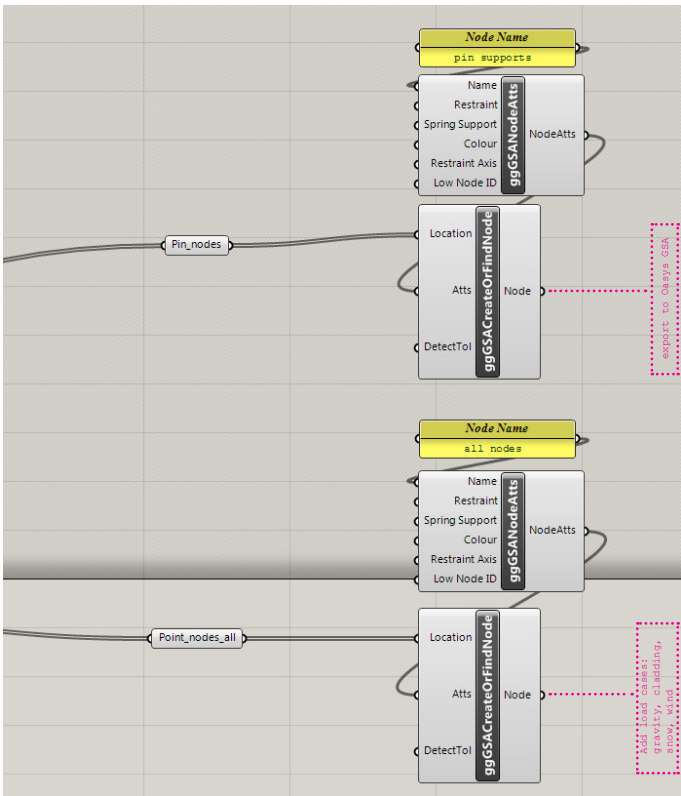
(a) Creating structural nodes and supports
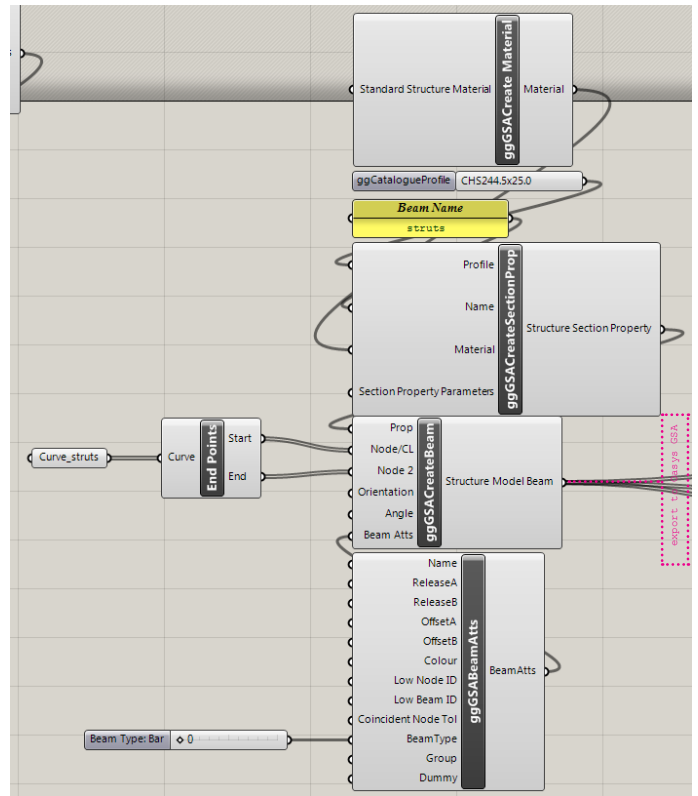
(b) Creating bar element, section, material for struts
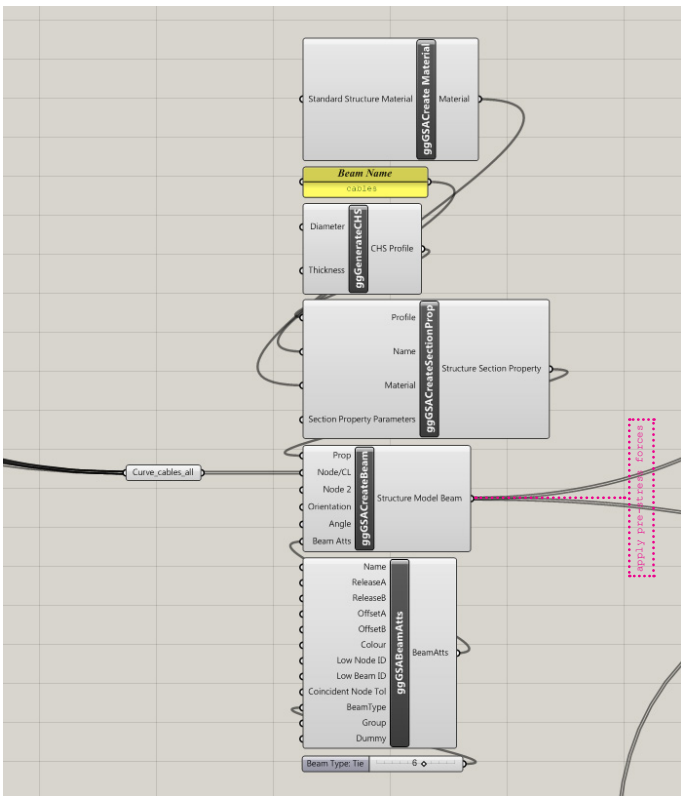
(c) Creating tie element, section, material for cables

(f) Double click this component to export the model
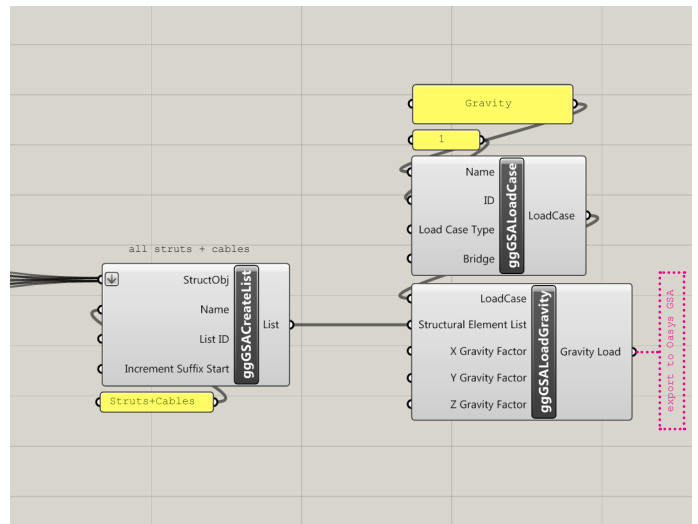
(d) Creating load case: Gravity
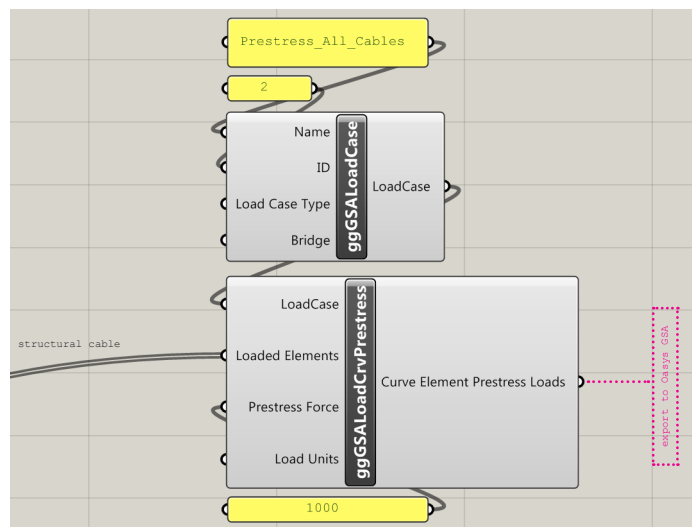
(e) Creating load case: Pre-stress forces in cables

3.12. Building structural model using GeometryGym in Grasshopper

similar to the digital model. There are a number of minor differences. The model has been constructed bottom-up from the compression ring first and then adding struts one by one, from the outer ring to the inner ring. The physical model performed as expected in structural principles following the Geiger's dome analysis of Pellegrino. In the physical model, it is observed that there are a number of cables which are not in loading so they can be removed. But on the other hand, for safety reason, they can stay in case other cables are broken in unexpected situations. The compression is clearly in loading. It can be seen that there are several struts bent (because of buckling, not bending forces, it is all axial forces). All structural members are subjected to axial forces following exactly the principle of tensegrity. No strut touches the others, and they are all floating in the network of cables.

Form-finding

After conducting form-finding with option 'ignore form-finding properties' in Oasys GSA, the tops of struts slightly deformed inwards, which is similar to the physical model. So this form-finding technique is the right choice for more complex ones.

Gravity

There is pure compression in struts and pure tension in cables. The entire structure became very rigid after form-finding, and it mostly works in tension strength. The inner ring deforms the most (0,1mm). From the outer ring to the inner ring, the magnitudes of pre-tensional forces decrease.

Nodal Loading

When a nodal load (-1000kn) is applied, the surrounding areas are affected in all directions. This behavior is also similar to the physical model. The rigidity of tensegrity structures depends on the pre-stress forces in cables that gives the structure the state of self-stress. Soap film and force density method cannot be applicable in this type of tensegrity, only 'ignore form-finding properties' works. This technique takes the deformed shape and internal loading from form-finding as the input for the next analysis.

3.3. Toward New Structural Topology and Geometry of Tensegrity Systems

Re-constructing Z-based Single-surface Tensegrity Structures

To construct Z-based single-surface tensegrity systems based on a polygonal tessellation, one needs to start with a certain polygon in the pattern, and then find adjacent polygons on the initial one. After that, using Z-based elementary cells, one can create a strut by connecting two vertices of two neighboring polygons in a way that it forms Z-shape, figure 3.13. In this method of constructing tensegrity systems, the relationship between the tessellation of cables and struts is critical. One has to define a network of cables beforehand to be able to determine struts by knowing adjacent polygons. Translating this logic directly to programming is challenging.

There is a better way to achieve such the systems. The method is going back to the fundamental of geometry: points. Everything will start from a quadrangular grid of vertices, considering u and v dimensions, in which one can set location (i,j) index pairs to every point. Taking this quadrangular grid as a platform, one can creaet a logic to build a network of cable and various networks of struts independently. In this step, there is no need to relate struts to the cable network. In the end, the pattern of struts will fit perfectly the network of cables, and exactly folloy Z-topology because they are initially defined on the same platform.
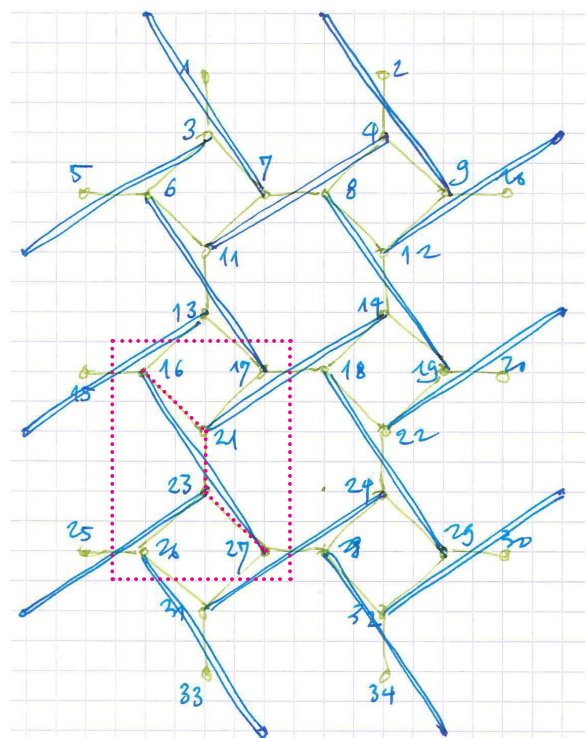
3.13. A network of struts within a network of cables with octagonal pattern, based on Z-topology
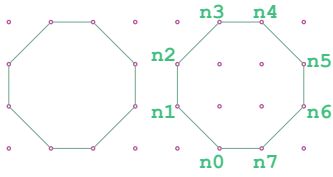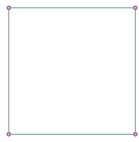
n0 = (i+1, j)
n1 = (i, j+1)
n2 = (i, j+2)
n3 = (i+1, j+3)
n4 = (i+2, j+3)
n5 = (i+3, j+2)
n6 = (i+3, j+1)
n7 = (i+2, j)
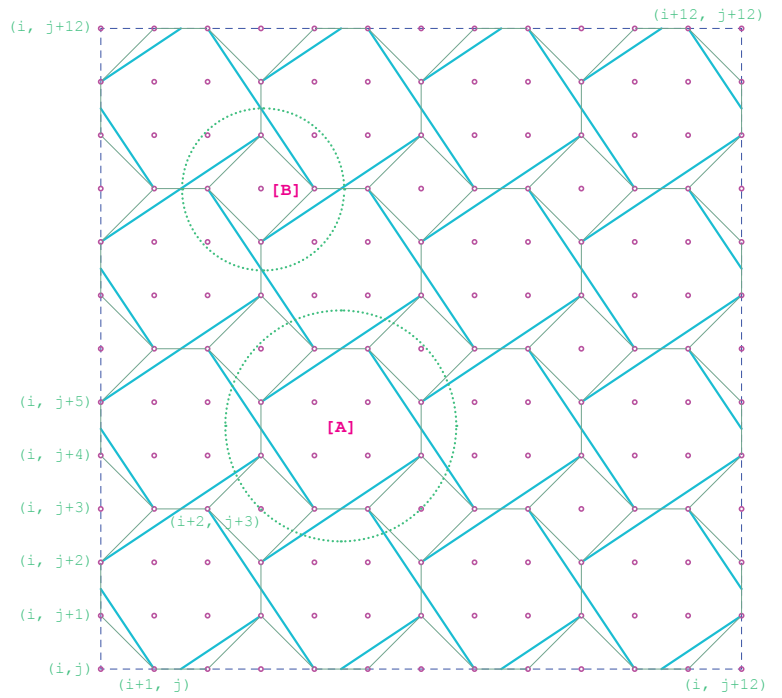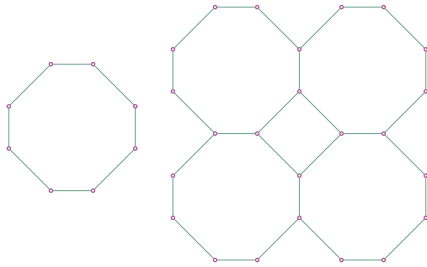
3.14b. Numbering the generic quadriangular grid which is the base for defining the network of struts and network of cables.

3.14a. Tessellation from a generic grid of vertices

n2 = (i, j+2)
n6 = (i+3, j+4)

n0 = (i+4, j)
n4 = (i+2, j+3)
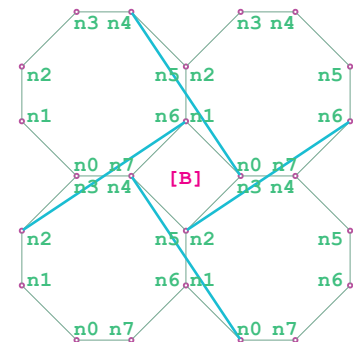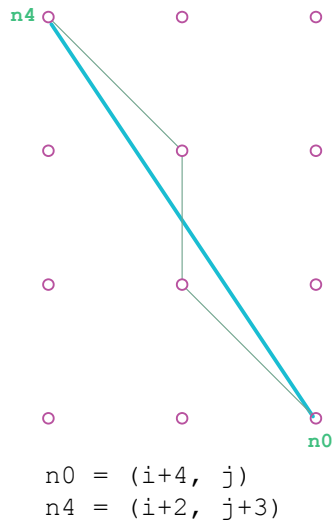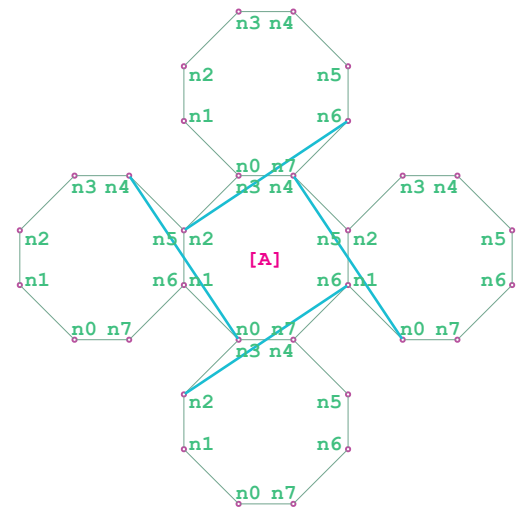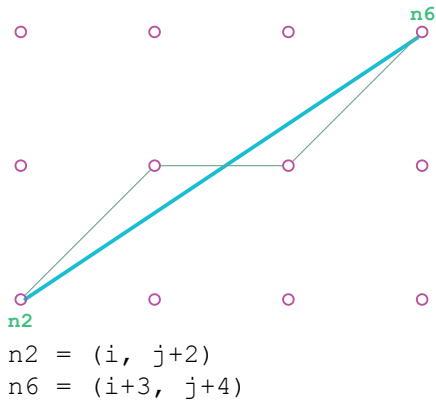
3.15. Procedural descriptions of struts and cables based on generic quadriangular grid

3.16. Two typical compositions of struts around an octagon or a square in the tessellation.
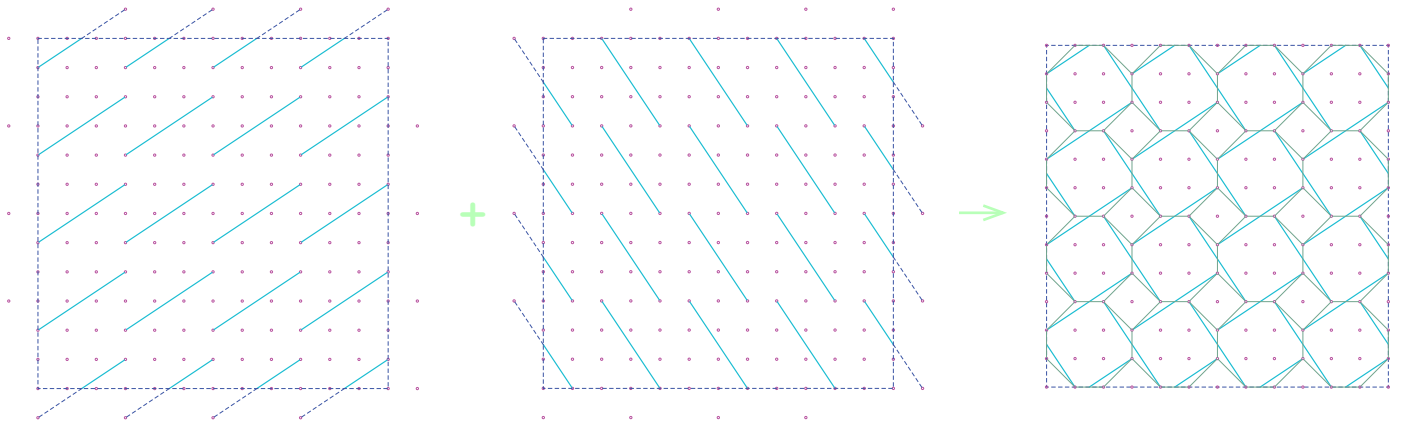
(b) Define the location of strut network on the quadriangular grid

(d) Strut network + cable network
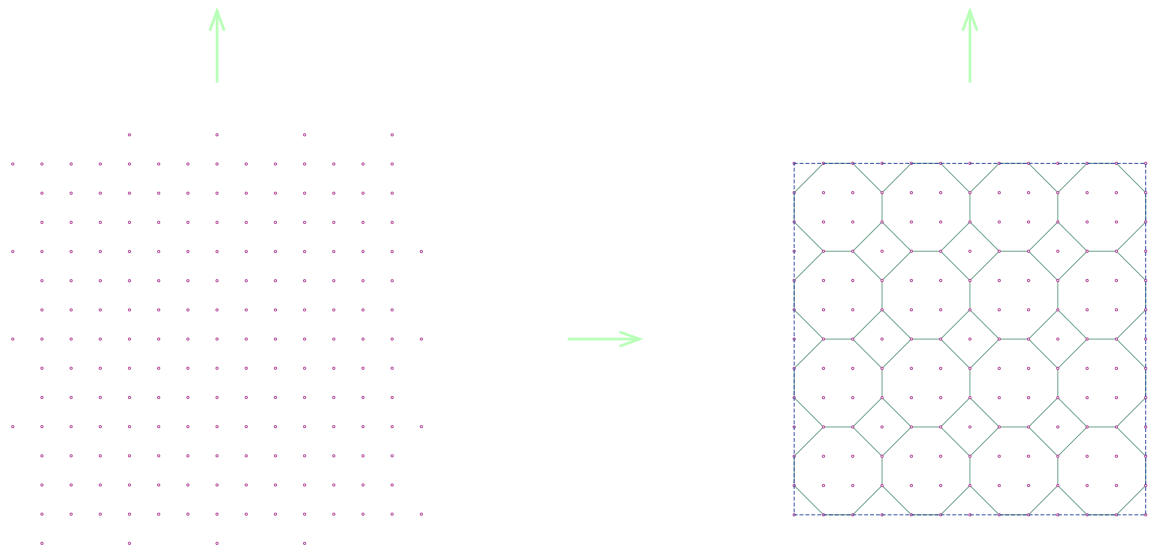
(a) Quadriangular grid based on grid of points

(c) Define the location of cable network on the quadriangular grid

3.17. The network of struts and network of cables are independently defined based on the generic quadrangular grid of points. In the end, they are assembled together to form a single-surface tensegrity structure. There is no need to figure out the z-topology or adjacent hexagons to define strut network which is no longer depending on the network of cable but the generic quadrangular grid.

(b)

(c)

(a)
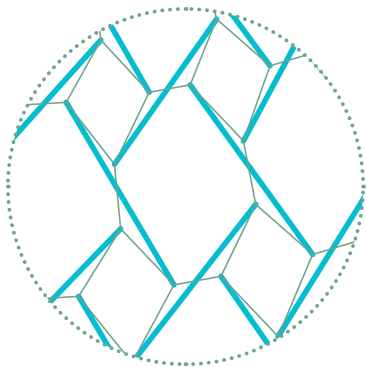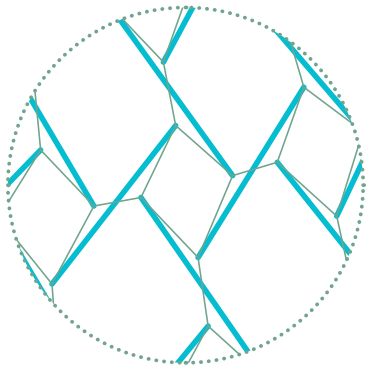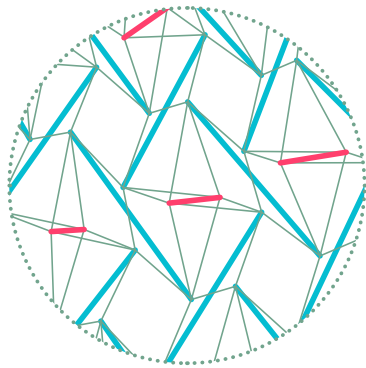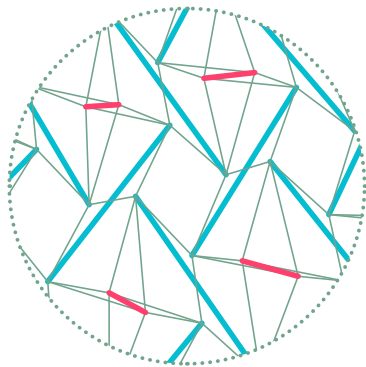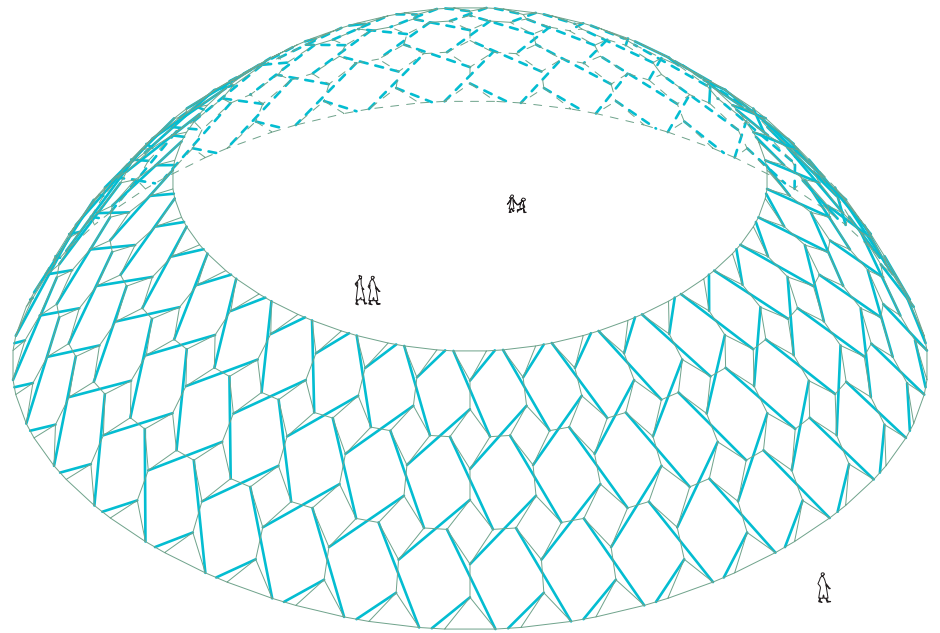
3.18. Tesselatizing and tensegritizing a simple dome with a central opening for an octagonal pattern (8-gon) | Single-surface tensegrity

(b)

(c)
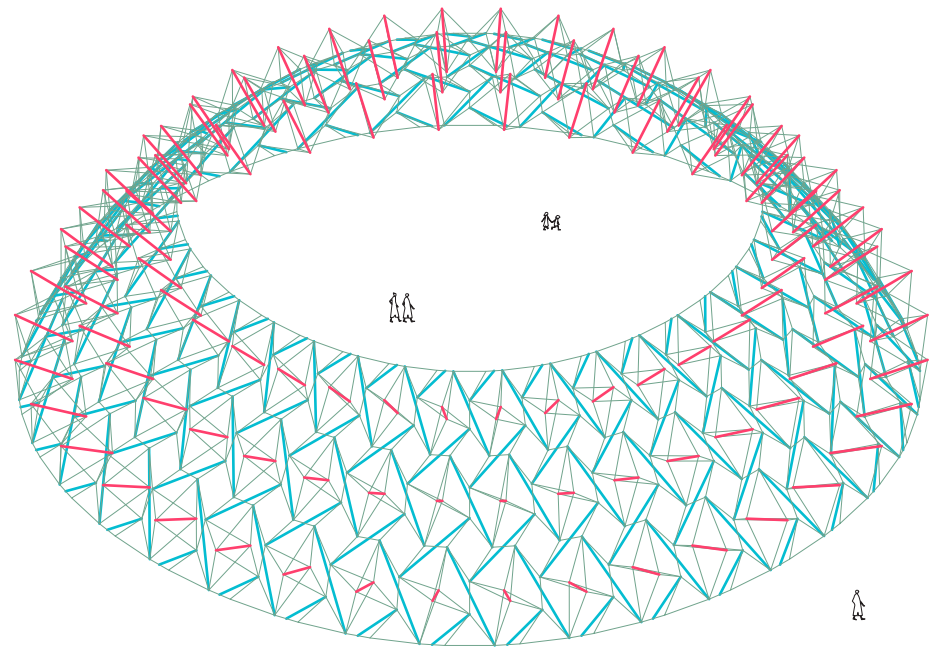
(a)

3.19. Adding normal struts (in pink) in the center of hexagonal cells to increase the thickness of the shell and handle out-plane loading applying to octagonal pattern (8-gon)
The in-plane struts (In blue) remain in the same reference surface extra cables are added to connect normal struts to in-plane struts
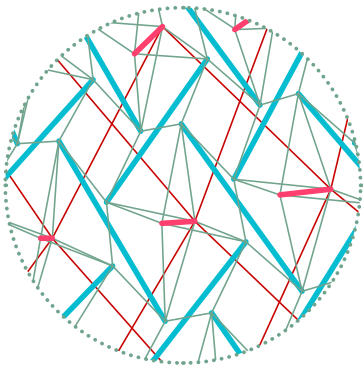
(b)
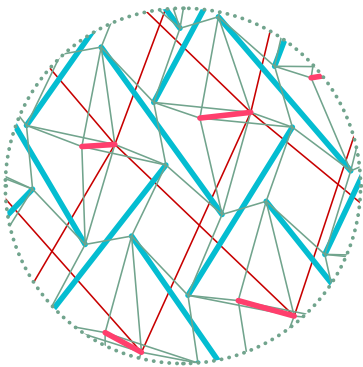
(c)
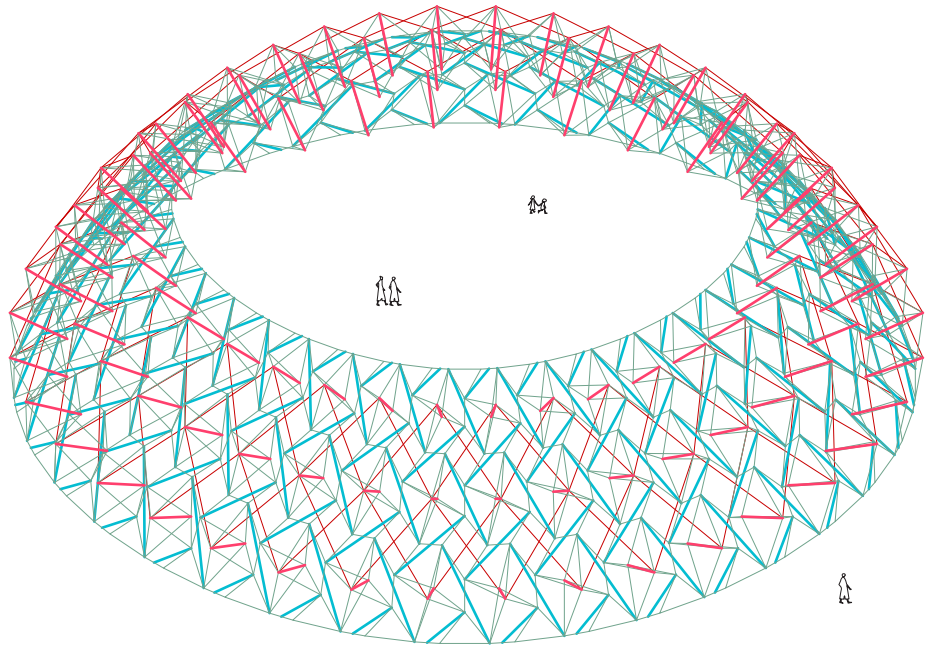
(a)

3.20. Adding outer bracing cables (thin lines in pink) to limit the rotation of pin-jointed connections
Applying to octagonal pattern (8-gon)
These bracing cables connect tops of normal struts in order

Double-surface Tensegrity Structures

As mentioned previously, with one-bar elementary cells, almost all kind of tensegrity systems can be constructed. But actually, this type of tensegrity is only based on one reference surface which is relatively fragile when the structure becomes large and complex because the entire structure almost has no height to handle out-plane loads. To achieve expected structural performance, the shell of tensegrity needs a certain height. One can argue that the height of the structure can be acquired by rotating every strut to make them out of the surface. This way would consume a lot of time, and it is difficult to rotate struts that way since the rotating axis needs to be defined and this axis will keep changing over the spherical (or even free-form) surfaces.

One simple way to add thickness to the system is to add normal struts in the center of n-gonal (hexagonal, octagonal) cells of the above system. In such a tessellation, at the center of every n-gon of the tensegrity shell, a normal strut will be added along with several cables to connect it to the vertices (the ends of struts) of these n-gons. Doing this way helps to increase the thickness of the system, and it performed better in the physical model. But there are two issues of this method. First of all, other struts still stay on a non-height surface, so it does not seem to be strong enough; thicknesses are desired locally in the system. Also because the number of struts is large, they are going to touch each other. So these struts should be made out of the co-surface to be better structurally. This requirement can be achieved by having a tensegrity with two reference surfaces; the second one could be simply the offset of the first reference surface from the one-bar elementary cells system. Using the similar logic of adding struts that Li et al proposed in 'Constructing tensegrity structures from one-bar elementary cells', but instead of staying on the same surface the first end of a strut will be on the first tessellation and then the second end will be the second tessellation. Repeating the logic, an expected space-shell of tensegrity structure will be achieved in the end.

From two reference shells of tessellation, one can build a space-shell of tensegrity structure in another way which is based on cylindrical tensegrity cell, one of the most popular and simplest tensegrity structures so far. Again, one needs to do the offsetting of the first reference of tessellation. When two reference tessellations are achieved, there are several n-gonal cylindrical geometries are automatically created; they are sitting next to each other. With a cylindrical 2n-gon, one can build n-gonal cylindrical tensegrity cells. For example, with a hexagonal cylindrical figure, one can add three struts evenly, or with an octagonal cylindrical figure, one can add four struts evenly to the network of cables, and so on. These cells are not tensegrity by themselves since they have more cables than they need and the topology is not exact for them as independent figures, but as a whole, they can form a very well-performed tensegrity structure.

In summary, there are two types of space-shell tensegrity structures that are based on two reference surfaces of tessellation. The tessellation should be a bridgeless cubic graph. The first one would have struts constructed following Z-based typology; the second one would have struts constructed based on cylindrical tensegrity types. To reinforce these systems, normal struts with extra cables are needed. In the first one, the two reference tessellations will be merged in the end into a single network of cable, the geometry of struts remain spatial. In the latter, the two surfaces of tessellation will stay; some extra cables will be introduced to connect these two separated networks of cables. Struts remain floating in both cases.

With double tensegrity, it is more convenient to locally vary the thickness of the tensegrity space-shell.
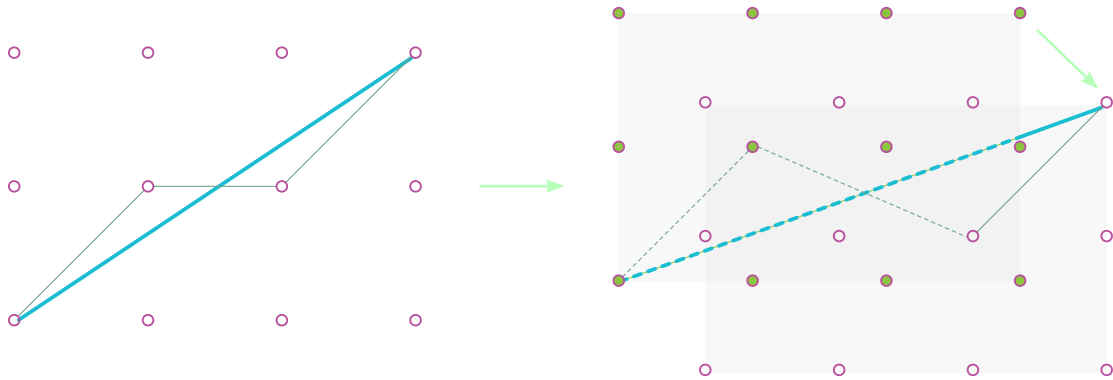
3.21. Based on Z-topology
(Mentioned in previous chapters)

MAKE IT SPATIAL!?
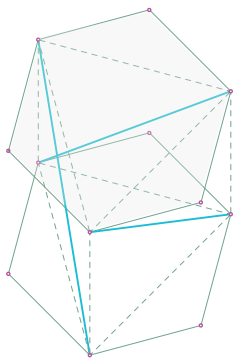
3 struts
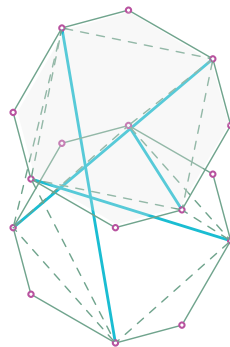
4 struts
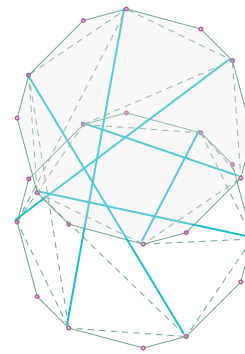
6 struts

3.22. Based on cylindrical tensegrity structures - 2n-gonal tesselation (n>2)
(The most popular tensegrity systems)

Type A: Double-surface tensegrity system based-on Z-topology
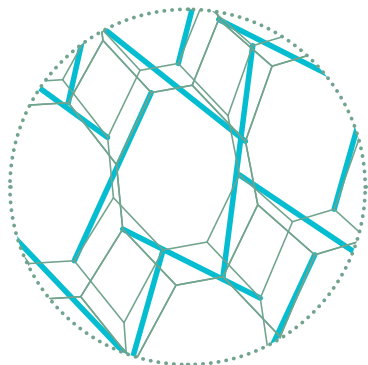
(b)
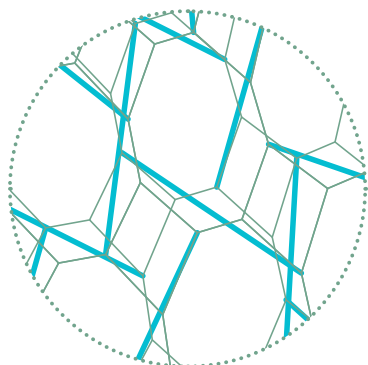
(c)
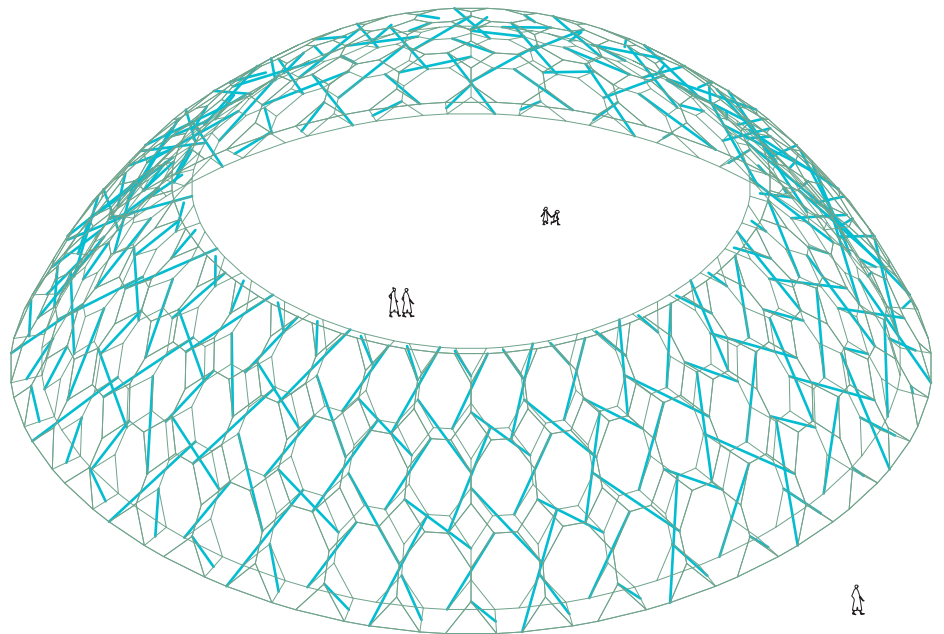
(a)

3.23. Using two reference surfaces with the same way of tessellating applying the method of single-surface tensegrity structures with z-topology, but in this case, two ends of a strut are located on two different surfaces. By doing this, the structure has the thickness, becomes more spatial. And touching between struts is avoided.
In this figure, the tesselation is an octagonal pattern.
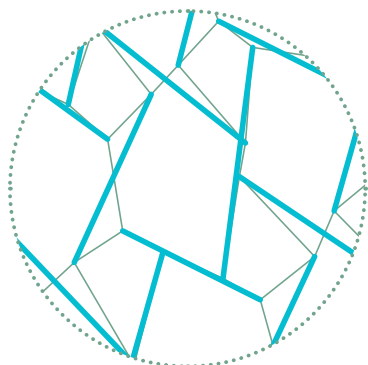
(b)
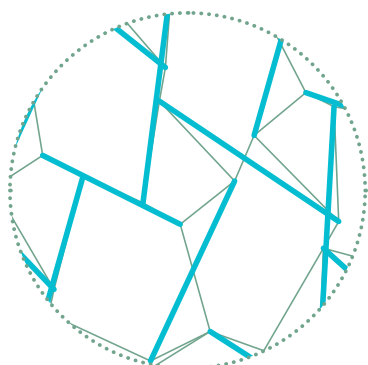
(c)
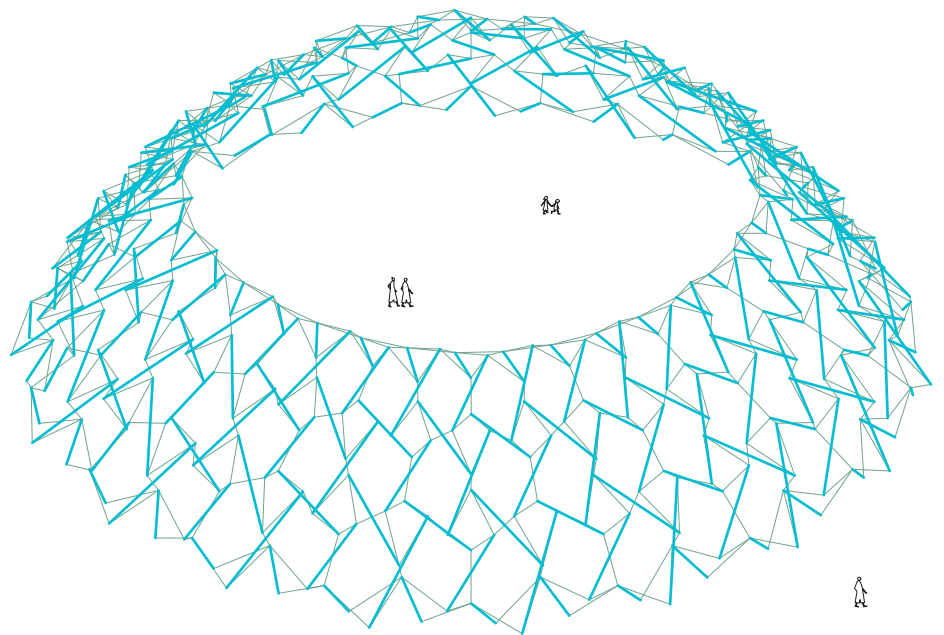
(a)

3.24. After having the network of struts, two reference cable networks are merged into one. In terms of topology, the system becomes similar to single-surface tensegrity structures again, but the geometry is different, and better in structural performance.
In this case, the tessellation is octagonal pattern.

Procedure: Tessellating and tensegritizing of octagonal pattern based on quadrangular grid, Z-topology, type A.
Inputs:
srf #first reference surface
srfx #second reference surface
udiv #u count, udiv % 3 == 0
vdiv #v count, vdiv % 3 == 0
Outputs:
nods #list of structural nodes
cabs #list of lines of cables
stra, strb #list of lines of struts

```
#Define the generic quadrangular grid of vertices which have (u, v) coordinates
for i in range (0, udiv - 2, 3):
    for j in range (0, vdiv - 2, 3):
        n0 = (i/udiv, (j+1)/vdiv, 0)
        n1 = (i/udiv, (j+2)/vdiv, 0)
        n2 = ((i+1)/udiv, (j+3)/vdiv, 0)
        n3 = ((i+2)/udiv, (j+3)/vdiv, 0)
        n4 = ((i+3)/udiv, (j+2)/vdiv, 0)
        n5 = ((i+3)/udiv, (j+1)/vdiv, 0)
        n6 = ((i+2)/udiv, j/vdiv, 0)
        n7 = ((i+1)/udiv, j/vdiv, 0)
        n8 = (i/udiv, (j+1)/vdiv, 0)

#Make the network of vertices to reference surfaces
        Evaluate (n0, n2, n4, n6) on srfx as (newn0,…,newn6)
        Evaluate (n1, n3, n5, n7) on srf as (newn1,…, newn7)
        AddPoint (newn0,…,newn7) to nods

#Define the network of cables or Constructing network of octagons
        AddLine ((newn0, newn1), (newn1, newn2), (newn2, newn3), (newn3, newn4),
(newn4, newn5), (newn5, newn6), (newn7, newn0)) to cabs

#Define the list of struts a
for i in range (0, udiv - 2, 3):
    for j in range (0, vdiv - 2, 3):
        a0 = (i/udiv, (j+2)/vdiv, 0)
        a1 = ((i+3)/udiv, (j+4)/vdiv, 0)
        Define a0 on srf as newa0
        Define a1 on srfx as newa1

        AddLine (newa0, newa1) to stra

#Define the list of struts b
for i in range (0, udiv - 2, 3):
    for j in range (0, vdiv - 2, 3):
        b0 = ((i+2)/udiv, (j+3)/vdiv, 0)
        b1 = ((i+4)/udiv, j/vdiv, 0)
        Define b0 on srf as newb0
        Define b1 on srfx as newb1

        AddLine (newb0, newb1) to strb
```
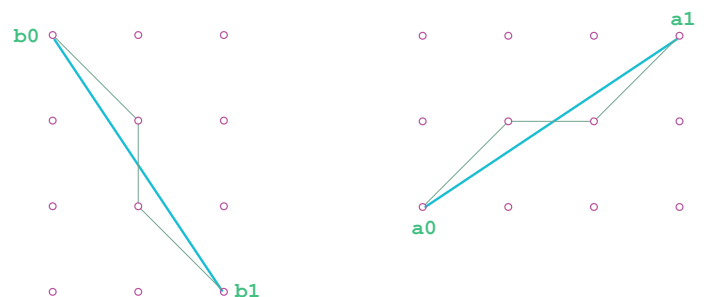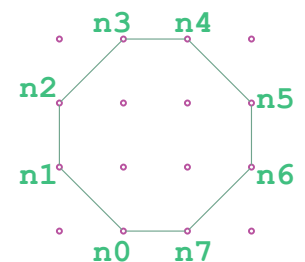

3.25. Cables and struts based on grid of vertices

Type B: Double-surface tensegrity system based-on cylindrical topology

(a)

(a)   (b)   (c)

(b)

X

X

(d)

(c)
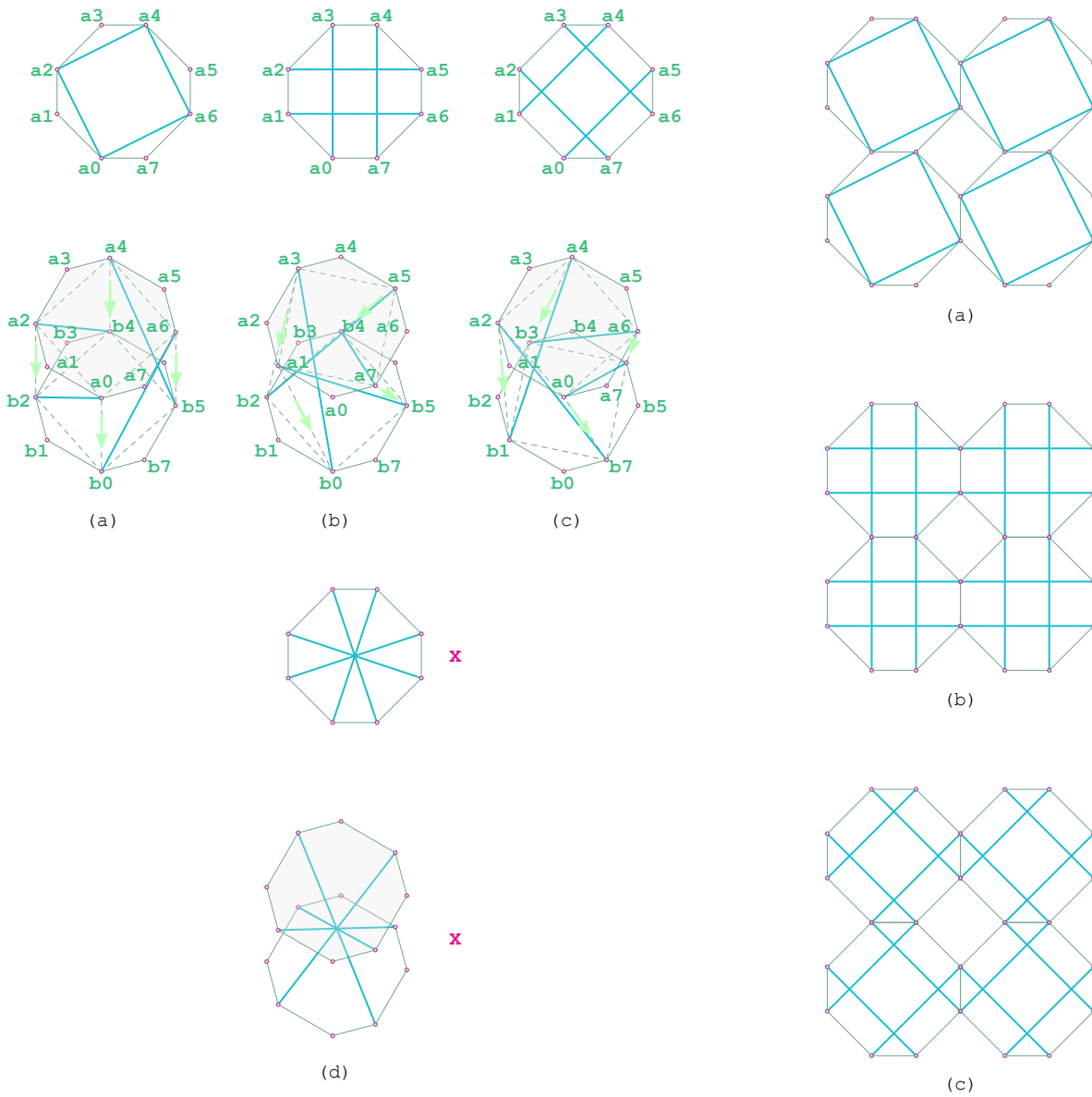
3.26. Within an octagonal tessellation, the system of quadrex tensegrity (quadrangular prism) can be constructed. n = 4
(x) Eliminated option because of touching struts in their centre points

3.27. Three different ways of placing struts in cable networks, which is creating different tessellations.
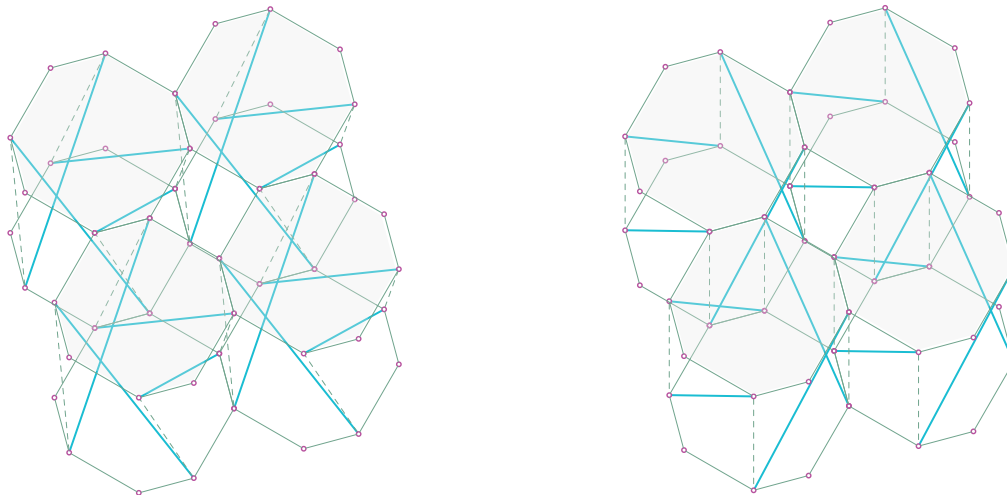
3.28. The cell of this system is a quadrex tensegrity inside an octagonal cylindrical geometry. They will be then combined in the way that struts do not touch each other.

Procedure: Tessellating and tensegritizing of octagonal pattern based on quadrangular grid, cylindrical topology, type B. (for cell 3.25(a))
Inputs:
srf #first reference surface
srfx #second reference surface
udiv #ucount, udiv % 3 == 0
vdiv #v count, vdiv % 3 == 0
Outputs:
nods #list of structural nodes
cabs #list of lines of cables
strs #list of lines of struts

```
#Define the generic quadrangular grid of vertices which have (u, v) coordinates
for i in range (0, udiv - 2, 3):
    for j in range (0, vdiv - 2, 3):
        a0 = (i/udiv, (j+1)/vdiv, 0)
        a1 = (i/udiv, (j+2)/vdiv, 0)
        a2 = ((i+1)/udiv, (j+3)/vdiv, 0)
        a3 = ((i+2)/udiv, (j+3)/vdiv, 0)
        a4 = ((i+3)/udiv, (j+2)/vdiv, 0)
        a5 = ((i+3)/udiv, (j+1)/vdiv, 0)
        a6 = ((i+2)/udiv, j/vdiv, 0)
        a7 = ((i+1)/udiv, j/vdiv, 0)
        a8 = (i/udiv, (j+1)/vdiv, 0)

#Make the network of vertices to reference surfaces
        Evaluate (a0,…,a7) on srfx as (xnewa0,…,xnewa7)
        Evaluate (a0,…,a7) on srf as (newa0,…,newa7)
        AddPoint (newa0,…,newa7) to nods

#Define the network of cables or Constructing network of octagons
        AddLine ((newa0, newa1), (newa1, newa2), (newa2, newa3), (newa3, newa4),
(newa4, newa5), (newa5, newa6), (newa7, newa0)) to cabs #cable network on srf
        AddLine ((xnewa0, xnewa1), (xnewa1, xnewa2), (xnewa2, xnewa3), (xnewa3,
xnewa4), (xnewa4, xnewa5), (xnewa5, xnewa6), (xnewa7, xnewa0)) to cabs #cable network
on srfx
        AddLine ((newa0, xnewa1), (newa1, xnewa2), (newa2, xnewa3), (newa3, xnewa4),
(newa4, xnewa5), (newa5, xnewa6), (newa7, xnewa0)) to cabs #connect two networks of
cables

#Define the network of struts
        AddLine ((newn0, xnewn2), (newn2, xnewn4), (newn4, xnewn6), (newn6, xnewn0)) to
strs #for each strut, one end is in srf, the other is in srfx
```
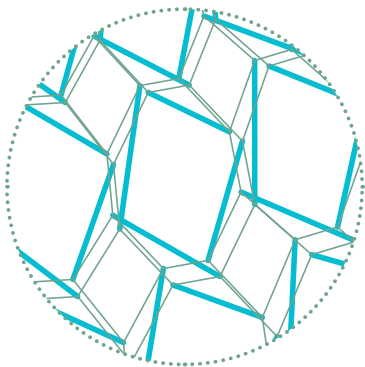
(b)
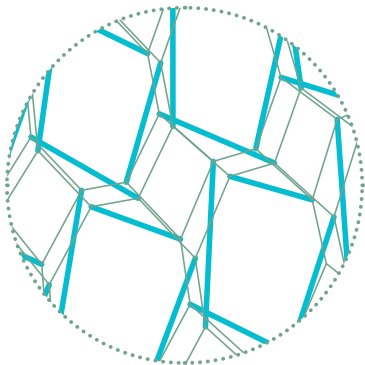
(c)
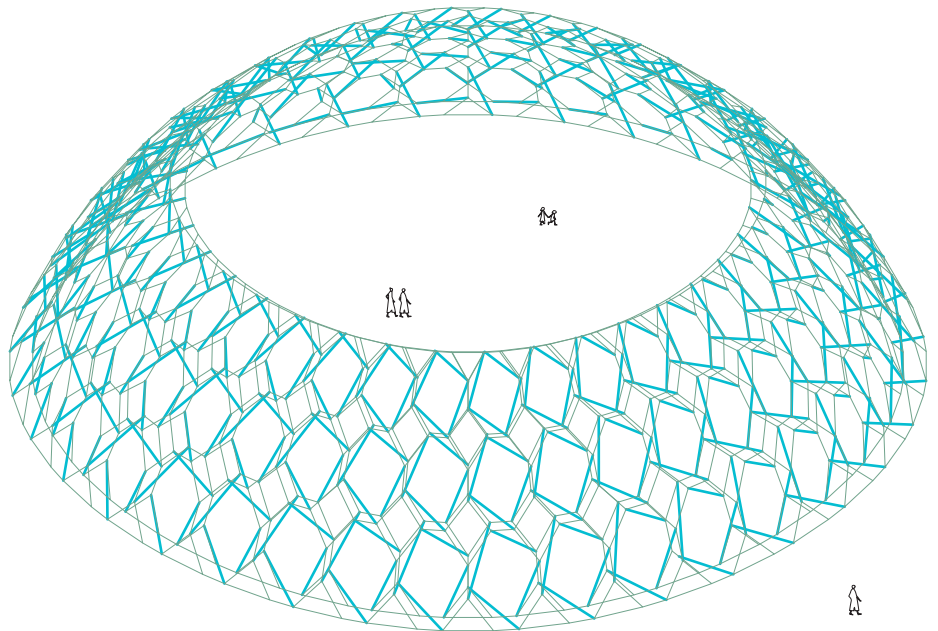
(a)

3.29. Applying to the dome with a central opening. There are a certain amount of cables which will be added to connect two reference tessellations. In this case, these reference tessellations are not merged.

With an octagonal pattern, a network of quadrex tensegrities is achieved.

3.4. Digital Form-finding of Double-surface Tensegrity Structures

GsRelax

GsRelax is a non-linear analysis solver in windows GSA. As a non-linear analysis solver, GsRelax can take the following special features into account in the analysis:
- Geometric non-linear effects (automatically considered)
- Geometric stiffness of beam elements (it can be turned on or off, default is on)
- Material non-linearity (Once non-linear material is defined for beam, bar, tie, and strut elements)

The advantages of using GsRelax solver in structure analysis:
- Since GsRelax analysis does not rely on small displacement assumption and geometric non-linear effects are always considered, GsRelax can produce more accurate and realistic results compared to linear analysis solver especially when the structure deformations are relatively large.
- Because a vector approach (Dynamic Relaxation) rather than a stiffness matrix method is used in GsRelax analysis, it does not impose any special requirements to the stiffness of the structure, for example, zero stiffness of some nodes in some directions are allowed in GsRelax analysis. Therefore, GsRelax can analyse virtually any type of structures even a mechanism, for example, normal structural analysis programs cannot cope with the following two special types of structures, but GsRelax will be able to give a solution as that in the real world.

Non-linear Analysis

To understand GsRelax and interpret its analysis results, it is important to know the differences between linear and non-linear analysis.

The linear structural analysis is using the following two assumptions:
- Material stress-strain relationship is linear (material Young's Modulus is constant)
- Displacement and strain relationship is linear (small displacement problem)

These two assumptions are acceptable in most cases of structural analysis since a majority of the structures (except light-weight structures) in practice are quite stiff and the deformations of the structures are relatively small compared with the size of the structure. In these situations, using linear analysis will not result in any significant error of the analysis results. However, if a structure is flexible or the deformation is relatively large compared with the size of the structures and/or real material property needs to be considered, these two assumptions become invalid and non-linear analysis should be used.

Ignoring Form-finding Properties

With simple tensegrity structures, soap film form-finding technique can be used efficiently to find the equilibrium state of the structures. But soft film form-finding requires the use of spacer elements. When the structure become complex, it is extremely difficult to set up these spacer properties. This is because a spacer should not be discontinued or bifurcated. That is why 'ignore form-finding properties' is used for complex tensegrity structures.

To start with the form-finding process, pre-stress forces should be applied firstly. After this form-finding, there are internal loads inside cables that lead to tensioning in a cable network. Consequently, discontinuous struts are in compression because of pre-stress forces. This step can be repeated several times until the system achieves a certain stiffness. At this point, we conduct the last form-finding which is the combination of the last internal loads from latest form-finding and self-weight before doing structural analysis. After this form-finding, the model will not deform under the similar load case.

3.5. Structural Analysis

Structural analysis in this chapter is only for checking the stiffness of the structural after form-finding. For this reason, only some simple load cases are considered such as self-weight and nodal loading.

The geometry received after the form-finding process deformed quite a lot compared to the original shape, but the general form is reserved. This shape can be improved by adjusting pre-stress forces in the cables. The model became very stiff and handled the nodal load well. There is some minor imperfection which does not seem to affect the global performance of the entire system. Therefore, it is time to move on with the design for Feyenoord.
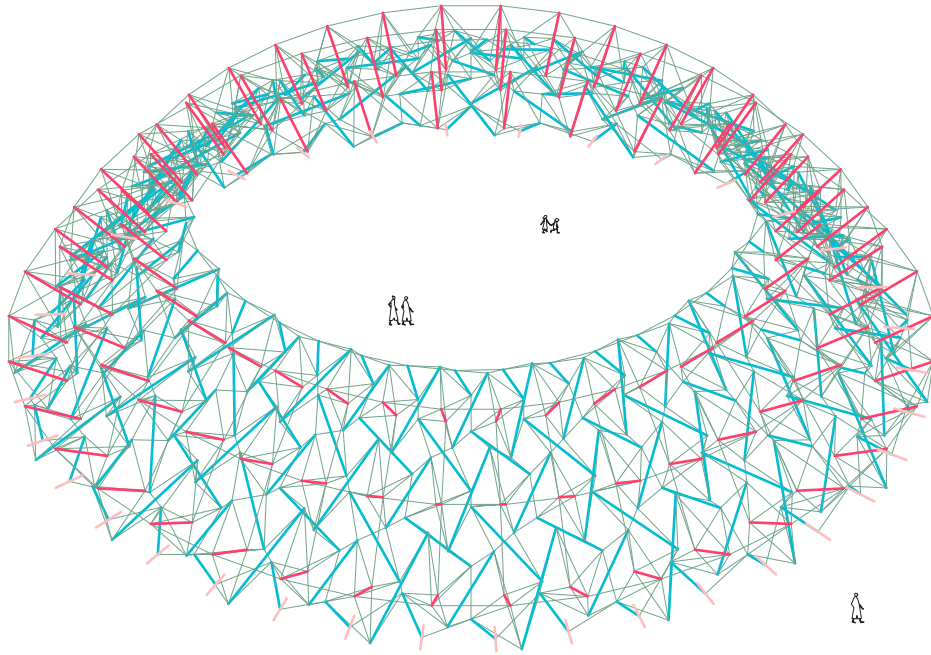
3.30(a). Double-surface tensegrity structures. octagonal tessellation.
z-base topology. normal struts. bracing cables.

Scale: 1.210.9
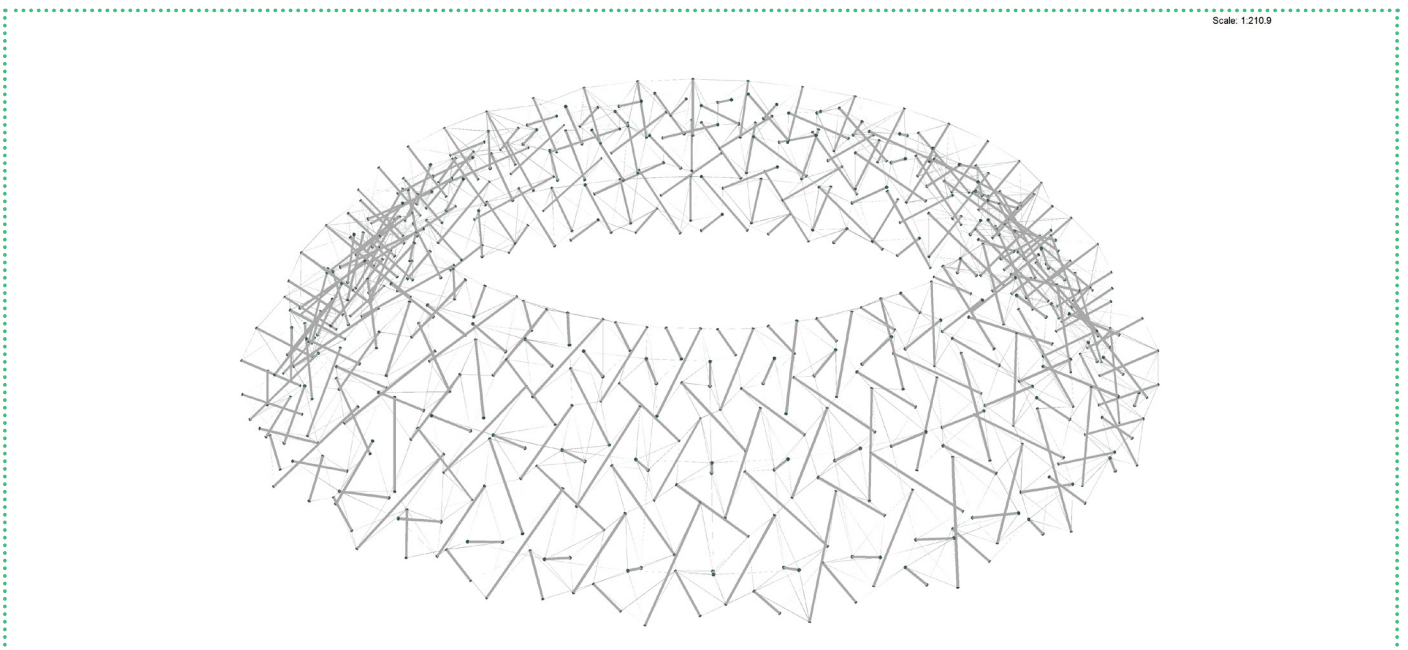
3.30(b). Designed form

Applying the form-finding method from 'bucky's dome with a central hole' to the structure. It deformed as expected and did behave the similar way to physical model which is a quater of the full model. In this case,it is also interesting that we see some large local deformations which are because of the imperfection in the modeling, but the model stand. So tWhe minor imperfection does not affect the global results, the model can be stable in case there are very small amount of local imperfections.
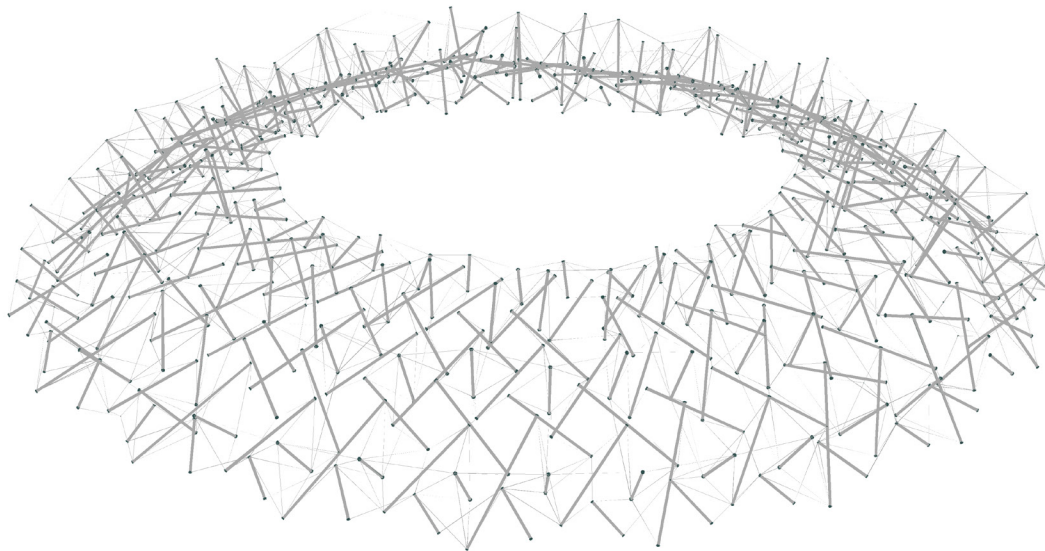
3.31. Form-finding result

Scale: 1:182.3
Deformation magnification: 1.000
Resolved Translation, |U|; 10000. mm/pic.cm
Output axis: global

	4500. mm
	4000. mm
	3500. mm
	3000. mm
	2500. mm
	2000. mm
	1500. mm
	1000. mm
	500.0 mm
	0.0 mm

Case: A4 : Analysis Case 4
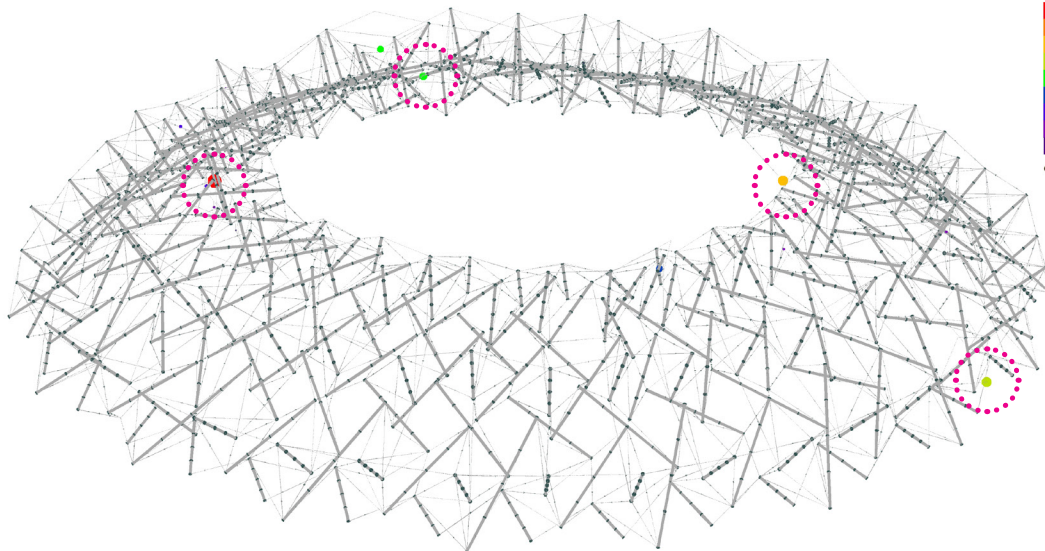
3.32. Nodal displacements

Scale: 1:182.3
Deformation magnification: 1.000
Resolved Element Translation, |U|; 10000. mm
Output axis: local

	4500. mm
	4000. mm
	3500. mm
	3000. mm
	2500. mm
	2000. mm
	1500. mm
	1000. mm
	500.0 mm
	0.0 mm

Case: A4 : Analysis Case 4
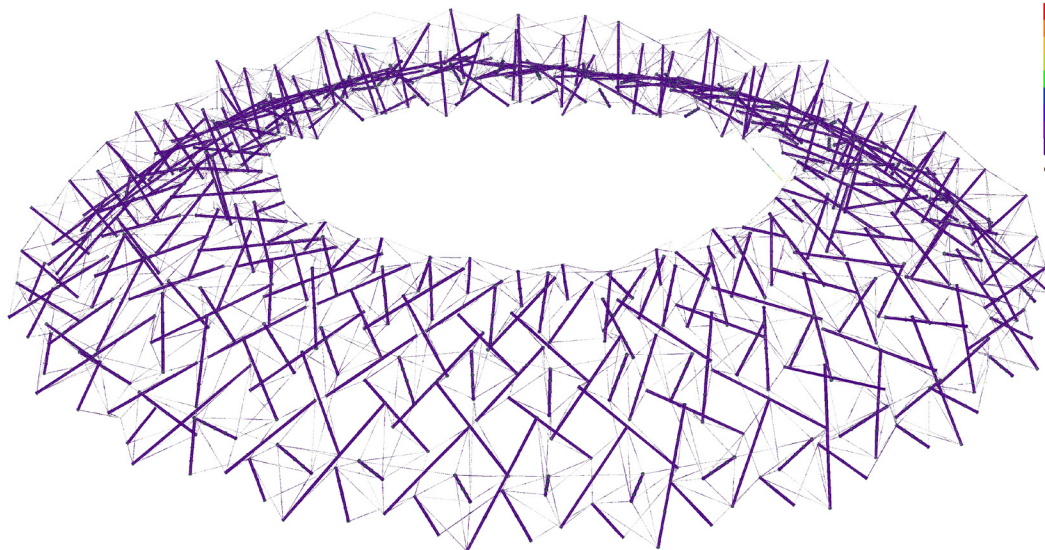
3.33. Beam displacements

(a)
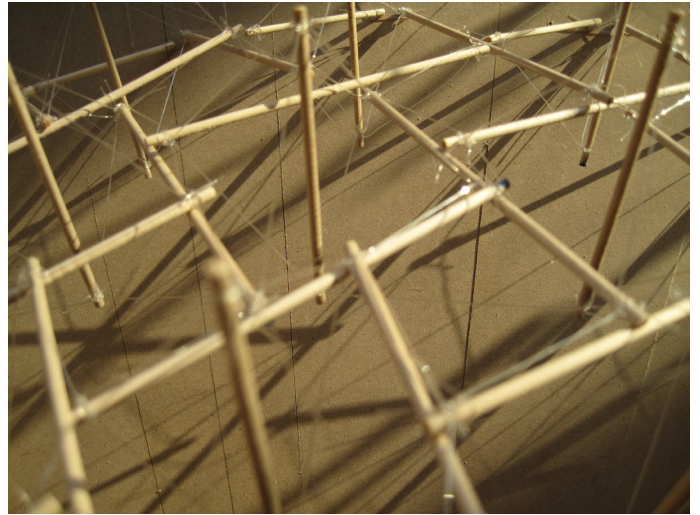
(b)
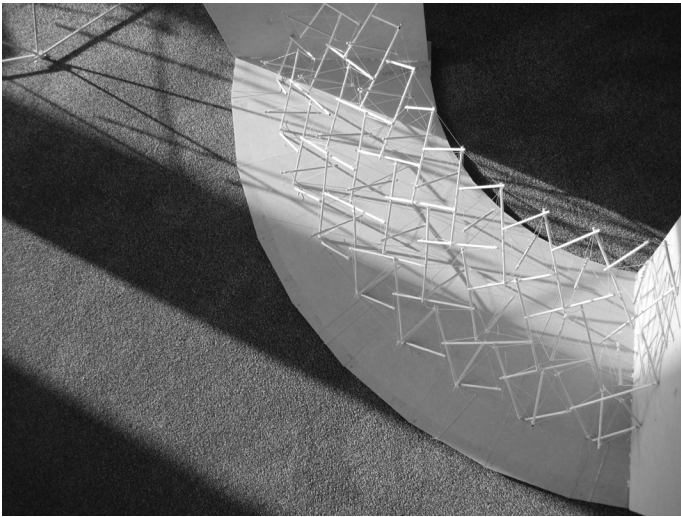
(c)
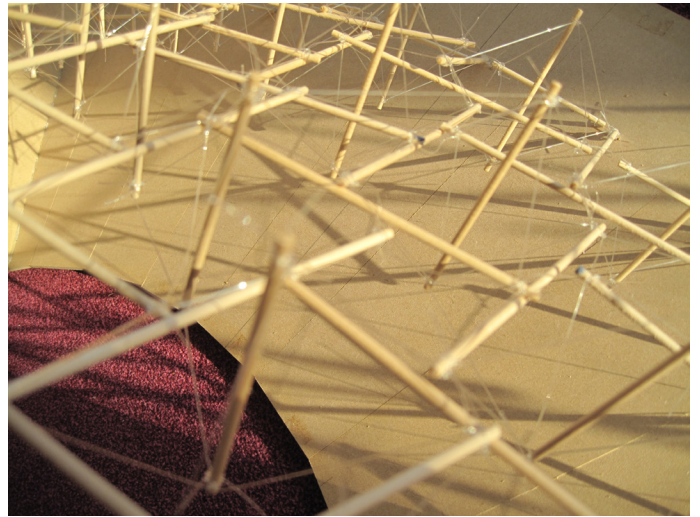
(d)
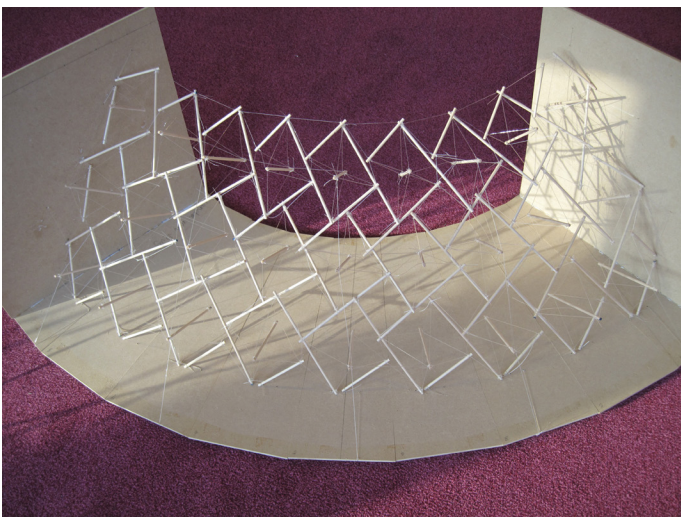
(e)
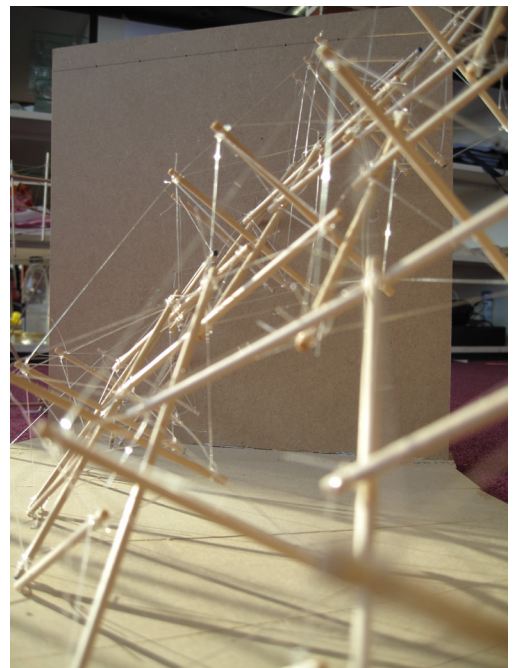
(f)

3.34. Physical model

(a)   (b)   (c)

(d)   (e)   (f)
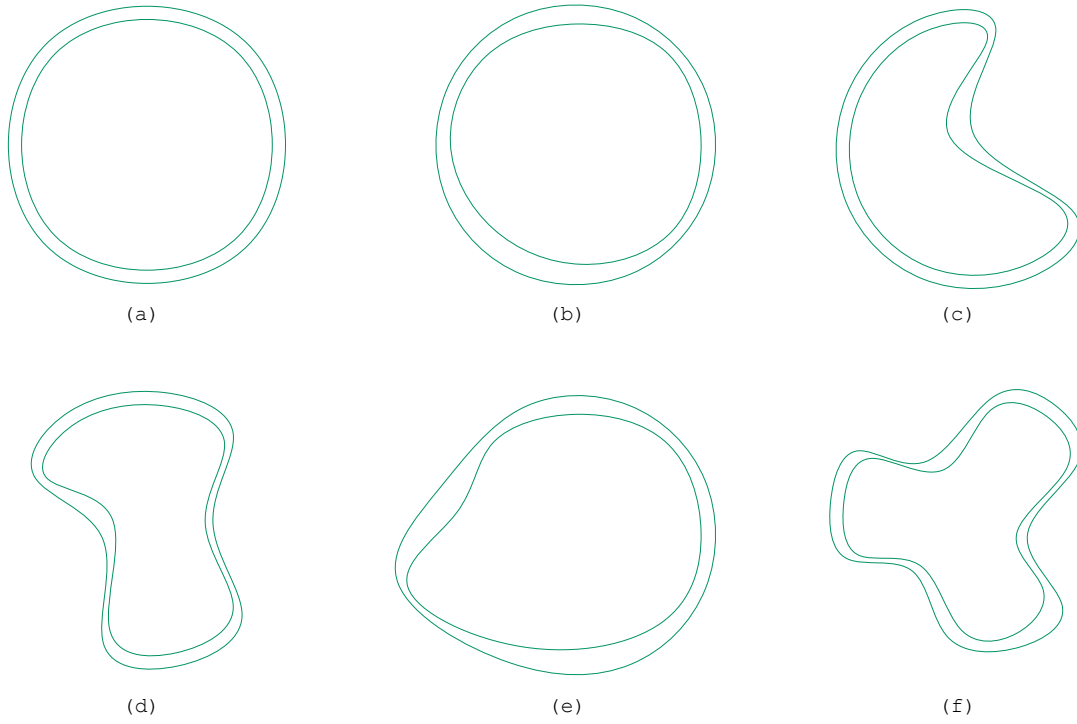
3.35. The double-surface tensegrity structures can be applied to given free-form, with two reference surfaces are slightly different, to locally change the thickness of the tensegrity shell, following structural purpose, architectural quality, and so on.

(a)   (b)   (c)

(d)   (e)   (f)
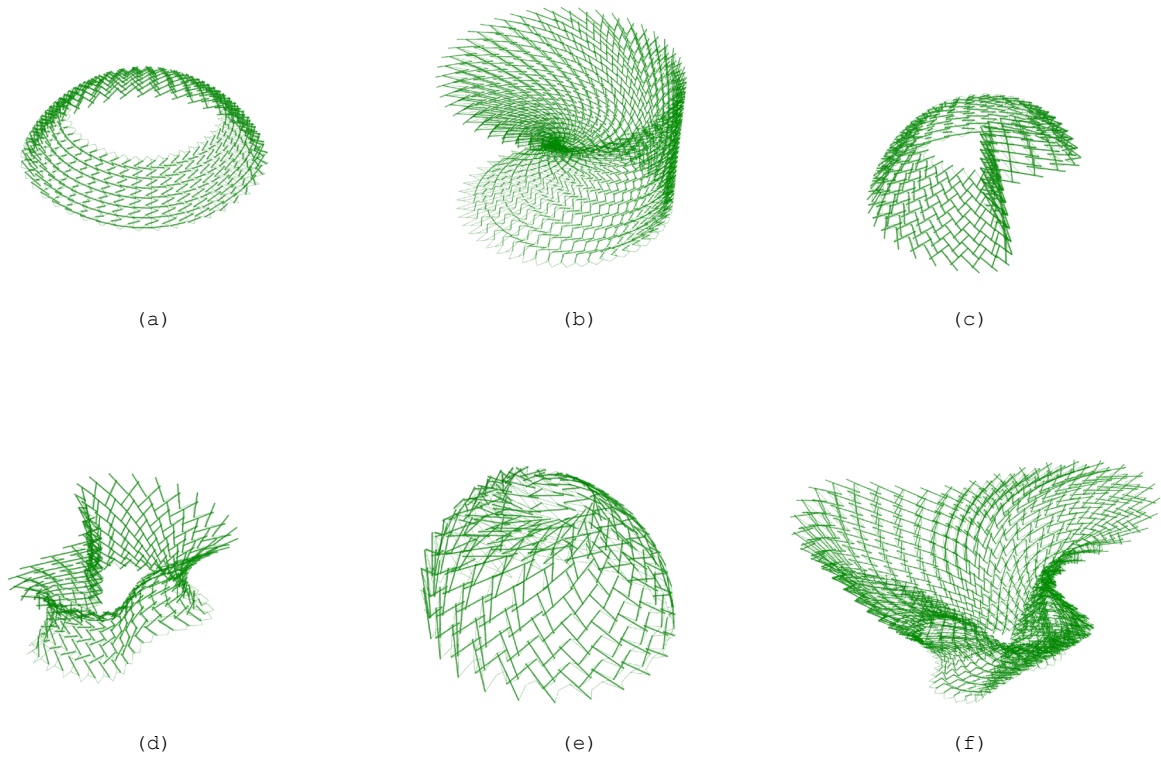
3.36. Double-surface tensegrity as a result of programming using Python in Grasshopper

Python coding on constructing double-surface tensegrity structures (can be applied to any free-form surfaces)

```python
#Input reference surfaces (srf, srfx), two dimensions of the surfaces (udiv, vdiv)

import rhinoscriptsyntax as rs

pts = [] #Quadrangular grid of vertices
noc = [] #Network of cables
nosa = [] #Network of struts a
nosb = [] #Network of struts b

#Define the network of vertices
for i in range (0, udiv - 2, 3):
    for j in range (0, vdiv - 2, 3):
        n0 = (i/udiv, (j+1)/vdiv, 0)
        n1 = (i/udiv, (j+2)/vdiv, 0)
        n2 = ((i+1)/udiv, (j+3)/vdiv, 0)
        n3 = ((i+2)/udiv, (j+3)/vdiv, 0)
        n4 = ((i+3)/udiv, (j+2)/vdiv, 0)
        n5 = ((i+3)/udiv, (j+1)/vdiv, 0)
        n6 = ((i+2)/udiv, j/vdiv, 0)
        n7 = ((i+1)/udiv, j/vdiv, 0)

#Make the network of vertices to surfaces
        srfxp = rs.SurfaceParameter (srfx, n0)
        newn0 = rs.EvaluateSurface (srfx, srfxp[0], srfxp[1])
        pts.append (rs.AddPoint(newn0))
        srfp = rs.SurfaceParameter (srf, n1)
        newn1 = rs.EvaluateSurface (srf, srfp[0], srfp[1])
        pts.append (rs.AddPoint(newn1))
        srfxp = rs.SurfaceParameter (srfx, n2)
        newn2 = rs.EvaluateSurface (srfx, srfxp[0], srfxp[1])
        pts.append (rs.AddPoint(newn2))
        srfp = rs.SurfaceParameter (srf, n3)
        newn3 = rs.EvaluateSurface (srf, srfp[0], srfp[1])
        pts.append (rs.AddPoint(newn3))
        srfp = rs.SurfaceParameter (srf, n4)
        newn4 = rs.EvaluateSurface (srf, srfp[0], srfp[1])
        pts.append (rs.AddPoint(newn4))
        srfxp = rs.SurfaceParameter (srfx, n5)
        newn5 = rs.EvaluateSurface (srfx, srfxp[0], srfxp[1])
        pts.append (rs.AddPoint(newn5))
        srfp = rs.SurfaceParameter (srf, n6)
        newn6 = rs.EvaluateSurface (srf, srfp[0], srfp[1])
        pts.append (rs.AddPoint(newn6))
        srfxp = rs.SurfaceParameter (srfx, n7)
        newn7 = rs.EvaluateSurface (srfx, srfxp[0], srfxp[1])
        pts.append (rs.AddPoint(newn7))

#Define the network of cables or Constructing network of octagons
        noc.append(rs.AddLine(newn0, newn1))
        noc.append(rs.AddLine(newn1, newn2))
        noc.append(rs.AddLine(newn2, newn3))
        noc.append(rs.AddLine(newn3, newn4))
        noc.append(rs.AddLine(newn4, newn5))
        noc.append(rs.AddLine(newn5, newn6))
        noc.append(rs.AddLine(newn6, newn7))
        noc.append(rs.AddLine(newn7, newn0))

#Define the network of struts a
for i in range (0, udiv - 2, 3):
    for j in range (0, vdiv - 2, 3):
```

```
        a0 = (i/udiv, (j+2)/vdiv, 0)
        a1 = ((i+3)/udiv, (j+4)/vdiv, 0)
        srfp = rs.SurfaceParameter (srf, a0)
        newa0 = rs.EvaluateSurface (srf, srfp[0], srfp[1])
        pts.append (rs.AddPoint(newa0))
        srfxp = rs.SurfaceParameter (srfx, a1)
        newa1 = rs.EvaluateSurface (srfx, srfxp[0], srfxp[1])
        pts.append (rs.AddPoint(newa1))

        nosa.append(rs.AddLine(newa0, newa1))

#Define the network of struts b
for i in range (0, udiv - 2, 3):
    for j in range (0, vdiv - 2, 3):
        b0 = ((i+2)/udiv, (j+3)/vdiv, 0)
        b1 = ((i+4)/udiv, j/vdiv, 0)
        srfp = rs.SurfaceParameter (srf, b0)
        newb0 = rs.EvaluateSurface (srf, srfp[0], srfp[1])
        pts.append (rs.AddPoint(newb0))
        srfxp = rs.SurfaceParameter (srfx, b1)
        newb1 = rs.EvaluateSurface (srfx, srfxp[0], srfxp[1])
        pts.append (rs.AddPoint(newb1))

        nosb.append(rs.AddLine(newb0, newb1))

a = pts #Structural nodes
b = noc #Network of cables
c = nosa #Network of struts a
d = nosb #Network of struts b
```
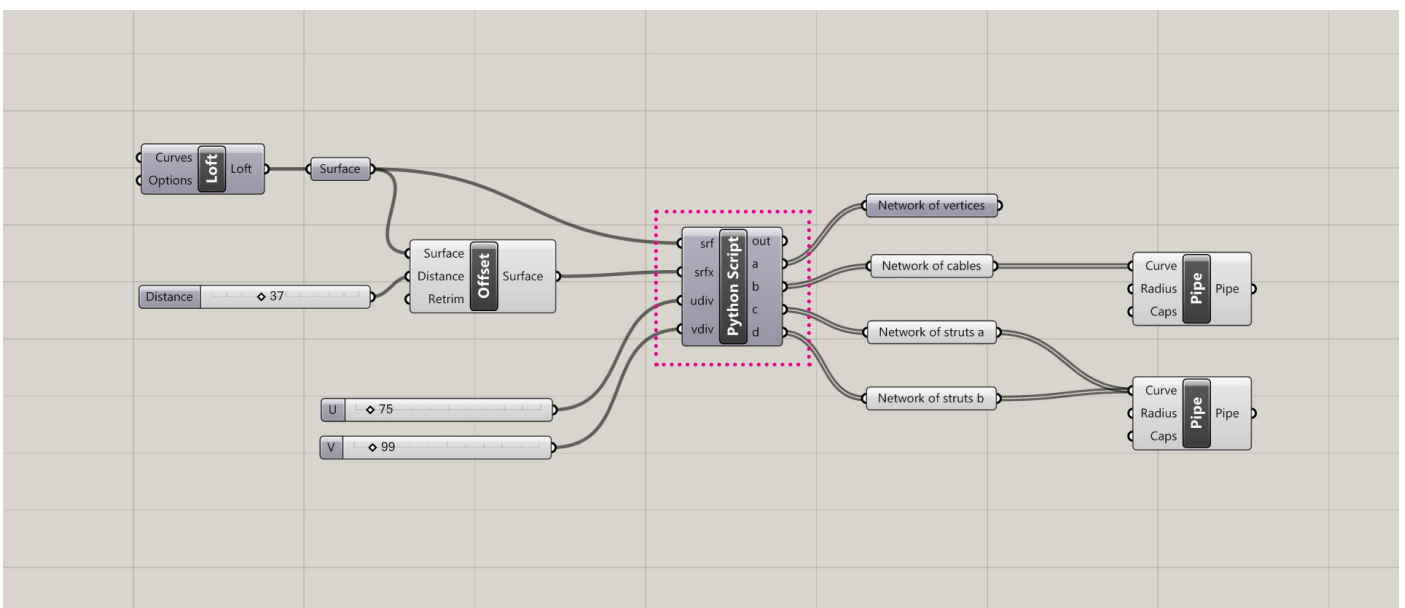

3.37. The grasshopper script to build double-surface tensegrity systems applied to any type of free form surfaces with the is Python code

Chapter 4. Design a Tensegrity Structure to Cover Original Feyenoord Stadium

4.1. History and Typology of Stadium Roof

Throughout almost 40 centuries of sports architecture construction, across five continents, the innovations of stadium engineering lie in the size of the stadium, stand's supporting structures and most recently the roof megastructures. From the ancient Greek to the 1900s, almost all stadiums around the world did not have a roof to cover people watching sports games.

In the beginning, it is obviously an impossible mission to build large-span structures in stone which is extremely heavy material. In Roman time, there are a number of technological innovations in construction but not any stadium roof was realized. This is because they mostly built in pure concrete which is relatively heavy material as well.

Until the beginning of 20th century, with the invention of reinforced concrete and the wide application of steel in construction, stadiums started having the roof to protect their spectators from extreme weather conditions, and bring a more comfortable environment for people to enjoy the games. But in these early years, there was a need of adding many columns to withstand the roof, these columns were in between the seats, and blocked the views of spectators.

Overtime, engineers explored solutions to get rid of those obstacles and step by step improved the structure of the roof with several methods of using megastructures. Since then, stadium roof becomes one of the most important parts of the stadium that expresses the characteristics of the site, of the people living there and their sports team. The roof helps to build up the sporting spirit and provides unique atmosphere and memories to all sports lovers.

In contemporary stadium design of the roof, there are mainly five typologies which are commonly applied nowadays:
(1) Geometrical stiffness
(2) Cantilevering from mega-columns
(3) Suspending from mega-columns
(4) Suspending from mega-trusses
(5) Tensioning to the mega-compression ring

4.2. Feyenoord Stadium

Feyenoord stadium is the home of Feyenoord football club the south of Rotterdam, the Netherlands. The stadium is more commonly known by its nickname De Kuip, meaning the Tub. It was designed by the famous Rotterdam's architect Leendert van der Vlught in 1935 and the construction was completed in 1937, making one of the most innovative football stadia at that time.

The capacity of the original stadium was 64.000. In World War II, the stadium was occupied by Nazis. After the war, it was expanded to 69.000 in 1949, stadium light was added in 1958. In 1994, it was renovated for a capacity of 51.117. In 1999, a significant amount of renovation work took place for UEFA Euro 2000 tournament, but the capacity was not primarily affected.

De Kuip was named in the monumental list of Rotterdam on 29 October 1991. The renovation in 1994 brought the stadium to its present form, the Olympic running pitch was transformed to all-seater, and the roof was extended to cover all the seats. The structure to support the roof was painted white to distinguish with the black part of original slender steel frames.

4.3. Design Proposal

After several renovations, the original characteristics of the stadium were lost. The innovative image of the extreme slender steel frame holding two floating tiers was replaced by the banal structure of the roof. After 20 years since the last renovation, De Kuip needs to have a new life, one more time.

The proposal is to take off the existing roof structure and four light flooding posts. The original structure of the stadium, which is used to be technologically innovative, is preserved. A new tensegrity roof will be added to cover the entire original stadium with an integrated lighting system.

The new tensegrity roof will show the extreme ability of structural engineering and architecture as well as the dynamicity of city of Rotterdam which has the second biggest harbor in the world. The floating compressional struts in the network of cable frankly against gravity will bring a real spiritual atmosphere to the Feyenoord area, and perfectly interacts with the monumental design of van der Vlugt.

zarzuela hippodrome
madrid
1935
© structurae.net

national olympic stadium
tokyo
1964
© Keystone Press

london stadium
london
2012
© treatch

panatheanic stadium
athens
330-329 BC
© Badseed

campo de les corts
barcelona
1943
© Peter Culley and John Pascoe

wembley stadium
london
2007
© Alamy

olympic stadium
munich
1972
© Jorge Royan

olympiastadia
stockholms
1912
© Sascha Uding

palazzeto dello sport
rome
1957
© Peter Culley and John Pascoe

la plata stadium
buenos aires
2003
© stadiumguide.com

past   future

4.1. Evolution of stadium engineering

taiwan national stadium
taipei
© Toyo Ito

feyenoord stadium
rotterdam
© skyscrapercity.com

olympic stadium
munich
© wikimedia.commons

emirate stadium
london
© wilson owens

cape town stadium
cape town
© warrenski

(1)
geometrical stiffness

(2)
cantilevering from columns

(3)
suspended to columns

(4)
suspended to mega-truss

(5)
outer compression ring and
inner tension ring
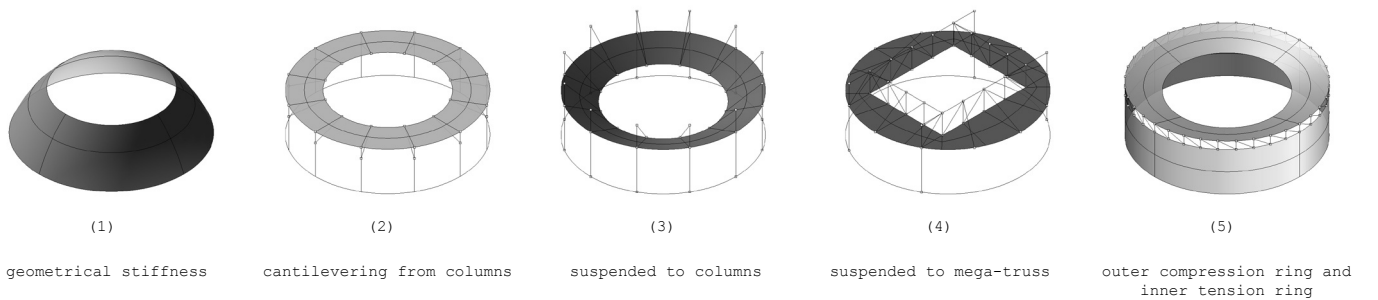
4.2. Stadium roof structural typology

4.3. Feyenoord stadium, Google Earth, 2017
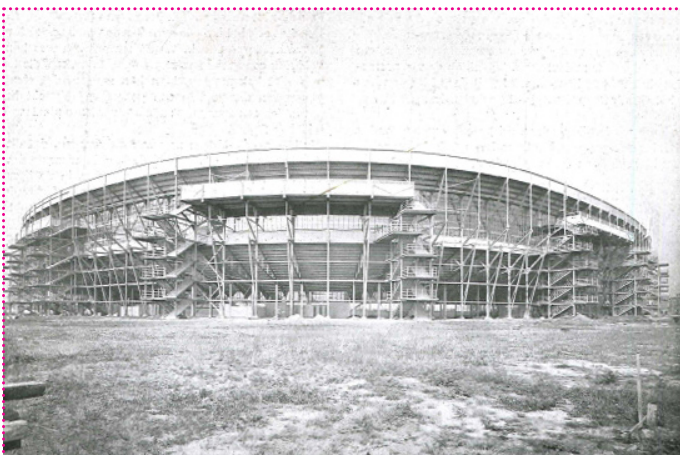
4.4. Feyenoord stadium, Bouwkundig weekblad magazine, 1936

4.5. Feyenoord stadium, Remy de Milde, flickr, 2011

160m

20m

210m
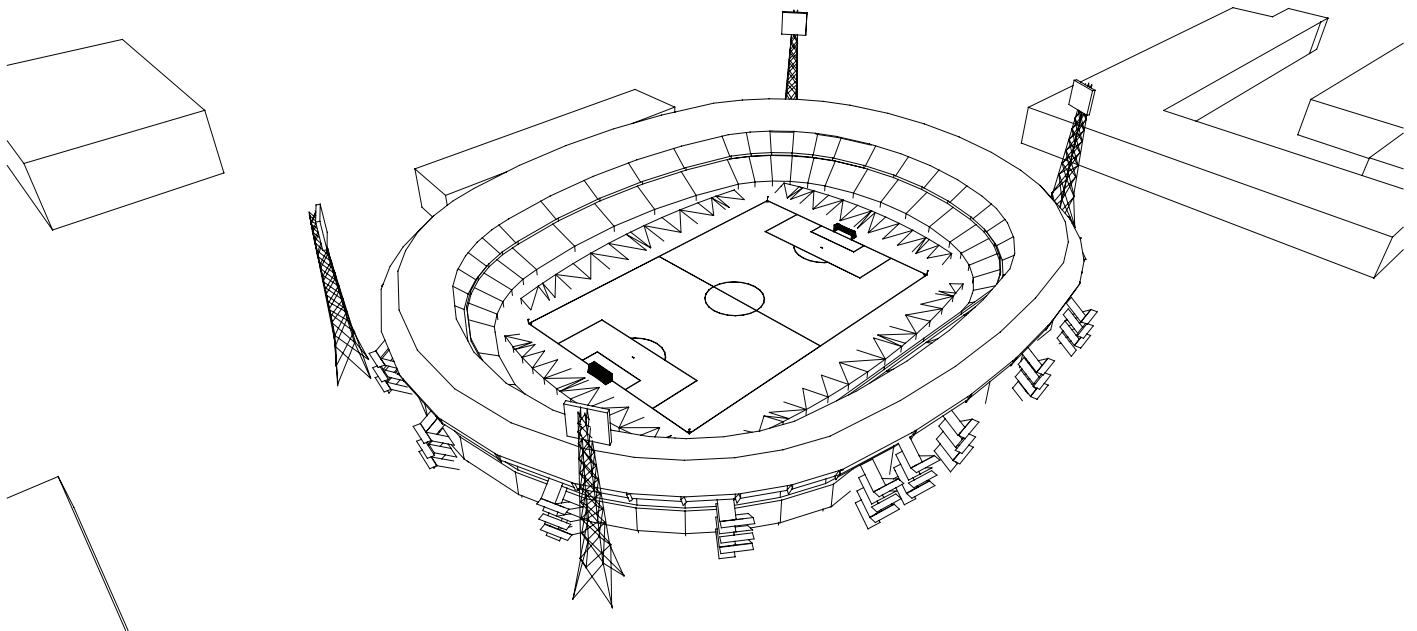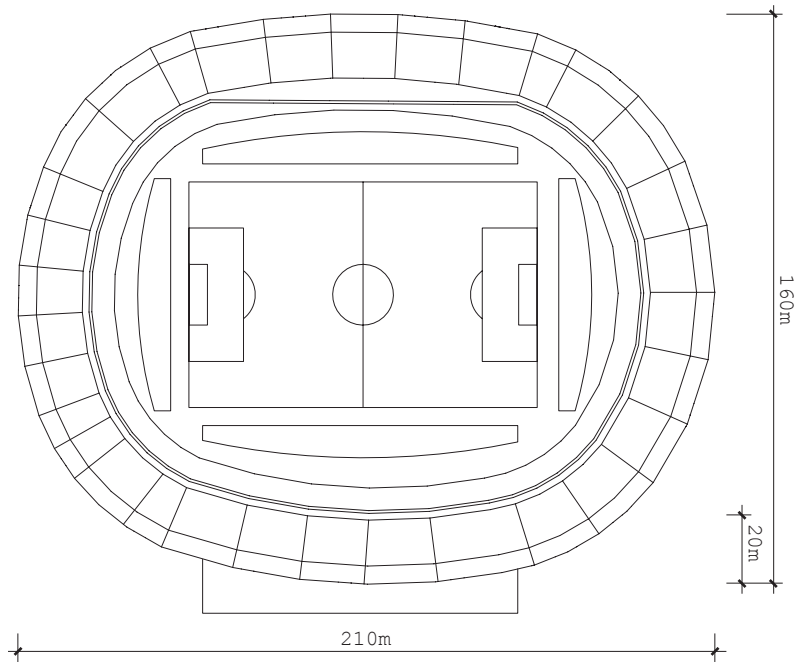
4.6. Current Feyenoord Stadium
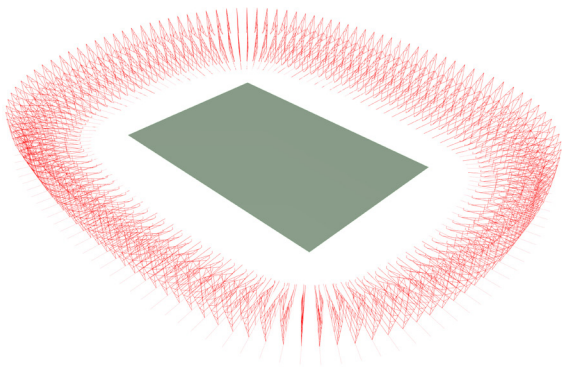
(a) Slender, minimum steel frames
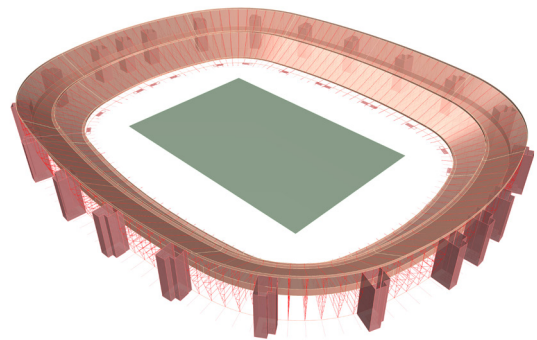
(c) Emergency stairs outside
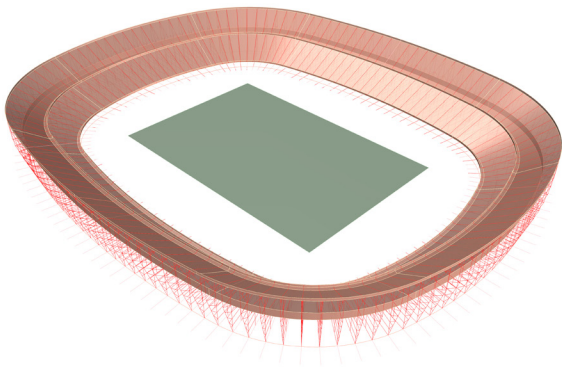
(b) Two hanging tiers
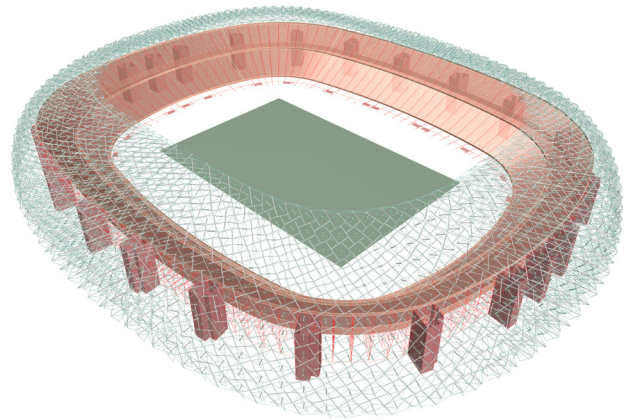
(d) New tensegrity roof

4.7. Adding new tensegrity structure to the original stadium rooted from 1936

4.8. The new roof on site
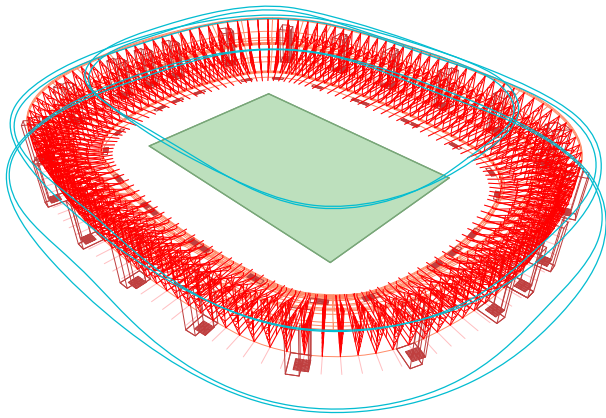
(a) Two reference surfaces
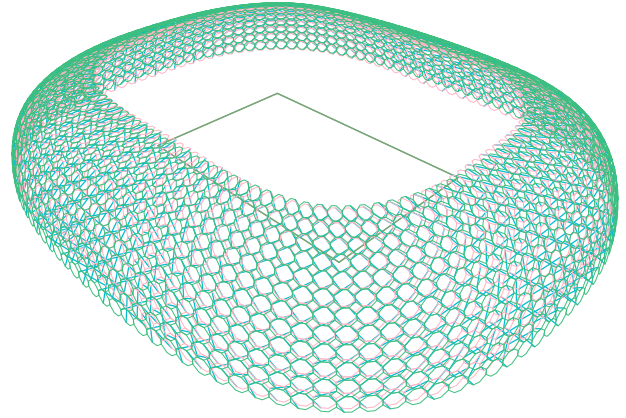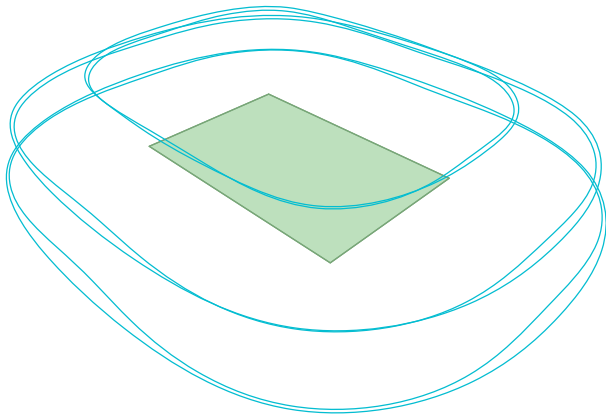
(b) Two reference surfaces are slightly different, creating vairied height

(c) Tessellatizing

(d) Tensegritizing
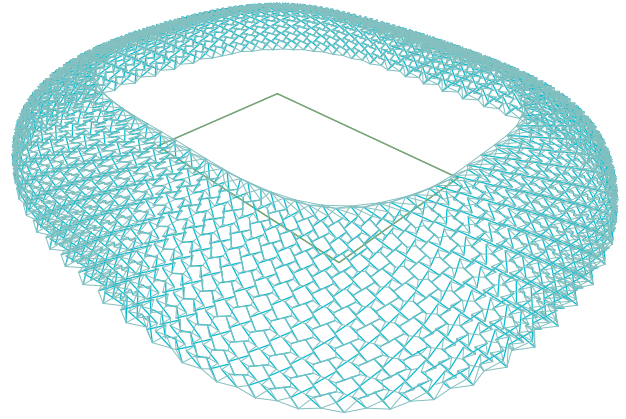
(e) Merging two reference surfaces
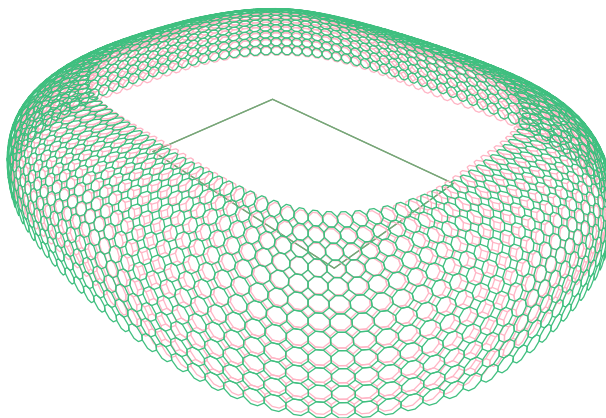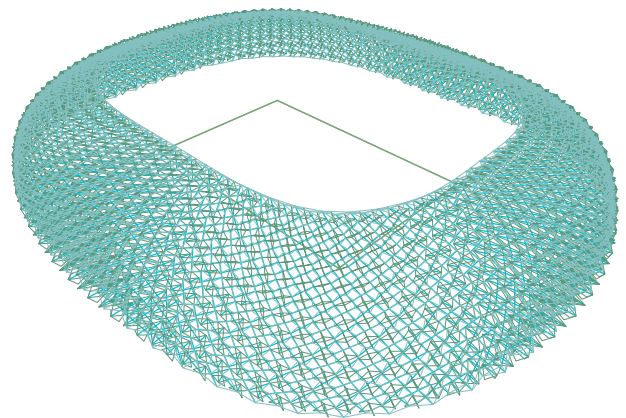
(f) Adding normal struts

4.9. Constructing the tesegrity roof
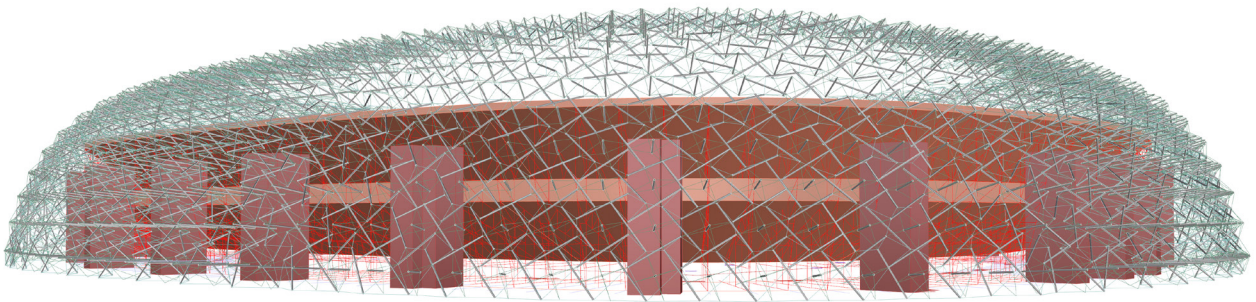
4.10. The original and the new are blending

MAAS RIVER

HOUSING

OFFICES

PARK

TRAIN LINES

TRAINING FIELDS

HOUSING

PARK
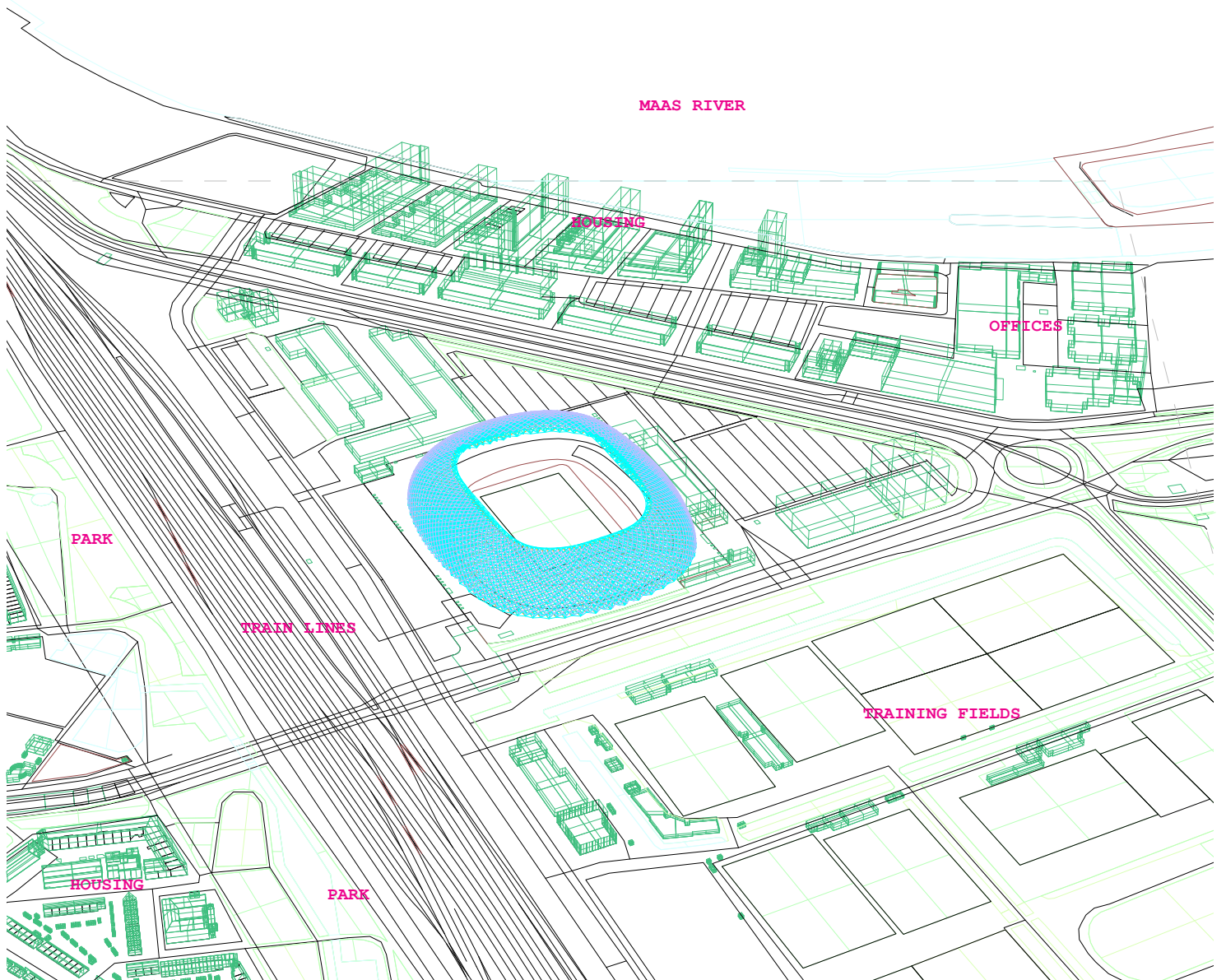
4.11. Bird-eye perspective
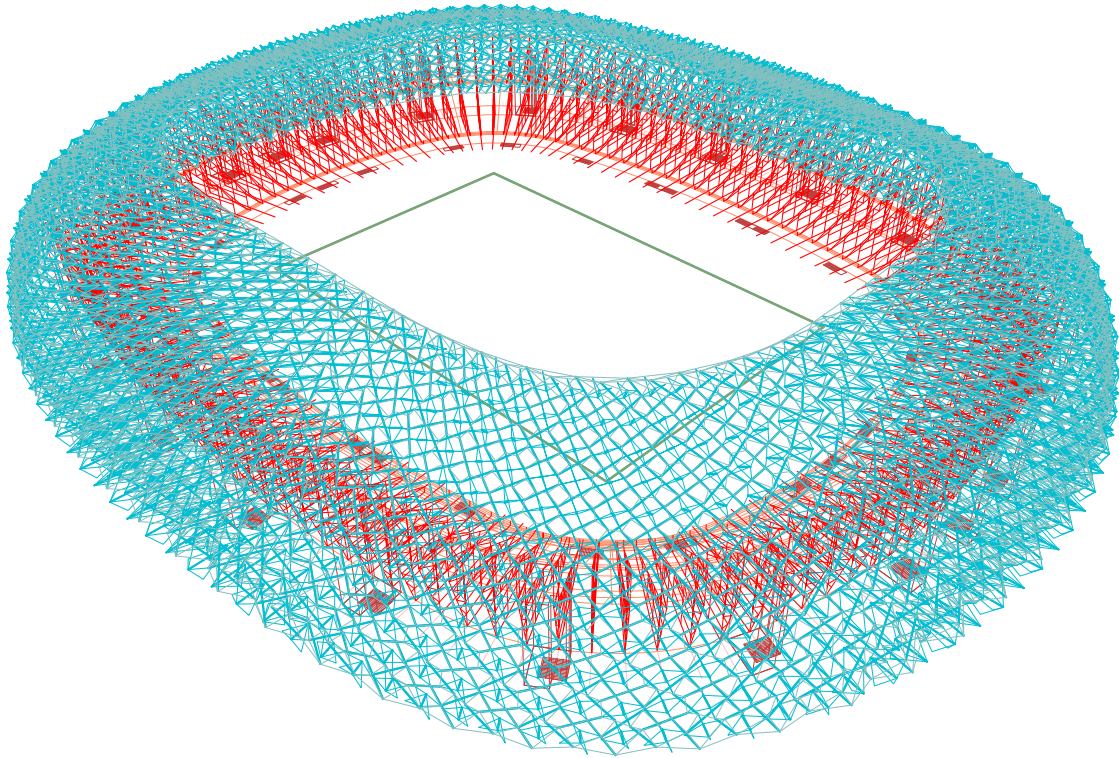
4.12. The original + The new

The entire structure: 200m x 240m x 37,5m
Cantilivering 37,5m
The central opening: 155m x 115m
4200 struts, 2,16-9,98m - CHS139,7X10
Cables: Ø10
Material: Steel (E = 2,05*E+11 PA)

4.13. A cloud of struts

4.4. Form-finding

Failure of Complexity

Using the method constructed in the
previous chapter, the full structural
model of the design was set up, added
properties and exported to Oasys GSA for
first form-finding analysis.

The size of the entire roof is
240x200x37,5 m. The distance between the
opening and the perimeter is 42,5 m. The
opening is 155x115 m. It has 4200 struts
CHS 139,7x10, length from 2,16 to 2,98 m.
The cable is steel cable Ø10, the lengths
vary.

It turned out that this structural model
is extremely computationally expensive.
Or in other words, it costs an enormous
amount of time to run a non-linear
analysis form-finding in Oasys GSA. I
realized it was a step too far from the
generic models built in chapter 3. So I
needed to take a step back.

Simplified Model

The simplified model is ten times smaller,
concerning the real scale model might
not work for the calculation, and has
a smaller amount of structural elements
(302 struts). But the structural topology
and geometry are completely similar. CHS
48.3x5 and steel cable Ø10 are used.

The size of the entire simplified roof
is 24x20x3,75 m. The central opening is
15,5x11,5 m. There are 211 spatial struts,
0,72 to 2,67 m. There are 91 normal
struts, 0,56 to 1,34 m.
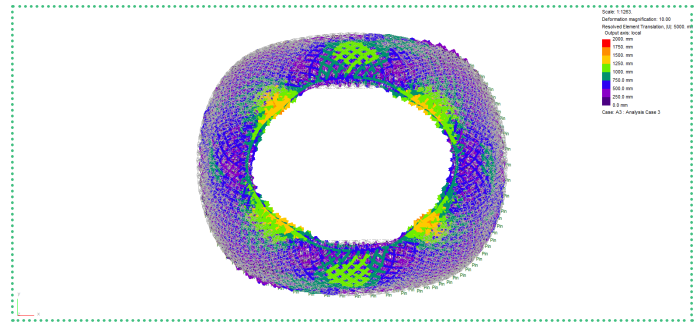
(a)
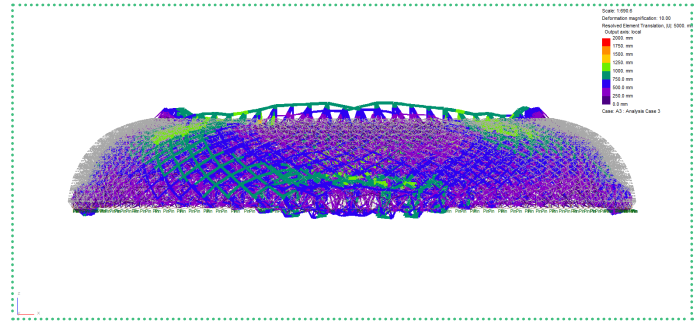
(b)
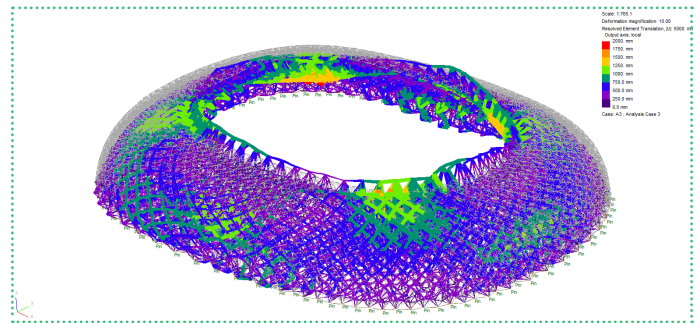
(c)

4.14. Full-scale model deformed because of gravity
after form-finding. While form-finding is being
conducted, the inner ring tends to from a circle
which is the minimal figure to find its own state of
self-stress while form-finding. But in the end, in
the equilibrium, the final shape will be close to the
original designed geometry.
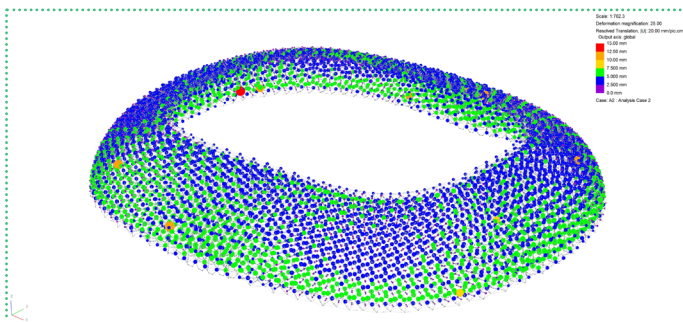
(a) Node displacements
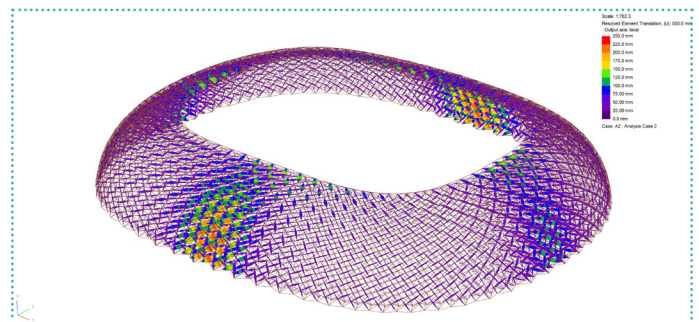
(b) Beam displacements

4.15. Full-scale model deformed because of gravity during and after form-finding. In the end, after form-
finding, the structure became very stiff as well. This is because of pre-stress forces, as well as the large
number of structural element. the geometry found is smoother and closer to the original version compared to
form-finding of simplified version.
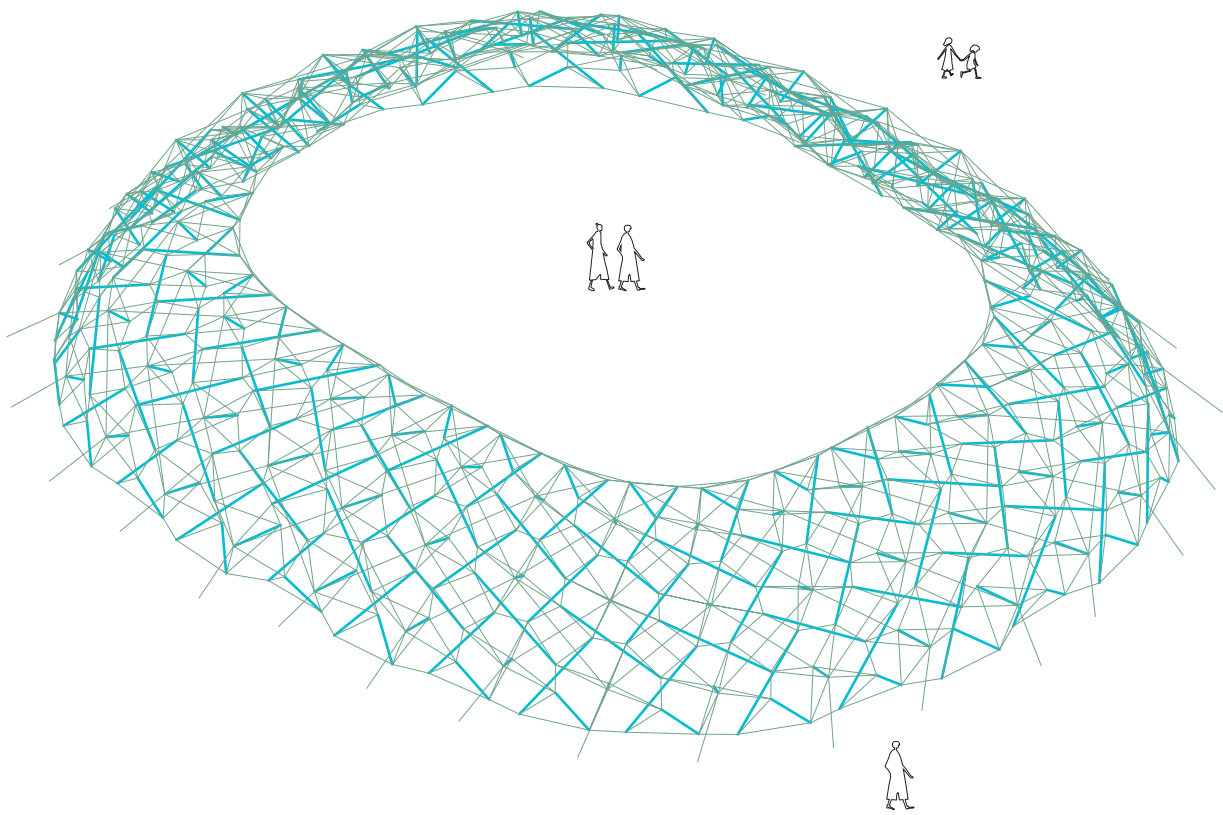
4.16. Simplified version of the structure

The entire structure: 20m x 24m x 3,7m
Cantilivering 3,7m
The central opening: 15,5m x 11,5m
211 spatial struts, 0,72-2,67m - CHS48,3X5
91 normal struts, 0,56-1,34m - CHS48,3X5
Cable: Ø10
Material: Steel (E = 2,05*E+11 PA)

GEOMETRIC MODEL

ADJUST PRE-STRESSING

PRE-STRESS FORCES
(FORM-FINDING)

PRE-STRESS FORCES
+ GRAVITY LOADING
(FORM-FINDING)

NO

EXPECTED
SHAPE

YES

INTERNAL FORCES FROM
FORM-FINDING + GRAVITY LOADING
(NON-LINEAR ANALYSIS)

INTERNAL FORCES FROM
FORM-FINDING + GRAVITY LOADING
+ NODE LOADING
(NON-LINEAR ANALYSIS)

ANALYSIS RESULTS
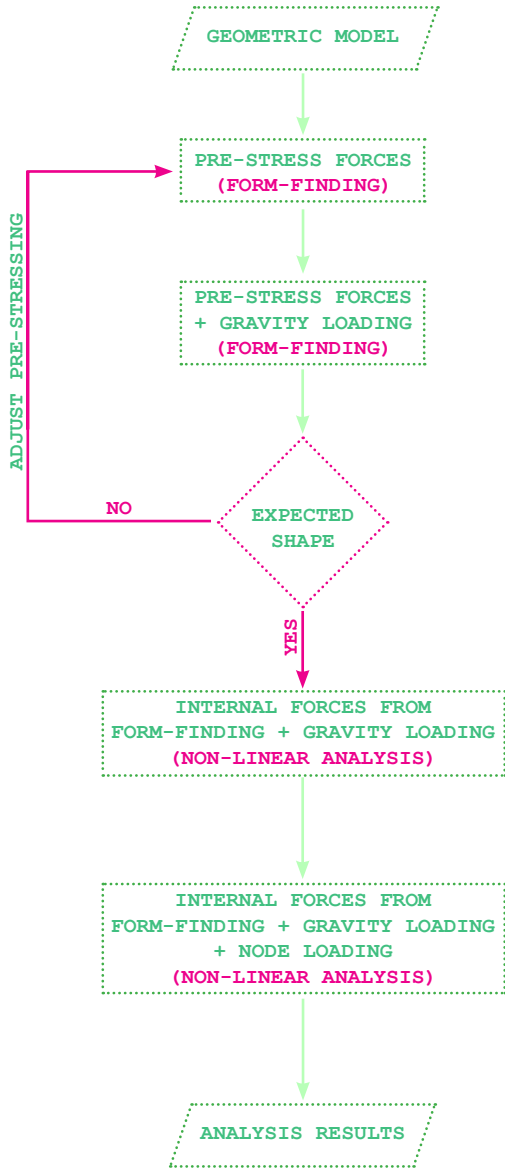
4.17. Form-finding work-flow

—— manual

—— digital
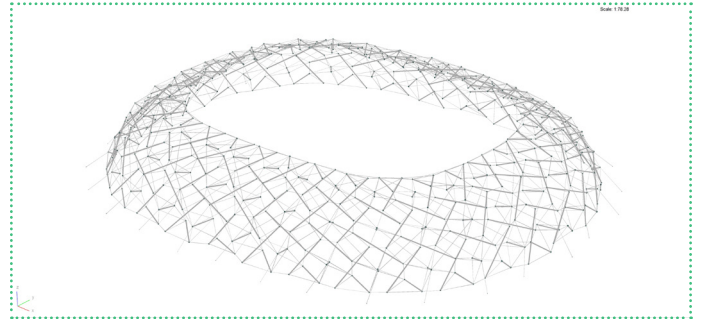
4.18. Designed form
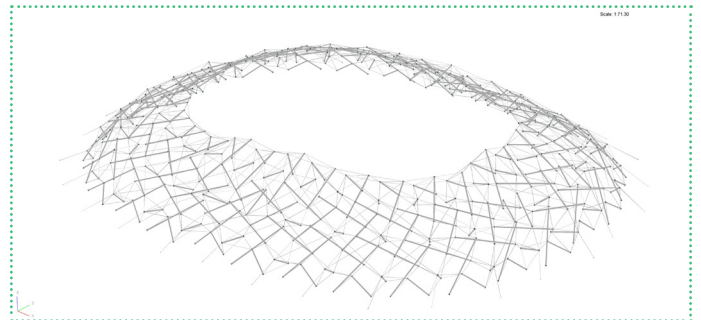
4.19(a). Form-found 1
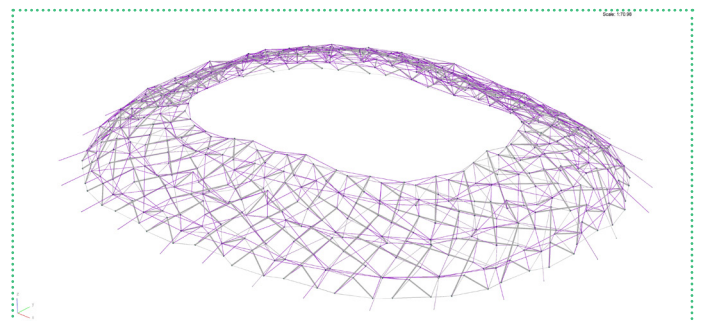
4.19(b). Form-found 2
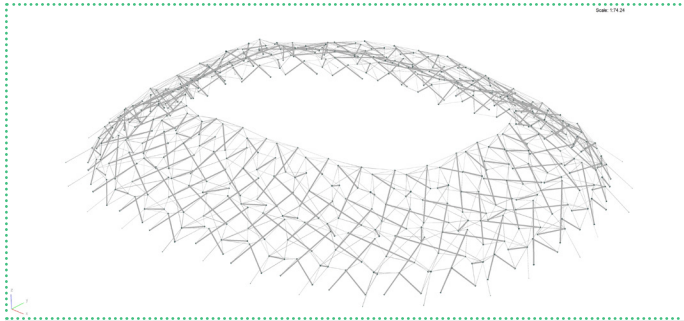
(a)
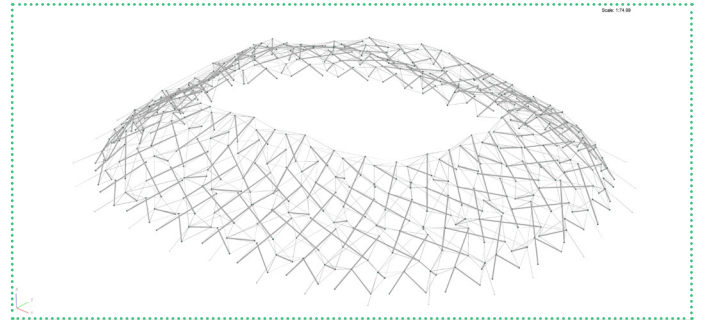
(b)
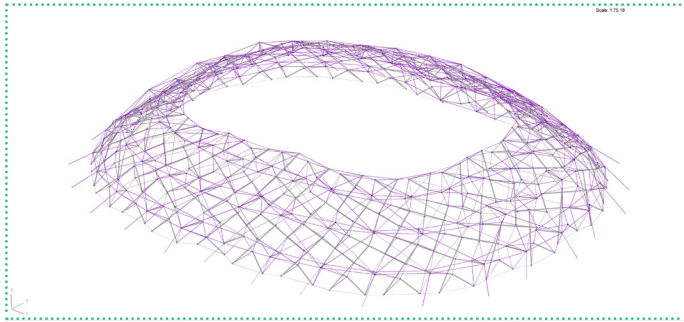
(c)
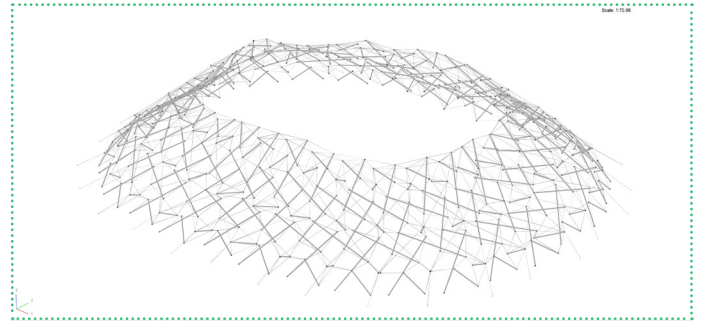
(d)
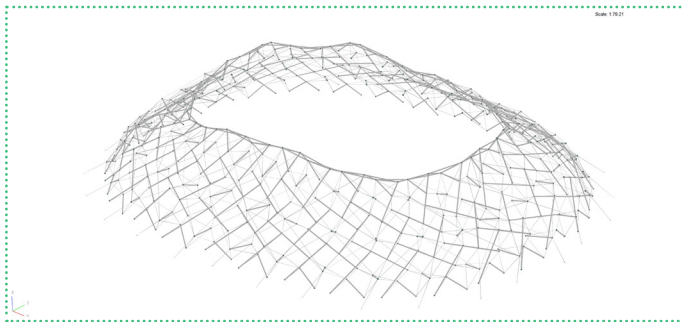
(e)
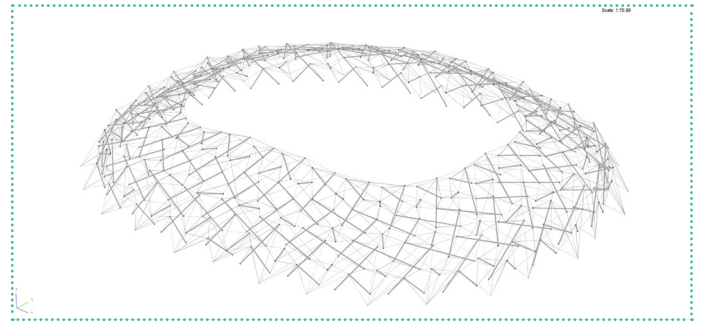
(f)

4.20. Form-finding results

The form-found shapes depend on the pre-stress forces. One has to repeat the form-finding process several times to make the structure less flat, becoming more domical geometries. the inner ring needs to be made out of a stiff 3d-frame which should be as lightweight as possible.
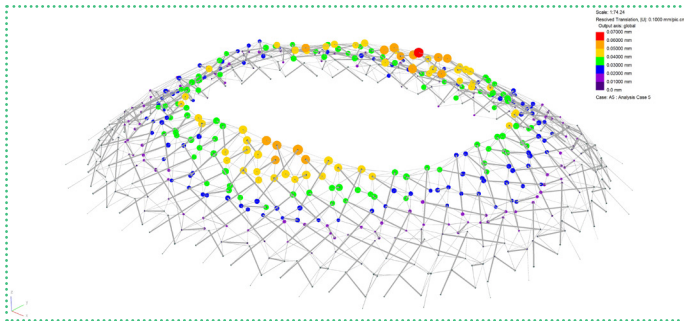
(a)
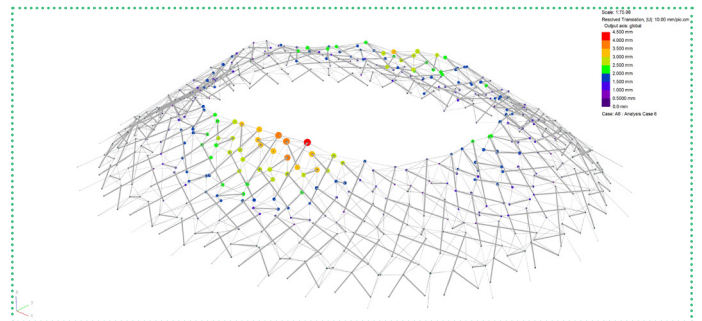
(b)
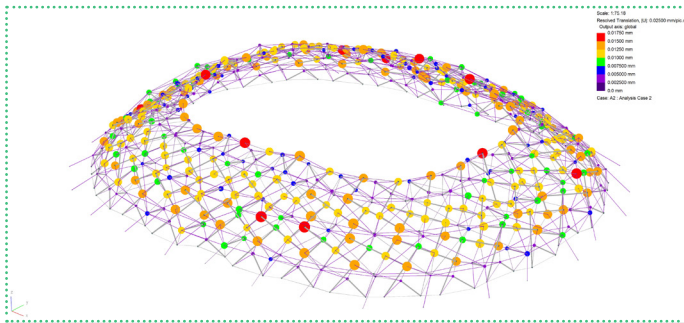
(c)
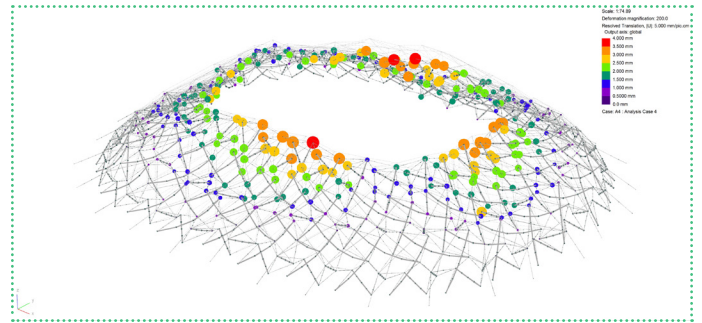
(d)
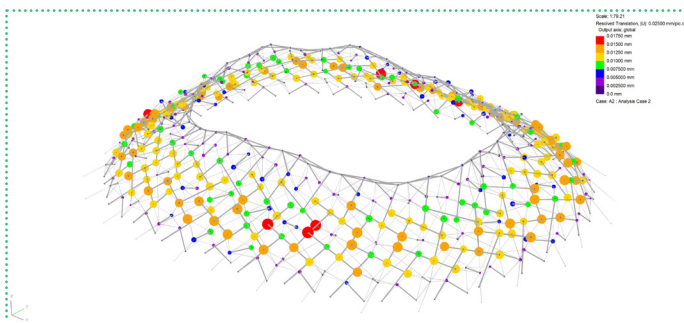
(e)
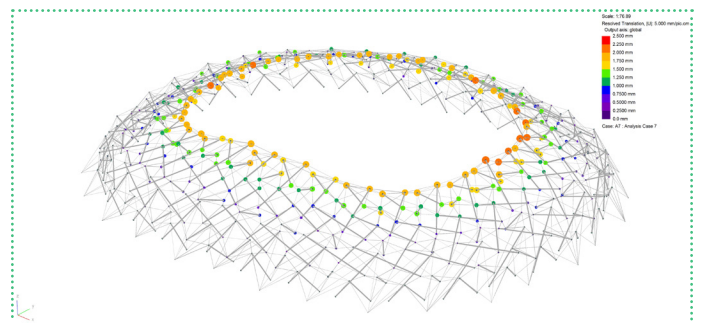
(f)

4.21. Node displacements caused by gravity

After form-finding processes in oasys gsa, the structures became very stiff, and it handled very well the gravity load. The displacements are relatively small, much smaller than the limts (l/250 = 3700/250 = 14.8mm).

The areas around the inner ring are the weakest areas. It is expected because of the large central opening.
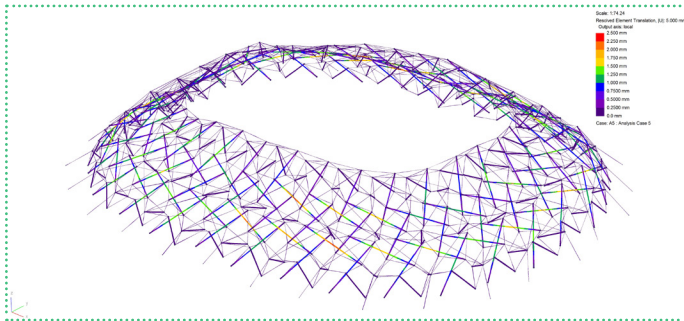
(a)
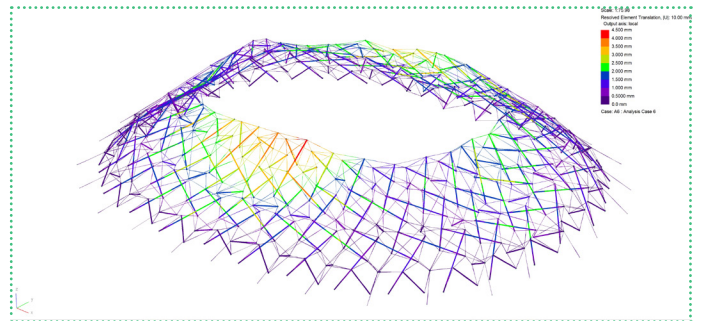
(b)
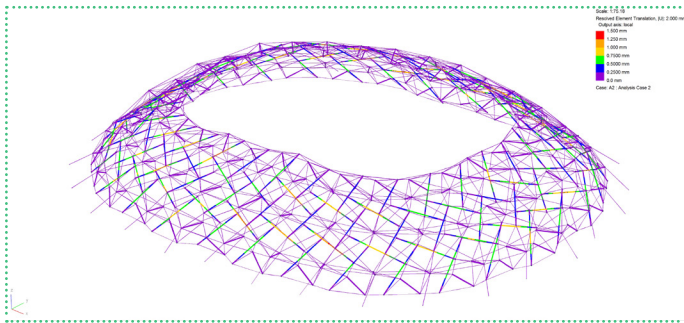
(c)
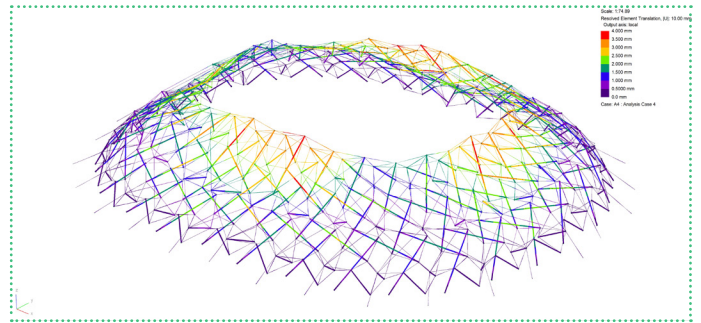
(d)
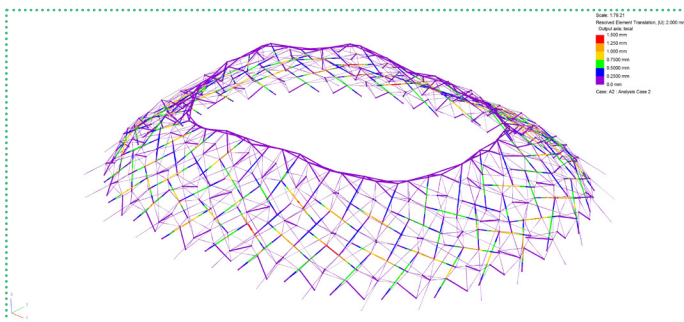
(e)
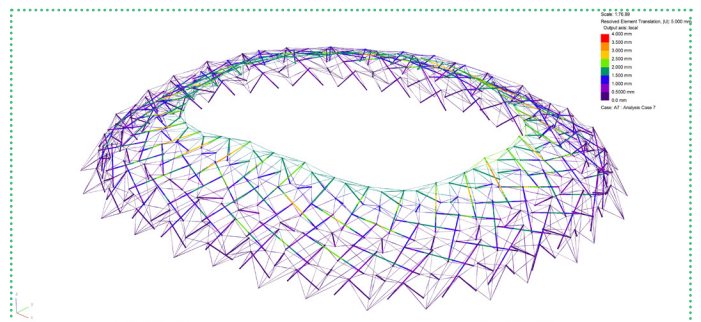
(f)

4.22. Beam displacements caused by gravity

Similar to node disppacements, beams deformed mostly around the central opening. the more pre-stress forces are applied, the stiffer the systems are. there are also displacements in the middle of struts which are caused by the large axial forces inside the structural elements.

When the bottom struts are fixed, the structure performed more equally. in other models, the largest deformations are in the middle on the edge of the inner ring.
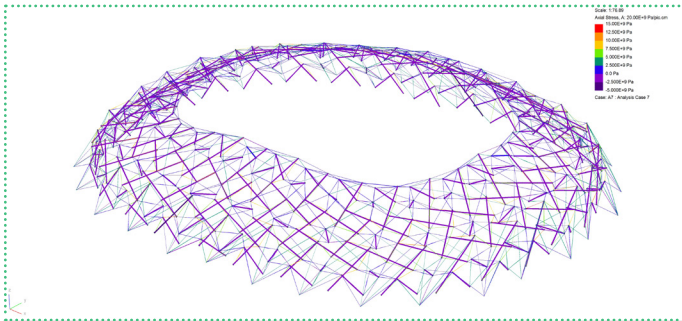
(a)
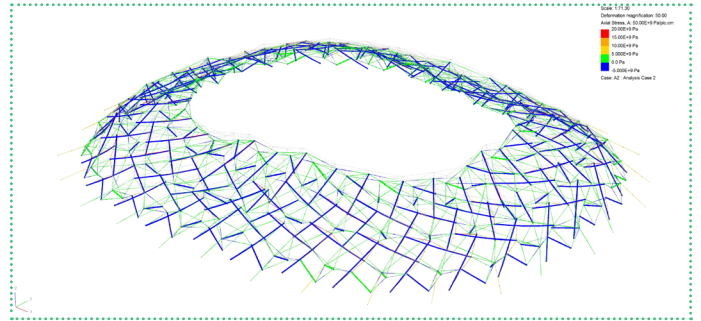
(b)
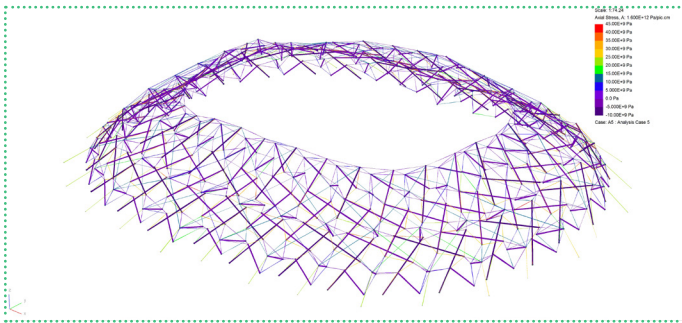
(c)

Both struts and cables are subjected to axial stresses. in these models, maximum axial stresses are relatively small compared to young's modulus of steel: 2,05e+11 pa.

4.23. Axial stresses caused by gravity
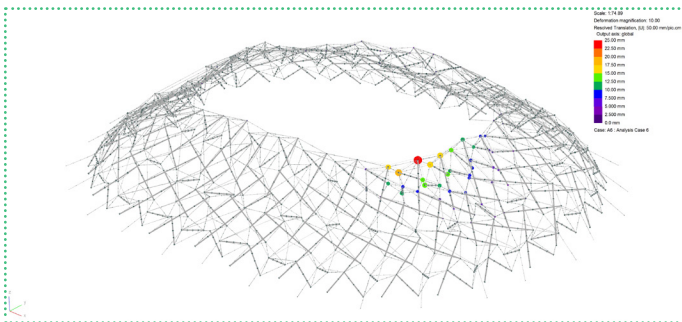
(a) Node deformations
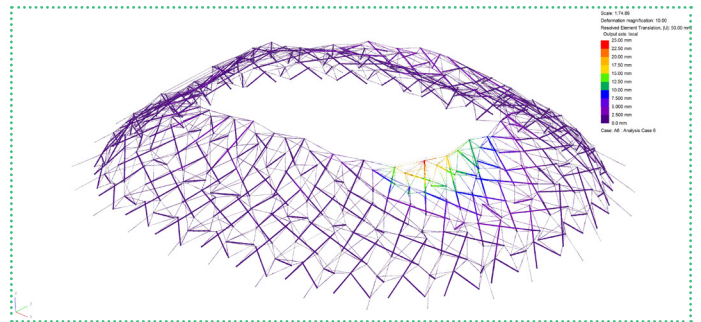
(b) Beam deformations

4.24. Displacements caused by nodal loading

When a nodal load is applied, the surrounding areas are affected in all directions. This behavior is also similar to the physical model. The rigidity of tensegrity structures depends on the pre-stress forces in cables which gives the structure the state of self-stress. Soap film and force density method cannot be applicable in this type of tensegrity, only 'ignore form-finding properties' works. This technique takes the deformed shape and internal loading from form-finding as the input for the next analysis.

(a)

(b)

(c)

(d)
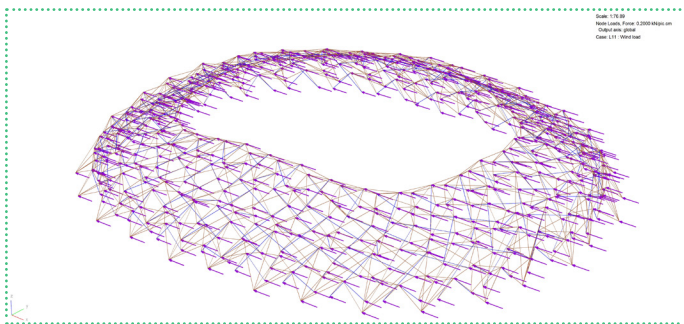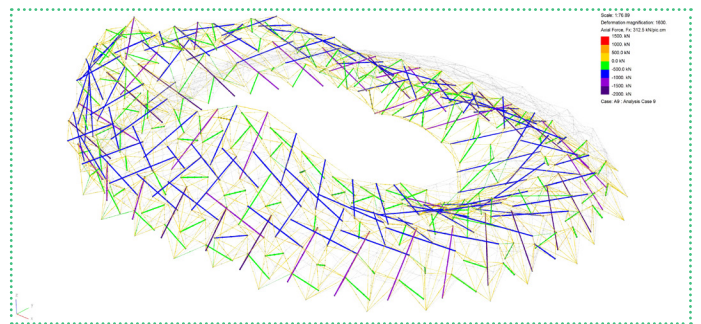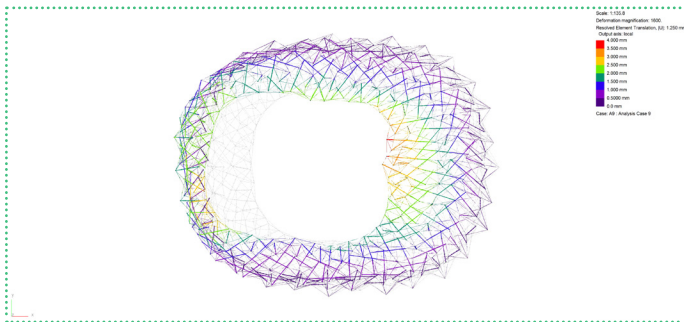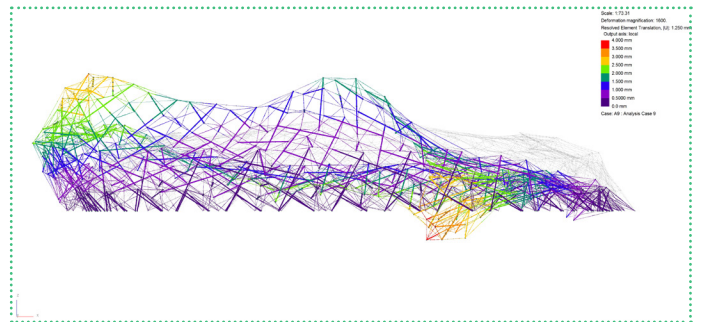
4.25. Wind loaidng

Checking the affect of lateral, asymetrical loading is crucial for such a flexible system like tensegrity. the roof performed very well. The displacement is relatively small compared to the span.

4.5. Final Structural Model

After several experiments with form-finding of simplified structural models, the real scale model is tested. This final model has the same amount of struts with the simplified model, but the size is in the real dimensions 240x240x45 m. In this model, a top truss and a bottom truss are introduced. Both of them are triangular truss. The top one is to stabilize the shape during the form-finding process and ensure a better structural performance after that. The bottom one is to lift up the entire tensegrity structure from the ground because of security reason in an emergency situation as well as to facilitate the circulation of such a complex public building. These following steps are applied:

(1) Constructing double-surface tensegrity roof within the perimeter using the Python code achieved from chapter 3. There is still a need to edit struts on the edges of the two surfaces.

(2) Adding structural properties to the geometric computational model. Bar element and tie element are chosen for struts and cables respectively. Struts have a CHS406,4x6,3 section. Steel cables are Ø40 and spiral. Bar element is also chosen for the top and bottom truss, the top ones have a CHS406,4x6,3 section, and the top ones have a CHS193,7x5 section. Different from previous models in which only the bottom of the model is pinned, the top is left free, this time both the top and bottom of the model are pinned initially.

(3) Adding load cases (will be explained with description for every load case as well as load combination)

(4) Form-finding. After (4.7), top truss nodes are unpinned for the last form-finding (4.8).
　　(4.1) Form-finding 1: Cable pre-stress forces (500 kN)
　　(4.2) Form-finding 2: Cable pre-stress forces (500kN) + Gravity
　　(4.3) Form-finding 3: Cable pre-stress forces (500 kN)
　　(4.4) Form-finding 4: Cable pre-stress forces (500 kN)
　　(4.5) Form-finding 5: Cable pre-stress forces (500 kN)
　　(4.6) Form-finding 6: Cable pre-stress forces (500 kN)
　　(4.7) Form-finding 7: Cable pre-stress forces (500 kN)
　　(4.8) Form-finding 8: Cable pre-stress forces + Gravity + Dead loads. After this, the model will not deform under gravity and dead loads
(5) Structural analysis (Serviceability Limit State - SLS, Ultimate Limit State - USL)
　　(5.1) Load combination 1
　　(5.2) Load combination 2
　　(5.3) Load combination 3
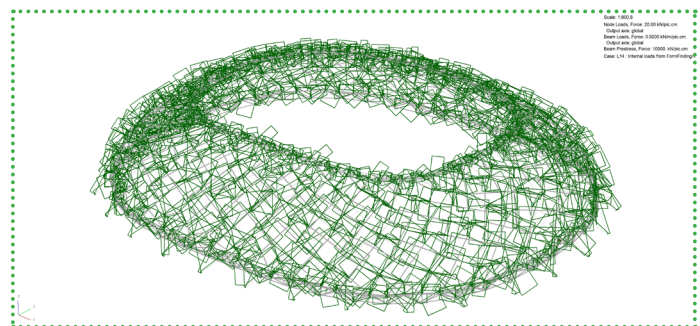　　(5.4) Load combination 4

Load Cases

There are five major load cases one should consider. These are the pre-stress forces, self-weight (or gravity), dead loads, snow load, and wind load. For each load, a description is given as well as an estimation of the magnitude of the load. Dead loads and live loads are always applied on struts as point loads. This means that when a surface load is given, the relevant area for the strut must be calculated. The pre-stress force is an axial load (or beam loading), and the self-weight is a line load.

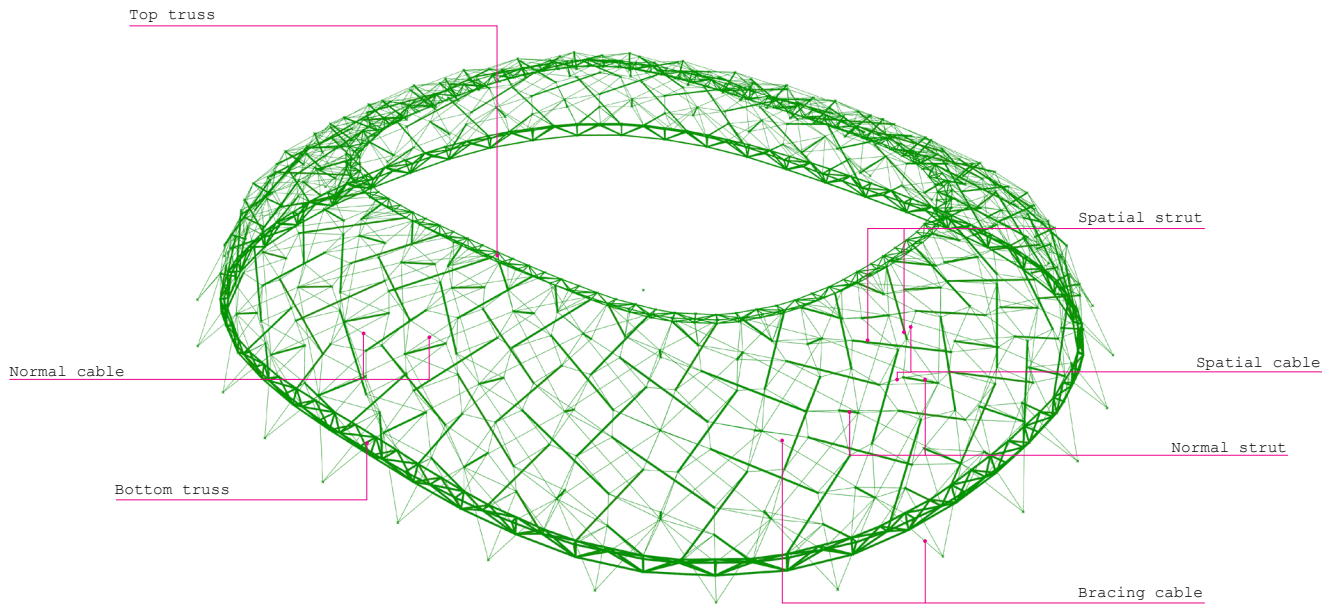Load case 1. Internal load given by form-finding process

After the form-finding process, cables (tie elements) have internal tensile forces and struts (bar elements) have internal compressive forces. Initial pre-stress forces given to cables is 5000 kN.
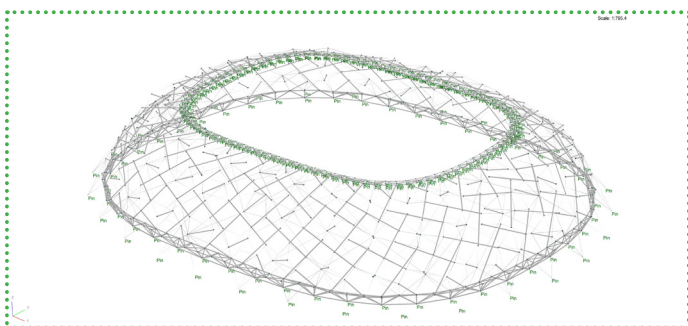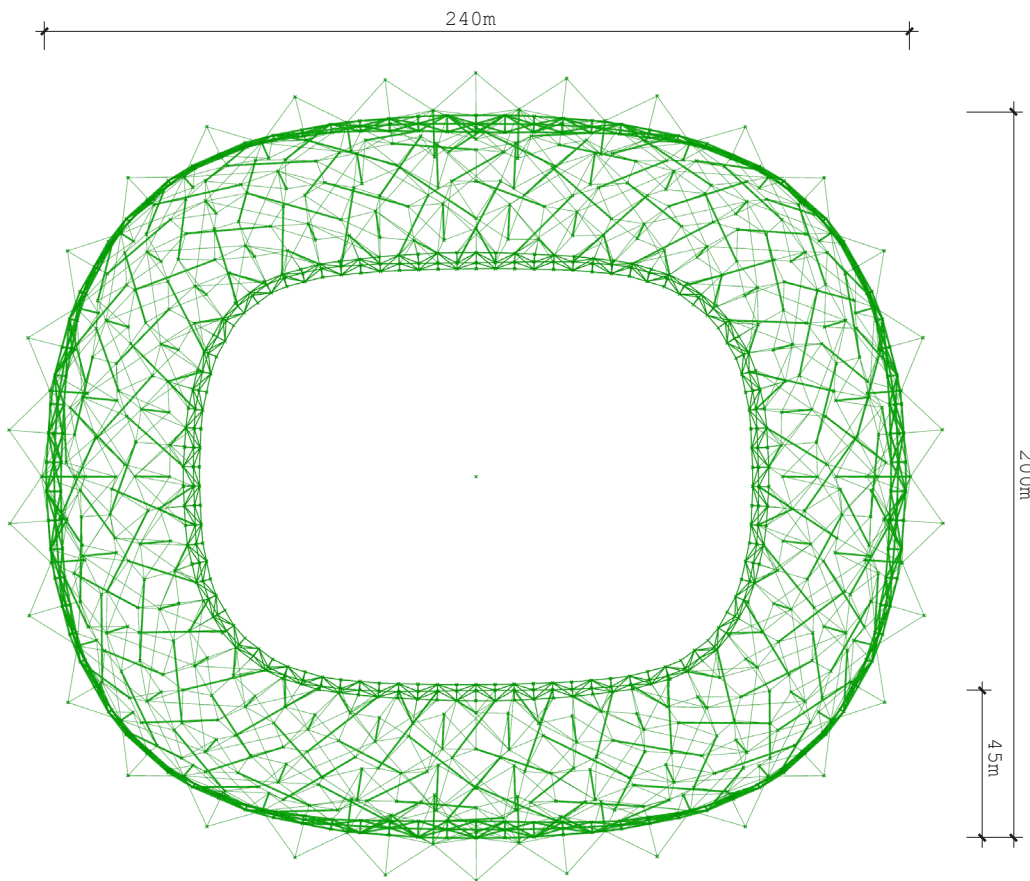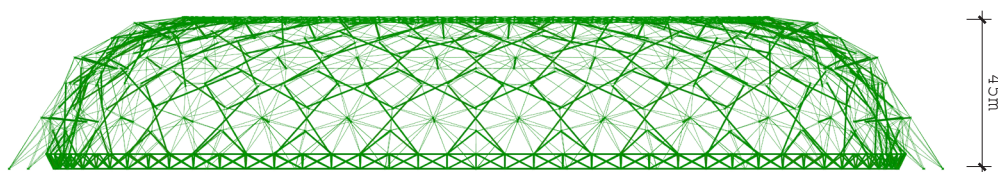

4.26. Restraint condition for form-finding

4.27. Internal loads from form-finding

Top truss

Spatial strut

Normal cable

Spatial cable

Normal strut

Bottom truss

Bracing cable

(a) Perspective

240m

200m

45m

(b) Plan

45m

(c) Elevation

4.28. Final Structural Model

Load case 2. Self-weight

Self-weight represents a significant load case for tensegrity structures since it provides the presence of gravity. Oasys GSA can calculate the self-weight of the model by itself after applying structural properties to the system. This load depends on the sectional properties of structural elements and materials in use.

4.29. Self-weight diagram

Load case 3. Dead load

Dead loads are loads consisting of the roof cladding, technical installations, and possible service walkways which are suspended from the roof structure. It is not possible to know these loads beforehand, yet these loads should be included depending on the function of the building on which the tensegrity dome is fitted. In the Netherlands, the number of installations suspended from the roof is very limited in, for example, football and ice-skating stadiums. Walkways and technical facilities are thus neglected. A small amount of dead loading can be determined.

Cladding:

4.30. Cladding layer is underneath the structure

ETFE foil: 2 to 3,5 kg/m2
Suppose 2 sheets (for instance when pneumatic cushion are used)
100kg = 1kN
$3,5*2/100 = 0.07$ kN/m2
Possible support system for the cladding:
Phi35 steel cable, with a weight of 6,8 kg/m2
Suppose a 3x3 grid, then 6 meters of cable per 9 m2 of roof surface
$6,8*6/9 = 4,53$ kg/m2 = 0,5 kN/m2
Total dead load:
$0,07 + 0,05 = 0,12$ kN/m2
The surface loads are applied on the struts. To simplify the load case, let's assume that the weight of cladding is distributed equally over the tensegrity netwrok on 600 nodes as ends of 300 struts.
Area of the roof: 13800 (m^2)
Nodal load: $13800*0,12/600 = 2.76$ kN

4.31. Cladding load diagram

Load case 4: Snow load

Snow loading is a variable load. It was chosen to use a uniform snow load, on a surface with an angle not steeper than 30°. It is convenient to define a uniform load per m2. The load is determined using the (Dutch) Eurocode.
q_{snow} = S = ν_I (at 0° inclination) = 0,8
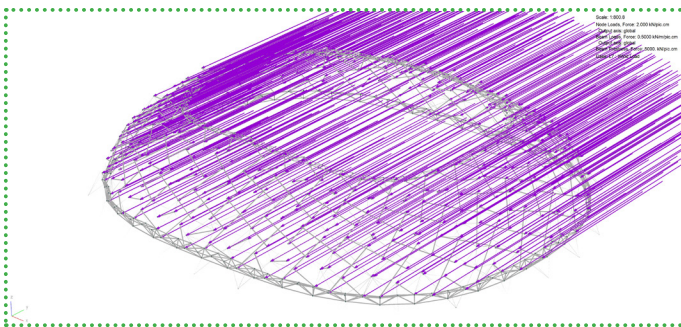Ce = 1,0
Ct = 1,0
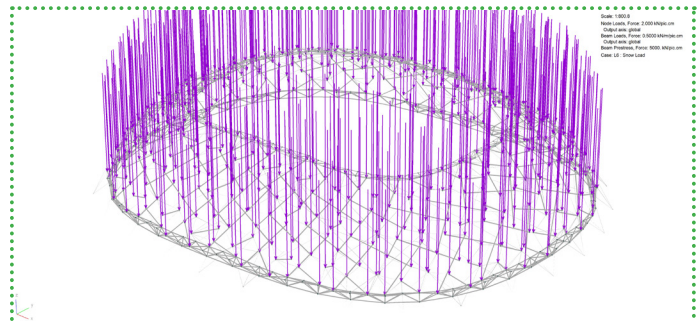
4.32. Snow load diagram
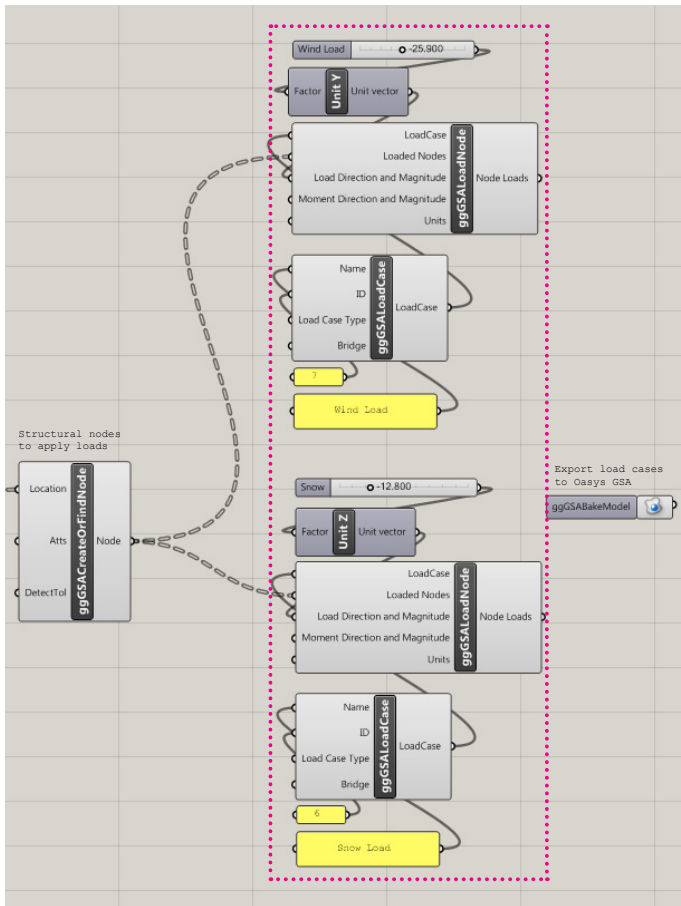
4.33. Grasshopper components for Snow load and Wind load

4.34. Wind load diagram, simplified the direction to horizontal y direction

$S_k = 0,7$ kN/m2

$q_{snow} = S = 0,8*1,0*1,0*0,7 = 0,56$ kN/m2

It was chosen to only investigate a uniform snow load. It is possible that a non-uniform load will be normative in some cases, but due to time restrictions, it is not included.

Load case 5: Wind load

In the case of a tensegrity structure which rises from the ground up to 45 m, the wind load is the non-uniform live load. To be able to calculate the winds on the roof, assumptions must be made for instance the location of the structure and the attitude of the structure.
It was chosen to use the geological features for a tensegrity structure in Rotterdam since this is the location of the Feyenoord stadium. Suction pressures are assumed to operate perpendicular to the surface of the structure with wind area II (Rotterdam, the Netherlands), built environment (in the city) and the presumed height above ground level of the tensegrity structure is 45m. This indicates:

$$q_{wind} = q_{p(Ze)} = 1,10 \text{ kN/m2}$$

$$C_s*C_d = 1$$

The wind load becomes:

$$W_e = q_{wind}*C_s*C_d = q_{p(Ze)}$$

It is also noted that the wind loads are largely simplified and do not always represent the actual wind loading on a real structure. The schematization may not reflect the load conditions on a concave shaped top cable that well.

Load Combinations

For the ultimate limit state load combinations, safety factors are used. The factors are chosen so that they represent the most unfavorable case. For the Serviceability Limit State, no safety factors are used. Not that no safety factor is included for the presentation load case. This is due to the measurability of this load case during construction.

The load combinations are:

Load combination 1: Pre-stress forces, self-weight and dead loads (LC1 + LC2 + LC3)

Ultimate Limit State (axial forces,

weights, and support reactions):
LC1 + 1,35*LC2 + 1,35*LC3

Serviceability Limit State (node
displacement):
LC1 + LC2 + LC3

Load combination 2: Pre-stress forces,
self-weight, dead loads, and snow load
(LC1 + LC2 + LC3 + LC4)

Ultimate Limit State (axial forces,
weights, and support reactions):
LC1 + 1,2*LC2 + 1,2*LC3 + 1,5*LC4

Serviceability Limit State (node
displacement):
LC1 + LC2 + LC3 + LC4

Load combination 3: Pre-stress forces,
self-weight, dead loads, and wind load
(LC1 + LC2 + LC3 + LC5)

Ultimate Limit State (axial forces and
support reactions)
LC1 + 0,9*LC2 + 0,9*LC3 + 1,5*LC5

Serviceability Limit State (node
displacement):
LC1 + LC2 + LC3 + LC5

Note: in this case, multiplying self-
weight and the dead loads with a safety
factor of 0,9 which is usually considered
a favorable safety factor, results in the
normative analysis case.

A very particular combination has been
examined.

Load combination 4: Pre-stress forces
(LC1)

Ultimate Limit State (axial forces and
support reactions):
LC1

This load combination is needed to figure
out the distribution of the pre-stress
forces in the tensegrity system so that
these pre-stress forces can be applied
directly to the cables and struts. In
this way, the actual distribution of pre-
stress forces in the system is preserved.
The pre-stress forces are varied over
the system, which made an impact on the
final form of the tensegrity shell. The
relationship between sizes of structural
elements and axial forces is essential in
a tensegrity system.

This load combination is never normative
for the finding the required sectional
properties in the tensegrity system. It is

only used to find the correct distribution
of pre-stress forces to form the expected
geometries.

Structural Requirements

The primary requirements for a building
are strength, stiffness, and stability.
This is an essential distinction for the
requirements of the structural design
of a building. Suppose a tensegrity
shell is strong enough to withstand any
occurring forces, then the structure
may still be considered unsafe due to
stiffness requirements. Stiffness is
required for building materials because
large displacements can break or tear
materials apart. But it is also required
for providing a safe feeling to the
users of a building. A well-performing
tensegrity structure must, therefore,
meet some safety requirements. Normally,
safety is divided between the Ultimate
Limit State (ULS) and the Serviceability
Limit State (SLS). Each of those states
has safety factors which are multiplied
by the occurring loads to simulate the
most extreme circumstances to which a
tensegrity structure may be exposed.
From analyzing the structure, there are
some observations that three cases of
failure can occur for a tensegrity shell:
1. The nodal displacements are too much
2. The distribution of pre-stress forces
are not expected
3. Element strengths can be small, which
leads to buckling
When an investigation is made to find the
lowest amount of required pre-stress
forces in the tensegrity structure, at
least one of the first two cases will be
the normative case. The element strengths
are always applicable.
Other structural requirements like
vibrations are also possible. To limit the
scope of the investigation, this is not
considered.

Displacements

The nodes in a tensegrity structure will
deformed because of the loads on the
system. It could be due to external loads,
pre-stress forces, and also there is
difference in node location between the
original design and the structure under
the dead loads inly (load combination 1),
since a tensegrity must always deform to
find equilibrium.

The deformation requirements are chosen to
be relative to the tensegrity structure
under dead loads. This means the two
extreme cases (snow and wind) and their

added nodal displacements must be within a certain margin.

The possible locations of a single node are provided in different conditions:
1. The original design location of the node
2. The location of that node when the tensegrity is loaded with pre-stress forces, self-weight, and dead load
3. The location under snow load
4. The location under wind load

Displacements for nodes under snow and wind conditions (3 and 4) are limited by the dashed boundary and are about the dead load case. The maximum displacement condition gives the distance between the dashed line and node location two.

Usually, the ratio between vertical nodal deformation and span length for roofs in the Netherlands is:
$$\sigma_{max} = l_{span} / 250 \text{ (mm)}$$
So that for a span of 25 m, the maximum allowed deformation would be 100 mm. The ratio may, however, be less applicable for tensegrity domes since the nodal deformations are in any direction x, y, z and the ration is usually used for shorter spans. Since the length of the span is equal to the diameter of the entire structure, 'S' can be substituted for lspan.
Finally, it was chosen to limit the direction of node deformation using:
$$\sigma_{max} = S/200 \text{ (mm)}$$
The maximum displacement for a 25m span is then 125mm in any direction.
Only the nodes at the tops of the struts are considered in the investigation. This choice is based on the idea that the bottom nodes are not connected to cladding system. Therefore, it cannot tear or break the cladding. It will be very difficult to notice node translation at the bottom parts of the struts for the general public, since it cannot be referenced to another point very well, unlike the top nodes, which relate directly to the cladding.
There are a few factors which influence the stiffness of the tensegrity dome. These are:
1. Geometry and topology of the dome
2. Young's modulus (E)
3. Sectional properties (A)
4. Pre-stress forces (F_p)
5. Steel grades (f_{Rk} or f_y)

The Young's modulus and the steel grades are kept constant. The choices are very critical, but they are dependent on the availability of products in the market.

It is evident that if a comparison among the various geometries and topologies is to be made, the other factors must be allowed to change between different tensegrity structures. Of course, when the geometry and topology are deliberately set at the given specifications beforehand in the variant study, we should optimize the system using the height of pre-stress forces and sectional properties.

If we were to build a tensegrity structure, we would choose different sectional properties for each element type. Changing the sectional properties leads to the changes in the stiffness and therefore the structural behavior of the entire system. Doing so will result in an iterative design process. This is, of course, demanding a lot of work, and limiting the time available to investigate other variations of geometry and topology. Sections can be chosen for each element group. It is noted that this will lead to an unknown error margin. Ideally, all the section sizes should be optimized for each comparison.

There is a large difference in the way the tensegrity system deforms under each type of load. The difference is caused by the magnitude, the direction, and the location of the load. Since the dead load combination and snow load combination consist of a uniformly distributed load, we expect all similar type nodes to perform identically.

The wind, on the other hand, is a non-uniformly distributed load due to the form factors. As a result, some nodes will deform more than others.
In these figures, the dashed lines indicate the design position of the elements. The normal lines indicate the deformation that the tensegrity experiences. In order to give a good impression, the deformations are scaled.

Distribution of Forces

If the distribution of forces is correct throughout the tensegrity structure, collapse can occur. Often the load on the outermost struts (the struts belonging to tension hoop number one) is the highest, due to the surface area which must be carried by that strut. The result is a failure mode which visually resembles lateral torsional buckling in steel beams. The top cable is not stiff enough for the occurring forces and also lacks any lateral support. The struts consequently overturn. Of course, deformations will

also increase largely when the collapse occurs.

The failure mode can only occur when loads are in the z direction. When decreasing the pre-stress forces, or when applying too much snow load, an element in the system can reach 0 kN axial force, after which the system can fail. This is not always the case; for instance, when a single element is unloaded, the system can still be stable.

It would be good engineering practice to set a minimally needed axial tension or compression forces for all elements so that a pre-specified amount of pre-stress is always available. This ensures the desired structural behavior always occurs. This is done by setting a margin for the minimal normal force in an element in the tensegrity structure.

Element Strengths

In structural design, it is a priority to choose the smallest section possible for an element in the structural system. This reduces the mass in the structure that helps to save materials and the construction budget at the same time. For each type of geometry and topology, the optimization of the sectional properties can be quite different. Basically, in such a system of double-surface tensegrity, every element is working in a different direction which may lead to differences in sections. To make it simpler for construction, it can be classified into some kinds:
(1) Spatial strut: initial struts from tessellation of reference surfaces
(2) Normal strut: added struts perpendicular to the two surfaces
(3) Spatial cable: connecting spatial struts
(4) Normal cable: connecting normal struts to spatial struts
(5) Top truss
(6) Bottom truss

For determination of the appropriate section of cables, the normative tension is used, meaning that some cables will be oversized slightly. Individual sections can be chosen for all types, but this will lead to a challenging and lengthy search for equilibrium.

According to the Eurocode, all sections must satisfy unity check:

$$N_{Ed}/N_{Rd} + M_{y;Ed}/M_{y;Rd} + M_{z;Ed}/M_{z;Rd} \leq 1$$

For sections in tension (the cables), the unity check can be reduced to:

$$N_{Ed}/N_{c;Rd} \leq 1,0$$

In which
N_{Ed}: The occurring tension force in the element
$N_{c;Rd}$: The capacity for tension force in the element

The cable products of Pfeifer Cable Structures are chosen for the system. The assumed cables are full locked cables, which allow limit tensions from 250 to 15000 kN. This is at the same time the maximum allowable tension in the tensegrity system when higher strengths are needed, the tensegrity will be assumed not to be efficient designed, and omitted from the analysis.

Choosing the best cable section is very important for the mass of the tensegrity shell. If a section is chosen which leads to a unity of 0,4, the section is strong enough for the load which is applied, but 60% of the section is not used. This is called over-dimensioning. To prevent this, a minimum unity check value was chosen at 0,8. This can occur when the load is too much to withstand (unity > 1) or when the section is over-dimensioned (unity check < 0,8). Therefore, the unity check becomes:

$$0,8 \leq N_{Ed}/N_{c;Rd} \leq 1,0$$

For sections in compression, a distinction can be made between members subjected to buckling (compression only) and lateral-torsional buckling (compression and bending).

Buckling occurs in compression members in the tensegrity structure. The unity check is:

$$N_{Ed}/(\chi*A*f_{y}/\gamma_{M1}) \leq 1,0$$

In which
χ: The reduction factor for the applicable buckling condition
A: The sectional area of the member
f_{y}: The yield tension of the member
γ_{M1}: A partial safety factor (assumed to be equal to 1)

Over-dimensioning can also be a problem for the struts, so (analogous to cables) the unity check is modified to:

$$0,8 \leq N_{Ed}/(\chi*A*f_{y}/\gamma_{M1}) \leq 1,0$$

Because of their favorite properties, hot

rolled circular hollow sections (CHS) are assumed in the tensegrity systems. It is also convenient to have the same moments of inertia for both axes; the buckling checks can then be reduced to a single check.

GF GALFAN Coated Steel - Full Locked Strands

PFEIFER

VVS-1   VVS-2   VVS-3

Material: Unalloyed quality steel
Modulus of Elasticity: 160 ± 10 kN/mm²
Tolerance Wire Diameter: +3%
Corrosion Protection: Inner layers: Hot dip galvanized with inner filling
Outer layers: GALFAN coated without inner filling

NOMINAL CABLE DIAMETER	CABLE CONSTRUCTION	METALLIC CROSS SECTION AREA	MINIMUM BREAKING LOAD			WEIGHT APPROX
mm		mm²	kN	kg	lb	kg/m
21.0	VVS-1	281.0	405	25000	91040	2.4
26.0	VVS-1	430.0	621	38360	139600	3.6
31.0	VVS-2	634.0	916	56630	205920	5.3
35.0	VVS-2	808.0	1170	72340	263020	6.8
40.0	VVS-2	1060.0	1520	93970	341710	8.9
45.0	VVS-2	1340.0	1930	119380	433880	11.2
50.0	VVS-2	1650.0	2380	147140	535040	13.8
55.0	VVS-3	2090.0	3020	186730	678920	17.2
60.0	VVS-3	2490.0	3590	222040	807060	20.5
65.0	VVS-3	2920.0	4220	261020	948690	24.1
70.0	VVS-3	3390.0	4890	302440	1099310	27.9
75.0	VVS-3	3890.0	5620	347550	1263420	32.1
80.0	VVS-3	4420.0	6390	395200	1436520	36,4
85.0	VVS-3	4990.0	7210	445910	1620870	41.1
90.0	VVS-3	5600.0	8090	500300	1818700	46.2
95.0	VVS-3	6310.0	9110	563360	2048000	52.0
100.0	VVS-3	6990.0	10100	624590	2270570	57.6

4.35(a). Pfeifer Cable Structure, GALFAN Coated Steel - FUll Locked Strands

SS Stainless Steel - Open Strands

1x19   1x61   1x91

Material: Grade 316

NOMINAL CABLE DIAMETER		CABLE CONSTRUCTION	METALLIC CROSS SECTION AREA	MINIMUM BREAKING LOAD			WEIGHT APPROX
mm	in.		mm²	kN	kg	lb	kg/m
2.5	-	1 x 19	3.7	4.9	500	1100	0.031
3.0	1/8	1 x 19	5.4	7.0	720	1580	0.045
4.0	5/32	1 x 19	9.6	12.6	1280	2830	0.079
-	3/16	1 x 19	13.5	18.9	1930	4255	0.113
5.0	-	1 x 19	15.0	19.6	2000	4410	0.124
-	7/32	1 x 19	18.0	24.2	2470	5440	0.145
6.0	-	1 x 19	21.5	28.0	2870	6340	0.178
-	1/4	1 x 19	24.1	34.0	3440	7584	0.198
7.0	9/32	1 x 19	29.2	35.0	3540	7800	0.243
8.0	5/16	1 x 19	38.2	45.4	4640	10220	0.317
-	3/8	1 x 19	54.2	64.0	6546	14434	0.446
10.0	-	1 x 19	59.7	71.0	7250	15980	0.495
-	7/16	1 x 19	73.7	86.0	8770	19335	0.624
12.0	-	1 x 19	86.0	102.0	10400	22930	0.713
-	1/2	1 x 19	96.3	119.0	12101	26678	0.804
14.0	9/16	1 x 19	117.0	139.0	14170	31240	0.971
16.0	5/8	1 x 19	153.0	182.0	18550	40910	1.270

4.35(b). Pfeifer Cable Structure, GALFAN Coated Steel - Open Strands

Form-finding Result
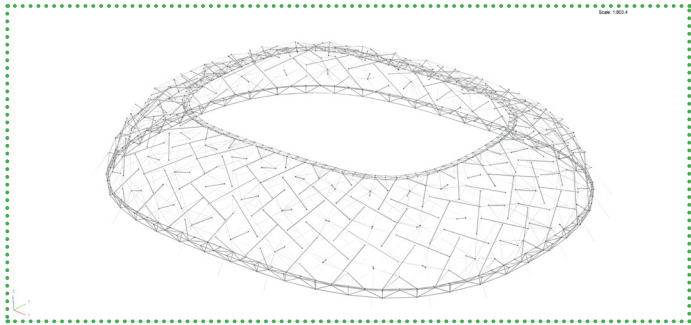
(a) Perspective
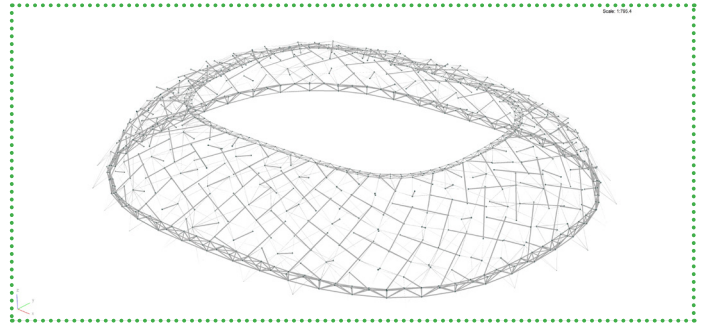
(a) Perspective
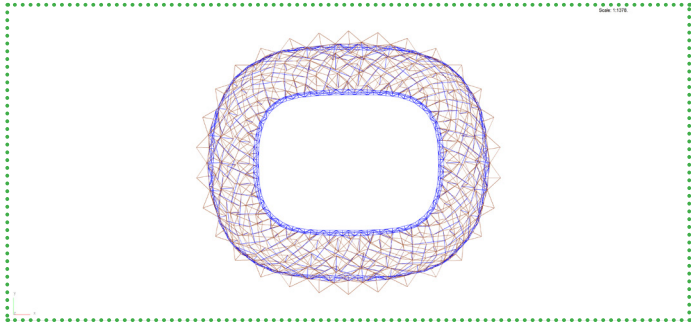
(b) Plan
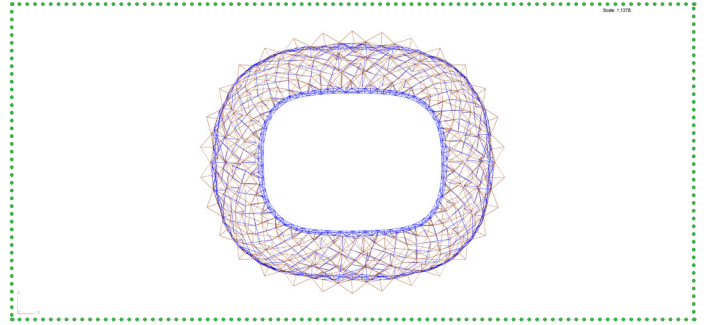
(b) Plan
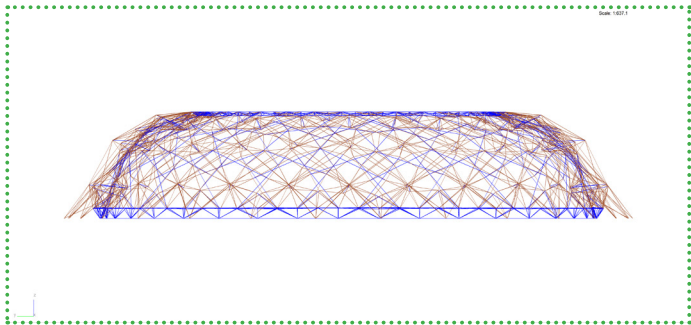
(c) Elevation, short side
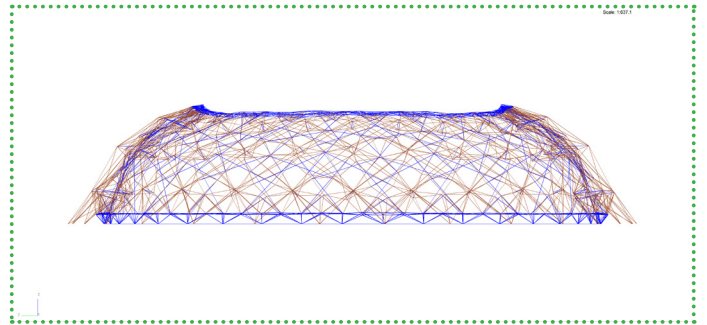
(c) Elevation, short side
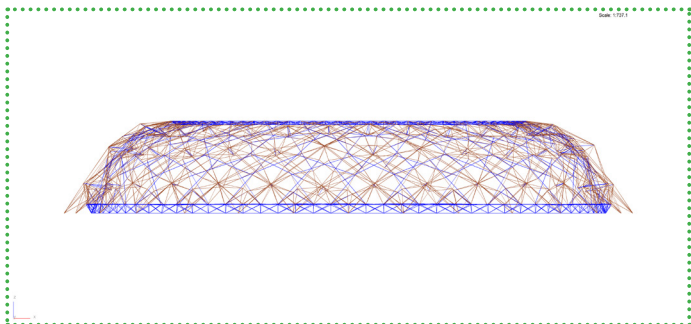
(d) Elevation, long side
4.36. Designed form
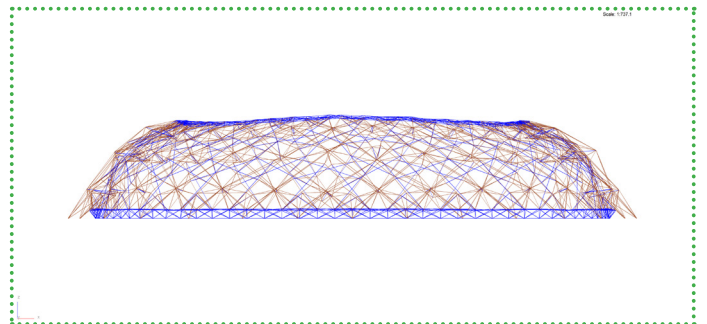
(d) Elevation, long side
4.37. Form-found

Compare to the previous form-finding results, the final one improved enormously. Although struts are slightly displaced locally, the shape, composition, and structural topology are reserved. The top ring helps to stabilize the geometry. Fixing while the form-finding were conducting leads to redistribute the right pre-stress forces until the structure achieves the right state of re-stress that it can stand by itself remarkably.

After the form-finding process, the top ring slightly deforms following sine-shape. On the long edge, it deformed upwards. On the short edge, it deforms downwards. The conners stay the same level with the pre-form-finding structure.

Structural Analysis Result

Displacement

Considering the span is 240m, the maximum deformation of 240/200 = 1.2m (1200mm) is allowed.

With load combination 1 (Pre-stress forces + Self-weight + Cladding), the maximum deformations are 0.3mm and 100mm for SLS and ULS respectively. These displacements are incredibly small that proves the stability of the structure against gravity with the help of appropriate pre-stress forces. In SLS case, critical deformations appear in the middle of the structure. In ULS case, the critical deformations appear in the middle of the longer edges of the top ring.

With load combination 2 (Pre-stress forces + Self-weight + Cladding + Snow), the maximum deformations are 400mm and 700mm for SLS and ULS respectively. They are in the limits. The largest displacements are in the middle of long edges of the top ring, and they are smaller towards the bottom ring.

With load combination 3 (Pre-stress forces + Self-weight + Cladding + Wind), the maximum deformations are 650mm and 1058mm for the SLS and ULS respectively. These numbers are large but they remain in the limits. Also, considering the height of the total structure is 45m, these numbers are obviously acceptable. When the wind hits the structure, it distorts the top part following sine-shape. One side of the structure directed to the wind deforms downwards while the opposite site deforms upwards.

With the last load combination, only pre-stress forces are taken into consideration. The structure deforms all the way upwards, the maximum deformation is 300mm on the mid-span of the long edges of the top ring. This explains that with the effect of gravity to its self-weight and cladding, the structure will move downwards to the designed levels.

Support Reaction

The results of support reactions are stable over different load combinations. Especially, in the last combination, there is no influence of gravity, the support reactions are very similar to other load cases. This proves that the pre-stress forces are the main factor which surpasses the impact of other load cases, such as gravity, snow, and wind. In almost all the cases, support reactions range from 2500 kN to 9000 kN. In the extreme case of the wind hitting the larger sides of the structure, the maximum increases slightly to 10000 kN.

Axial Force

The axial forces vary from -1500 kN to 1250 kN which is the range of 40mm GALFAN Coated Steel - Full Locked Strands cable from Pfeifer Cable Structure from Germany. Axial forces inside normal cables are relatively small compared to the rest. There are pure compressive forces in struts and pure tensile forces in cables. Compression and tension both occur in the top and bottom truss, the magnitudes are small compared to forces inside struts and cables. In most of the cases, these numbers remain stable.

Axial Stress

Axial stresses vary from -400 MPa to 1000 MPa while the modulus of elasticity of cable is 160000 Mpa. The results are in the limits. Axial stresses in the elements in the middle of the structure are the largest numbers. These numbers become smaller towards the top and bottom rings.

From 300 Struts to 4200 Struts

There are 300 struts in structural model due to computational expensive calculation. In reality, the structure will have 4200 struts. Therefore, the maximum axial forces and stresses will be smaller. As a result, the structural element will be more optimized. This mean diameter of cables can be decrease from 40mm to 12mm or smaller, picture 4.35-36. And the diameter of CHS struts can be decrease from 400mm to 150-100mm.

$$\frac{\text{the number of struts in model}}{\text{the number of struts in reality}} = \frac{300}{4200} = 0,07$$

$F_{compression;max;reality}$ = 1500.0,07 = 105 kN
$F_{tension;max;reality}$ = 1250.0,07 = 87.5 kN
$\sigma_{compression;max;reality}$ = 400.0,07 = 28 MPa
$\sigma_{tension;max;reality}$ = 1000.0,07 = 70 MPa

Buckling of Struts

The longest strut is 10 [m] with two ends pinned K = 1, CHS139x10, I = 868.10^4 [mm^4]. Maximum load can be handled by strut following Euler's formula:
$F_{max\ (139.3x10)}$ = π^2.EI/(KL)^2
= 3,14^2.210000.868.10^4/(1.10000)^2
= 85810 [N] = 179,72 [kN]

$F_{max(139x10)}$ > $F_{compression;max;reality}$, so there is no buckling.

Scale: 1:800.8
Deformation magnification: 20.00
Resolved Translation, |U|: 0.5000 mm/pic.cm
Output axis: global
0.3000 mm
0.2750 mm
0.2500 mm
0.2250 mm
0.2000 mm
0.1750 mm
0.1500 mm
0.1250 mm
0.1000 mm
0.07500 mm
0.05000 mm
0.02500 mm
0.0 mm

Case: A10 : Load combination 1 (SLS): Pre-st

(a) Nodal displacements

Scale: 1:800.8
Deformation magnification: 20.00
Reaction Force, Fx: 5000. kN/pic.cm
Output axis: global
Reaction Force, Fy: 5000. kN/pic.cm
Output axis: global
Reaction Force, Fz: 5000. kN/pic.cm
Output axis: global
Resolved Reaction Force, |F|: 12500. kN/pic.s
Output axis: global
9000. kN
8500. kN
8000. kN
7500. kN
7000. kN
6500. kN
6000. kN
5500. kN
5000. kN
4500. kN
4000. kN
3500. kN
3000. kN
2500. kN
2000. kN
1500. kN
1000. kN
500.0 kN
0.0 kN

Case: A10 : Load combination 1 (SLS): Pre-s

(b) Support reactions

4.38. Load combination 1 (SLS): Pre-stress forces + Gravity + Cladding

■	1250. kN
■	1000. kN
■	750. kN
■	500. kN
■	250. kN
■	0.0 kN
■	-250. kN
■	-500. kN
■	-750. kN
■	-1000. kN
■	-1250. kN
■	-1500. kN

Case: A10 : Load combination 1 (SLS): Pre-s

(c) Axial forces

■	10.00E+8 Pa
■	9.000E+8 Pa
■	8.000E+8 Pa
■	7.000E+8 Pa
■	6.000E+8 Pa
■	5.000E+8 Pa
■	4.000E+8 Pa
■	3.000E+8 Pa
■	2.000E+8 Pa
■	1.000E+8 Pa
■	0.0 Pa
■	-1.000E+8 Pa
■	-2.000E+8 Pa
■	-3.000E+8 Pa
■	-4.000E+8 Pa

Case: A10 : Load combination 1 (SLS): Pre-s
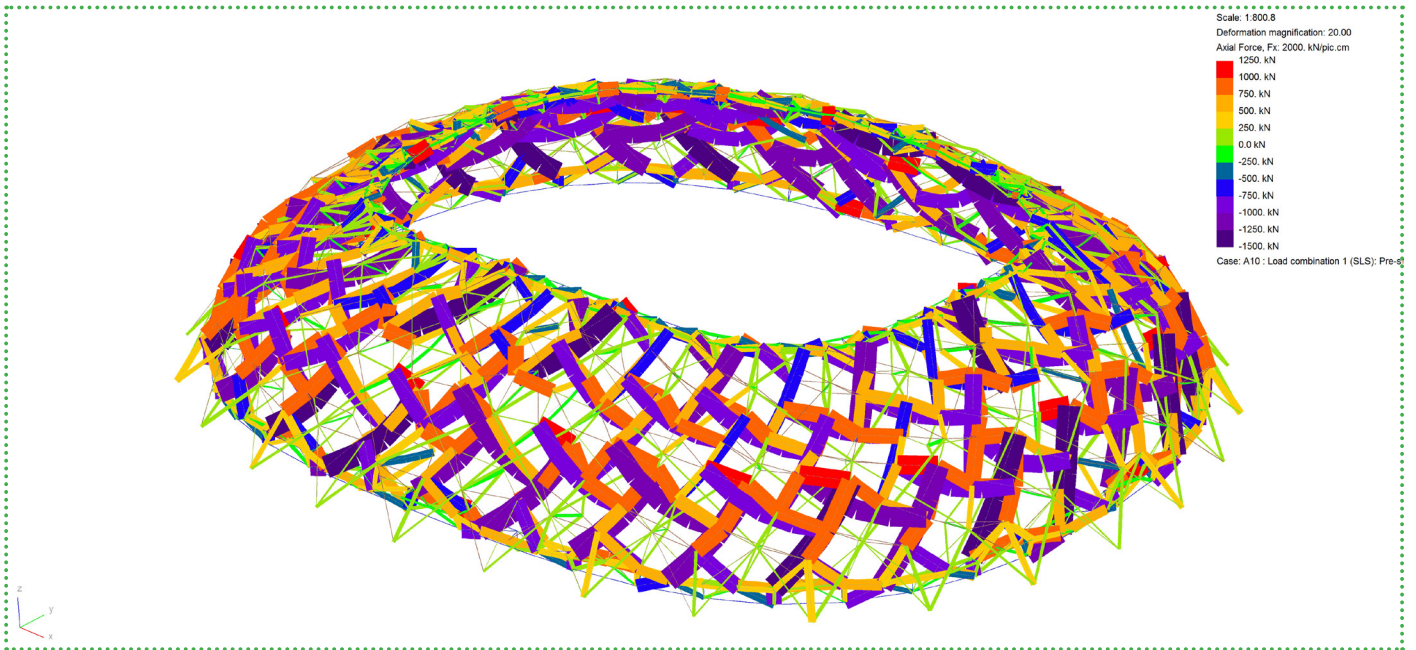
(d) Axial stresses

4.38. Load combination 1 (SLS): Pre-stress forces + Gravity + Cladding
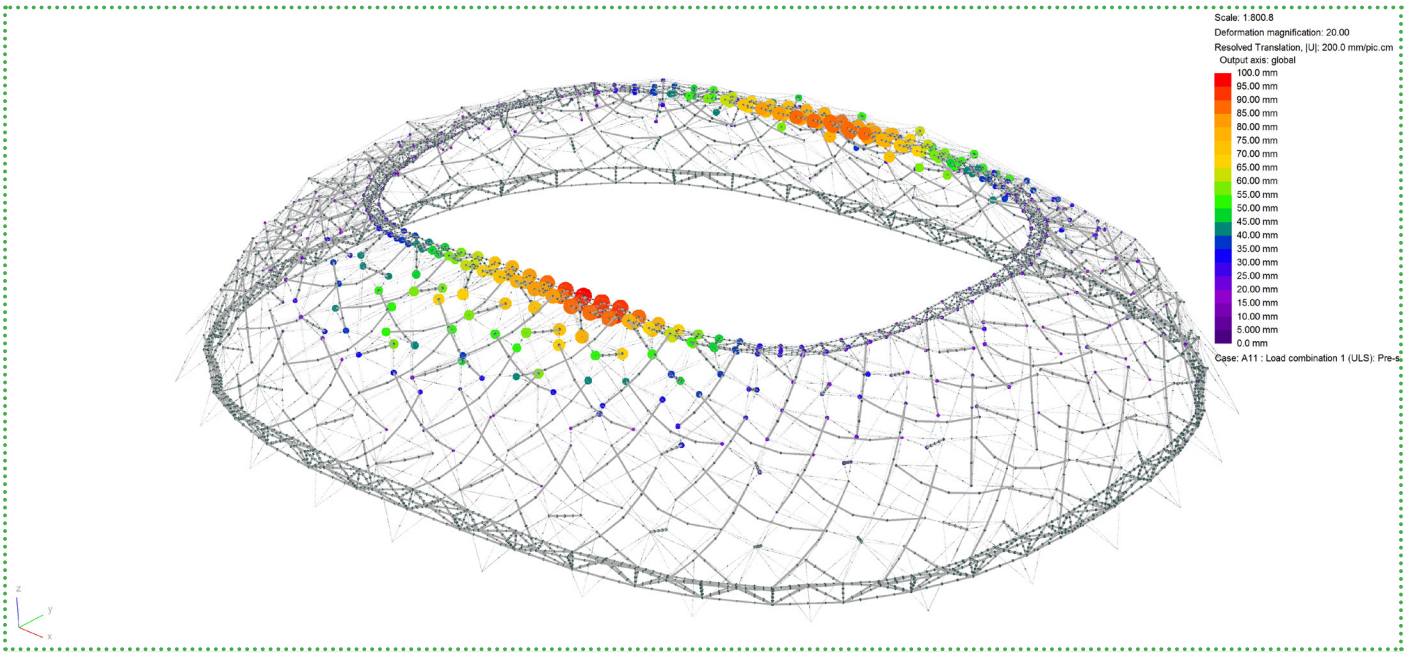
(a) Nodal displacements
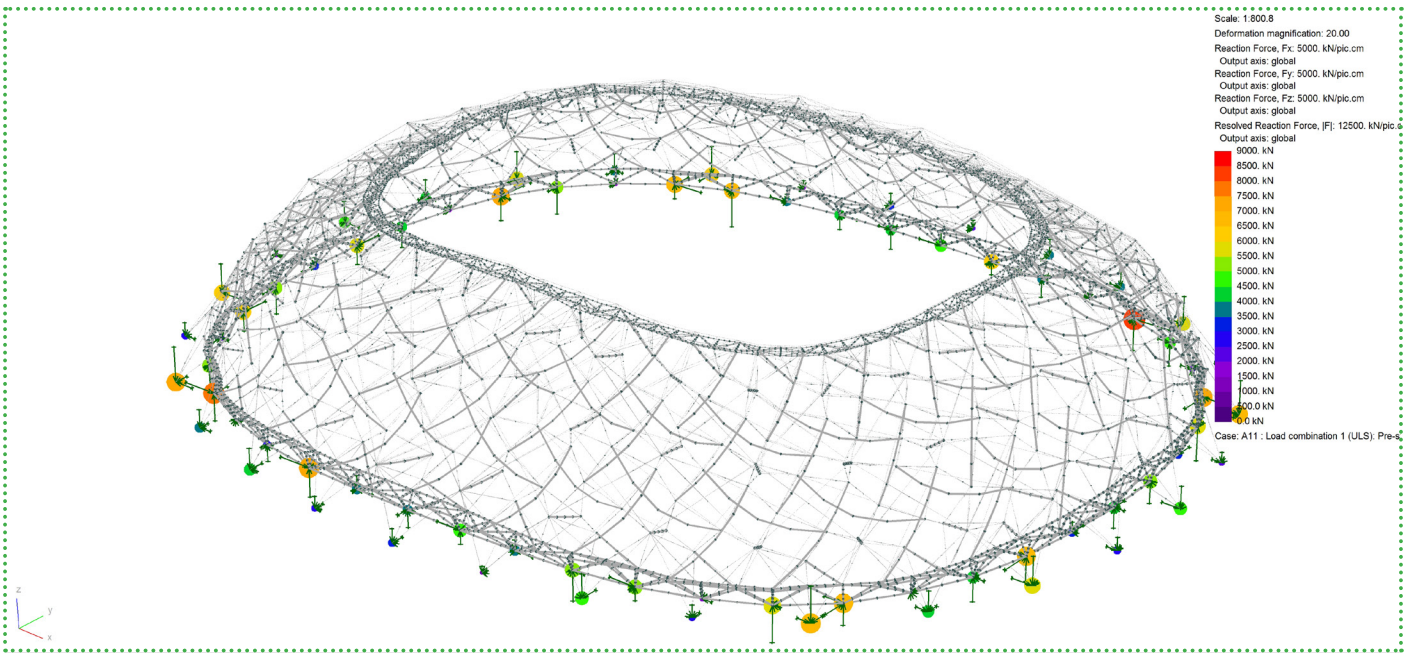
(b) Support reactions

4.39. Load combination 1 (ULS): Pre-stress forces + Gravity + Cladding
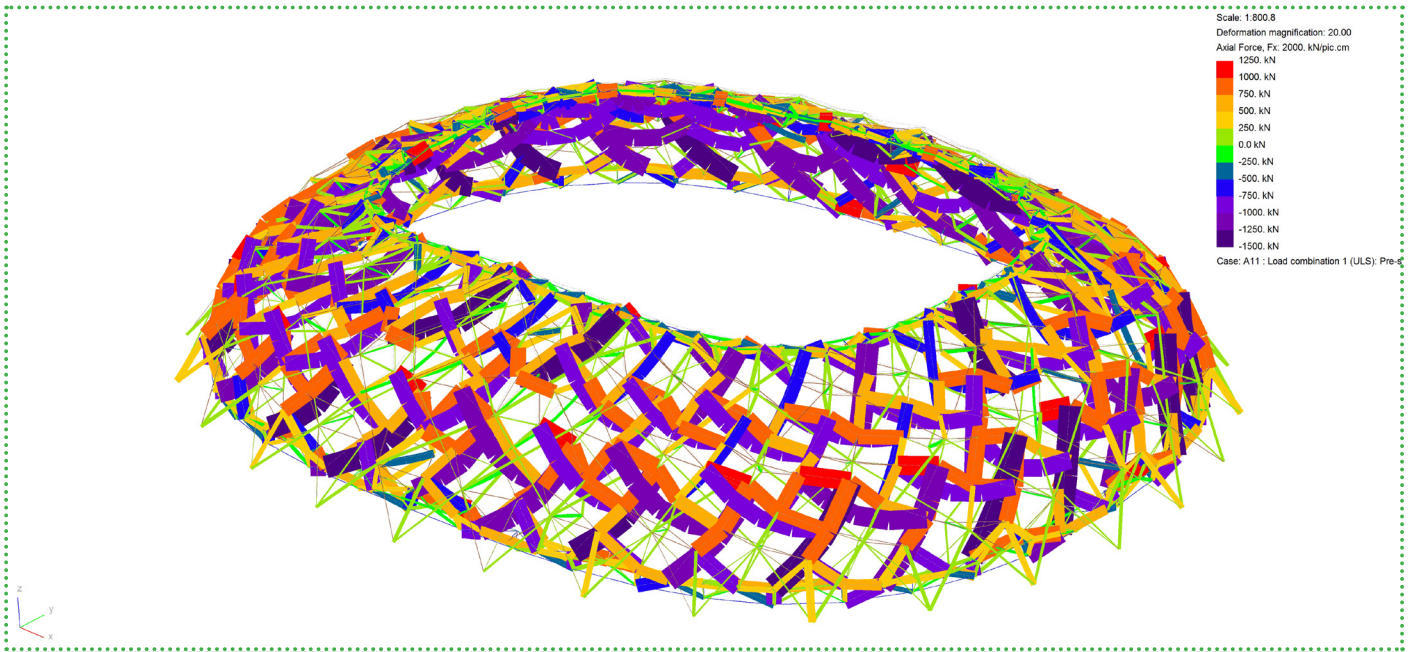
(c) Axial forces
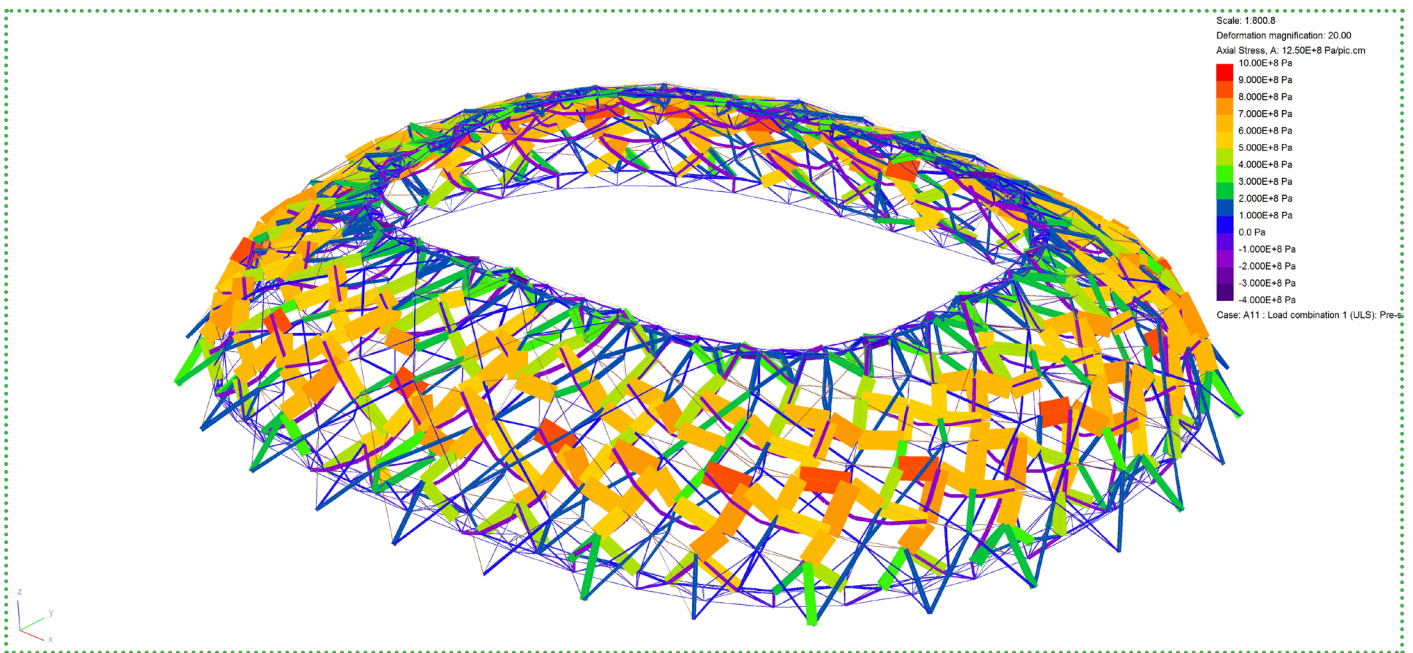
(d) Axial stresses

4.39. Load combination 1 (ULS): Pre-stress forces + Gravity + Cladding
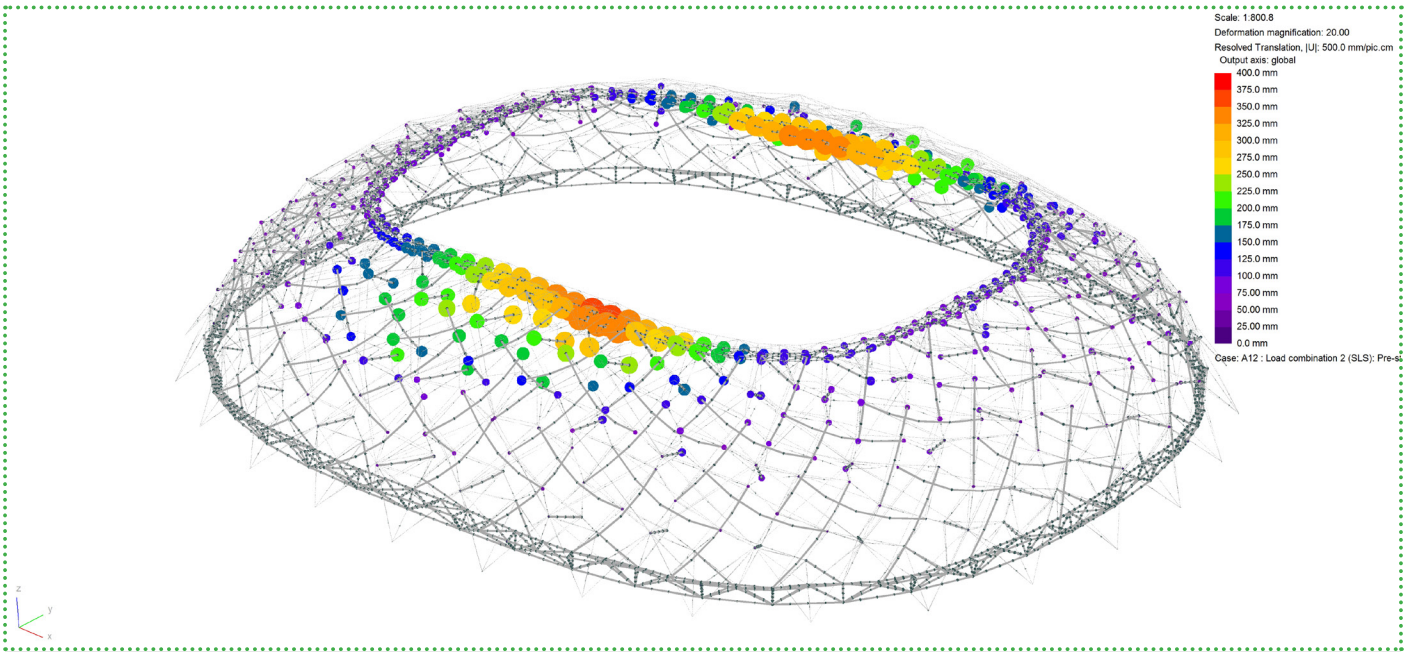
(a) Nodal displacements
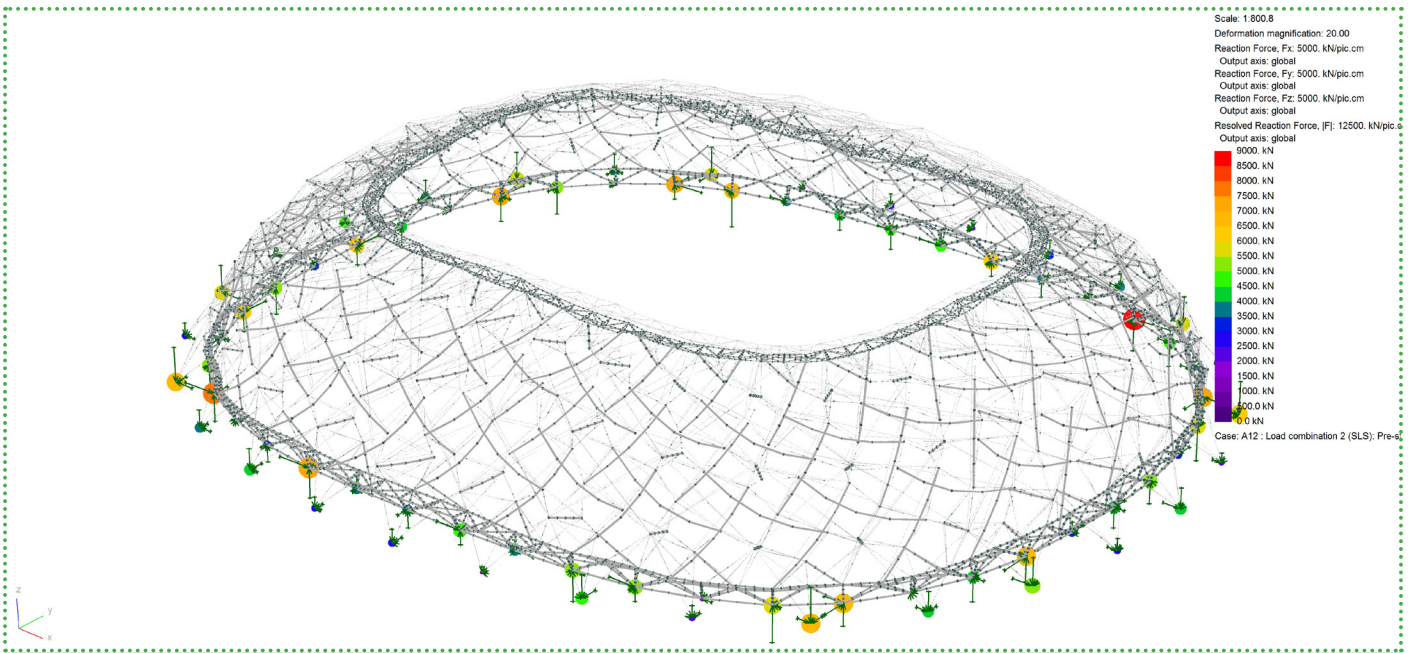
(b) Support reactions

4.40. Load combination 2 (SLS): Pre-stress forces + Gravity + Cladding + Snow

🟥	1250. kN
🟧	1000. kN
🟧	750. kN
🟨	500. kN
🟨	250. kN
🟩	0.0 kN
🟩	-250. kN
🟦	-500. kN
🟦	-750. kN
🟪	-1000. kN
🟪	-1250. kN
🟪	-1500. kN

Case: A12 : Load combination 2 (SLS): Pre-st

(c) Axial forces

🟥	10.00E+8 Pa
🟧	9.000E+8 Pa
🟧	8.000E+8 Pa
🟨	7.000E+8 Pa
🟨	6.000E+8 Pa
🟩	5.000E+8 Pa
🟩	4.000E+8 Pa
🟩	3.000E+8 Pa
🟩	2.000E+8 Pa
🟦	1.000E+8 Pa
🟦	0.0 Pa
🟪	-1.000E+8 Pa
🟪	-2.000E+8 Pa
🟪	-3.000E+8 Pa
🟪	-4.000E+8 Pa

Case: A12 : Load combination 2 (SLS): Pre-st
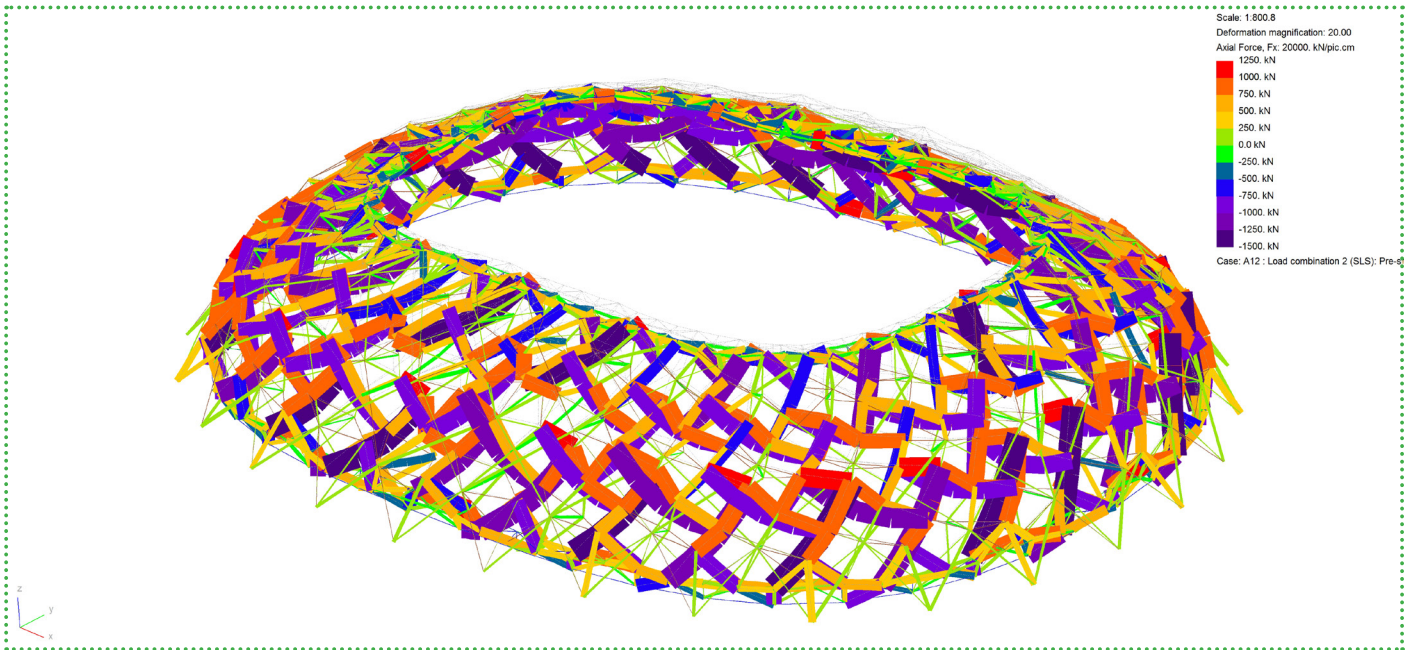
(d) Axial stresses

4.40. Load combination 2 (SLS): Pre-stress forces + Gravity + Cladding + Snow
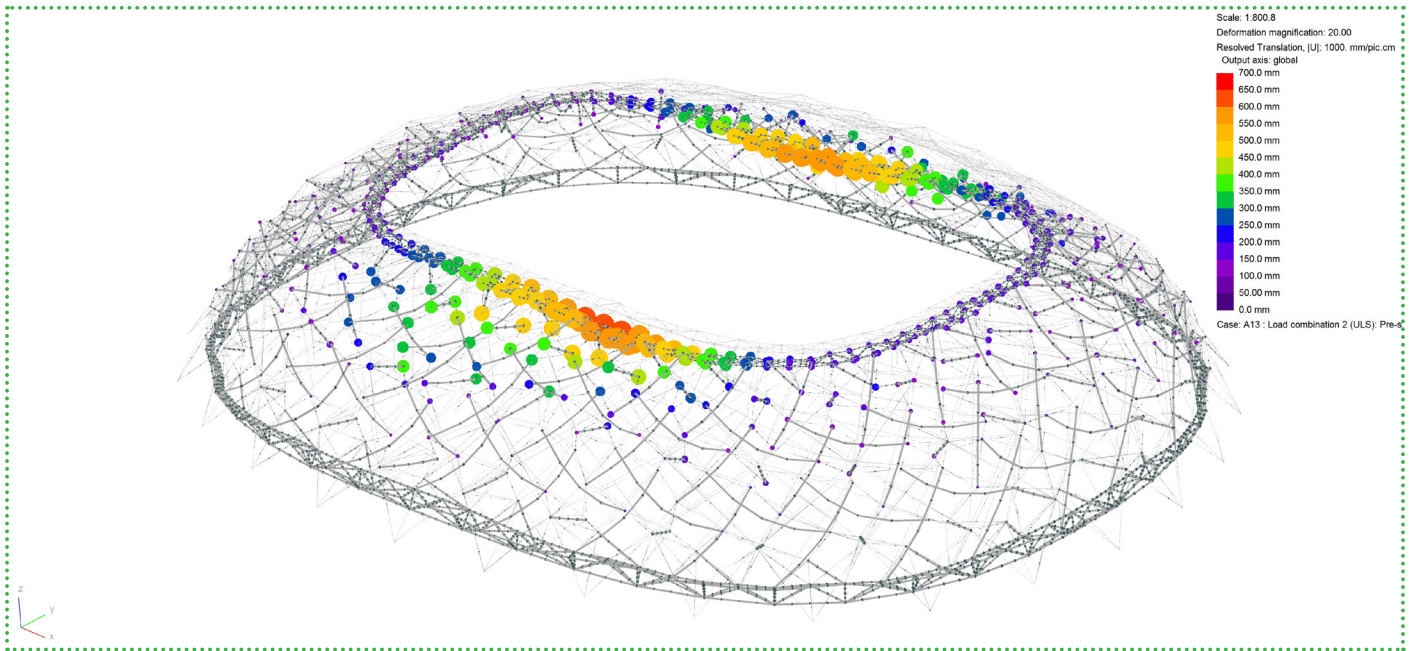
(a) Nodal displacements
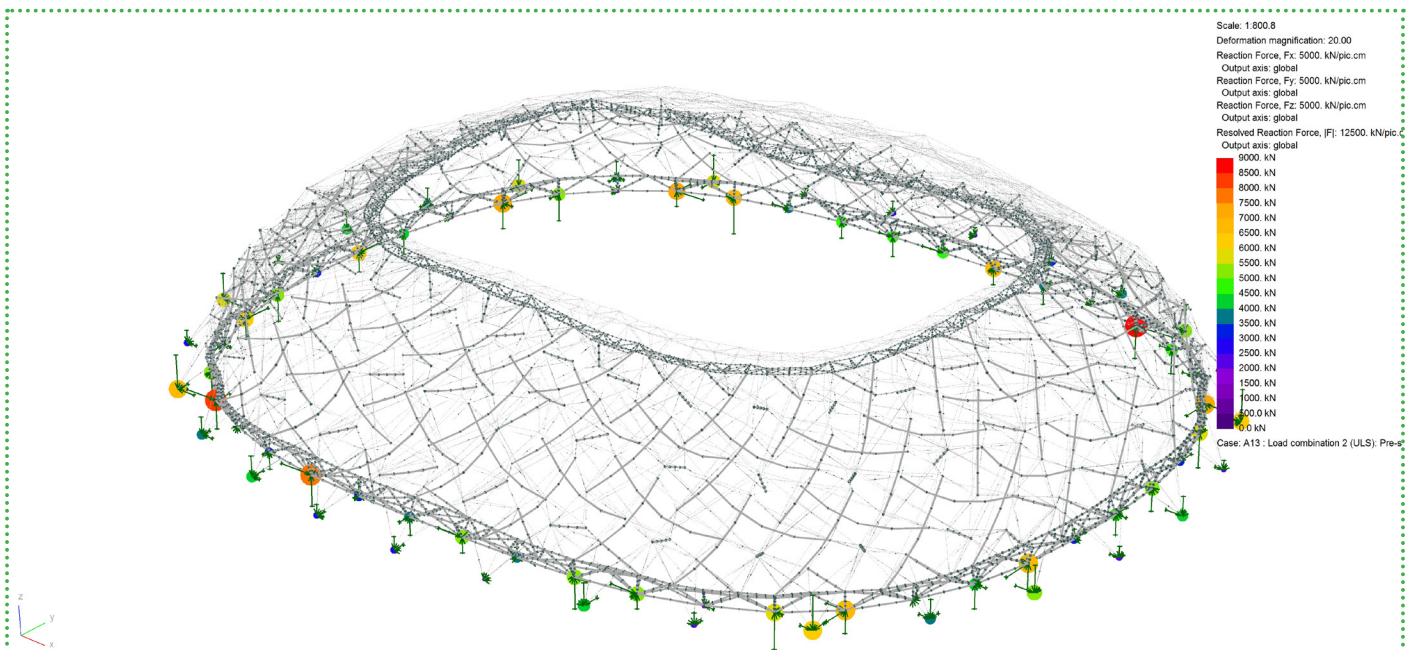
(b) Support reactions

4.41. Load combination 2 (ULS): Pre-stress forces + Gravity + Cladding + Snow
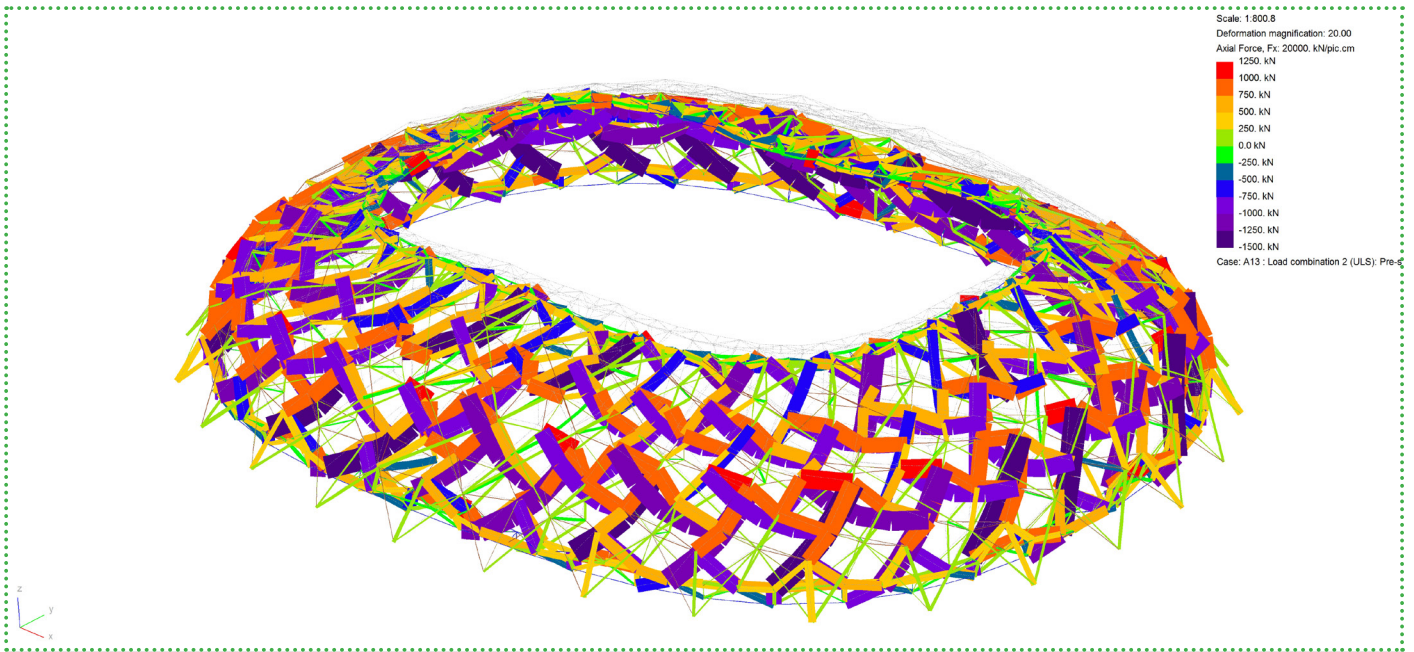
(c) Axial forces
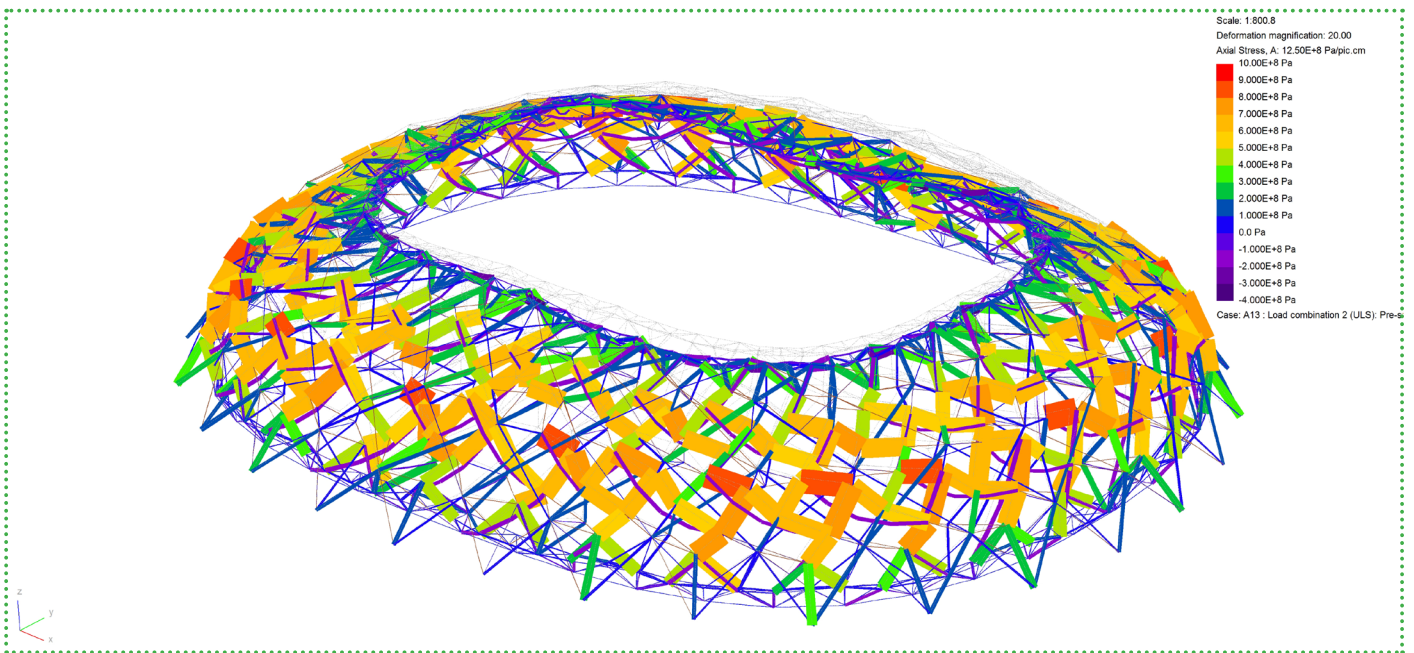
(d) Axial stresses

4.41. Load combination 2 (ULS): Pre-stress forces + Gravity + Cladding + Snow
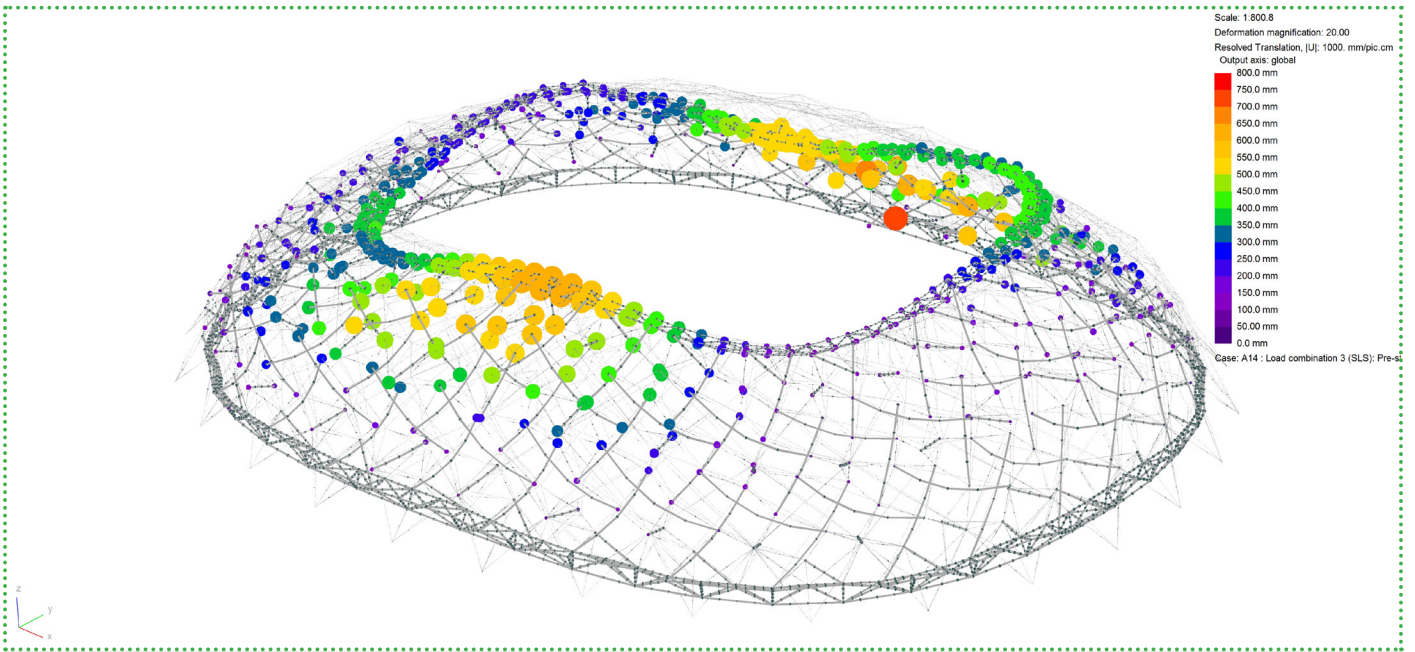
(a) Nodal displacements
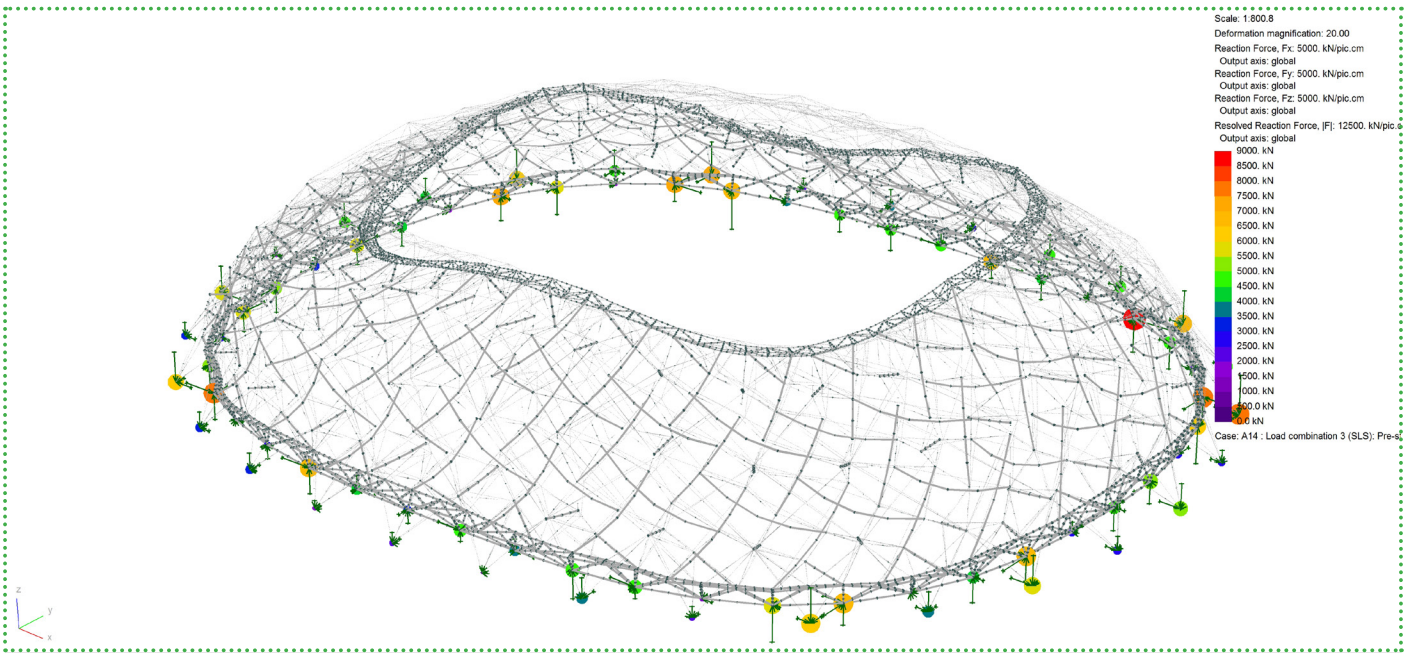
(b) Support reactions

4.42. Load combination 3 (SLS): Pre-stress forces + Gravity + Cladding + Wind (y direction)
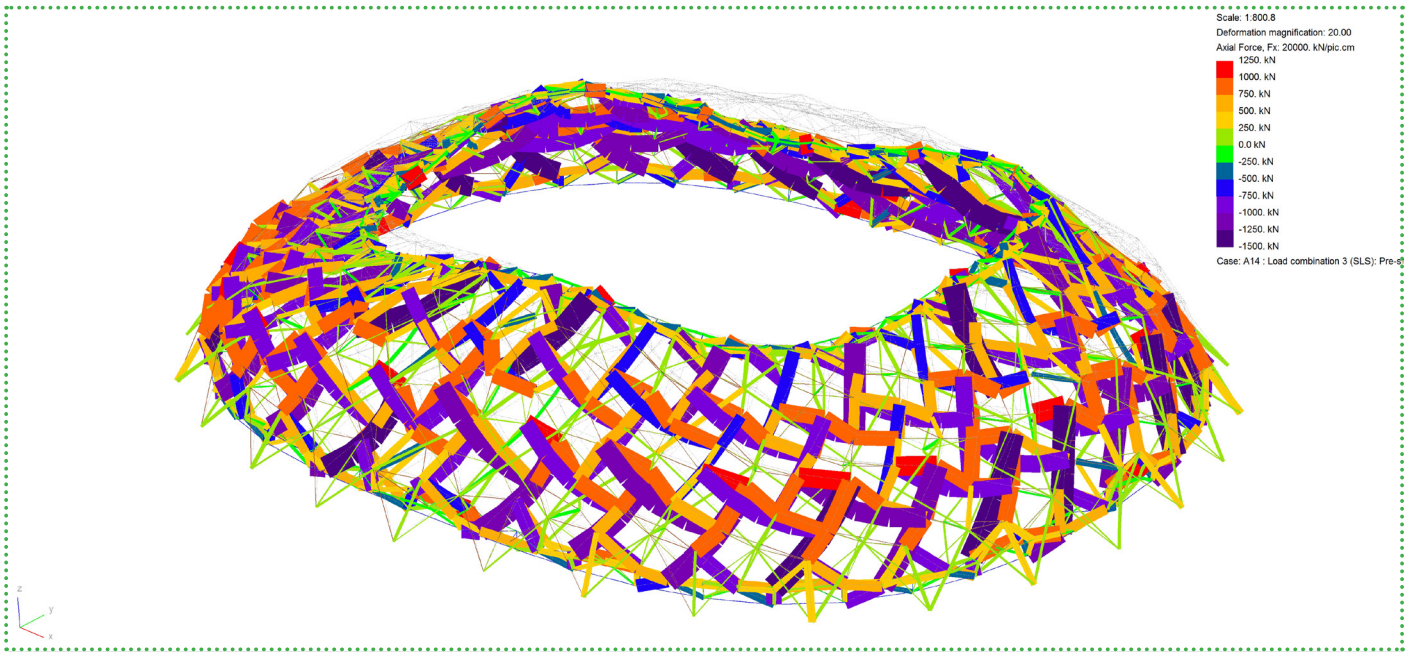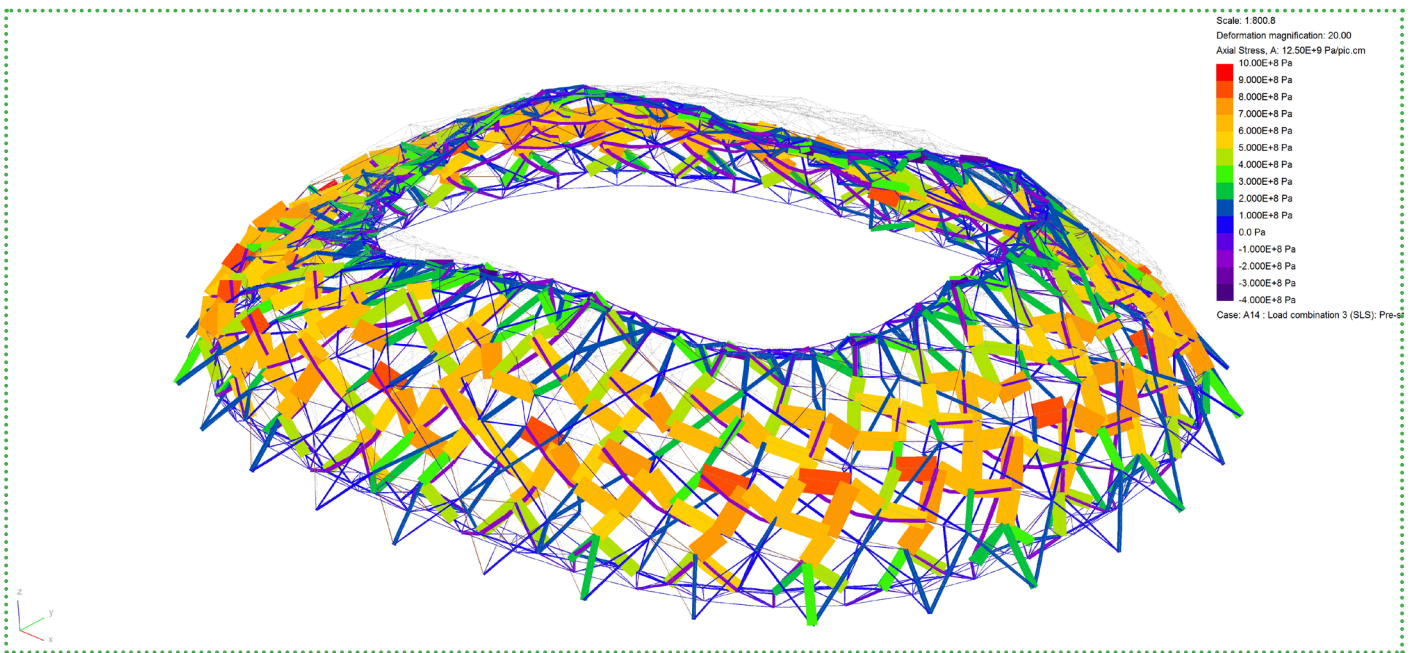
(c) Axial forces

(d) Axial stresses

4.42. Load combination 3 (SLS): Pre-stress forces + Gravity + Cladding + Wind (y direction)
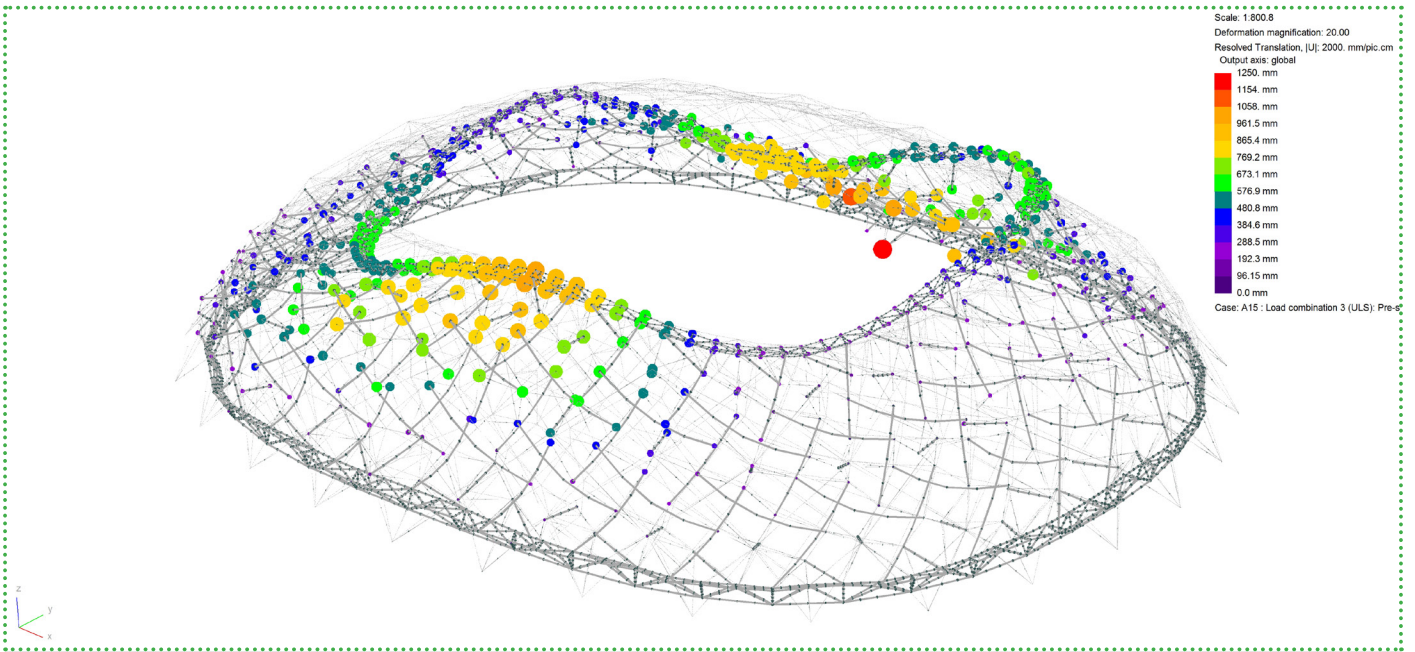
(a) Nodal displacements
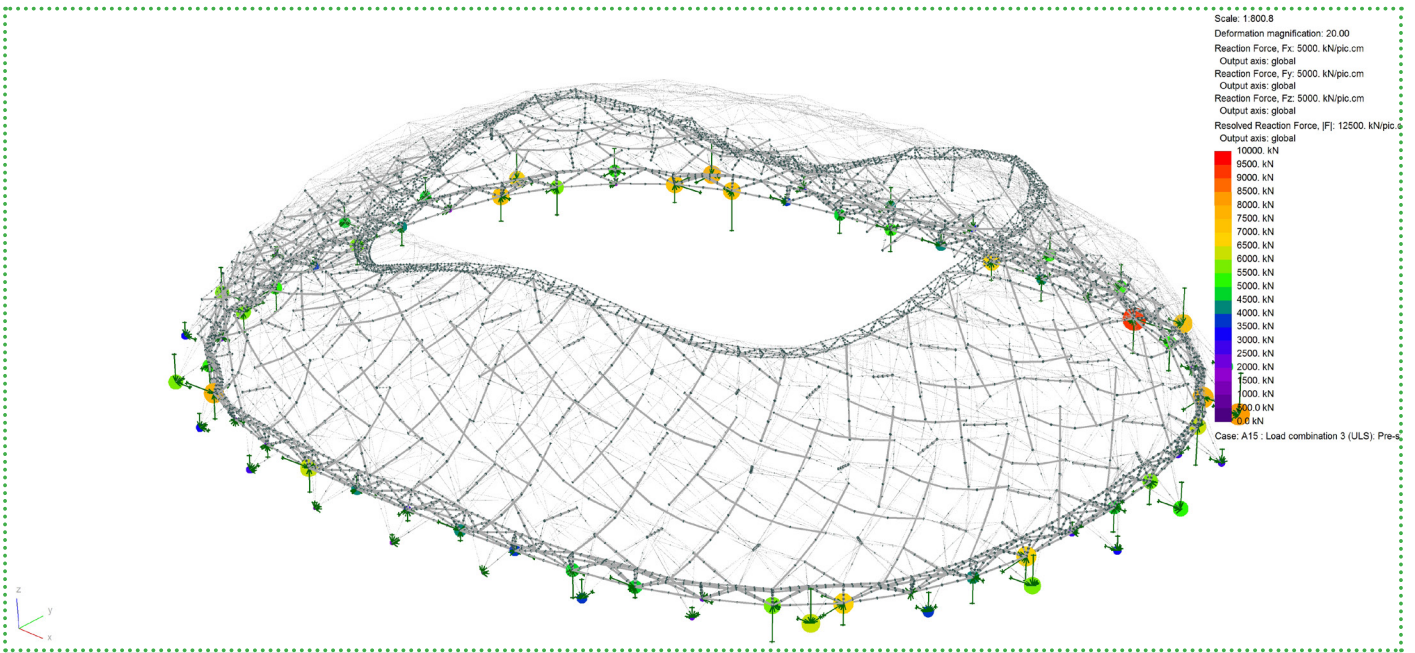
(b) Support reactions

4.43. Load combination 3 (ULS): Pre-stress forces + Gravity + Cladding + Wind (y direction)
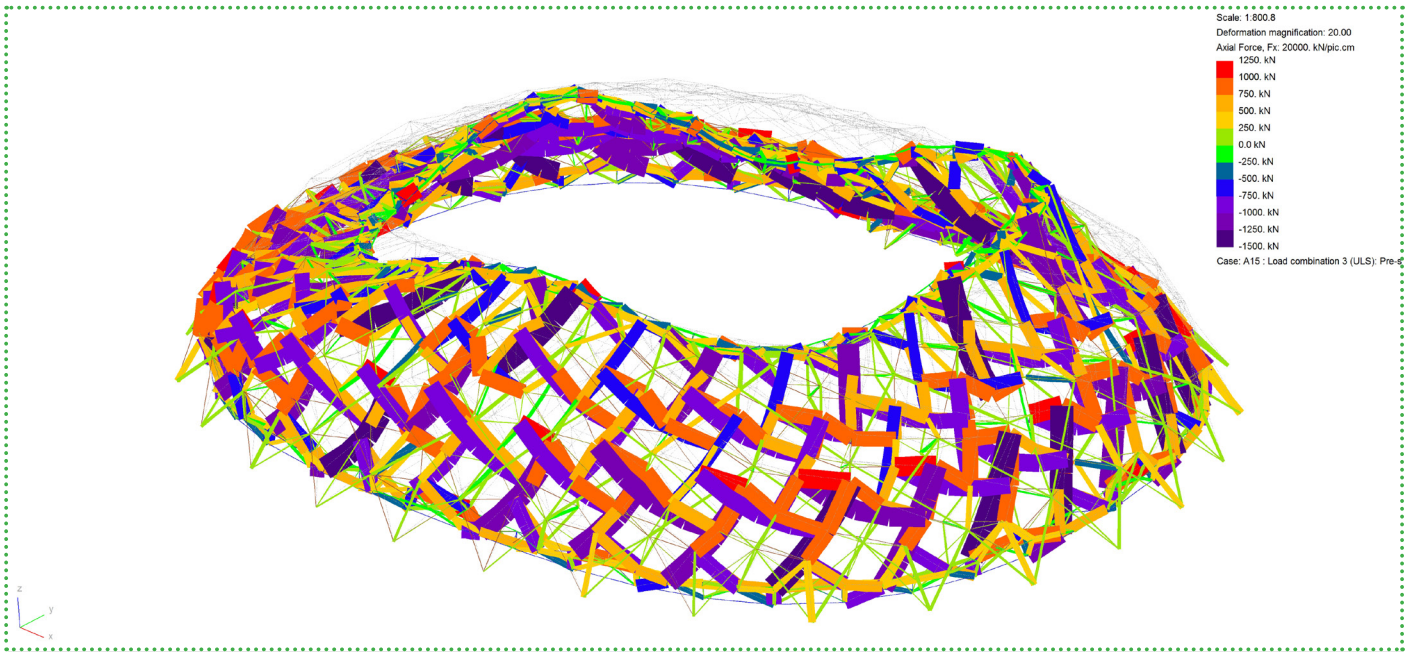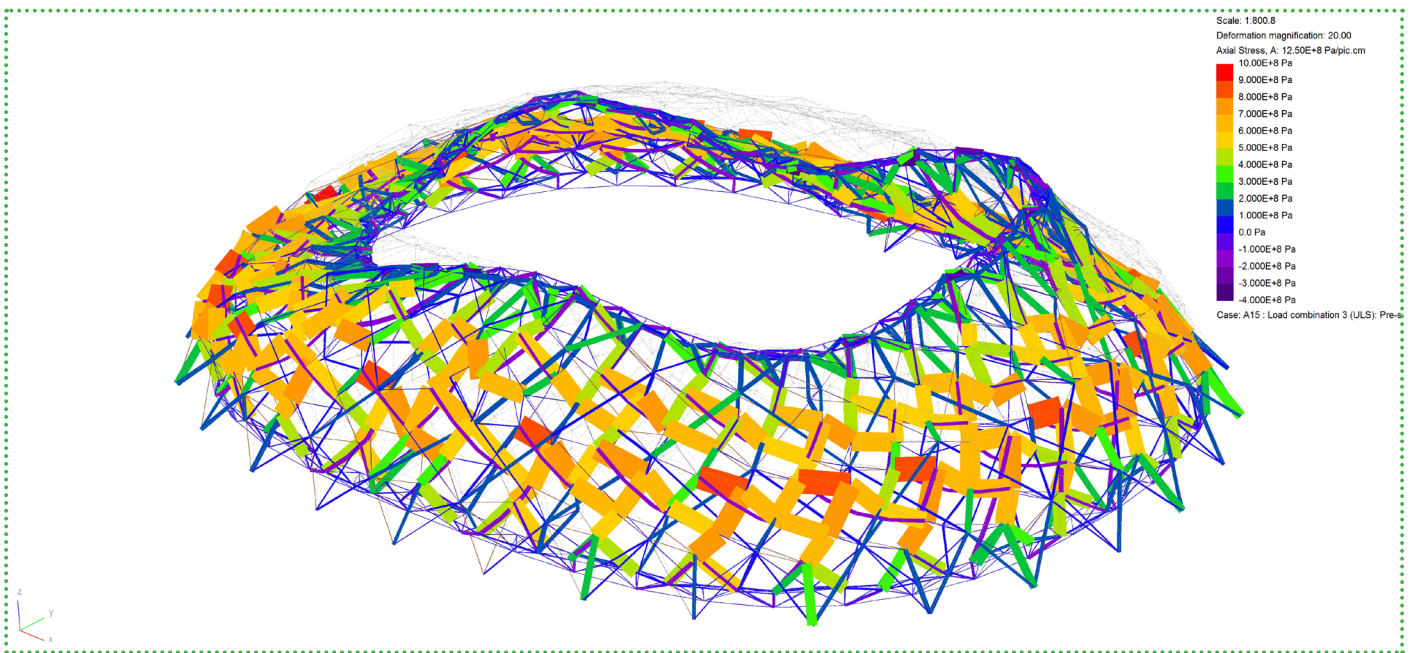
(c) Axial forces

(d) Axial stresses

4.43. Load combination 3 (ULS): Pre-stress forces + Gravity + Cladding + Wind (y direction)
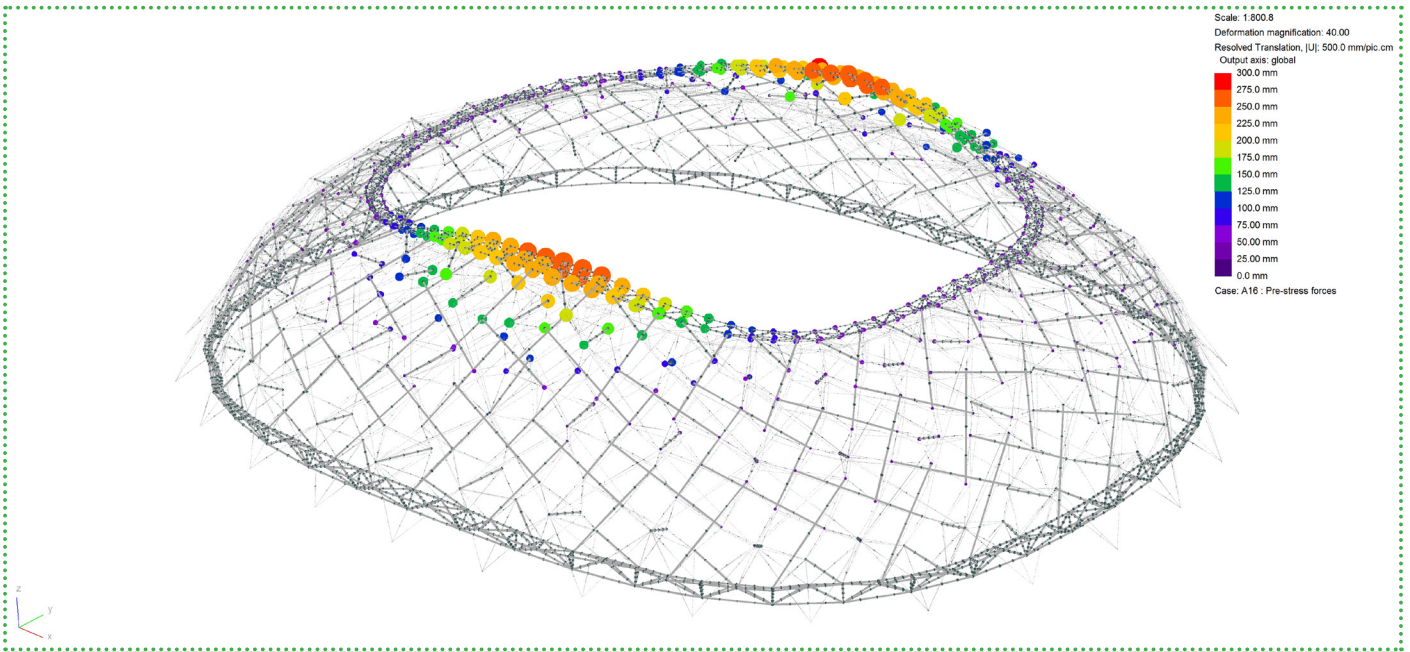
(a) Nodal displacements
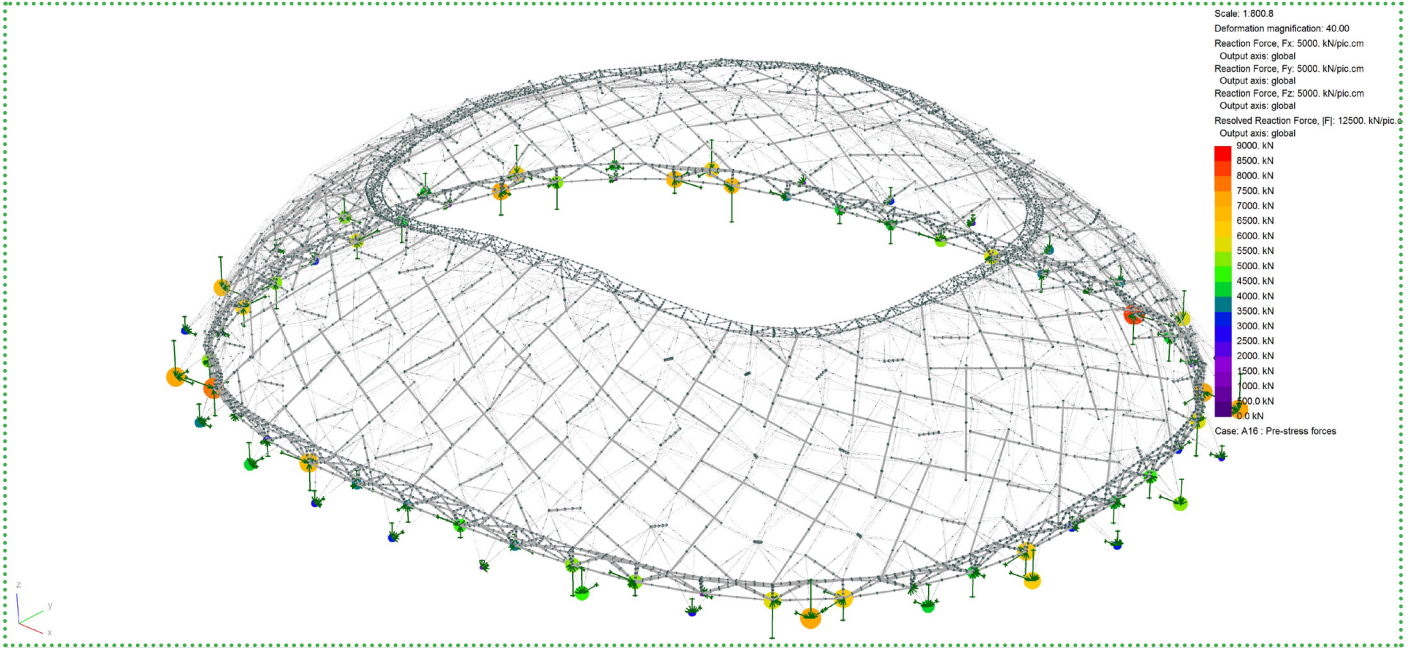
(b) Support reactions

4.44. Load combination 4: Pre-stress forces

92

Scale: 1:800.8
Deformation magnification: 40.00
Axial Force, Fx: 20000. kN/pic.cm

	1250. kN
	1000. kN
	750. kN
	500. kN
	250. kN
	0.0 kN
	-250. kN
	-500. kN
	-750. kN
	-1000. kN
	-1250. kN
	-1500. kN

Case: A16 : Pre-stress forces

(c) Axial forces

Scale: 1:800.8
Deformation magnification: 40.00
Axial Stress, A: 12.50E+8 Pa/pic.cm

	9.000E+8 Pa
	8.000E+8 Pa
	7.000E+8 Pa
	6.000E+8 Pa
	5.000E+8 Pa
	4.000E+8 Pa
	3.000E+8 Pa
	2.000E+8 Pa
	1.000E+8 Pa
	0.0 Pa
	-1.000E+8 Pa
	-2.000E+8 Pa
	-3.000E+8 Pa
	-4.000E+8 Pa

Case: A16 : Pre-stress forces
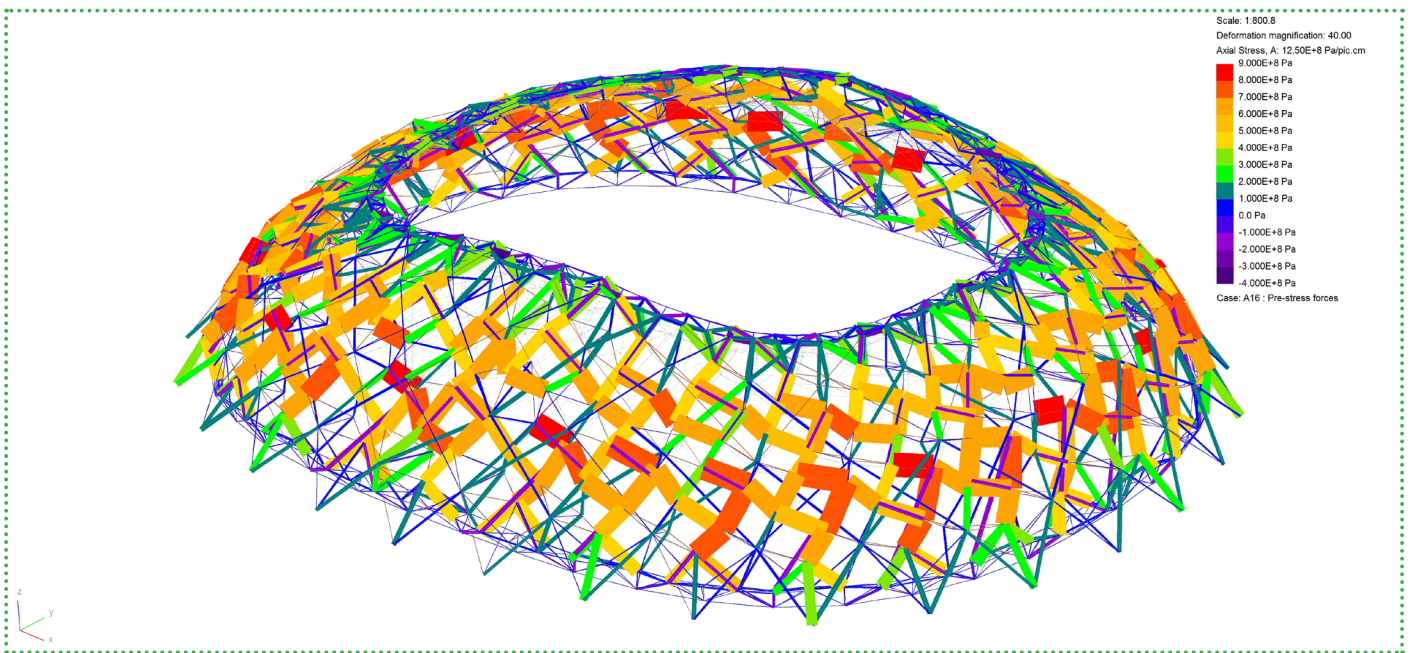
(d) Axial stresses

4.44. Load combination 4: Pre-stress forces

4.6. Detailing and Construction

Connections

One of the crucial parts of tensegrity design is the connection, or the joint. In a true tensegrity system, the typical connection is the one in which there is only one strut linking with many other cables, and the minimum amount is three cables. Normally there are six cables in a joint connecting to one strut. At most, the number of cables is eight. So it is utterly essential that the connection has to accommodate forces coming from all directions but creating no bending moment. To achieve this, a connection needs to hold all the structural elements in a way that the central lines of these elements are meeting at one point. Aesthetically, the size of the joint should be as small as possible, so that it is not distinguished from the body of struts. At best, they should naturally be a part of struts to receive cables coming. Achieving this, there will be no connection anymore but only the network of struts and cables. The connections between the tensegrity shell and the bottom truss as well as top truss are also necessary, they are pinned joints.

Foundation

Although the new structure is covering the whole Feyenoord stadium is massive, it remains a lightweight structure which does not put much mass to the ground. Pre-stress forces play an important role to give the pressure on the foundation. It is assumed that the existing ground condition is already stiff enough with the construction of Feyenoord stadium over these years. For this reason, there is no need to introduce more piles to the ground to support the new structure, and only a shallow concrete foundation is necessary to fix the bottom truss of the tensegrity shell to the ground. The connections between the shallow foundation and the bottom truss are pinned.

Construction Sequence

The construction of the new roof for Feyenoord stadium will follow these steps:

(1) Taking off the roof and four lighting posts of the current stadium, steel material from these structures can be recycled for the new roof. This way is very sustainable.
(2) Setting the concrete shallow foundation ring to the ground. Moving steel elements of the bottom truss to the site.
(3) Installing the bottom truss. Moving the struts and cables for the first ring of tensegrity to the site.
(4) Installing the first round of struts, for the first time, every longer strut will be fixed to its designed positions in space by three cables to the ground. The shorter struts will be fixed to bottom truss and longer struts by cable with measured lengths. Moving material of the next round to the site.
(5) Lifting normal struts to fix them to the first round of tensegrity by normal cables. Making sure that all cables will be in tension. Moving material of the next round to the site.
(6) Keep adding struts and cables bottom-up until the last round of tensegrity part. Moving material of top truss to the site.
(7) Installing the top truss on the ground, lifting it up to the designed level, fixing it to the tensegrity shell with pinned joints.
(8) Adjusting the tension in the cable network to get expected geometry, stiffening the entire structure. Moving cladding material to the site.
(9) Installing ETFE roof underneath the new structure to cover all the stadium's stands.
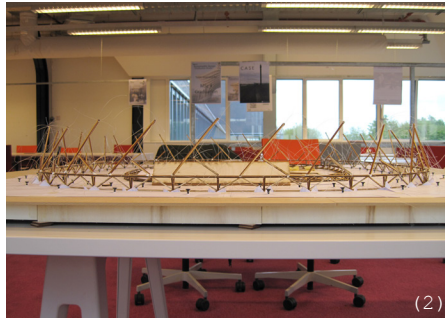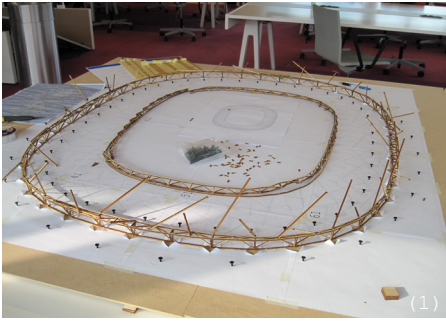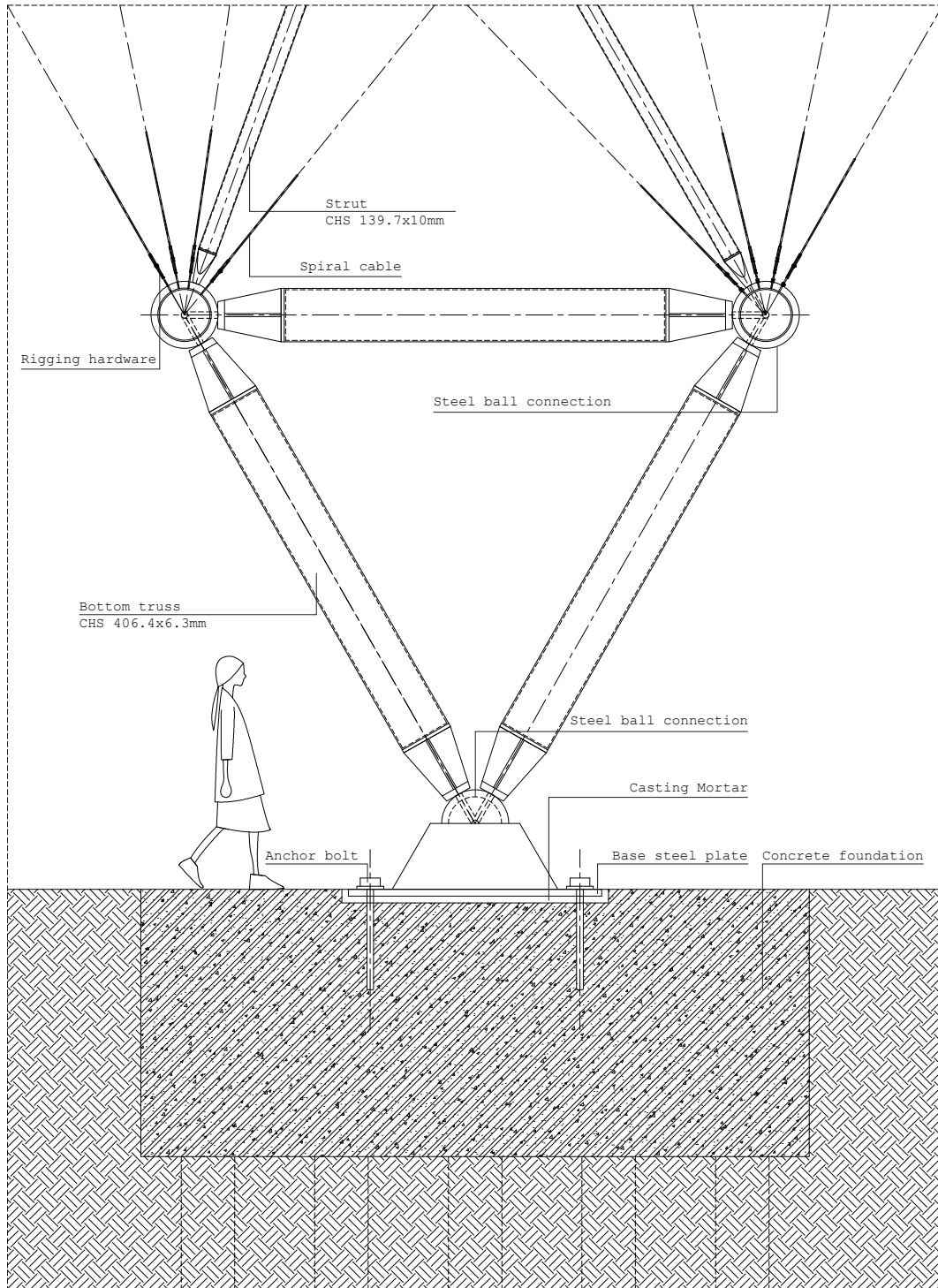(10) Finishing
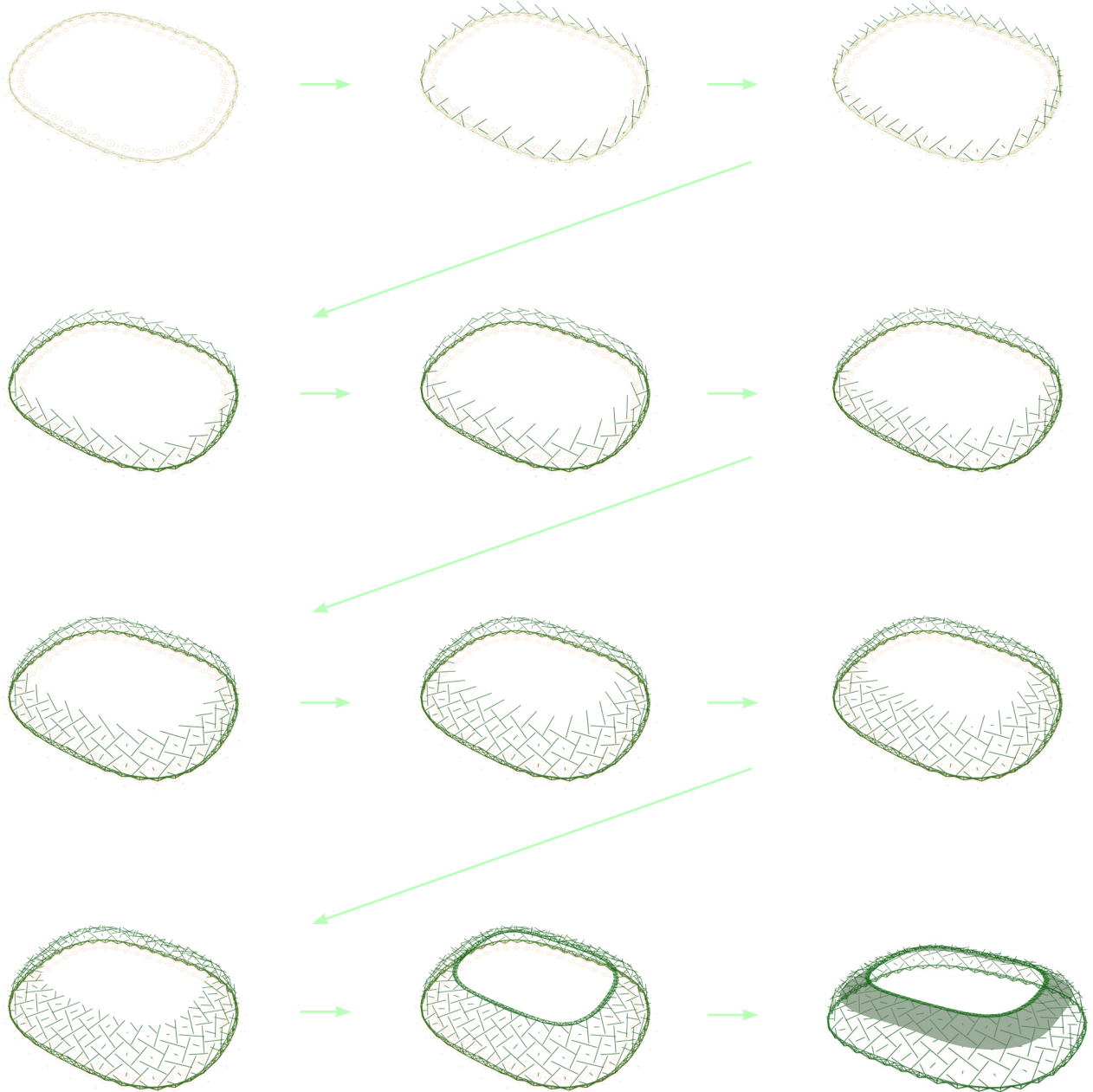
45. Construction sequence
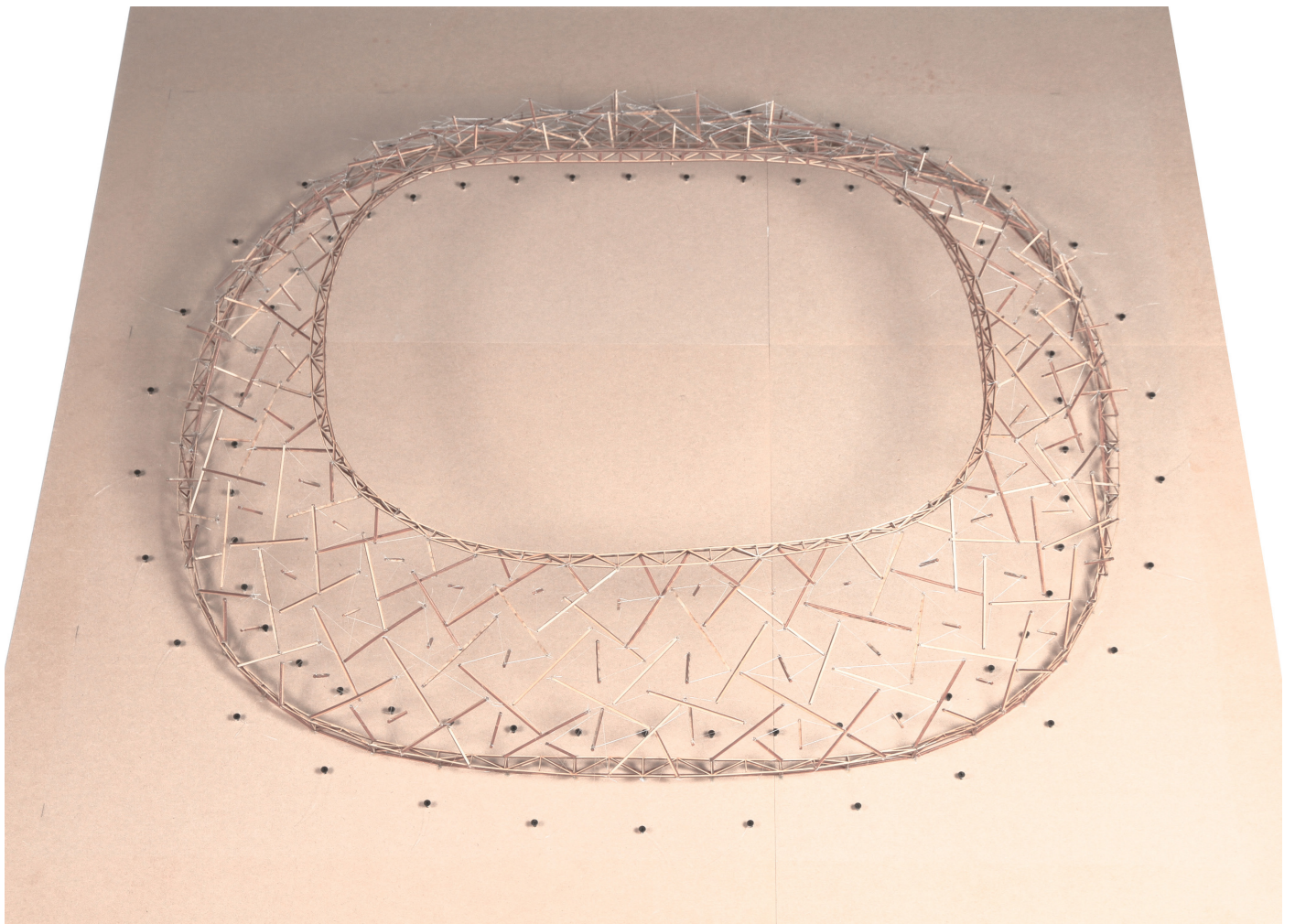
46. Final model 1:200 (above)
47. Construction of the final model (next page)

(1)

(2)

(3)

(4)

(5)

(6)

(7)

(8)

(9)

(10)

(11)

(12)

(13)

(14)

(15)

(16)

(17)

(18)

Strut
CHS 139.7x10mm

Spiral cable

Rigging hardware

Steel ball connection

Bottom truss
CHS 406.4x6.3mm

Steel ball connection

Casting Mortar

Anchor bolt   Base steel plate   Concrete foundation
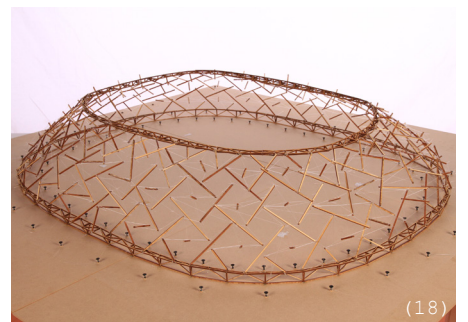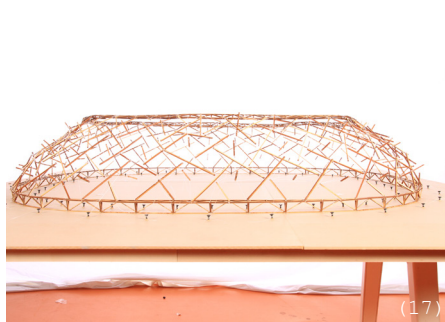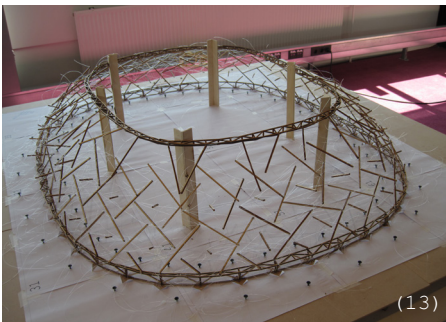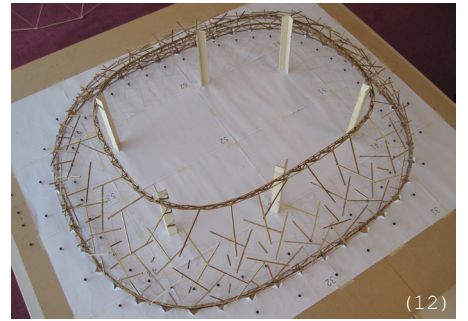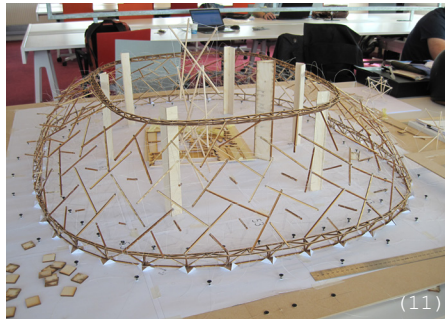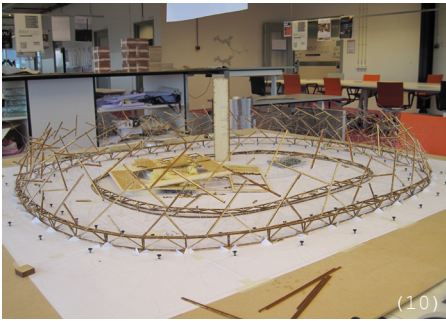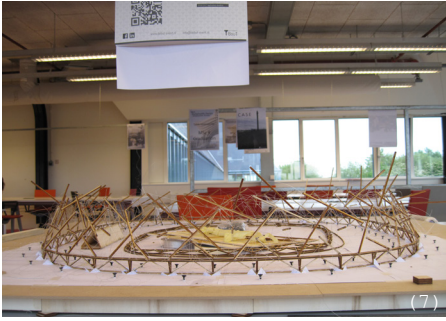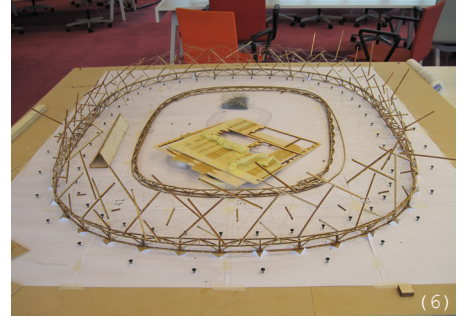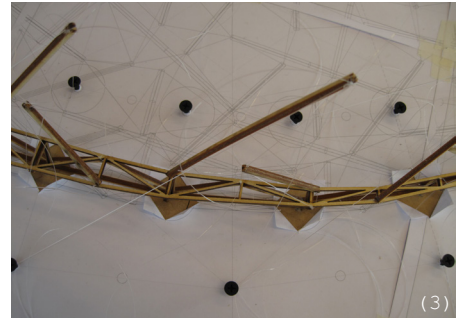
4.48. Foundation - Bottom truss - Tensegrity (Strut and cable network)

Strut
CHS 139.7x10mm

Spiral cable Ø12

Rigging hardware

Steel ball connection

Bottom truss
CHS 406.4x6.3mm
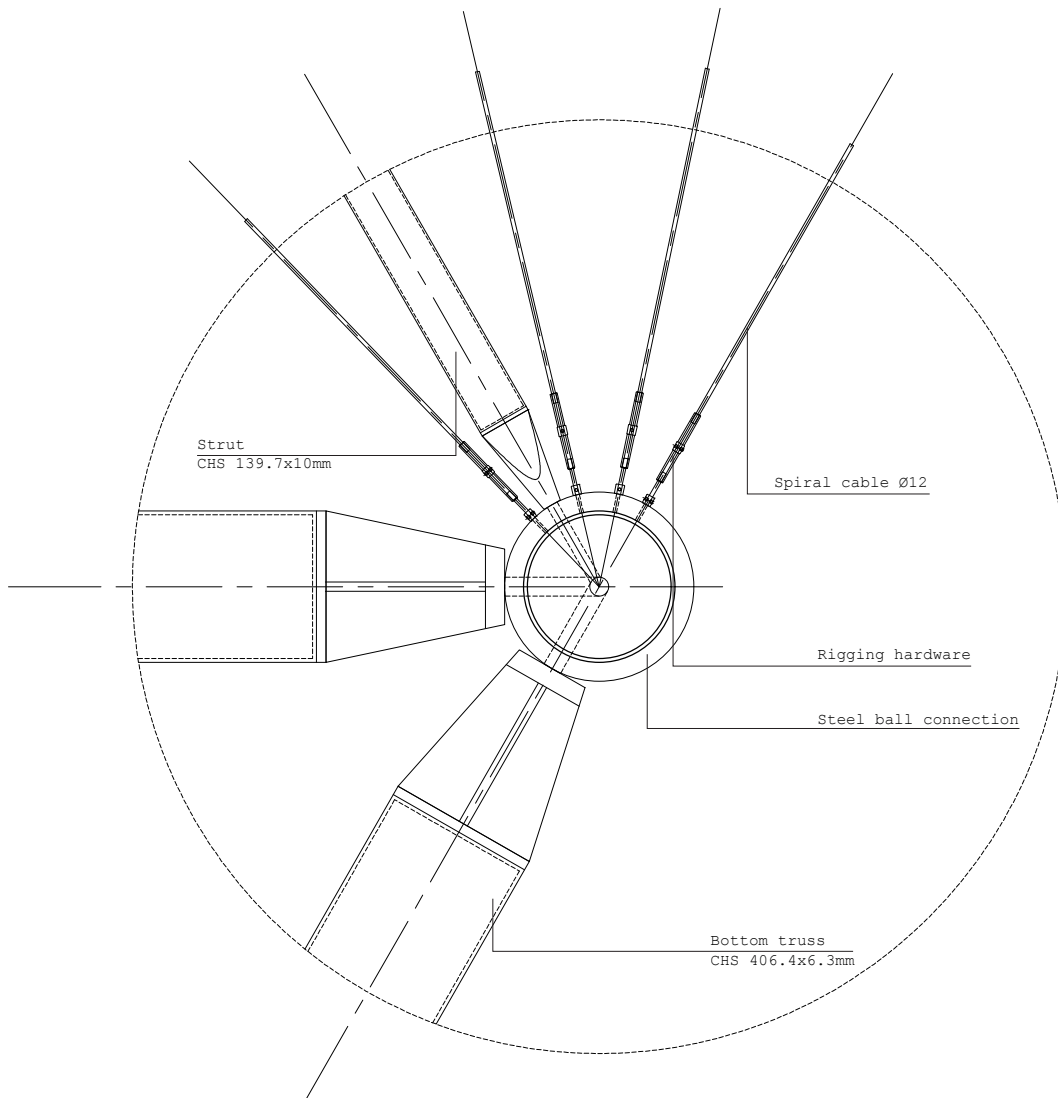
4.49. Bottom truss - Strut - Cables

Molded steel piece with 6 wings
Can receive up to 18 cables

Spiral cable Ø12

Steel cap
Can integrate LED lighting

Strut
CHS 139.7x10mm

Rigging hardware
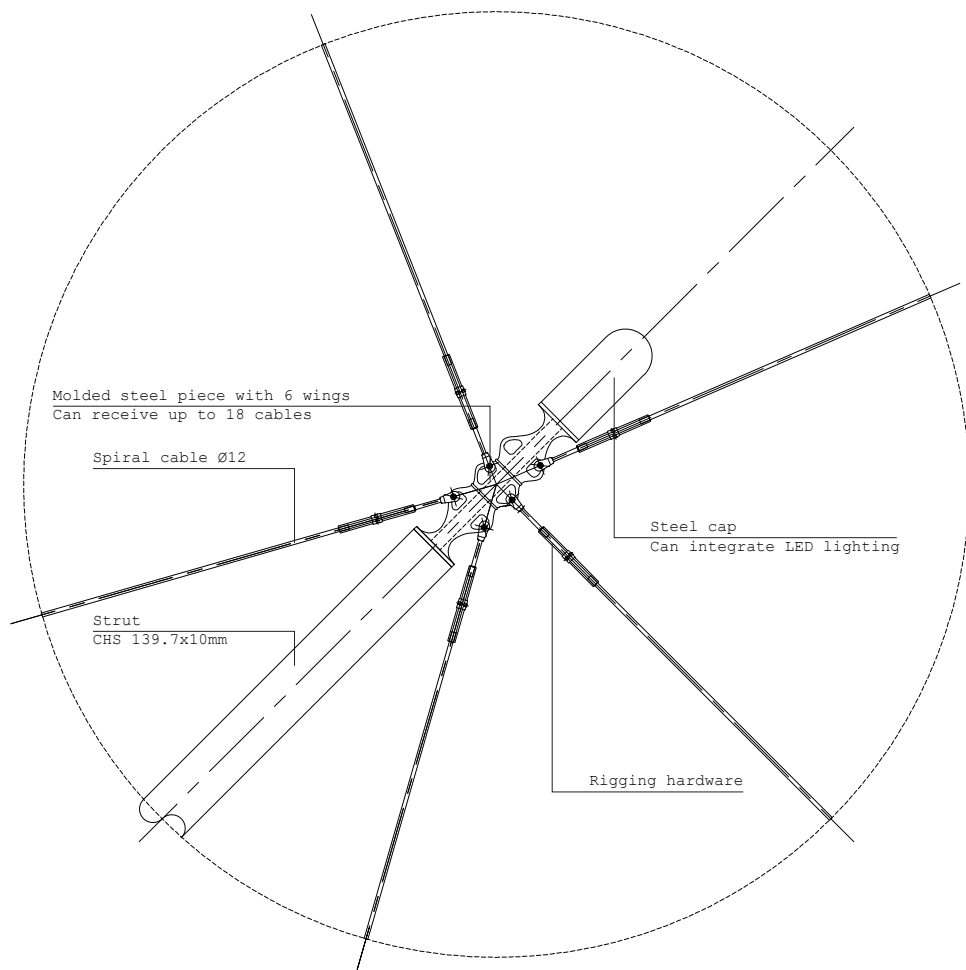
4.50. Tensegrity joint - Side view

Molded steel piece with 6 wings
Can receive up to 18 cables

Spiral cable Ø12

Strut
CHS 139.7x10mm

Rigging hardware
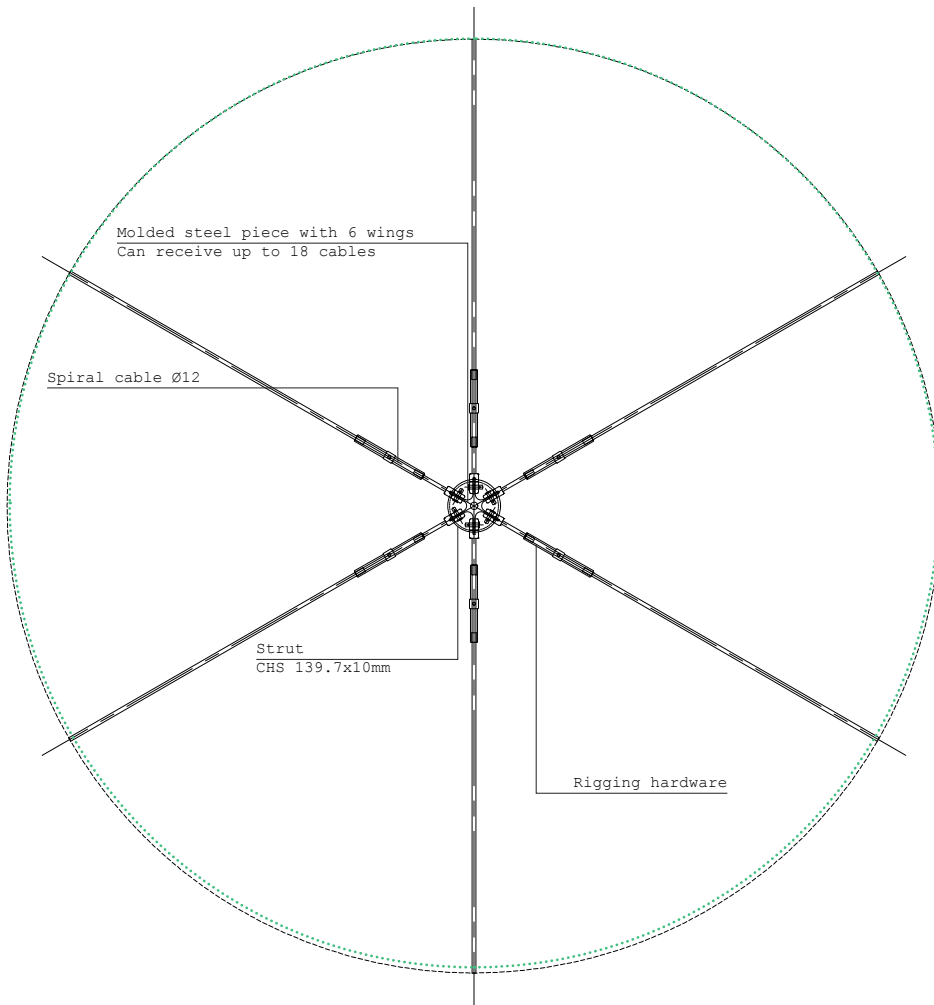
4.51. Tensegrity joint - Horizontal section

(a)   (b)   (c)

4.52. Connection profile

Steel cap
Can integrate LED lighting

Rigging hardware

Spiral cable Ø12

Molded steel piece with 6 wings
Can receive up to 18 cables

Strut
CHS 139.7x10mm
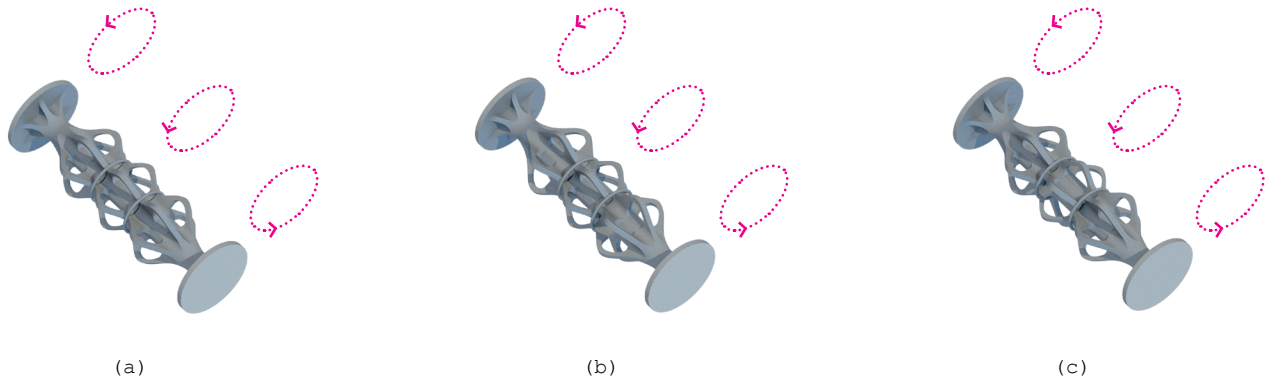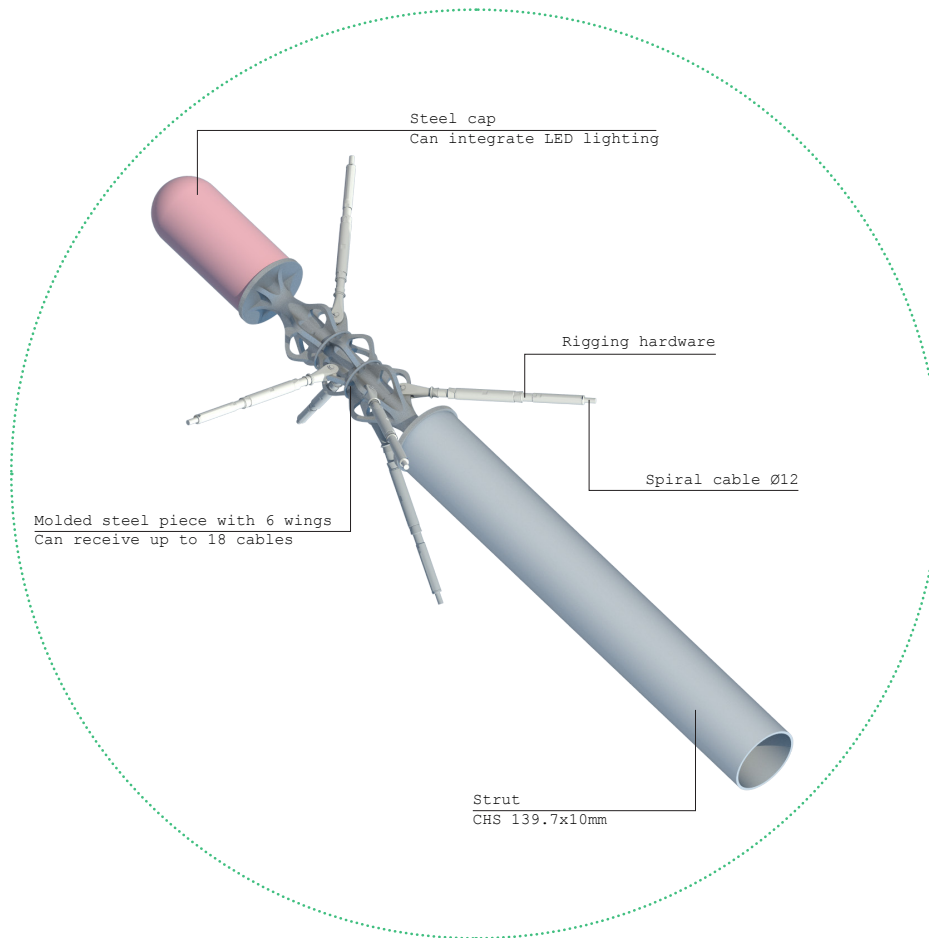
4.53. Perspective view

The connection contains 3 pieces which can rotate independently around an axis to receive cables from almost all directions. The movement of these pieces in one connection also helps to reduce bending moments created because of the imperfection of details. Since tensegrity systems are enormously flexible, it is almost impossible to create a perfect connection taken into account that the angles of cables vary. In addition, my intention is to create a generic connection which can use in almost all location rather than specify for each position of detail. By doing that, it would be more efficient and economical in mass production which contributes to buildability of tensegrity structures. Although there are rooms for developments of this detail in terms of element strength and its flexibility of minimizing bending moments.

Strut
CHS 139.7x10mm

Molded steel piece with 6 wings
Can receive up to 18 cables

Spiral cable Ø12

Rigging hardware

Teflon®-coated woven fiberglass membrane

Steel cap
Can integrate LED lighting
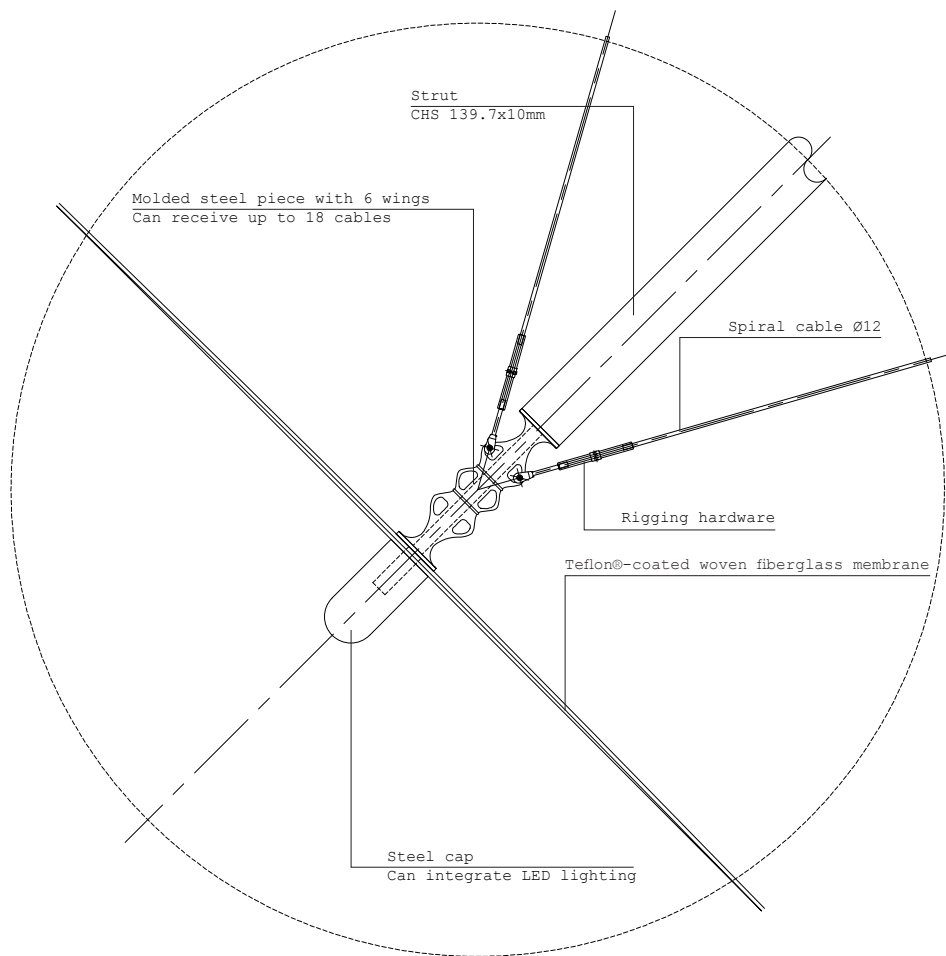
4.54. Connecting to the cladding at the bottom of strut

Chapter 5. Conclusion and Discussion

5.1. Conclusion

- The new design method for double-surface tensegrity systems is generated along this thesis. There are two families of double-surface tensegrity structures that are discovered.

- Double-surface tensegrity structures are buildable.

- Based on a generic grid of vertices, the structural can be computationally generated by programming which will bring a lot of possibilities to develop such a system.

- The modeling is conducted in rhino and grasshopper, so the model is not entirely parametric yet. Structural model can be built in grasshopper along with all the structural properties, such as material, element type, sectional profile.

- Oasys GSA is only a calculation platform, and the design time is shortened.

- After form-finding, the found shapes are very stiff. The geometries handle very well its own weight as well as some other loading conditions, such as dead loads, snow load, and wind load.

- Finding the right pre-stress forces is the key of a successful form-finding using 'ignore form-finding properties' in Oasys GSA.

- The areas around inner ring deformed the most.

- The more elements a structure has, the smoother it is after form-finding.

- The process is not linear, but it is expected. There is always a need to go back to check and redo to be able to move forward.

- It is crucial to compare behaviors of physical models and digital model to direct the research and design to the right direction. This is similar to checking hand calculation and the results given by the computer.

5.2. Recommendation

- Making an entire parametric model

- Develop programming part of other typologies presented in the appendix

- Integrating calculation part to Grasshopper, and exploring a computationally cheap way for form-finding

- Optimization of pre-stress forces and sections to deal with complex load cases and ultimate situations

- Experimenting carbon fiber for cables, and wood or bamboo for struts

5.3. Reflection

On the Theme Graduation Lab and the Chosen Method, Topic, Outputs of the Thesis

This thesis contributed to constructing the library of tensegrity structures with a design method for application in large-scale construction. There is a new method of making double-surface tensegrity structures that is created. In fact, there are some studies on double tensegrity structures, but in these systems, struts are touching each other. The method propose by this thesis makes sure that one can build a pure tensegrity structure with almost any given geometry, struts are completely floating in the network of cables, the connections between compression members are prevented. It helps to resolve the obstacles posed by the complexity of such the systems by the innovative use of computational tools. Also, a way of improving the rigidity and usability of tensegrity in mega-structure is explored, which paves a way to realize the construction and fabrication of the buildings using this structural system.

The thesis provides a plenty of possibilities to develop further in terms of structural composition, computational programming, topological mathematics, and possibly the combination of them. The thesis constructs a new way of structural approach towards structural skin to potentially make the systems more transparent and integrated within urban contexts, architectural quality, technical installations, and services. The design helps to make the building honest in its own way of structural performance and raises attractions from the general public as a sort of inspiration for technological innovation in architectural design. It not only celebrates the innovation but also technologically uses the advanced method to build.

On Wider Social Context

A new way of tensegrity application can reflect the technological innovation of our time in a complex type of building covering a huge open space, a stadium. A stadium is a major component in social interaction in the culture around the world. It is currently the place where people are able to come together to celebrate sport, enjoy a concert, or congregate for self-expression, or some other similar social events. Society would obviously benefit from the impact of using tensegrity systems for the redevelopment of a current urban context.

Throughout the history of stadium construction, the stadium roof is always reflecting the technological innovation in structural engineering of that time, which is an inspiration to push architecture going forwards. The structural span of a stadium roof is always enormously large, and normally coming along with a big central opening which makes it even more challenging. Being able to use new composition of tensegrity structures for a stadium roof is absolutely an innovation. Feyenoord stadium, as well as the city of Rotterdam, has its own tradition of applying high-end technology and innovation in architecture. To continue this avant-garde tradition, the singularity of a tensegrity structure will be the right answer.

On Relationship between Design and Research

There is a strong coherence from design method, structural principles, constructing digital models, physical models, and structural models towards the construction in real scale. Research and design have always been going along. They have a dialectical relationship. One has always been moving back and forth to achieve positive results at the end of the process. Since nothing comes from the blue, one cannot design without research. They are not two separate areas. Research provides inputs to design process, and in turn, design helps to redirect the research procedures, programs. One cannot create an invention from scratch, but by transforming the existing materials, one can acquire a new thing.

One could choose either 'Research by Design' or 'Design by Research' or the combination of them as the way of conducting the thesis. 'Research by Design' seems to fit me well since I feel it is very enjoyable while I was trying

out a number of design options, comparing them, and sometimes a new design appears in-between these options. The physical modeling, critical thinking, and the combination of computational tools are crucial in both design or research process of tensegrity study.

Evaluating the Design Process

The process was not linear from one step to another as expected in the research framework, but it is always moving back and forth, evaluating, redirecting, redoing, resetting, and recalculating. I went from very generic model to specific one, then to very complex one. But with the complex one which is computationally expensive, it is almost impossible to calculate in the beginning, even with the computer, the calculation time is just too long, for days. For this reason, I had to simplify the complex model to the simplest version of the type to be able to perform simulations in Oasys GSA. For computational form-finding, physical models are essential. One has to play around with these form-finding techniques in Oasys GSA many times to achieve the right method. When the behavior of physical models and form-finding models are similar, the right form-finding method is selected. To do the form-finding, the model needs to be designed beforehand, concerning structural topology and geometry. The form-finding did give some interesting alternatives. In the end, it is mostly about giving the right pre-stress forces to the tensegrity structures, and it needs to be locally customized.

To sum up, I successfully created a new design method for new types of tensegrity structures which can stand by itself in reality. I have gone through all the steps planned in P2 and achieved positive results. Although the full-scale structural model of Feyenoord stadium still has some difficulties to analysis, it can be handled afterward. Also, I have not managed to have a fully parametric structural model, which is a pity. But in a way, doing certain parts manually helps me build up the understanding of tensegrity structures very well. I could consider that the lack of programming part helps me to construct the new design method for double-surface tensegrity structures. I realized that slowing down the process is essentially valuable for both research and design.

Reference

- R. W. Burkhardt, A Practical Guide to Tensegrity Design, 2nd Edition, Cambridge, USA.
- R. Motro and N. Vassart, Tensegrity Systems, Laboratoire de Mecanique et Genie Civil, Universite de Montpellier, France.
- K. Miura and S. Pellegrino, Structural Concepts - Structural Concepts and Their Theoretical Foundations, Chapter 1 and Chapter 4.
- A. Puth, An Introduction to Tensegrity, University of California Press, 1976, USA.
- R. Motro, Tensegrity: from Art to Structural Engineering, 2012 IASS-APCS Symposium, May 2012, Seoul, South Korea.
- T. Tachi, Interactive Freeform Design of Tensegrity, the University of Tokyo, Japan.
- H. Ohmori, Computational Morphogenesis - Its Current State and Possibility for the Future, IASS-IACM 2008, Cornell University, Ithaca, New York, USA.
- Q. Li, A. Borgart, Y. Wu, How to understand "Structural Morphology"?, Journal of the International Association for Shell and Spatial Structures, 145 p., Vol. 57 (2016) No. 2, Madrid, Spain.
- A. van Waart, Exploring Structural Design - An Introduction to A Workflow for Parametric Structural Design, August 2012.
- R.E. Skelton, J.P. Pinaud, D.L. Mingori, Dynamics of the Shell Class of Tensegrity Structures, Journal of the Franklin Institute 338 (2001) 255-320.
- M. Lazzari, R.V. Vitaliani, M. Majowiecki, A.V. Saetta, Dynamic Behavior of a Tensegrity System Subjected to Follow Wind Loading, Computers and Structures 81 (2003) 2199-2217.
- R. Motro, Structural Morphology of Tensegrity Systems, Meccanica 46 (2011) 27-40.
- R. Issa, Robert McNeel & Associates, Essential Mathematics for Computational Design, Second Edition.
- J. Wallgren, Tension at Saltholm, The Royal Danish Academy of Fine Arts, School of Architecture, 2013.
- V. G. Jauregui, Tensegrity Structures and Their Application to Architecture, School of Architecture, Queen's University Belfast.
- M.V. van Telgen, Parametric Design and Calculation of Circular and Elliptical Tensegrity Domes, TU Eindhoven, Department of Architecture, Building and Planning, 2013.
- D.M. Smidt, Freeform Follows Functions, TU Delft, Faculty of Architecture and Built Environment, 2014.

Appendix

The content following is the logic and
design development for double-surface
tensegrity with other tessellations, such
as hexagonal or dodecagonal patterns, with
both type 1 (based on Z-based elementary
cells) and type 2 (based on cylindrical
tensegrity cells).

Z-topology tensegrity, hexagonal tessellation, single-surface
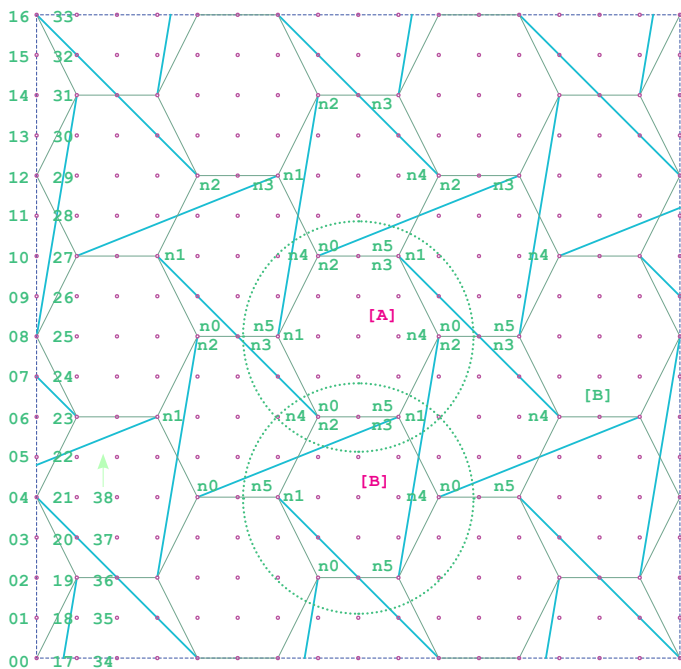
Numbering the generic quadriangular grid which is the base for defining the network of struts and network of cables.

$$n0 = i$$
$$n3 = n0 + 5u + 2$$

$$n1 = i$$
$$n4 = n1 + 4u - 4$$

$$n5 = i$$
$$n2 = n5 + u + 6$$
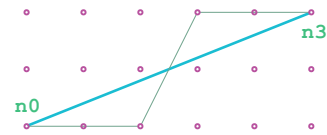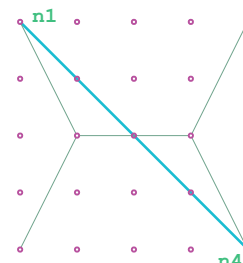
Two typical compositions of struts around a hexagon in the tessellation.
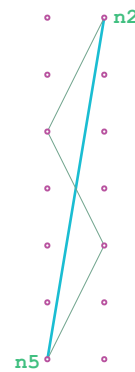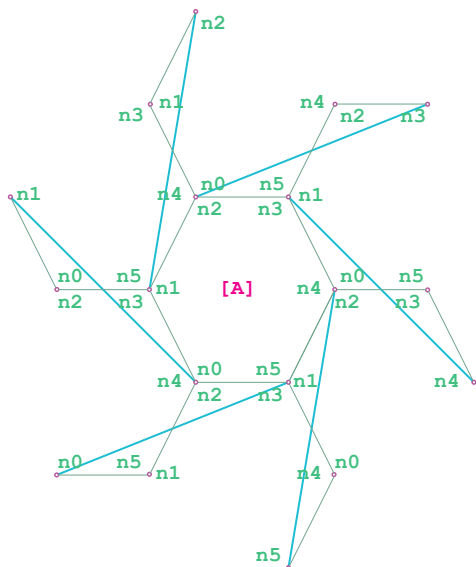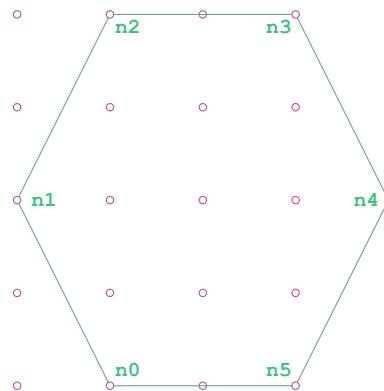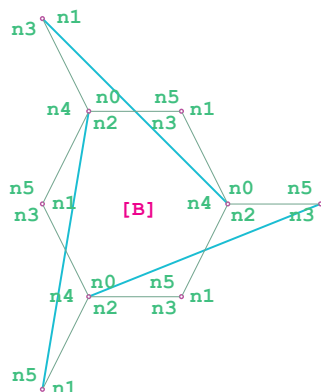
$$n0 = i$$
$$n1 = n0 - u + 2$$
$$n2 = n1 + u + 2$$
$$n3 = n2 + 2$$
$$n4 = n3 + u - 2$$
$$n5 = n4 - u - 2$$

Procedural descriptions of struts and cables based on generic quadriangular grid.

Define the location of strut network
on the quadriangular grid

Strut network + cable network

Quadriangular grid based on grid of
points

Define the location of cable network
on the quadriangular grid

The network of struts and network of cables are independently defined based on the generic quadriangular
grid of points. In the end, they are assemblied together to form a single-surface tensegrity structure.
There is no need to figure out the z-topology or adjacent hexagons to define strut network which is no
longer depending on the network of cable but the generic quadriangular grid.

Z-topology tensegrity, hexagonal tessellation, single-surface
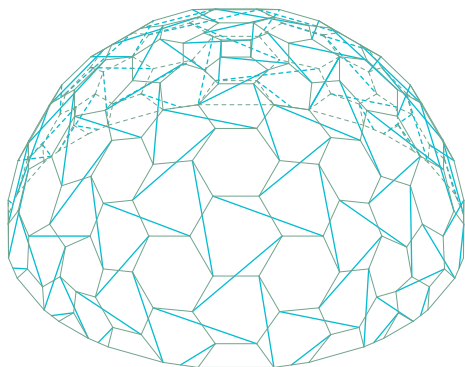
Bucky's half-sphere class-1
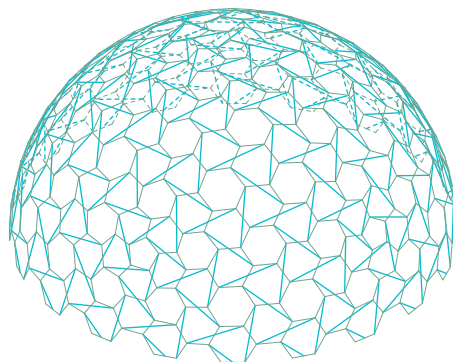
Bucky's half-sphere class-0
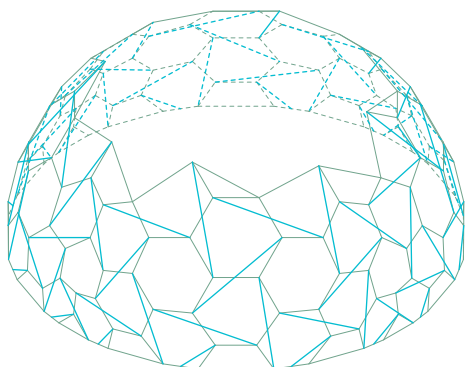
Bucky's half-sphere class-1
with opening
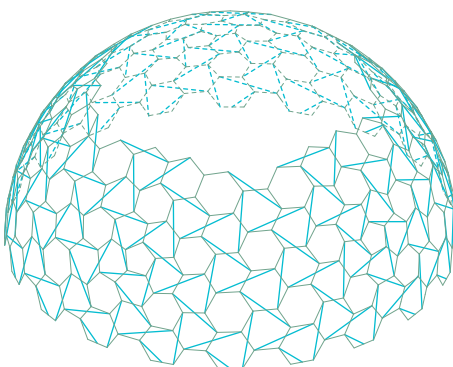
Bucky's half-sphere class-0
with opening
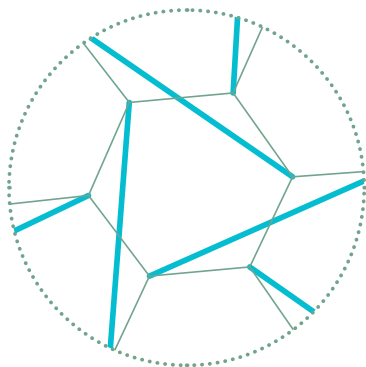
Topology type 1
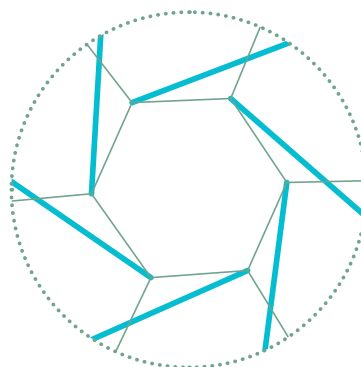
Topology type 2
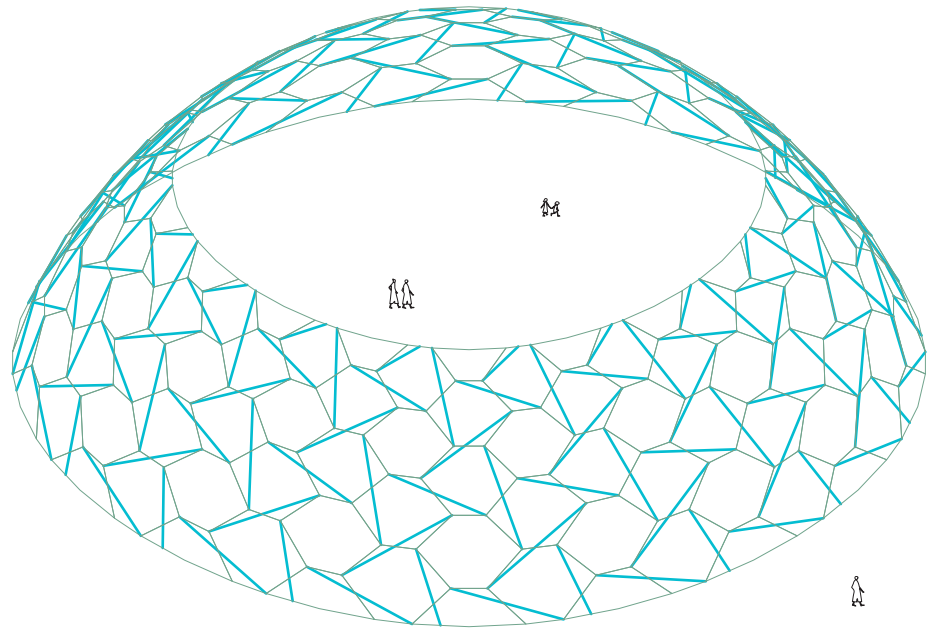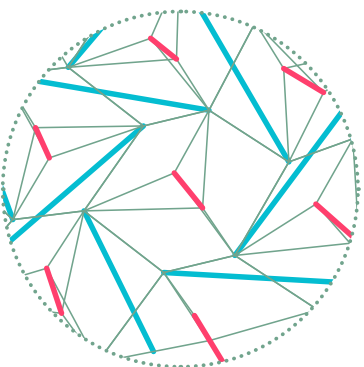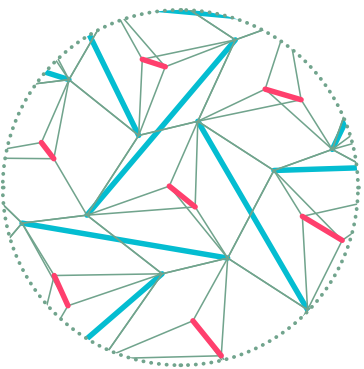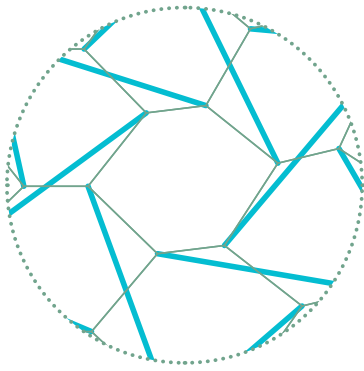
Tesselatizing and tensegritizing a simple dome with a central opening using hexagonal pattern (6-gon)
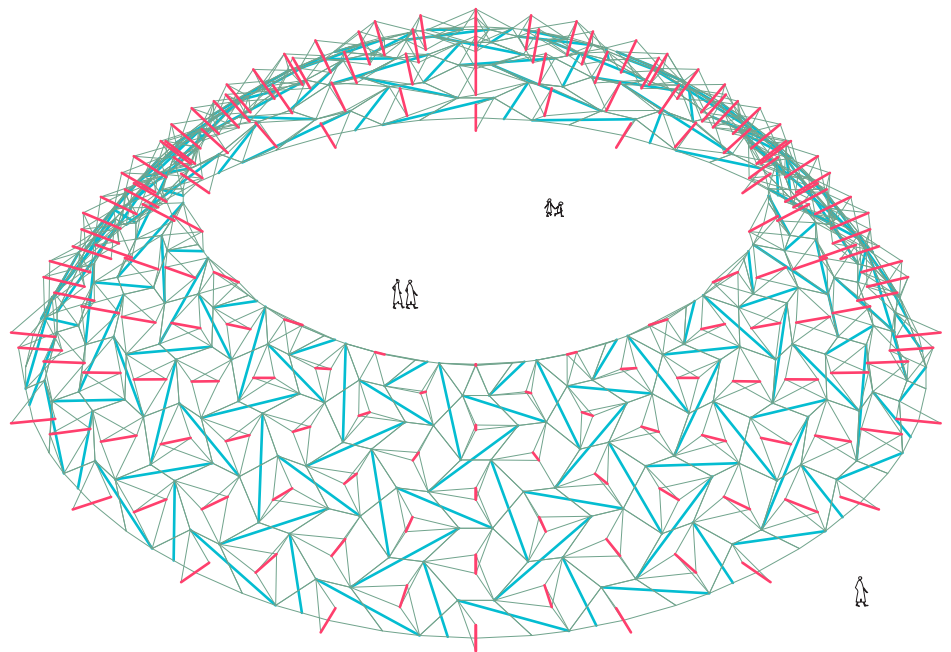
Adding normal struts (in pink) in the center of hexagonal cells, to increase the thickness of the shell,to handle out-plane loading applying to hexagonal pattern (6-gon)
The in-plane struts (In green) remain in the same reference surface extra cables are added to connect normal struts to in-plane struts

Z-topology tensegrity, hexagonal tessellation, single-surface
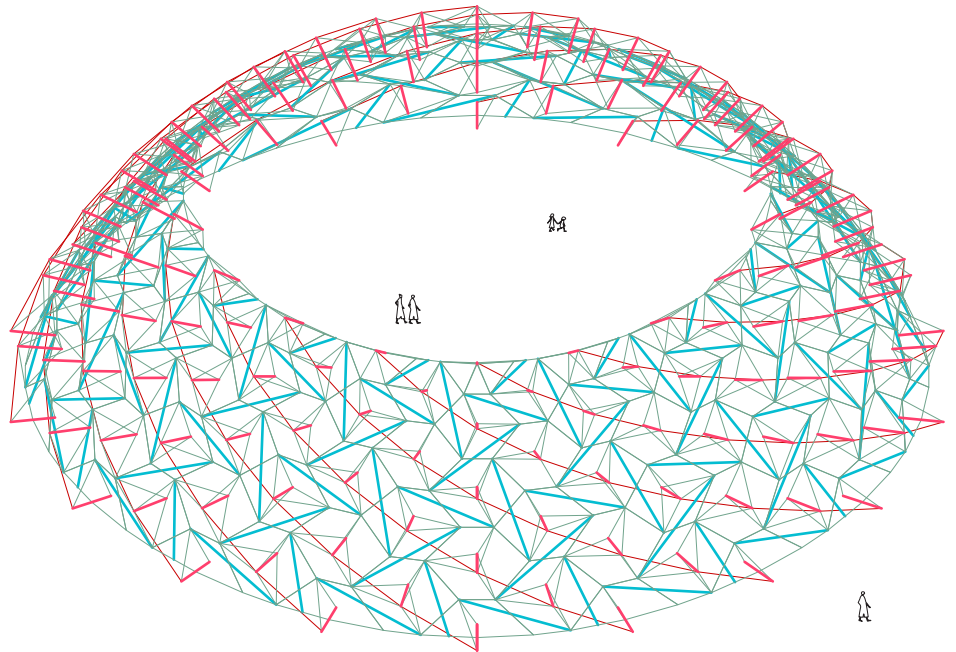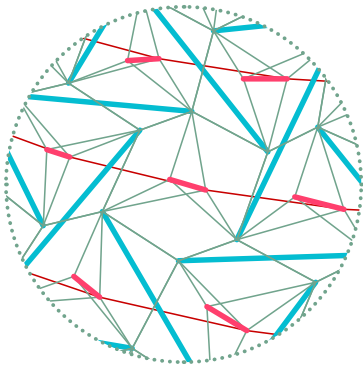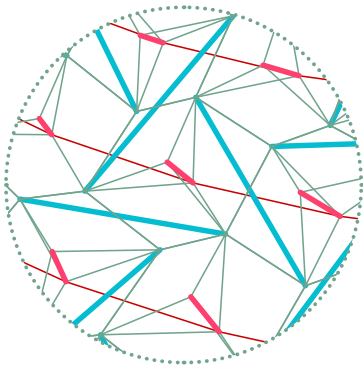
Adding outer bracing cables (thin lines in pink) to limit the rotation of pin-jointed connections
Applying to hexagonal pattern (6-gon)
These bracing cables connect tops of normal struts in order

Using two reference surfaces with the same way of tessellating applying the method of single-surface tensegrity structures with z-topology, but in this case, two ends of a strut are located on two different surfaces. by doing this, the structure has the thickness, becomes more spatial. and touching between struts are avoided.
In this figure, the tesselation is hexagonal pattern.
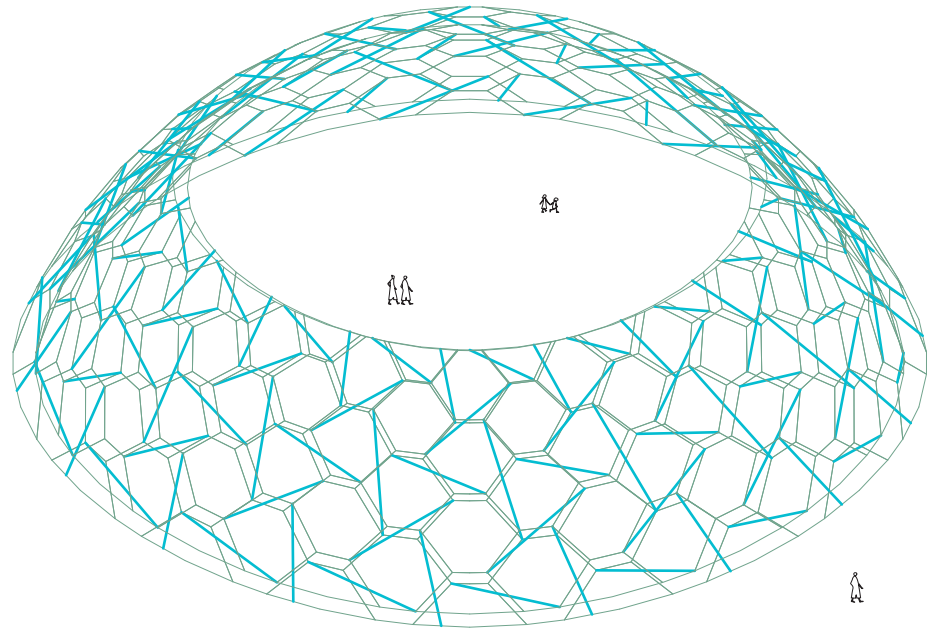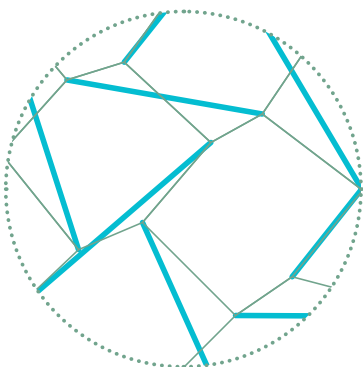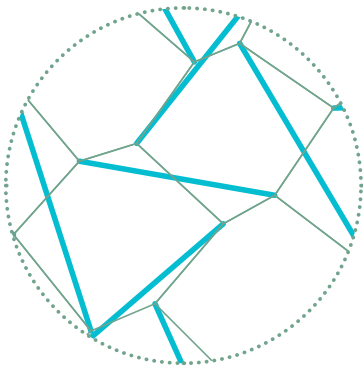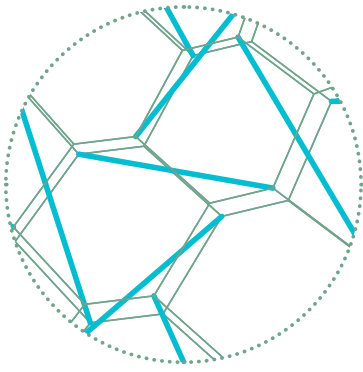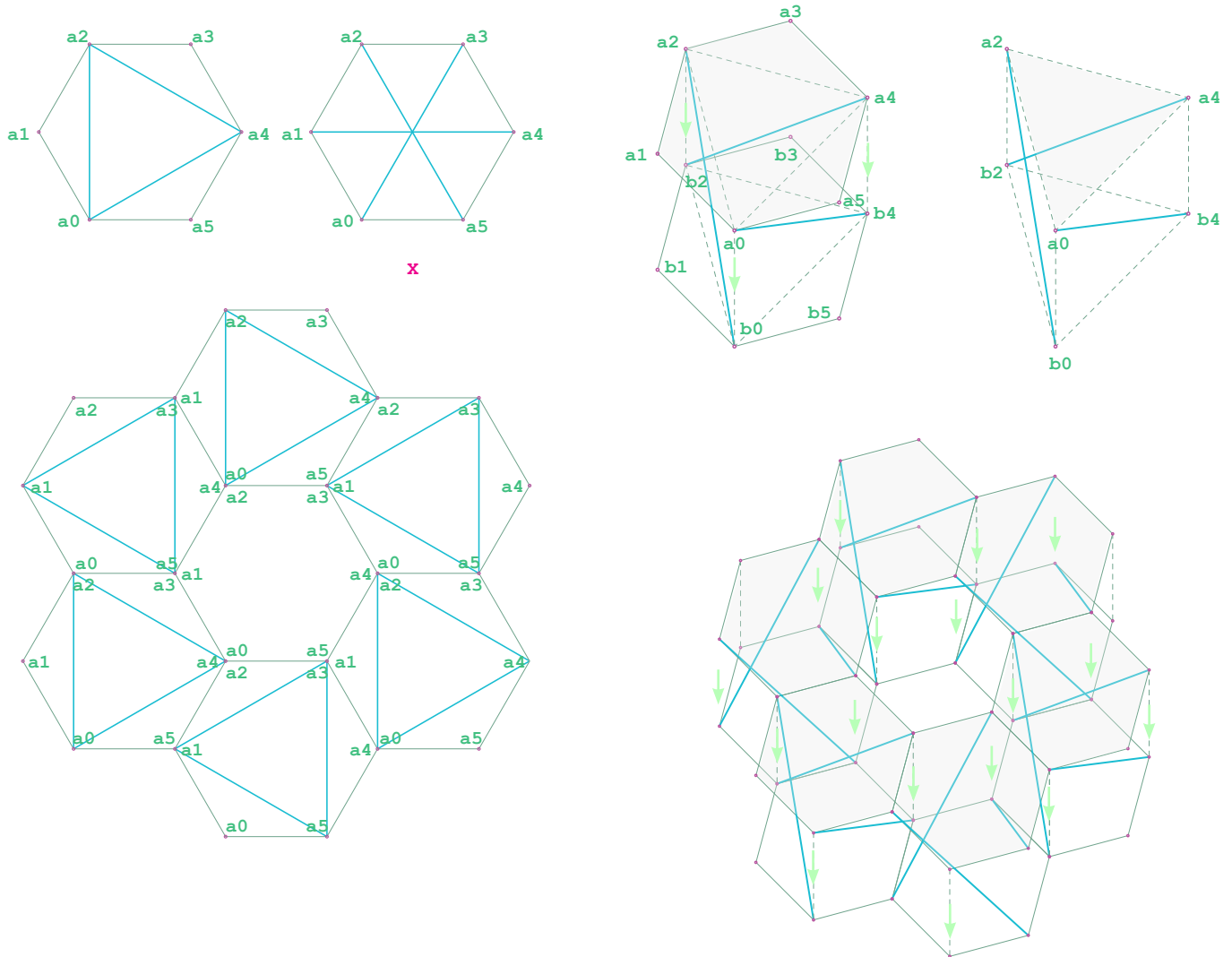

After having the network of struts, two reference cable networks are merged into one. so in terms of topology, the system becomes similar to single-surface tensegrity structures again, but the geometry is different, and better in structural performance.
In this case, the tessellation is hexagonal pattern.

Z-topology tensegrity, dodecagonal tessellation, single-surface
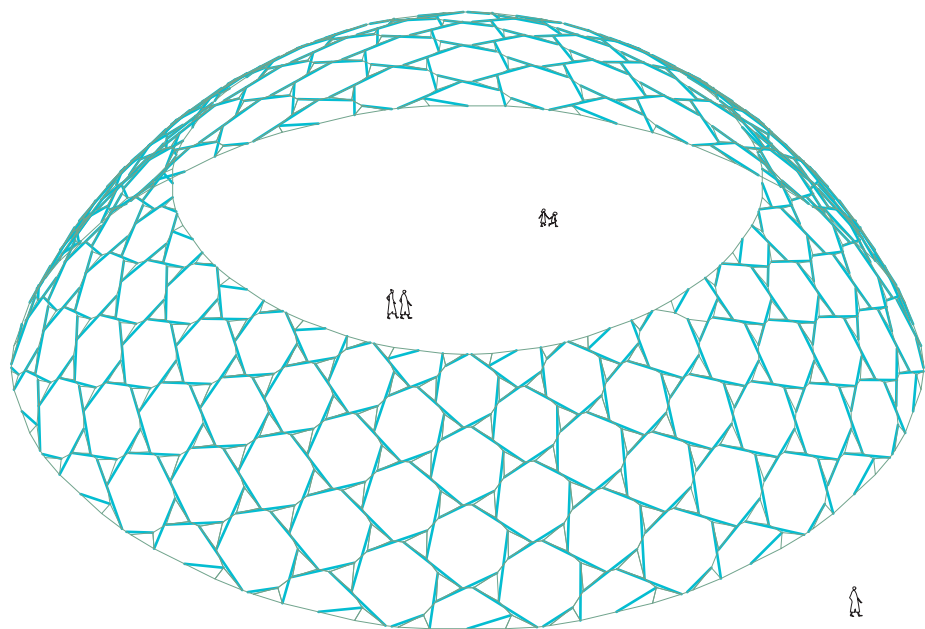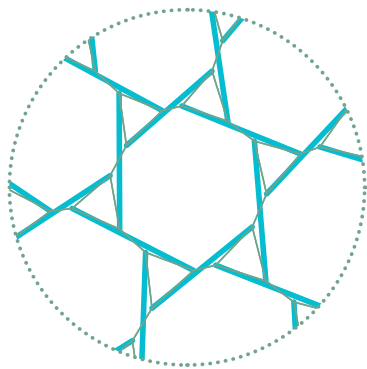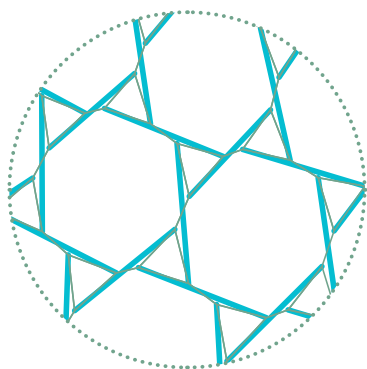
Tesselatizing and tensegritizing a simple dome with a central opening
using dodecagonal pattern (12-gon)

Z-topology tensegrity, dodecagonal tessellation, double-surface
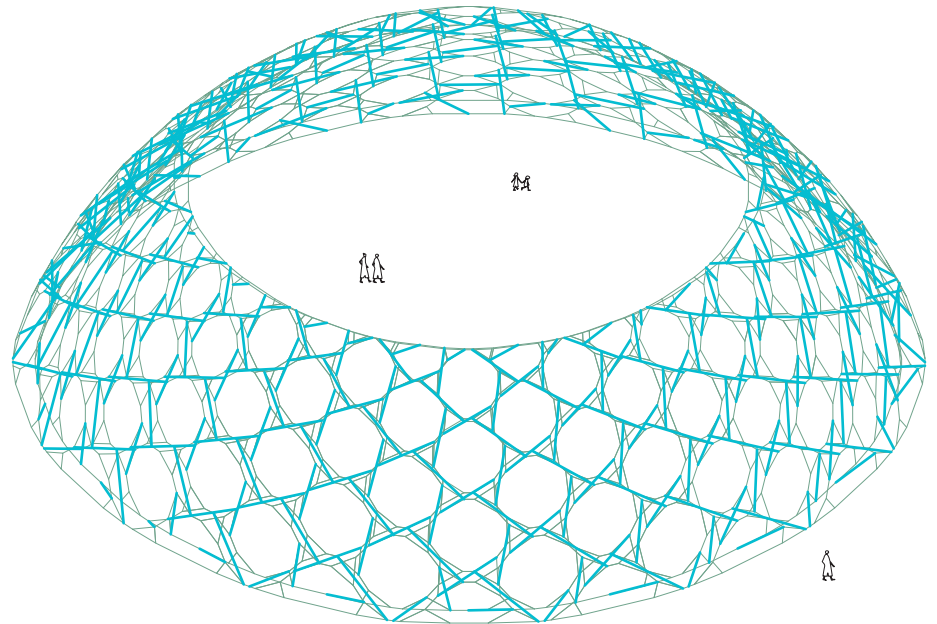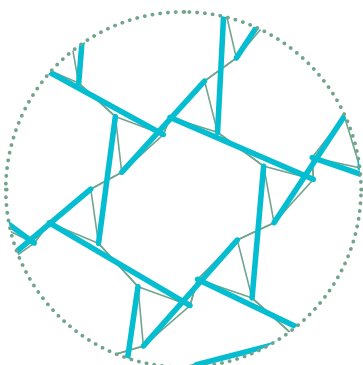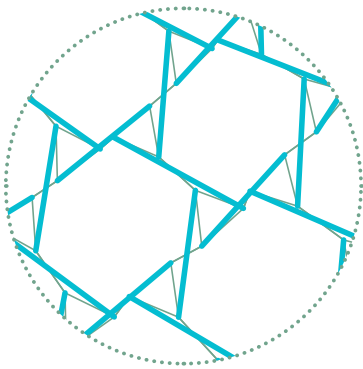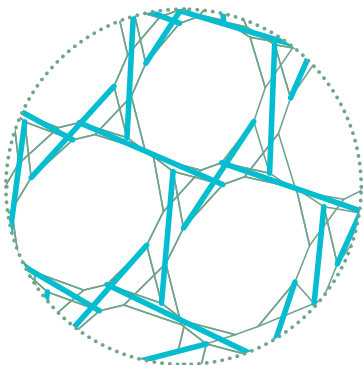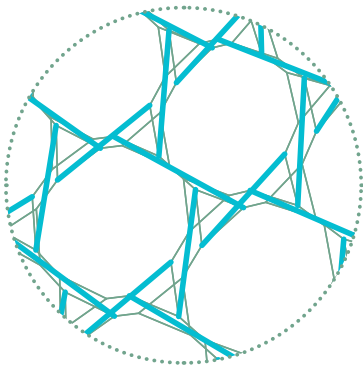
Using two reference surfaces with the same way of tessellating
applying the method of single-surface tensegrity structures with
z-topology, but in this case, two ends of a strut are located on two
different surfaces. By doing this, the structure has the thickness,
becomes more spatial. and touching between struts are avoided.
In this figure, the tesselation is octagonal pattern.
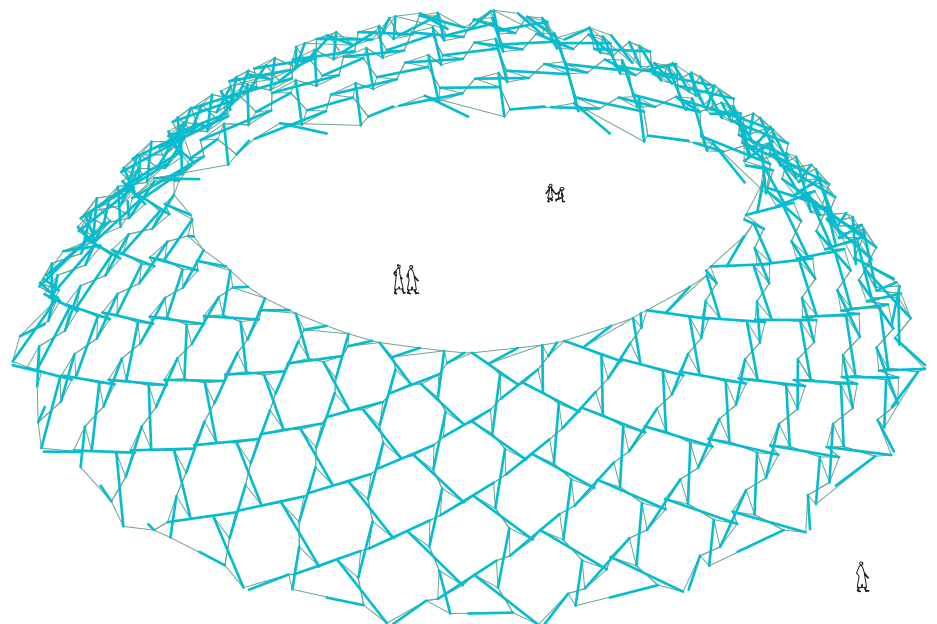
After having the network of struts, two reference cable networks are
merged into one. so in terms of topology, the system becomes similar
to single-surface tensegrity structures again, but the geometry is
different, and better in structural performance.
In this case, the tessellation is dodecagonal pattern.

Cylindrical tensegrity, n = 2, hexagonal tessellation, double-surface
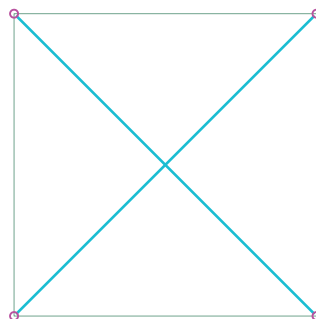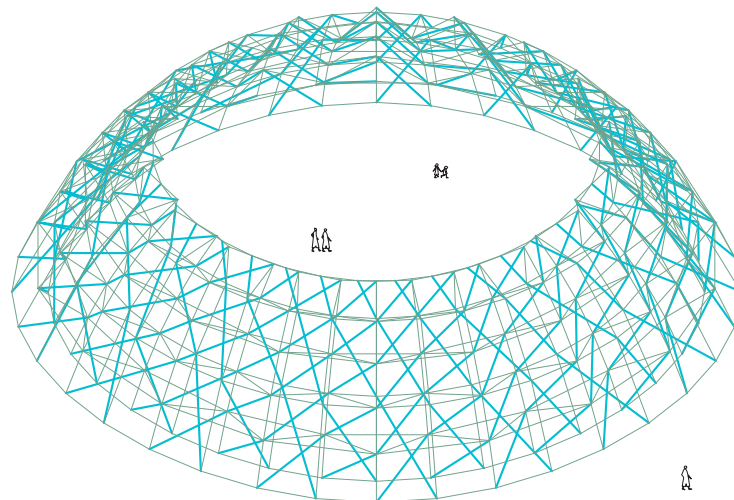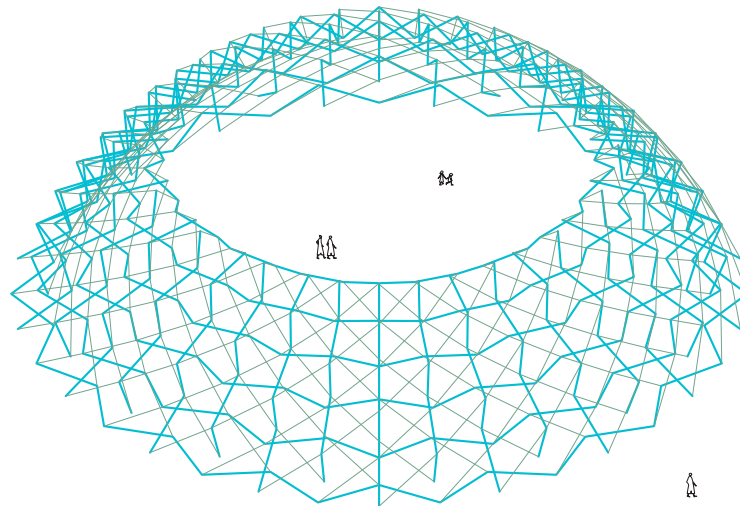
In this case, n = 2. these are tensegrity structures, but not pure types since there are a certain amount of struts touching the others. In general, the network of struts is discontinuous while the cable network is continuous.
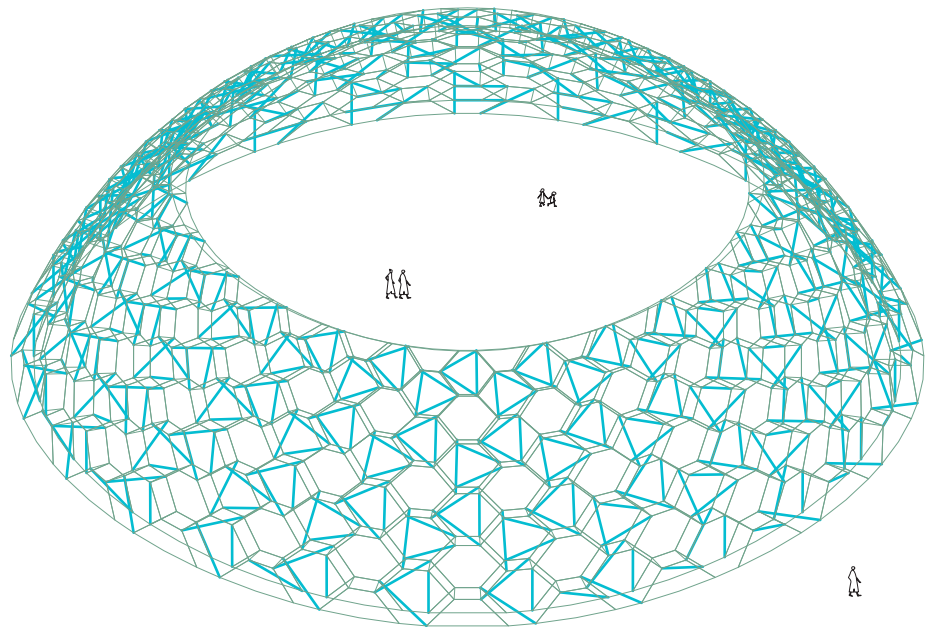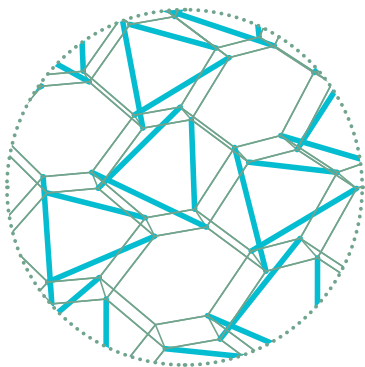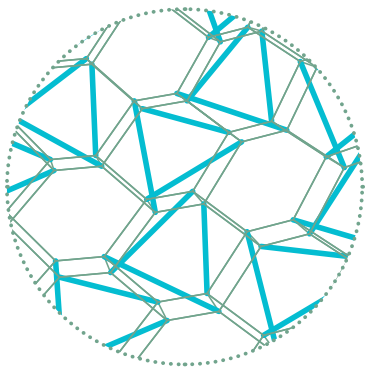
within a hexagonal tessellation, the system of simplex tensegrity (triangular prism) can be constructed. n = 3 in this case.
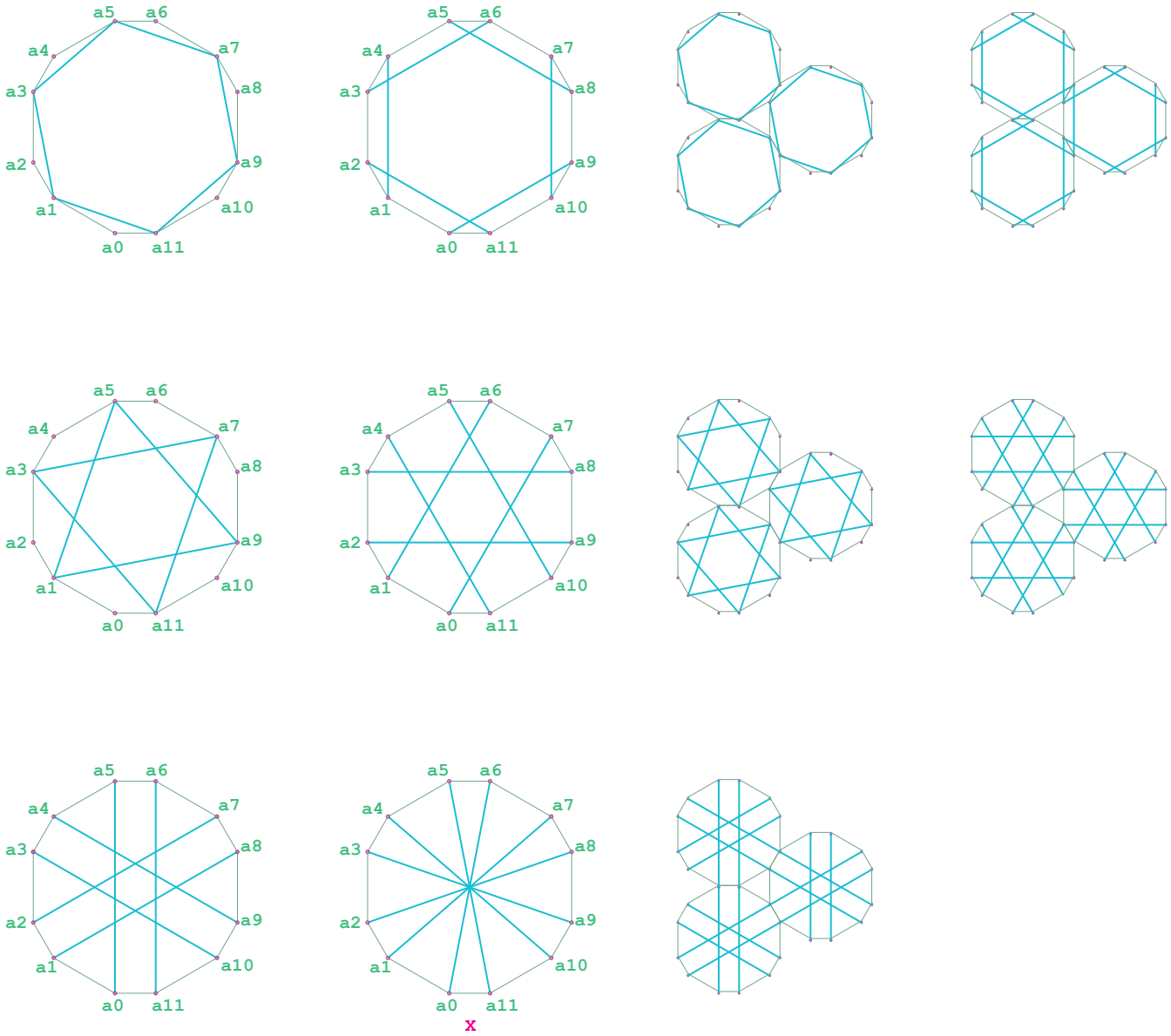
The cell of this system is a simplex tensegrity inside a hexagonal cylindrical geometry.They will be then combined in the way that struts do not touch each other.

Cylindrical tensegrity, n = 3, hexagonal tessellation, double-surface

Applying to the dome with a central opening. There are a certain amount
of cables which will be added to connect two reference tessellations.
in this case, these reference tessellations are not merged.
With a hexagonal pattern, a network of simplex tensegrities is achieved.
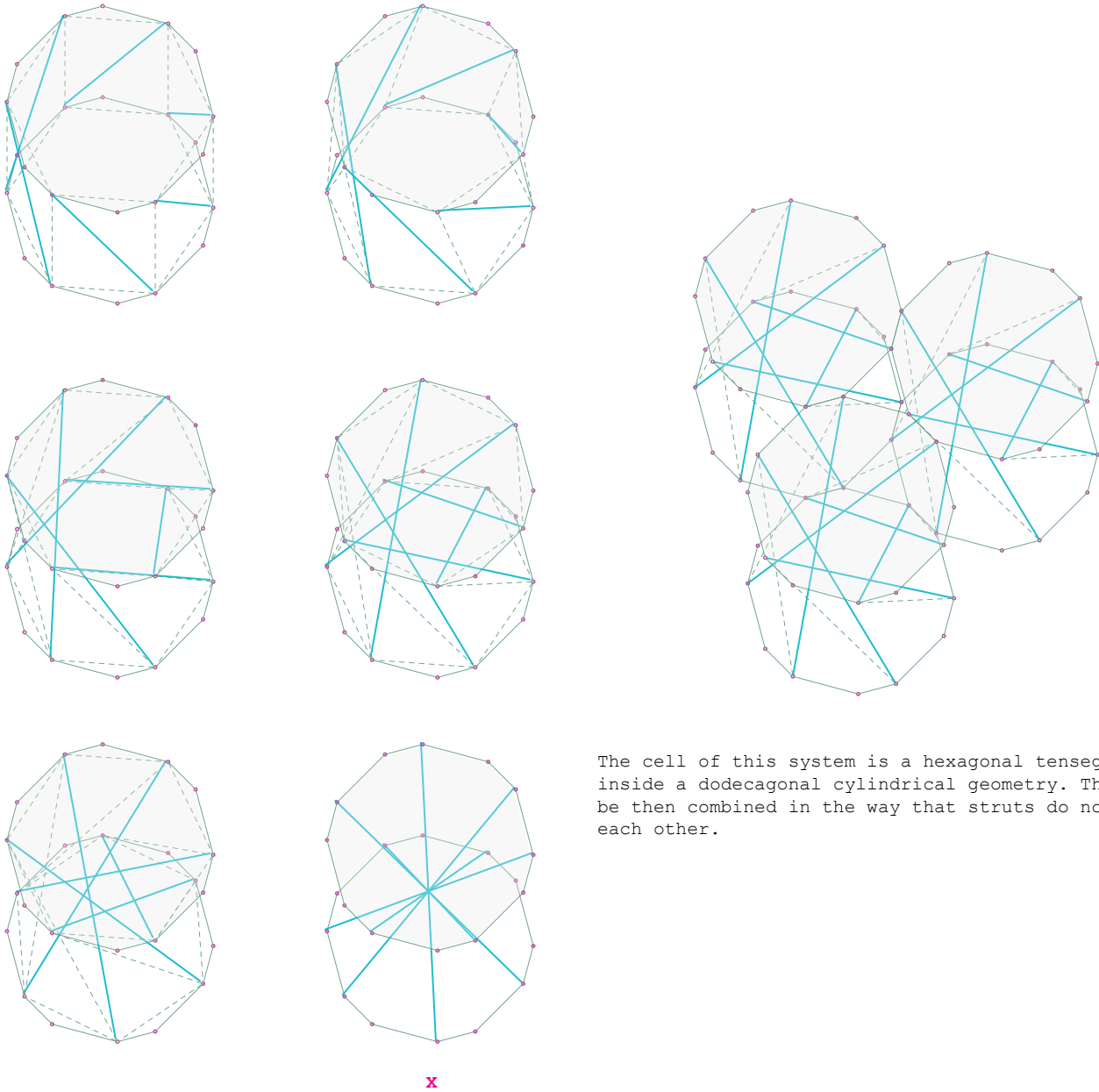
There are five possible compositions of six struts within a dodecagonal prism. The last one is useless because struts touch each other in the middles.

By combining these five possible types of cells together, 5 different tessellations are achived.

Cylindrical tensegrity, n = 6, dodecagonal tessellation, double-surface

The cell of this system is a hexagonal tensegrity inside a dodecagonal cylindrical geometry. They will be then combined in the way that struts do not touch each other.

X
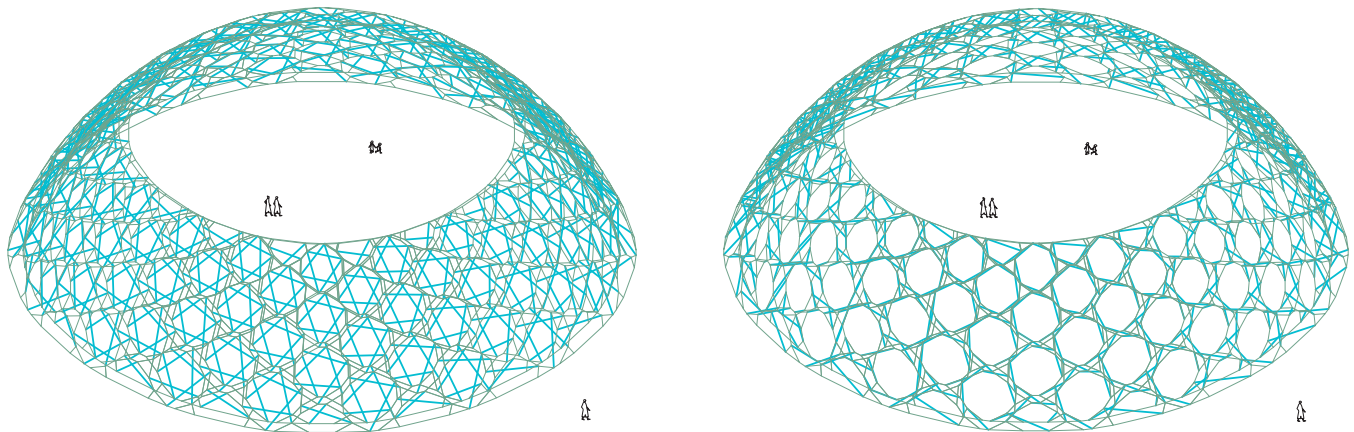
Applying to the dome with a central opening. There are a certain amount of cables which will be added to connect two reference tessellations. In this case, these reference tessellations are not merged.
with a dodecagonal pattern, a network of hexagonal tensegrities is achieved. There are five alternatives of them. two of these systems are visualized in the figure.